



HAL
open science

Modèles de dimères : comportements limites

Cédric Boutillier

► **To cite this version:**

Cédric Boutillier. Modèles de dimères : comportements limites. Mathématiques [math]. Université Paris Sud - Paris XI, 2005. Français. NNT: . tel-00011334

HAL Id: tel-00011334

<https://theses.hal.science/tel-00011334>

Submitted on 10 Jan 2006

HAL is a multi-disciplinary open access archive for the deposit and dissemination of scientific research documents, whether they are published or not. The documents may come from teaching and research institutions in France or abroad, or from public or private research centers.

L'archive ouverte pluridisciplinaire **HAL**, est destinée au dépôt et à la diffusion de documents scientifiques de niveau recherche, publiés ou non, émanant des établissements d'enseignement et de recherche français ou étrangers, des laboratoires publics ou privés.

N° D'ORDRE :

**UNIVERSITE PARIS XI
UFR SCIENTIFIQUE D'ORSAY**

THESE

Présentée

Pour obtenir

**Le GRADE de DOCTEUR EN SCIENCES
DE L'UNIVERSITE PARIS XI ORSAY**

PAR

Cédric BOUTILLIER

Sujet : **MODÈLES DE DIMÈRES :
COMPORTEMENTS LIMITES**

Rapporteurs : **M. Nikolai RESHETIKHIN
 M. Scott SHEFFIELD**

Soutenue le 26 octobre 2005 devant la Commission d'examen

M. Philippe CHASSAING
Mme Alice GUIONNET
M. Richard KENYON **(directeur de thèse)**
M. Yves LE JAN
M. Vincent PASQUIER
M. Wendelin WERNER

Résumé. Le modèle de dimères est un système de mécanique statistique qui modélise l'adsorption de molécules diatomiques sur la surface d'un cristal, représentée par un réseau périodique plan biparti. On attribue à chaque type d'arête une énergie, correspondant à la facilité avec laquelle une molécule va pouvoir s'y fixer. Il existe une famille à deux paramètres de mesures de Gibbs, dont les comportements sont classifiés en trois phases : gazeuse, liquide, solide.

La première partie de cette thèse est consacrée à l'étude d'un tel système près de la transition de phase liquide-solide. En examinant le cas du réseau hexagonal, nous exhibons deux types de comportements limites. Le premier est une collection de chemins aléatoires conditionnés à ne pas se toucher. Le deuxième, appelé le modèle du collier de perles, est un processus ponctuel sur $\mathbb{Z} \times \mathbb{R}$. Ces comportements limites possèdent tous les deux des marginales données par le processus déterminantal sur \mathbb{R} avec noyau sinus, décrivant aussi les statistiques des valeurs propres des grandes matrices aléatoires de l'ensemble GUE. Le modèle du collier de perles est universel : nous montrons qu'il apparaît comme la limite de tout modèle de dimères sur un graphe planaire biparti périodique.

Dans une deuxième partie, on s'intéresse à la statistique des motifs dessinés par des dimères. Nous montrons que les fluctuations de densité d'un motif convergent à la limite d'échelle vers un champ gaussien. Dans le cas liquide, l'objet limite est la somme d'une dérivée du champ libre et d'un bruit blanc indépendant. Pour une mesure gazeuse, la limite est un bruit blanc.

Dans le dernier chapitre, on aborde un problème de dénombrement de chemins sur le graphe-échelle, lié à l'étude du noyau de la chaleur sur le groupe de l'allumeur de réverbères, ainsi qu'à celle des opérateurs de Schrödinger aléatoires.

Mots-clés. mécanique statistique, dimères, pavages, transitions de phase, marches aléatoires, groupe de l'allumeur de réverbères, opérateurs de Schrödinger aléatoires.

MSC2000. 82B20, 82B41, 82B44, 60B15.

Abstract. The dimer model is a system from statistical mechanics modelizing the adsorption of diatomic molecules on the surface of a crystal, represented by a bipartite biperiodic planar graph. A weight is assigned to every type of edge. This weight is related to the energy needed for a molecule to settle at a particular place. For such a distribution of weights, there exists a two-parameter family of Gibbs measures on configurations. The behaviour of these measures can be classified into phases: gaseous, liquid or solid.

The first part of this thesis is devoted to the study of such a system near the liquid-solid phase transition. Considering first the case of the honeycomb lattice, we exhibit two sorts of limit behaviours. The first one is an infinite collection of non-colliding random paths. The second one, called the bead model, is described by a point random field on $\mathbb{Z} \times \mathbb{R}$. They both have marginals given by the determinantal point random field on \mathbb{R} with the sine kernel, describing also the eigenvalues statistics in the bulk of the spectrum of large random matrices of the GUE ensemble. Then, we prove that the bead model is universal: it appears as the limit of any dimer model on a bipartite planar periodic graph.

In the second part, we study the statistics of patterns made of a finite number of dimers. We prove that the fluctuations of pattern density converge in the scaling limit to a Gaussian random field. When the measure is liquid, the limiting object is a linear combination of a derivative of the massless free field and an independent white noise. In the case of a gaseous measure, the limit is simply a white noise.

In the last chapter, we solve a counting problem of paths on the ladder graph. This problem is related to the asymptotics of the heat kernel on the lamplighter's group, as well as to spectral theory of Schrödinger operators with random potential.

Keywords. statistical mechanics, dimer models, tilings, phase transitions, random walks, lamplighter's group, random Schrödinger operators.

Remerciements

Richard, je te remercie d'avoir accepté de diriger mes recherches. J'ai beaucoup appris avec toi au cours de nos conversations aux quatre coins du monde : Orsay, Princeton, Vancouver, Amsterdam. Merci pour ta générosité, ta simplicité, ta gentillesse. Pendant les deux dernières années, tu as continué malgré la distance à suivre l'avancement de mes travaux. Je te dois beaucoup.

I would like to thank Nikolai Reshetikhin and Scott Sheffield to have accepted to report my thesis and to give me some of their precious time.

Wendelin, je te remercie d'avoir toujours été là pour répondre à mes questions, sans doute souvent un peu naïves, et me prodiguer de précieux conseils. Merci de faire partie de mon jury.

Yves Le Jan, Vincent Pasquier, Alice Guionnet, Philippe Chassaing, vous m'honorez en faisant partie de mon jury.

Je remercie le département de Mathématiques de l'Université de Colombie Britannique, son directeur Bryan Marcus, et notamment l'équipe de probabilité de m'avoir accueilli durant l'automne 2004. Je remercie tout particulièrement Ed Perkins pour les discussions que nous avons eues mais qui n'ont malheureusement pas réussi à trouver leur place dans cette thèse.

Je tiens à remercier Kirone Mallick, qui a guidé mes premiers pas dans le monde de la recherche académique. Son enthousiasme et sa passion pour la recherche sont pour beaucoup dans le choix de mon orientation.

Un grand merci à Martine Justin et à Valérie Lavigne. Votre efficacité m'a été toujours d'un grand secours, et votre accueil toujours chaleureux.

À tous les doctorants du bâtiment 430 que j'ai côtoyés pendant ces trois années. D'abord les anciens et les nouveaux du bureau le plus sympa, le 110 : Antoine, Magali, Khaled, Mina, Aurélien, Marie, Besma, Marion, cela a été un grand plaisir que de partager avec vous ce deuxième chez-moi. Merci à Ismaël de mettre autant de vie dans notre cher couloir. Reda, ta présence m'a manqué pendant ma dernière année. J'espère que nos routes vont se recroiser très bientôt. Béatrice, tu es en quelque sorte ma grande sœur dans la famille de la recherche. Je te remercie pour toutes nos discussions, tes conseils et ton amitié. Merci à Mathieu, Graham, et tous les autres ...

Merci aussi à tous mes amis non mathématiciens : David, mes amis russes de FizFak et d'ailleurs. Merci à Thomas, mon vieux pote des bois.

Merci à mes parents de m'avoir encouragé et soutenu dans dans mes choix.

Olya, mon petit soleil, pour m'avoir laissé partir au Canada juste quelques semaines après notre mariage, pour m'avoir soutenu et supporté pendant mes mauvais jours, pour tout ça et beaucoup d'autres choses, merci. Я тебя люблю.

Contents

Introduction	13
1 Combinatorics of the dimer model	24
1.1 Dimer configurations of a graph	24
1.2 The dimer model on planar graphs	26
1.3 The dimer model on bipartite graphs	29
1.4 Dimers on bipartite graphs and flows	30
1.4.1 Forms on a graph embedded in an orientable surface	31
1.4.2 Unit white-to-black flows and height function	32
1.4.3 Gauge transformation and magnetic field	32
2 Dimers and Amoebæ	34
2.1 Gibbs measures on dimer configurations	34
2.2 Spectral curve and related objects	35
2.3 Changing the magnetic field and computing...	36
2.3.1 ...the partition function	37
2.3.2 ...the local statistics	38
2.4 Harnack curves and consequences of maximality	40
2.5 The gaseous phase	41
2.6 The liquid phase	41
2.6.1 Map from G^* to \mathbb{R}^2	42
2.6.2 Asymptotics of $K_B^{-1}(\mathbf{b}, \mathbf{w})$	44
2.7 The solid phase	45
2.8 The dimer on the honeycomb lattice	47
3 Determinant random point fields	50
3.1 Definitions	50
3.2 Examples of determinantal random point fields	54
3.2.1 Eigenvalues of Random matrices	54
3.2.2 Dimer models	56
4 Lozenge tilings and the Dyson model	58
4.1 Non colliding random paths	59
4.2 The Dyson model and the sine process	61
4.3 Convergence to the sine process	62
4.4 Proof of proposition 4.1	66

4.5	Proof of proposition 4.2	68
5	The bead model	73
5.1	Presentation of the bead model	73
5.2	Discrete bead model and dimers	75
5.3	Explicit expression of the Gibbs measures	77
5.4	Comments and possible developments	81
5.4.1	The bead model as an asymmetric exclusion process	81
5.4.2	The bead model and spanning trees	82
6	The bead model – Generalization	84
6.1	Tentacles of the amoeba	84
6.2	Deep inside a tentacle	86
6.2.1	Analytic results about the roots of P	86
6.2.2	Asymptotics of the inverse Kasteleyn operator for beads	87
6.3	Convergence to the bead model	92
6.4	Interaction between bead models	93
7	Pattern densities in fluid dimer models	101
7.1	Introduction	101
7.1.1	Scaling limits of pattern densities	101
7.1.2	The fluid phases of the dimer model	102
7.1.3	Gaussian Fields	103
7.1.4	Statement of the result and structure of the proof	104
7.1.5	Density fields and partition function	105
7.2	The liquid case: edge densities	106
7.2.1	Convergence of the second moment	106
7.2.2	Convergence of higher moments	111
7.2.3	A word about the non generic case	117
7.3	The liquid case: general pattern densities	117
7.3.1	Notations	118
7.3.2	Asymptotics of correlations	119
7.3.3	Convergence of the second moment	123
7.3.4	Convergence of higher moments	123
7.4	The gaseous case	124
7.4.1	Convergence of the second moment	125
7.4.2	Higher moments	126
7.4.3	Patterns in gaseous phase	127
7.5	Correlations between density fields	128
7.6	Examples	129
7.6.1	Tilings of the plane by dominos	129
7.6.2	Dimer densities on the square-octagon graph	132

8	Curl-free walks and the lamplighter's problem	135
8.1	The lamplighter's problem	136
8.2	Strategy	137
8.3	Approximation of the first eigenvalue	139
8.3.1	Lower bound	139
8.3.2	Upper bound	140
8.4	Main contribution to $ \mathcal{P}_n $	142
8.5	Spectral gap	145
8.6	Generalization	146
8.7	Paths counting and random Schrödinger operators	148

Introduction

La mécanique statistique cherche à décrire l'état d'un système complexe composé d'un très grand nombre de constituants élémentaires. Le but est de donner une description probabiliste globale pour le système à partir de la combinatoire locale qui régit l'arrangement des configurations microscopiques de celui-ci.

Des exemples de tels systèmes sont:

- un gaz formé d'atomes identiques dont le volume, la pression, la température décrivent l'état macroscopique. Ces grandeurs sont la traduction à grande échelle du mouvement chaotique des atomes.
- un aimant, modélisé par un cristal sur les sites duquel se trouvent des *spins* qui, malgré l'agitation thermique, cherchent à s'aligner avec leurs voisins.

Le formalisme canonique de la mécanique statistique consiste à attribuer à chaque configuration microscopique du système \mathcal{C} une énergie $\mathcal{E}(\mathcal{C})$, calculée à partir des interactions microscopiques. Une configuration est d'autant plus favorisée que son énergie est basse. Pour traduire ce fait, la probabilité $p(\mathcal{C})$ associée à chaque configuration est

$$p(\mathcal{C}) = \frac{1}{Z(\beta)} e^{-\beta \mathcal{E}(\mathcal{C})} \quad (1)$$

où β désigne l'inverse de la température. Cette mesure de probabilité est appelée mesure de Boltzmann. Le coefficient de normalisation,

$$Z(\beta) = \sum_{\mathcal{C}} e^{-\beta \mathcal{E}(\mathcal{C})} \quad (2)$$

est appelé *fonction de partition*. Cette fonction de partition joue un rôle très important puisqu'à partir de celle-ci, il est possible de calculer des grandeurs macroscopiques telles que la pression dans le cas du gaz, ou bien l'aimantation dans le cas de l'aimant.

Il n'existe que peu de modèles non triviaux pour lesquels on connaît une formule exacte pour la fonction de partition. Parmi ces rares exemples, on trouve le modèle des dimères, qui est l'objet d'étude principal de cette thèse. Ce modèle possède en effet une structure sous-jacente très riche, qui rend son étude tout à fait intéressante.

Le modèle des dimères

Le modèle des dimères fut introduit la première fois en 1937 dans la littérature par les physiciens Fowler et Rushbrooke [15] pour modéliser l'adsorption de molécules diatomiques sur la surface d'un cristal. Les premiers calculs exacts sur ce modèle sont dus à Kasteleyn [24] et Temperley et Fisher [60] qui obtiennent indépendamment la fonction de partition. Le modèle des dimères a fait l'objet de nombreux travaux, non seulement pour son intérêt propre, mais aussi, grâce à des bijections, comme outil d'étude d'autres modèles : modèle d'Ising [14, 39], arbres couvrants [59, 5], fonte de cristal [44, 13], marches aléatoires annihilantes [38], ...

À partir des années 1990, les mathématiciens s'approprient le sujet. Citons entre autres les travaux de Thurston [62], Cohn, Kenyon et Propp [8], et Kenyon [27], qui posent les bases d'une étude mathématique systématique de ce modèle.

Récemment, le modèle des dimères connaît un nouveau gain d'intérêt en théorie topologique des cordes, grâce notamment aux travaux d'Okounkov, Reshetikhin et Vafa [45], qui proposent une dualité entre les cordes topologiques du A -modèle sur une variété de Calabi-Yau de dimension 3 et un modèle de dimères sur lequel on impose des contraintes aux bords.

Définitions et notations

Dans le lexique des chimistes, un *dimère* est une molécule constituée de deux atomes liés par une liaison chimique. Par analogie, nous emploierons ce terme pour désigner parfois les arêtes d'un graphe G : une arête \mathbf{e} représente la liaison chimique entre deux atomes, modélisés par les sommets extrémités de \mathbf{e} .

Une *configuration de dimères* \mathcal{C} est un sous-ensemble d'arêtes de G tel que chaque sommet de G est incident à exactement une arête de ce sous-ensemble. En théorie des graphes, elle est appelée aussi *couplage parfait*.

Supposons que le graphe G est fini et qu'il admet au moins une configuration de dimères. Une mesure de probabilité sur l'ensemble des configurations de dimères $\mathcal{M}(G)$ est construite de la manière suivante : on attribue à chaque arête \mathbf{e} une énergie $\mathcal{E}(\mathbf{e})$. La fonction d'énergie est ensuite étendue à une configuration de dimères comme la somme de l'énergie des dimères qu'elle contient

$$\mathcal{E}(\mathcal{C}) = \sum_{\mathbf{e} \in \mathcal{C}} \mathcal{E}(\mathbf{e}). \quad (3)$$

On associe alors à la configuration \mathcal{C} la probabilité

$$\mathbb{P}_{\mathcal{E}}[\mathcal{C}] = \frac{1}{Z(\mathcal{E})} e^{-\mathcal{E}(\mathcal{C})} \quad (4)$$

où $Z(\mathcal{E})$ est la fonction de partition

$$Z(\mathcal{E}) = \sum_{\mathcal{C} \in \mathcal{M}(G)} e^{-\mathcal{E}(\mathcal{C})}. \quad (5)$$

La mesure de probabilité ainsi obtenue est appelée *mesure de Boltzmann*. La quantité $\nu_{\mathbf{e}} = e^{-\mathcal{E}(\mathbf{e})}$ est appelée *poids* de l'arête \mathbf{e} .

Lorsque le graphe G est planaire, Kasteleyn a montré que la fonction de partition $Z(\mathcal{E})$ s'exprime comme le *pfaffien* d'une matrice d'adjacence orientée de G . Lorsque le graphe est biparti, la structure du modèle est plus riche. $Z(\mathcal{E})$ peut s'écrire plus simplement sous la forme du déterminant d'un opérateur K , appelé opérateur de Kasteleyn (voir par exemple [27]). Par ailleurs, les configurations de dimères sont en bijection avec des *fonctions de hauteurs*, ce qui permet d'interpréter le modèles de dimères comme un modèle de surface aléatoire discrète.

Quand le graphe G est infini, la fonction de partition en général est infinie, et on ne peut définir simplement de mesure de Boltzmann. Cette notion est remplacée par celle de *mesure de Gibbs*. Pour une telle mesure, une fois la configuration fixée dans une région annulaire, la configuration à l'intérieur et à l'extérieur sont indépendantes, et la mesure induite à l'intérieur est la mesure de Boltzmann. Dans [34], Kenyon, Okounkov et Sheffield généralisent les résultats de [8, 27] et étudient l'ensemble des mesures de Gibbs sur les configurations de dimères des graphes planaires bipartis \mathbb{Z}^2 -périodiques. Elles forment une famille paramétrée par le *champ magnétique* $B = (B_x, B_y)$. Le comportement de ces mesures peut être décomposé en trois catégories ou *phases* : gazeux, liquide ou solide suivant la vitesse de décroissance des corrélations entre les dimères.

On donne maintenant un aperçu des questions abordées dans cette thèse.

Transitions de phase et comportement limites

Un dimère \mathbf{e} d'un graphe biparti planaire \mathbb{Z}^2 -périodique se comporte en quelque sorte comme un petit dipôle magnétique, dont la direction est celle de son arête duale \mathbf{e}^* . En présence d'un champ magnétique B , le système privilégie les arêtes dont les dipôles sont alignés avec le champ.

Un des exemples les plus simples de graphes planaires bipartis \mathbb{Z}^2 -périodiques est le réseau hexagonal H , dont le graphe dual est le réseau triangulaire T . Un dimère peut être vu comme un lien entre deux faces adjacentes de T , formant ainsi un losange. Le fait que chaque sommet de H est couvert par un seul dimère implique que les losanges constitués de cette façon forment un *pavage du plan*. Le modèle de dimères sur H s'interprète par dualité comme un modèle de pavages aléatoires du plan par des losanges.

On distingue trois types de losanges, a , b , c , caractérisés par leur orientation, et représentés sur la figure 2.

Si l'on affecte une énergie nulle aux arêtes de H , en l'absence de champ magnétique les trois types de losanges sont équiprobables.

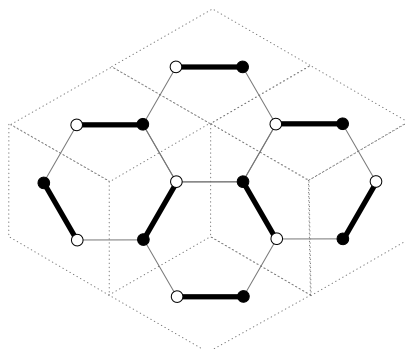


Figure 1: Un morceau de configuration de dimères sur H et le pavage par losanges correspondant.

Lorsqu'on augmente progressivement la composante verticale de B , la proportion de losanges de type a augmente progressivement jusqu'à atteindre 1 pour une *valeur critique* finie de B . Pour cette valeur de B , le graphe de cette proportion n'est plus dérivable : on assiste à une *transition de phase*. Le système est passé d'un *état liquide* où tous les types de losanges apparaissent avec une probabilité positive, à un *état solide* où un seul type de losanges est présent avec probabilité 1. Ce modèle peut représenter un cristal de glace qui se fissure et qui fond progressivement.

Peut-on donner une description quantitative du comportement des fissures lorsque la glace commence juste à fondre ?

Au contraire, lorsqu'on applique un champ magnétique très fortement dirigé vers le bas, la probabilité d'apparition des losanges de type a , même si elle décroît avec l'amplitude de B , reste toujours strictement positive. Elle n'atteint 0 que quand la composante verticale de B tend vers $-\infty$. Dans ce cas, on n'a pas à proprement parler de transition de phase. En revanche, le comportement limite des losanges horizontaux est tout à fait intéressant.

Quelle est, à la limite, la distribution des losanges horizontaux ?

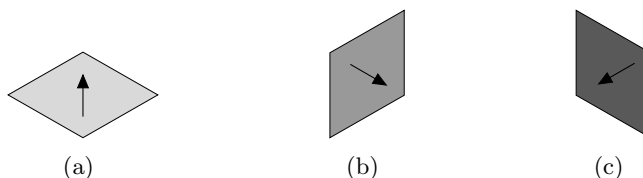


Figure 2: Les différents types de losanges d'un pavage correspondant à une configuration de dimères sur H , ainsi que les directions des dipôles associés.

Une partie de cette thèse est consacrée à l'étude détaillée de ces phénomènes, ainsi que leur généralisation à des graphes plus complexes, et qui se trouve reliée à la statistique des valeurs propres des matrices aléatoires.

Densités de motifs

Depuis [27], on sait, pour un champ magnétique fixé, calculer la densité moyenne de n'importe quel *motif* dessiné par un nombre fini de dimères dans une configuration aléatoire. Le nombre moyen de motifs dans une grande boule est alors donné grossièrement par le nombre de domaines dans la boule fois la densité du motif. Il nous parut intéressant d'essayer de comprendre les fluctuations de ce nombre autour de sa valeur moyenne, du moins à la *limite d'échelle* : tout en gardant la taille de la boule fixée, on fait tendre la maille du réseau vers 0, de sorte que le nombre de domaines fondamentaux dans la boule tend vers l'infini.

Comment se comportent à la limite d'échelle les fluctuations des densités de motifs ?

Combinatoire des chemins

Les méthodes de la mécanique statistique peuvent aussi s'appliquer à des problèmes plus proches de la combinatoire, comme par exemple le dénombrement de grands chemins sur des graphes. L'étude de la marche aléatoire simple ou de la marche aléatoire auto-évitante sur \mathbb{Z}^2 en sont des exemples.

Un raisonnement élémentaire sur la marche aléatoire simple montre que, sur \mathbb{Z} , la proportion de chemins de longueur $2n$ qui reviennent à leur point de départ est de l'ordre de $\frac{1}{\sqrt{\pi n}}$. On se pose ici une question similaire, qui est la suivante :

Sur un graphe en forme d'échelle, quel est le nombre de chemins de longueur n passant un nombre pair de fois par chaque barreau ?

Il se trouve que cette question, d'apparence pourtant anodine, et ses généralisations, ont de profondes conséquences en théorie des groupes.

Contenu de la thèse

Cette thèse est composée de huit chapitres dont les sept premiers sont consacrés aux modèles de dimères. Le dernier chapitre aborde le problème du dénombrement d'une certaine classe de chemins. Les résultats principaux, présentés dans les chapitres 4 à 8, sont expliqués brièvement à la fin de cette section.

Le chapitre 1 présente en détails le modèle des dimères sur un graphe fini G . Après avoir rappelé dans le cas général la définition de configuration de dimères ainsi que celle de mesure de Boltzmann, nous discutons plus en détails le cas particulier des graphes planaires bipartis pour lesquels la fonction de partition, ainsi que les statistiques locales s'expriment en termes de *déterminants* d'un opérateur K , apparenté à la matrice d'adjacence du graphe, et de son inverse K^{-1} . L'opérateur K est appelé *opérateur de Kasteleyn*.

Dans le chapitre 2, il est question du modèle de dimères sur des graphes planaires bipartis et \mathbb{Z}^2 -périodiques. Dans le cas d'un graphe infini, la mesure de Boltzmann telle qu'elle est définie dans le chapitre 1 n'a plus de sens. Elle est remplacée par la notion de *mesure de Gibbs* qui en est une extension naturelle. Nous résumons les travaux de Kenyon, Okounkov et Sheffield [34] dans lesquels ils montrent que pour un tel graphe, il existe une famille à deux paramètres de mesures de Gibbs. Le comportement de ces mesures peut être divisé en trois catégories ou *phases* : gazeux, liquide, solide, suivant la vitesse de décroissance des corrélations. Le diagramme de phase est donné par l'*amibe* de la *courbe spectrale*. La théorie générale est appliquée au cas particulier du réseau hexagonal H .

On trouve dans le chapitre 3 des éléments de la théorie des *champs aléatoires déterminantaux* ou *fermioniques*. Une présentation plus complète peut être trouvée dans [56]. Un exemple de tels champs est donné par la distribution des valeurs propres d'une matrice hermitienne aléatoire de l'ensemble GUE.

Le contenu des chapitres de 4 à 8 est décrit dans les paragraphes suivants.

Un modèle de chemins auto-évitants

Le chapitre 4 présente une étude de la transition de phase que subit le modèle des dimères sur le réseau hexagonal H , lorsque le champ magnétique, dirigé vers le haut, approche sa valeur critique par valeurs inférieures.

La riche structure algébrique du modèle permet d'étudier en détails cette transition. Un pavage est décrit complètement par les chemins que dessinent les losanges de type b et c de gauche à droite. Lorsque l'intensité du champ magnétique suivant la verticale augmente, les chemins s'écartent de plus en plus. En effectuant le changement d'échelle brownien, nous montrons que lorsque le champ magnétique tend vers cette valeur critique, la distribution de ces chemins converge vers une distribution de courbes aléatoires.

Théorème 1. *La famille de chemins aléatoires de losanges converge faiblement dans la limite d'échelle vers le processus sinus étendu.*

Le processus *sinus étendu* est un processus déterminantal qui décrit un système stationnaire et invariant par translation de chemins browniens soumis à une force de rappel vers l'origine, et conditionnés à ne pas se toucher. À un instant fixé, les corrélations entre les

positions des différents chemins s'expriment comme un déterminant du noyau *sinus*

$$\frac{\sin(x-y)}{\pi(x-y)}$$

et sont donc données par les mêmes formules que celles des valeurs propres des grandes matrices aléatoires de l'ensemble GUE.

Ce système homogène de chemins aléatoires a été étudié par Spohn [58], Osada [46], Nagao et Forrester [42], et plus récemment par Katori, Nagao et Tanemura [26], comme la limite lorsque le nombre de particules tend vers l'infini du cœur du modèle de Dyson [12].

Notons que dans cette même limite, la distribution du premier chemin est donnée par le *processus d'Airy*. Ce processus, introduit par Prähofer et Spohn [50], se retrouve aussi dans l'étude de pavages aléatoires auxquels on impose certaines contraintes aux bords [13, 22], ainsi que dans d'autres modèles de mécanique statistique, tels que le *modèle de croissance polynucléaire* (PNG) [50].

Alors que dans les précédentes études, le processus sinus étendu est obtenu en partant d'un nombre fini de chemins – continus ou discrets – puis en faisant tendre ce nombre vers l'infini, notre modèle de départ décrit déjà une famille infinie de chemins discrets, ce qui constitue l'originalité de notre approche.

Le modèle du collier de perles

Dans le chapitre 5, nous présentons un modèle de mécanique statistique que nous appelons le *modèle du collier de perles*. Les configurations pour ce modèle sont des collections de points (les perles) sur $\mathbb{Z} \times \mathbb{R}$ représentant une succession de brins sur lesquels les perles sont enfilées, qui vérifient les deux conditions suivantes

- Les configurations de points sont localement finies : sur un morceau fini de fil, il n'y a qu'un nombre fini de perles.
- Entre deux perles successives sur un même fil, on doit trouver exactement une perle sur le fil situé juste à gauche, ainsi que sur celui situé juste à droite.

Un exemple de configuration de perles est présenté sur la figure 3.

Si nous avons seulement un nombre fini de fils de longueur finie avec un nombre fixé N de perles, l'espace des configurations serait un convexe borné de \mathbb{R}^N et la mesure uniforme sur ce domaine définirait une mesure de probabilité. Nous nous proposons dans ce chapitre de construire des mesures de probabilité sur l'espace Ω de ces configurations qui sont uniformes en un certain sens. Elles doivent :

- être ergodiques sous l'action de $\mathbb{Z} \times \mathbb{R}$ par translation,
- posséder la propriété suivante : si l'on conditionne une configuration sur un anneau, la mesure de probabilité induite à l'intérieur est la mesure uniforme.

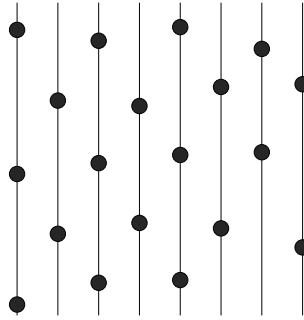


Figure 3: Un exemple de configuration de perles.

De telles mesures sont appelées des mesures de Gibbs. On prouve le théorème suivant :

Théorème 2. *À densité moyenne de perles fixée, il existe une famille $(\mathbb{P}_\gamma)_{\gamma \in]-1,1[}$ à un paramètre de mesures de Gibbs sur Ω . Pour chaque valeur de γ , $(\Omega, \mathbb{P}_\gamma)$ est un processus ponctuel déterminantal, dont la marginale sur chacun des brins est le processus déterminantal à noyau sinus.*

Idée de la démonstration:

Les mesures de Gibbs sont contruites comme limites de mesures sur des modèles de perles *discrétisés* pour lesquels les perles sont contraintes à occuper des sites d'un réseau dont on fait tendre la maille vers 0.

Le point-clé est la bijection que nous construisons entre les configurations de perles et les pavages du plan par losanges présentés plus haut : étant donné un pavage par losanges, on place une perle au centre de chaque losange de type a . La famille à deux paramètres de mesures de Gibbs sur les pavages par losanges se transporte aux configurations de perles discrétisées. Pour conserver la densité de perles lorsque la maille tend vers 0, il faut dans le modèle de pavages pénaliser les losanges horizontaux, en dirigeant fortement le champ magnétique vers le bas.

À la limite, la grandeur γ paramétrant la famille de mesures correspond à la composante horizontale du champ magnétique : en favorisant ou en pénalisant les losanges de type b par rapport à ceux de type c , elle influence la position relative d'une perle par rapport à ses deux voisins sur le fil à sa droite, comme on peut le voir sur la figure 5.2, page 75. \square

Le modèle du collier de perles décrit donc la statistique limite des losanges de type a dans un pavage aléatoire, lorsque leur densité tend vers zéro, c'est-à-dire lorsque le champ magnétique est très fortement dirigé vers le bas. En fait, il se trouve que les liens entre le modèle du collier de perles et le modèle des dimères ne sont pas limités au réseau hexagonal, comme on l'explique dans le chapitre 6.

En effet le diagramme de phase d'un modèle de dimères sur un graphe planaire bipartite bipériodique, dans l'espace des paramètres (B_x, B_y) , est représenté par l'*amibe* d'une

certaines courbes algébriques, associées au modèle. L'amibe présente sur son bord extérieur des *tentacules* qui séparent la phase liquide des différentes phases solides. Lorsque le champ magnétique tend vers l'infini, en restant dans l'une de ces tentacules, la probabilité d'apparition de certains types d'arêtes, dits *rare*s tend vers 0. Le théorème que l'on démontre dans le chapitre 6 peut être formulé de la manière suivante :

Théorème 3. *Lorsque la densité des arêtes rares tend vers 0, leur distribution est décrite à la limite par le modèle de perles.*

Idée de la démonstration:

Les corrélations entre les arêtes s'écrivent sous forme de déterminants de l'opérateur inverse de Kasteleyn K_B^{-1} , dépendant du champ magnétique. L'essentiel de la démonstration réside dans la dérivation des asymptotiques des coefficients de cet opérateur lorsque le champ magnétique s'enfonce dans une tentacule, qui fait appel de manière non triviale aux propriétés algébriques des *courbes de Harnack* dont la courbe spectrale fait partie. \square

Les corrélations déterminantales avec un noyau sinus (discret) avaient déjà été remarquées dans des cas particuliers par Johansson [21], Baik *et al.* [1]. Nous fournissons ici une méthode systématique pour obtenir des sous-ensembles d'arêtes dont les corrélations sont arbitrairement proches du processus déterminantal sinus, et ce à partir de n'importe quel modèle de dimères sur un graphe périodique planaire biparti.

Densités de motifs

Dans le chapitre 7, nous étudions la limite d'échelle de champs aléatoires construits à partir d'un modèle de dimères sur un graphe G planaire biparti et bipériodique, appelés *champs de densités de motifs*.

Ces champs fournissent une alternative au point de vue adopté précédemment dans les études par Kenyon [29, 31] et de Tilière [10] des limites d'échelle de dimères, qui utilisaient la *fonction de hauteur* dont les fluctuations à la limite sont décrites par le *champ libre sans masse* [54].

On appelle *motif* tout sous-ensemble d'arêtes de G . Si Ψ est un plongement de G dans le plan, pour tout $\varepsilon > 0$ on définit G^ε comme étant l'image de G par le plongement $\varepsilon\Psi$. G^ε représente le graphe G vu à l'échelle ε .

Étant donné un facteur d'échelle ε et un motif \mathcal{P} , on construit un champ aléatoire $N_{\mathcal{P}}^\varepsilon$ qui associe à tout domaine borné du plan D , le nombre aléatoire $N_{\mathcal{P}}^\varepsilon(D)$ de motifs observés dans une configuration de dimères aléatoire de G^ε dans la région D . Ces champs peuvent être étendus en *distributions aléatoires* en s'appliquant à des fonctions-tests φ lisses et à support compact. On s'intéresse aux fluctuations de ces distributions aléatoires autour de leurs valeurs moyennes, lorsque ε tend vers 0.

Alors que l'espérance de $N_{\mathcal{P}}^\varepsilon(\varphi)$ est de l'ordre de ε^{-2} , ses fluctuations

$$\tilde{N}_{\mathcal{P}}^\varepsilon(\varphi) = N_{\mathcal{P}}^\varepsilon(\varphi) - \mathbb{E}[N_{\mathcal{P}}^\varepsilon(\varphi)]$$

sont de l'ordre de ε^{-1} . Nous montrons que dans le cas d'une mesure de Gibbs fluide – c'est-à-dire liquide ou gazeuse – les fluctuations, correctement normalisées, convergent vers un champ aléatoire continu complètement explicite :

Théorème 4. *Pour une mesure de Gibbs fluide, $\varepsilon\tilde{N}_{\mathcal{P}}^\varepsilon$ converge faiblement, au sens des distributions, vers un champ gaussien $\mathcal{N}_{\mathcal{P}}$ dont la structure de covariance a la forme suivante*

$$\mathbb{E}[\mathcal{N}_{\mathcal{P}}(\varphi)\mathcal{N}_{\mathcal{P}}(\psi)] = \frac{1}{\pi} \int_{\mathbb{R}^2 \times \mathbb{R}^2} \partial_{\mathcal{P}^*} \varphi(u) G(u, v) \partial_{\mathcal{P}^*} \psi(v) |du| |dv| + B_{\mathcal{P}} \int_{\mathbb{R}^2} \varphi(u) \psi(u) |du|. \quad (6)$$

La fonction $G(u, v)$ est le noyau de Green sur le plan $-\frac{1}{2\pi} \log|u - v|$, et l'opérateur $\partial_{\mathcal{P}^*}$ désigne la dérivation selon un vecteur qui dépend du motif \mathcal{P} et de la mesure de Gibbs. Pour une mesure liquide et un motif formé d'une seule arête, ce vecteur coïncide avec l'image de l'arête duale par un plongement bien adapté. C'est le vecteur nul si la mesure est gazeuse, car comme les corrélations décroissent exponentiellement vite, elles ne persistent pas à la limite d'échelle.

Cette structure de covariance peut être interprétée physiquement comme l'énergie d'interaction magnétique entre deux dipôles macroscopiques, pointant dans la direction \mathcal{P}^* , soumis en plus à une interaction à courte distance pénalisant leur interpénétration. Ceci pousse donc un peu plus loin l'analogie entre dimères et dipôles déjà relevée plus haut.

Idée de la démonstration:

Bien que les arguments soient différents suivant le type de mesure et la complexité du motif, la structure de la démonstration reste la même. Dans un premier temps, on montre par l'analyse que le deuxième moment converge en utilisant notamment les asymptotiques de l'opérateur de Kasteleyn inverse K^{-1} obtenus dans [34]. Ensuite, la deuxième partie de la démonstration, plus combinatoire, consiste à vérifier à la limite la formule de Wick, donnant les moments d'un champ gaussien en fonction de sa covariance. Les raisons pour lesquelles la formule est vérifiée à la limite sont non triviales et dépendent fondamentalement des propriétés de chaque phase. \square

Dans la suite du chapitre, on étudie aussi les corrélations entre les champs de densités correspondant à différents motifs. Nous montrons que leurs corrélations sont elles-aussi données par la formule de Wick. Les résultats sont alors appliqués à deux cas particuliers : le graphe \mathbb{Z}^2 et le réseau régulier aux faces carrées et octogonales.

Chemins dénoués et l'allumeur de réverbères

Le chapitre 8 aborde un problème de combinatoire de chemins. Sur un graphe en forme d'échelle, quel est le cardinal de l'ensemble \mathcal{P}_n de chemins fermés passant un nombre pair de fois par chacun des barreaux ?

Il se trouve que cette question est liée au problème d'estimation du noyau de la chaleur pour le groupe de l'*allumeur de réverbères*. Ce groupe fait partie de la classe des groupes engendrés par des automates [19], qui est aujourd'hui un sujet très actif de la théorie des groupes. Obtenu comme le produit en couronne $\mathbb{Z}_2 \wr \mathbb{Z}$, il modélise une rue avec une infinité de lampes indexées par \mathbb{Z} , dont seulement un nombre fini est allumé, ainsi qu'un allumeur qui peut se déplacer le long de cette rue et allumer ou éteindre les réverbères devant lesquels il se trouve. Le groupe est engendré par les éléments correspondant aux trois mouvements élémentaires de l'allumeur : se déplacer d'une lampe vers la gauche, d'une lampe vers la droite, et changer l'état de la lampe devant laquelle il se tient. Dans la configuration correspondant à l'élément neutre du groupe, toutes les lampes sont éteintes et l'allumeur de réverbères se tient en face de la lampe 0.

La proportion de chemins de longueur n sur le graphe en échelle appartenant à \mathcal{P}_n donne la probabilité p_n que l'allumeur réussisse en n actions à ramener les lampes à leur état initial, et revenir à sa position de départ.

On donne une estimation asymptotique de cette probabilité :

Théorème 5.

$$p_n = \frac{|\mathcal{P}_n|}{3^n} \asymp n^{\frac{1}{6}} e^{-\left(\frac{3\pi \log 2}{2}\right)^{\frac{2}{3}} n^{\frac{1}{3}}} \quad (7)$$

où le symbole \asymp signifie que le quotient des deux membres est borné loin de 0 et de l'infini.

Ce résultat avait déjà été obtenu par Revelle [53], sous une forme légèrement plus précise, mais pour d'autres générateurs du groupe $\mathbb{Z}_2 \wr \mathbb{Z}$ et par une autre méthode que celle employée ici.

Idée de la démonstration:

Le principe de la preuve se fonde sur le fait combinatoire suivant : si on affecte des poids aux arêtes d'un graphe, on peut définir la matrice d'adjacence M du graphe qui reflète les propriétés de connectivité de celui-ci. En particulier, l'élément (i, j) de M^n est la somme des poids des chemins de longueur n allant de i à j . En combinant les contributions obtenues pour différents poids bien choisis – en l'occurrence, ici on attribue des poids ± 1 sur les barreaux et 1 ailleurs – on arrive à sélectionner uniquement la contribution des chemins qui nous intéresse. Lorsque n est grand, les asymptotiques de M^n sont données en première approximation par λ_1^n , où λ_1 est la plus grande valeur propre de M . En analysant finement la matrice pour chaque donnée de poids ± 1 , on obtient une valeur approchée de λ_1 . Ces estimations sont ensuite recombinaées pour obtenir les asymptotiques de $|\mathcal{P}_n|$. \square

Le chapitre s'ouvre ensuite sur une généralisation de ce problème en dimension 2, en faisant le lien avec les opérateurs de Schrödinger avec potentiel aléatoire. La résolution de ce problème permettrait d'évaluer la croissance du sous groupe de F_2 , le groupe libre à deux générateurs, engendré par les commutateurs de commutateurs.

1 Combinatorics of the dimer model

The goal of this chapter is to give a combinatorial presentation of the dimer model on a graph G . Following Kasteleyn [24, 25], we explain how to compute the partition function of this model in particular cases, including the case when G is planar, using the so-called *Pfaffian-Hafnian method*. We then specialize the study to the case of bipartite graphs, and discuss some aspects of the dimer model related to the homology of the graph.

1.1 Dimer configurations of a graph

Dimer configurations and partition function

Let $G = (V, E)$ be a connected graph with no multiple edge and no loop. A *dimer configuration* or *perfect matching* of G is a subset of edges $\mathcal{C} \subset E$ such that every vertex $v \in V$ is incident with exactly one edge of \mathcal{C} .

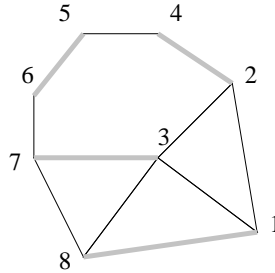


Figure 1.1: An example of a dimer configuration on a graph G .

We will always suppose in what follows that G has at least one dimer configuration. If positive weights are assigned to edges by the mean of a *weight function* $\nu : E \rightarrow \mathbb{R}^+$, then one can define the *weight of a dimer configuration* \mathcal{C} as

$$\nu(\mathcal{C}) = \prod_{e \in \mathcal{C}} \nu_e$$

These weights on dimer configurations can be used to define a *Boltzmann probability measure* on the set of all dimer configurations: the probability that the random dimer configuration \mathcal{C}_ω is equal to a given configuration \mathcal{C}_0 is given by

$$\mathbb{P}[\mathcal{C}_\omega = \mathcal{C}_0] = \frac{\nu(\mathcal{C}_0)}{Z(G, \nu)}$$

where the normalizing coefficient $Z(G, \nu)$ equals the sum of the weights of all the dimer configurations of G

$$Z(G, \nu) = \sum_{\mathcal{C}} \nu(\mathcal{C}) = \sum_{\mathcal{C}} \prod_{\mathbf{e} \in \mathcal{C}} \nu_{\mathbf{e}}.$$

$Z(G, \nu)$ is called the *partition function*.

In fact, the role played by the partition function in the dimer model — and in every statistical mechanical model in general — is much greater than just the role of a normalizing constant. Notice that

$$\nu_{\mathbf{e}} \frac{\partial \nu(\mathcal{C})}{\partial \nu_{\mathbf{e}}}$$

is equal to $\nu(\mathcal{C})$ if the edge \mathbf{e} belongs to \mathcal{C} , and 0 if not. Therefore,

$$\nu_{\mathbf{e}} \frac{\partial Z(G, \nu)}{\partial \nu_{\mathbf{e}}}$$

is the sum of the weights of the dimer configurations containing the edge \mathbf{e} . Hence, the probability of seeing the edge \mathbf{e} in the random configuration is given by

$$\mathbb{P}[\mathbf{e} \in \mathcal{C}_{\omega}] = \frac{\nu_{\mathbf{e}}}{Z(G, \nu)} \frac{\partial Z(G, \nu)}{\partial \nu_{\mathbf{e}}} = \frac{\partial \log Z(G, \nu)}{\partial \log \nu_{\mathbf{e}}}.$$

More generally, the probability of seeing k edges $\mathbf{e}_1, \dots, \mathbf{e}_k$ is given by the following formula

$$\mathbb{P}[\mathbf{e}_1, \dots, \mathbf{e}_k \in \mathcal{C}_{\omega}] = \frac{\nu_{\mathbf{e}_1} \cdots \nu_{\mathbf{e}_k}}{Z(G, \nu)} \frac{\partial^k Z(G, \nu)}{\partial \nu_{\mathbf{e}_1} \cdots \partial \nu_{\mathbf{e}_k}}.$$

As the elementary events “ $\mathbf{e} \in \mathcal{C}_{\omega}$ ” generate the algebra of all events, the probability of any event can be expressed in terms of derivatives of $Z(G, \nu)$. Therefore, the partition function plays the role of a generating function for the Boltzmann probability measure.

Dimer configurations as tilings

If the graph G is embedded on an orientable compact surface Σ , one can give a dual description of dimer configurations of G in terms of tilings of Σ . The embedding of G on Σ induces a cellular decomposition D of Σ . One can define a dual cellular decomposition¹ D^* of Σ : the dual vertices correspond to faces of D , and there is a dual edge between two dual vertices if the corresponding faces in D share an edge. The vertices v of D correspond to the dual faces v^* of D^* . To an edge $\mathbf{e} = (v_1, v_2)$ of G is associated a compact domain $T_{\mathbf{e}} = v_1^* \cup v_2^*$ of Σ . The fact that in a dimer configuration \mathcal{C} every vertex is incident with exactly one edge implies that $(T_{\mathbf{e}})_{\mathbf{e} \in \mathcal{C}}$ satisfies

$$\forall \mathbf{e}, \mathbf{e}' \in \mathcal{C}, \quad T_{\mathbf{e}} \cap T_{\mathbf{e}'} = \emptyset \quad (1.1)$$

$$\bigcup_{\mathbf{e} \in \mathcal{C}} T_{\mathbf{e}} = \Sigma \quad (1.2)$$

¹This dual cellular decomposition is not unique.

1. Combinatorics of the dimer model

and hence $(T_e)_{e \in \mathcal{C}}$ is a tiling of Σ . Reciprocally, if a subset \mathcal{C} of edges is such that $(T_e)_{e \in \mathcal{C}}$ is a tiling of Σ , then \mathcal{C} is a dimer configuration of G . Dimer models can be seen as particular cases of random tiling models. Two cases are particularly important:

- Dimer configurations of a piece of the square grid \mathbb{Z}^2 are dual to tilings with 2×1 rectangles, also known as *dominos*.
- Dimer configurations of a piece of the honeycomb lattice H are dual to tilings with rhombi with a 60° angle, also known as *lozenges*.

When these dimer models are discussed as examples, it will be useful to have in mind their dual interpretation.

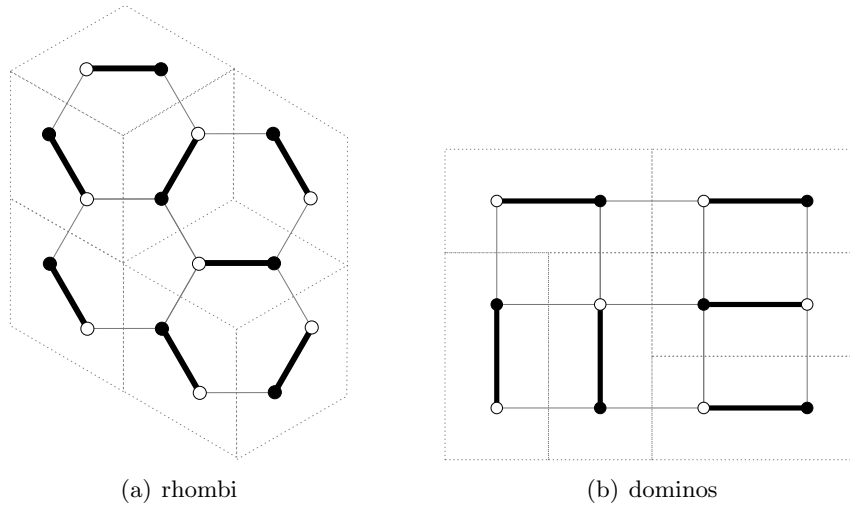


Figure 1.2: Two examples of dimer configurations on bipartite graphs and the corresponding tilings.

1.2 The dimer model on planar graphs

In this section we explain how to compute the partition function of the dimer model on a planar graph. A *planar graph* is a graph that can be embedded on the plane. This means that one can draw the graph on a sheet of paper in such a way that no edge intersects another edge.

A dimer configuration of G is a particular case of a partition of the set of its vertices into parts of length 2. An obvious necessary condition for G to have a perfect matching is to have an even number, say $2n$, of vertices.

For instance, the dimer configuration represented in figure 1.1 corresponds to the partition

$$\{\{i_1, j_1\}, \dots, \{i_n, j_n\}\} = \{\{1, 8\}, \{2, 4\}, \{3, 7\}, \{5, 6\}\}.$$

Such a partition can be conveniently encoded by a permutation of \mathfrak{S}_{2n} with the two following constraints:

$$\begin{aligned} \forall k \in \{1, \dots, n\} \quad \sigma(2k-1) < \sigma(2k) \\ \forall k \in \{1, \dots, n-1\} \quad \sigma(2k-1) < \sigma(2k+1). \end{aligned}$$

The images of two successive integers $\sigma(2k-1)$ and $\sigma(2k)$ correspond to a component of the partition. The permutation encoding the dimer configuration of figure 1.1 is

$$\sigma = \begin{pmatrix} 1 & 2 & \cdots & 2n-1 & 2n \\ i_1 & j_1 & \cdots & i_n & j_n \end{pmatrix} = \begin{pmatrix} 1 & 2 & 3 & 4 & 5 & 6 & 7 & 8 \\ 1 & 8 & 2 & 4 & 3 & 7 & 5 & 6 \end{pmatrix}.$$

This point of view yields a new expression for the partition function

$$Z(G, \nu) = \sum_{\sigma}' A_{\sigma(1), \sigma(2)} \cdots A_{\sigma(2n-1), \sigma(2n)}.$$

where the sum is performed over the partitions with the restrictions indicated above and $A_{i,j}$ is equal to $\nu_{\mathbf{e}}$ if i and j are the ends of the edge \mathbf{e} , and is 0 if not. This expression is sometimes called the *Hafnian* of the matrix A .

Given an orientation of G , the weighted adjacency matrix \mathcal{K} is defined as follows: if the edge \mathbf{e} is oriented from vertex i to vertex j , then

$$\mathcal{K}_{i,j} = \nu_{\mathbf{e}} \quad \text{and} \quad \mathcal{K}_{j,i} = -\nu_{\mathbf{e}}.$$

If there is no edge between i and j , then $\mathcal{K}_{i,j} = 0$. The partition function, expressed in terms of the matrix \mathcal{K} as

$$Z(G, \nu) = \sum_{\sigma}' |\mathcal{K}_{\sigma(1), \sigma(2)} \cdots \mathcal{K}_{\sigma(2n-1), \sigma(2n)}|$$

is very similar to the *Pfaffian* of \mathcal{K} defined by the following formula

$$\text{Pfaff } \mathcal{K} = \sum_{\sigma}' \text{sgn}(\sigma) \mathcal{K}_{\sigma(1), \sigma(2)} \cdots \mathcal{K}_{\sigma(2n-1), \sigma(2n)}. \quad (1.3)$$

The Pfaffian of a matrix is much easier to compute than the Hafnian. In particular, it is a square root of the determinant. If there exists an orientation for which all the terms in the sum defining the Pfaffian have the same sign, then the partition function is equal to the Pfaffian of the adjacency matrix \mathcal{K} for this orientation, up to a global sign

$$Z(G, \nu) = |\text{Pfaff } \mathcal{K}|. \quad (1.4)$$

An orientation for which equation (1.4) is satisfied is called an *admissible orientation* or *Pfaffian orientation*, and the corresponding adjacency matrix \mathcal{K} is called the *Kasteleyn matrix*.

Kasteleyn proved that if the graph G is planar, then there exists an admissible orientation. Such an orientation is given by the *odd clockwise rule*: around every face, the number of edges oriented clockwise is odd.

The reason why the odd clockwise rule gives an admissible orientation is the following: if we superimpose two dimer configurations \mathcal{C} and \mathcal{C}' encoded by permutations σ and σ' respectively, then we see a collection of cycles of even length and double edges, representing graphically the decomposition in cycles of the permutation $\sigma' \circ \sigma^{-1}$, the double edges corresponding to the fixed points of this permutation. Consider one of these nontrivial cycles. Its length is even and, up to reindexation of the vertices of G , we can suppose that the vertices of this cycles are labelled from 1 to $2m$ counterclockwise. It is formed by edges $(1, 2), \dots, (2m-1, 2m)$ from \mathcal{C} and edges $(1, 2m), (2, 3), \dots, (2m-2, 2m-1)$ from \mathcal{C}' , and represents thus an even cycle of $\sigma' \circ \sigma^{-1}$. Besides, the odd-clockwise rule is preserved by deletion of edges, so the number of edges oriented clockwise is odd along any cycle of G , and in particular, the one we consider. Consequently, the number of edges with negative orientation among $(1, 2), \dots, (2m-1, 2m)$ has the same parity as the number of edges with negative orientation among $(1, 2m), (2, 3), \dots, (2m-2, 2m-1)$. It follows that the contribution of each of these cycles in $\text{sgn}(\sigma) \prod_j \mathcal{K}_{j, \sigma(j)}$ and $\text{sgn}(\sigma') \prod_j \mathcal{K}_{j, \sigma'(j)}$ have the same parity, and therefore, all the terms in the sum (1.3) have the same sign.

Let us now explain how to compute probabilities with Pfaffians in the dimer model on the planar graph G . Let $\mathbf{e}_1 = (v_1, w_1), \dots, \mathbf{e}_k = (v_k, w_k)$ be k disjoint edges of G . The graph \tilde{G} obtained from G by removing the edges $\mathbf{e}_1, \dots, \mathbf{e}_k$ has an admissible orientation that is induced by that of G . Therefore the Pfaffian of the matrix $\tilde{\mathcal{K}}$ obtained from \mathcal{K} by deleting rows and columns corresponding to the vertices v_i, w_i represents the partition function of the dimer model on \tilde{G} (which can be zero). The following expression

$$\nu_{\mathbf{e}_1} \cdots \nu_{\mathbf{e}_k} |\text{Pfaff } \tilde{\mathcal{K}}|$$

is then the sum of the weights of the dimer configurations of G containing the edges $\mathbf{e}_1, \dots, \mathbf{e}_k$. The probability of seeing $\mathbf{e}_1, \dots, \mathbf{e}_k$ in a random dimer configuration of G is thus given by

$$\mathbb{P}[\mathbf{e}_1, \dots, \mathbf{e}_k] = \nu_{\mathbf{e}_1} \cdots \nu_{\mathbf{e}_k} \frac{|\text{Pfaff } \tilde{\mathcal{K}}|}{|\text{Pfaff } \mathcal{K}|}.$$

what can be rewritten, using the correspondance between Pfaffians of submatrices \mathcal{K} and that of \mathcal{K}^{-1} , as

$$\mathbb{P}[\mathbf{e}_1, \dots, \mathbf{e}_k] = \nu_{\mathbf{e}_1} \cdots \nu_{\mathbf{e}_k} |\text{Pfaff}(\mathcal{K}^{-1})_{\mathbf{e}_1 \dots \mathbf{e}_k}|$$

where $(\mathcal{K}^{-1})_{\mathbf{e}_1 \dots \mathbf{e}_k}$ is the restriction of \mathcal{K}^{-1} to the vertices v_i, w_i .

In general, if the graph is drawn on an orientable surface of genus $g \geq 1$, the situation is more complicated: some cycles are not homotopic to zero, and the odd-clockwise rule does not work directly any more, and some terms in (1.3) come with the wrong sign. However, the partition function can be written as a linear combination of 4^g Pfaffians obtained from different orientations [61, 11].

1.3 The dimer model on bipartite graphs

In this section, we assume that the graph G is bipartite, *i.e.* that we can color the vertices of G in black and white such that any two adjacent vertices have different colors. Since an edge links a white vertex with a black vertex, an obvious necessary condition for G to have a dimer condition is to have the same number, say n , of white and black vertices.

If the vertices of G are labelled in such a way that in the Kasteleyn matrix, the first n lines and columns refer to white vertices and the last n to black vertices, then \mathcal{K} has the following form

$$\mathcal{K} = \left(\begin{array}{c|c} 0 & \mathbf{K}_{\bullet \rightarrow \circ} \\ \hline \mathbf{K}_{\circ \rightarrow \bullet} & 0 \end{array} \right)$$

where

$$\mathbf{K}_{\bullet \rightarrow \circ} : \mathbb{C}^{\text{black vertices}} \rightarrow \mathbb{C}^{\text{white vertices}}$$

acts on functions defined on black vertices and $\mathbf{K}_{\circ \rightarrow \bullet}$ is the transpose of $-\mathbf{K}_{\bullet \rightarrow \circ}$. For simplicity, we will denote the operator $\mathbf{K}_{\bullet \rightarrow \circ}$ simply by \mathbf{K} . In this particular context, a dimer configuration can be encoded by a permutation $\sigma \in \mathfrak{S}_n$. For all $i \in \{1, \dots, n\}$, $\sigma(i)$ is the label of the black vertex with which \mathbf{w}_i is incident in the configuration represented by σ .

The partition function of the dimer model can be expressed only in terms of \mathbf{K}

$$Z(G, \nu) = \sum_{\sigma \in \mathfrak{S}_n} |\mathbf{K}(\mathbf{w}_1, \mathbf{b}_{\sigma(1)}) \cdots \mathbf{K}(\mathbf{w}_n, \mathbf{b}_{\sigma(n)})|$$

Like in the previous section, a simpler expression for Z can be given if G is planar, *i.e.* if it can be embedded in the plane, whereas the situation is more intricate if G can only be embedded on surfaces of higher genus.

If G is planar, and more generally if it admits a Pfaffian orientation, then the partition function is, up to a sign, the determinant of \mathbf{K}

$$Z(G, \nu) = |\det \mathbf{K}|.$$

The odd-clockwise rule in this particular case introduces minus signs in the matrix \mathbf{K} when comparing with the natural orientation of the edges of G (from white to black vertices). The number of minus signs around a face is even if the face is bordered by $2 \bmod 4$ edges, and odd if it is bordered by $0 \bmod 4$. Thanks to correspondance between determinants of submatrices of \mathbf{K} and that of \mathbf{K}^{-1} , the probability of seeing k edges $\mathbf{e}_1 = (\mathbf{w}_1, \mathbf{b}_1), \dots, \mathbf{e}_k = (\mathbf{w}_k, \mathbf{b}_k)$ in a random configuration is given by a determinant of a submatrix of \mathbf{K}^{-1} of size k :

$$\mathbb{P}[\mathbf{e}_1, \dots, \mathbf{e}_k \in \mathcal{C}] = \left(\prod_{j=1}^k \nu_{\mathbf{e}_j} \right) \det[\mathbf{K}^{-1}(\mathbf{b}_i, \mathbf{w}_j)] = \det[\nu_{\mathbf{e}_j} \mathbf{K}^{-1}(\mathbf{b}_i, \mathbf{w}_j)]. \quad (1.5)$$

Using multilinearity of the determinant and an inclusion-argument argument, one can also express as a determinant the probability of the following events:

$$\begin{aligned} & \mathbb{P} [\mathbf{e}_1, \dots, \mathbf{e}_k \notin \mathcal{C} ; \mathbf{e}_{k+1}, \dots, \mathbf{e}_{k+l} \in \mathcal{C}] \\ &= \det \left(\left[\begin{array}{c|c} \mathbb{1}_k & \\ \hline & \mathbb{0}_l \end{array} \right] + \left[\begin{array}{c|c} -\nu_{\mathbf{e}_j} \mathbf{K}^{-1}(\mathbf{b}_i, \mathbf{w}_j) & -\nu_{\mathbf{e}_j} \mathbf{K}^{-1}(\mathbf{b}_i, \mathbf{w}_j) \\ \hline \nu_{\mathbf{e}_j} \mathbf{K}^{-1}(\mathbf{b}_i, \mathbf{w}_j) & \nu_{\mathbf{e}_j} \mathbf{K}^{-1}(\mathbf{b}_i, \mathbf{w}_j) \end{array} \right] \right) \end{aligned} \quad (1.6)$$

where the diagonal square blocks of the matrices have size k and l . $\mathbb{1}_k$ and $\mathbb{0}_l$ are the identity matrix of size k and the null matrix of size l .

The superposition of two dimer configurations of the planar graph G is a collection of cycles and double edges. One can pass from one configuration to another by performing a succession of elementary operations [51], reducing gradually the length of the non-trivial cycles. If G is not planar but can be embedded on a torus, the situation is different: in such a superposition, some of the cycles are not homotopic to zero. There are in fact four equivalence classes of dimer configurations, coinciding with the homology class in $H_1(\mathbb{T}^2, \mathbb{Z}/2\mathbb{Z})$ of the collection of cycles obtained from the superimposition with a reference dimer configuration \mathcal{C}_0 , *i.e.* the horizontal and vertical winding number of this collection of cycles modulo 2. Let \mathbf{K} be a Kasteleyn matrix as above. Configurations in different classes give terms with different signs in $\det \mathbf{K}$. One can chose properly the orientation so that the class $(0, 0)$ give positive terms and the others negative terms. Let γ_x and γ_y , and denote by $\mathbf{K}^{(\theta\tau)}$ the matrix obtained from \mathbf{K} by multiplying the entries corresponding to edges crossing γ_x (resp. γ_y) by $(-1)^\theta$ (resp. by $(-1)^\tau$). The expression of the partition function is given by the following linear combination:

$$Z = \frac{1}{2} (-Z^{(00)} + Z^{(01)} + Z^{(10)} + Z^{(11)}) \quad (1.7)$$

where $Z^{(\theta\tau)} = \det \mathbf{K}^{(\theta\tau)}$. The expression for the probability of seeing $\mathbf{e}_1, \dots, \mathbf{e}_k$ in a random dimer configuration of G is

$$\begin{aligned} \mathbb{P} [\mathbf{e}_1, \dots, \mathbf{e}_k] &= \left(\prod_{l=1}^k \mathbf{K}_{\mathbf{w}_l \mathbf{b}_l} \right) \times \frac{1}{2} \left(-\frac{Z^{(00)}}{Z} \det(\mathbf{K}^{(00)})_{\mathbf{b}_i, \mathbf{w}_j}^{-1} + \right. \\ & \left. \frac{Z^{(10)}}{Z} \det(\mathbf{K}^{(10)})_{\mathbf{b}_i, \mathbf{w}_j}^{-1} + \frac{Z^{(01)}}{Z} \det(\mathbf{K}^{(01)})_{\mathbf{b}_i, \mathbf{w}_j}^{-1} + \frac{Z^{(11)}}{Z} \det(\mathbf{K}^{(11)})_{\mathbf{b}_i, \mathbf{w}_j}^{-1} \right) \end{aligned} \quad (1.8)$$

where $\mathbf{e}_j = (\mathbf{w}_j, \mathbf{b}_j)$.

1.4 Dimers on bipartite graphs and flows

In the case of a bipartite graph, interesting interpretations of a dimer configuration can be given in terms of flows.

1.4.1 Forms on a graph embedded in an orientable surface

The embedding of G in an orientable compact closed surface Σ yields a cellular decomposition of Σ . For $k \in \{0, 1, 2\}$, a k -chain is a formal combination of oriented k -cells with integer coefficients, and a k -form is a function on k -chains. Let $\Omega^k(G)$ be the linear space of the k -forms². The coupling between k -chains and k -forms will be denoted by the integral sign.

The spaces $\Omega^k(G)$ come with the standard exterior derivative d , the adjoint of the border operator ∂ on chains: if f is a 0-form and \mathbf{e} is an oriented edge from v to w , then

$$\int_{\mathbf{e}} df = d f(\mathbf{e}) = f(\partial \mathbf{e}) = f(v) - f(w).$$

Similarly, if α is a 1-form and \mathbf{f} is a positively oriented face, bordered by edges $\mathbf{e}_1, \dots, \mathbf{e}_m$ oriented counterclockwise, then

$$\iint_{\mathbf{f}} d\alpha = \oint_{\partial \mathbf{f}} \alpha = \sum_{i=1}^m \int_{\mathbf{e}_i} \alpha.$$

Finally, the derivative $d\omega$ of a 2-form ω is 0.

One can associate to the graph G embedded in Σ a dual graph G^* embedded in Σ . The vertices of G^* are the faces of G and there is an edge \mathbf{e}^* between f_1^* and f_2^* of G^* if the two corresponding faces of G , f_1 and f_2 , share an edge \mathbf{e} . The faces of G^* are associated to vertices of G . This duality extends to oriented chains: an orientation of \mathbf{e} induces an orientation of \mathbf{e}^* so that $(\mathbf{e}, \mathbf{e}^*)$ is a direct frame. Note that for 0-chains and 2-chains, the duality operator is an involution

$$(v^*)^* = v \quad (\mathbf{f}^*)^* = \mathbf{f},$$

whereas it is an anti-involution on 1-chains

$$(\mathbf{e}^*)^* = -\mathbf{e}.$$

This $*$ -operator induces a bijection between $\Omega^k(G)$ and $\Omega^{2-k}(G^*)$ for $k \in \{0, 1, 2\}$, also noted by $*$. For any k -chain γ and any k -form α ,

$$*\alpha(\gamma) = (-1)^k \alpha(\gamma^*)$$

²Note that whereas $\Omega^0(G), C_0(G), \Omega^1(G)$ and $C_1(G)$ depend only on the structure of the graph G , the spaces $\Omega^2(G)$ and $C_2(G)$ depends strongly on the embedding in the surface Σ , since it is the embedding that defines the faces of G .

1.4.2 Unit white-to-black flows and height function

A dimer configuration \mathcal{C} defines a *unit white-to-black flow* ω , i.e a flow with divergence $+1$ at every white vertex, and -1 at every black vertex: the amount of flow $\int_{\mathbf{e}} \omega$ in the edge \mathbf{e} equals 1 if \mathbf{e} belongs to \mathcal{C} , and 0 if not.

Let \mathcal{C}_0 be a reference dimer configuration of G with flow ω_0 . For any dimer configuration \mathcal{C} with flow ω , The difference $\omega - \omega_0$ is a *divergence-free* flow: its dual is a closed 1-form.

- If the surface in which the graph is embedded is a sphere, then the dual closed form is *exact*: there exists a function on faces of G , $h \in \Omega^2(G)$, such that the flux of $\omega - \omega_0$ across any dual 1-chain γ from face \mathbf{f}_1 to face \mathbf{f}_2 is

$$\int_{\gamma} *(\omega - \omega_0) = h(\mathbf{f}_2) - h(\mathbf{f}_1).$$

This function h is called the *height function*.

- If the graph G is embedded in a torus, the form $*(\omega - \omega_0)$ is not always exact. If γ_x and γ_y are dual paths with respective homology class $(1, 0)$ and $(0, 1)$, then $*(\omega - \omega_0)$ can have periods along these paths: after m horizontal and n vertical winds, the change in height is

$$\oint_{m\gamma_x + n\gamma_y} *(\omega - \omega_0) = mh_x + nh_y.$$

(h_x, h_y) is called the *height change* of \mathcal{C} . It is an element of \mathbb{Z}^2 , and can be identified with the homology class in $H_1(\mathbb{T}^2, \mathbb{Z})$ of the flow $\omega - \omega_0$.

1.4.3 Gauge transformation and magnetic field

The edges of the bipartite graph G have a natural orientation: from their white end to their black end. The functions on edges can be identify with the 1-forms of G . Similarly, we identify the functions on the vertices and on the faces of G with the elements of $\Omega^0(G)$ and $\Omega^2(G)$ respectively.

Define the *energy* \mathcal{E} as the logarithm of the weight function ν

$$\mathcal{E} = -\log \nu.$$

If a dimer configuration is identified with the sum of the edges it contains, the energy of a configuration is given by

$$\mathcal{E}(\mathcal{C}) = \int_{\mathcal{C}} \mathcal{E} = \sum_{\mathbf{e} \in \mathcal{C}} \int_{\mathbf{e}} \mathcal{E}.$$

When superposing two dimer configurations \mathcal{C}_1 and \mathcal{C}_2 , one sees double edges and a union of cycles γ_j . The difference of energy between the two configurations is therefore the (alternate) sum of the energy of edges of each cycle γ_j

$$\mathcal{E}(\mathcal{C}_1) - \mathcal{E}(\mathcal{C}_2) = \sum_j \oint_{\gamma_j} \mathcal{E}.$$

The relative weights of dimer configurations are determined by the flux of energy through cycles $\oint_{\gamma} \mathcal{E}$. In particular, adding to the energy the derivative df of a 0-form, *i.e.* replacing the energy of an edge $\mathbf{e} = (\mathbf{w}, \mathbf{b})$ by

$$\int_{\mathbf{e}} \mathcal{E} + df = \mathcal{E}(\mathbf{e}) + f(\mathbf{w}) - f(\mathbf{b})$$

will not affect the Boltzmann probability measure. Such a transformation is called a *gauge transformation*.

- When the graph G is planar, the set of gauge equivalence classes is parameterized \mathbb{R}^{F-1} , where F is the number of faces of G : An equivalence class $[\mathcal{E}]$ is represented by the element $d\mathcal{E} \in \Omega^2(G) \simeq \mathbb{R}^F$ giving the flux of energy through faces, and subject to the relation that the sum of all the fluxes is zero. Following [34], we will refer to the element $d\mathcal{E} \in \Omega^2(G)$ as B_z .
- When the graph is embedded in a torus, the situation is different for topological reasons. The set of gauge equivalence classes is parameterized by $\mathbb{R}^{F-1} \oplus \mathbb{R}^2$: in addition to the previous fluxes through the faces of G , there are also the fluxes through the non trivial cycles γ_x and γ_y , that are controlled by the last two parameters, B_x and B_y . B_x represents an extra energy that is added (resp. subtracted) to edges crossing γ_x from left to right (resp. from right to left). Similarly, B_y is the amount of energy that is added (resp. subtracted) to edges crossing γ_y from left to right (resp. from right to left). Modifying the magnetic field B by

$$B' = B + (0, \Delta B_x, \Delta B_y)$$

will affect the energy of a configuration \mathcal{C} . The change in energy depends linearly in the magnetic modification through the height change (h_x, h_y) of the configuration:

$$\mathcal{E}_{B'}(\mathcal{C}) - \mathcal{E}_{B'}(\mathcal{C}_0) = \mathcal{E}_B(\mathcal{C}) - \mathcal{E}_B(\mathcal{C}_0) + \Delta B_x h_x + \Delta B_y h_y \quad (1.9)$$

This influence of the magnetic field on the relative weight of a configuration through its height change will be used in the next chapter to classify the translation invariant probability measures on dimer configurations of a planar \mathbb{Z}^2 periodic graph.

2 Dimers and Amoebæ

The title of this chapter is borrowed from an article written by Kenyon, Okounkov and Sheffield [34]. In that article, the authors describe the set of all translation invariant Gibbs measures for the dimer model of a planar bipartite periodic graph, as well as its phase diagram. That is what we propose to explain in this chapter.

Let G be a bipartite \mathbb{Z}^2 -periodic planar graph: the vertices of G are colored in black and white such that any two adjacent vertices have different colors, and \mathbb{Z}^2 acts on G by color-preserving translations. For a chain α and $\mathfrak{x} \in \mathbb{Z}^2$, we will denote by $\alpha_{\mathfrak{x}}$ the image of α by the translation of \mathfrak{x} . We denote also by G_n the quotient of G by the action of $(n\mathbb{Z})^2$.

Fix a white-to-black unit flow ω_0 on G_1 . This flow can be lifted to any G_n and to G and will serve as a reference flow to define the height function. We will suppose that this flow corresponds to a dimer configuration \mathcal{C}_0 of G_1 .

Let \mathcal{E} be an energy function on edges of G_1 , which defines also a periodic energy function on edges of G_n and G . We define like in the previous chapter a probability measure μ_n on the set $\mathcal{M}(G_n)$ of dimer configurations of G_n by the formula

$$\forall \mathcal{C} \in \mathcal{M}(G_n) \quad \mu_n(\mathcal{C}) = \frac{e^{-\mathcal{E}(\mathcal{C})}}{Z(G_n, \mathcal{E})}$$

The graphs G_n are naturally embedded in a torus, and therefore dimer configurations on G_n have a height change. For a fixed $(s, t) \in \mathbb{R}^2$, we also define $\mathcal{M}_{s,t}(G_n)$ be the set of dimer configurations of G_n with a height change $([ns], [nt])$ and $\mu_n(s, t)$ be the conditional measure induced by μ_n on $\mathcal{M}_{s,t}(G_n)$.

2.1 Gibbs measures on dimer configurations

Since G is an infinite graph, the notion of Boltzmann measure as presented in the previous chapter cannot be applied here. It is replaced by the notion of Gibbs measure, which is a natural extension of it:

Definition 2.1. A probability measure μ on dimer configurations of G is a *Gibbs measure* if it has the property that if we fix the matching in an annular region, the dimer configurations outside and inside the region are independent, and the probability of any interior matching is proportionnal to the weight of this matching. Moreover, if μ is invariant and ergodic under the action of \mathbb{Z}^2 , then μ is said to be an *ergodic Gibbs measure* (EGM).

For an EGM μ , let $s = \mathbb{E} [h(\mathbf{f}_{(1,0)}) - h(\mathbf{f})]$ and $t = \mathbb{E} [h(\mathbf{f}_{(0,1)}) - h(\mathbf{f})]$ be respectively the expected horizontal and vertical height changes. (s, t) is called the *slope* of μ . Sheffield proved in [55] a theorem about unicity of ergodic Gibbs measures

Theorem 2.1 ([55]). *For each (s, t) for which $\mathcal{M}_{s,t}(G_n)$ is non empty for n sufficiently large, $\mu_n(s, t)$ converges as n goes to $+\infty$ to a EGM $\mu(s, t)$ of slope (s, t) . Moreover, μ_n itself converges to a EGM $\mu(s_0, t_0)$, where (s_0, t_0) is the limit of the slopes of μ_n .*

If (s_0, t_0) lies in the interior of the set of (s, t) for which $\mathcal{M}_{s,t}(G_n)$ is non empty for n sufficiently large, then every EGM of slope (s, t) is of the form $\mu(s, t)$ as above: that is $\mu(s, t)$ is the unique EGM of slope (s, t) .

The *surface tension* or *free energy* per fundamental domain of a measure $\mu(s, t)$ is defined to be the following limit

$$\sigma(s, t) = -\frac{1}{n^2} \log \sum_{\mathcal{C} \in \mathcal{M}_{s,t}(G_n)} e^{-\mathcal{E}(\mathcal{C})}. \quad (2.1)$$

This quantity describes how fast the number of dimer configurations of a given slope grows with n . The slope of the measure $\mu(s_0, t_0)$ is the slope that realizes the minimum of σ . The minimum is unique since the surface tension σ is strictly convex [55].

2.2 Spectral curve and related objects

Since the weights on G are periodic, a Kasteleyn operator on G can be defined by lifting that of the finite graph G_1 .

The Kasteleyn operator K commutes with the translation action of \mathbb{Z}^2 . In particular, it preserves the \mathbb{Z}^2 -eigenspaces, that are indexed by multipliers $(z, w) \in (\mathbb{C}^*)^2$. These eigenspaces are finite-dimensional, and a basis (δ_v) is given by the functions supported on a single \mathbb{Z}^2 -orbit, and taking value 1 on a vertex v inside a fixed fundamental domain. Let $K(z, w)$ be the matrix of the restriction of K to the \mathbb{Z}^2 -eigenspace indexed by (z, w) in the basis (δ_v) .

This matrix can also be viewed as the *magnetically altered* Kasteleyn operator of the graph G_1 , that is a Kasteleyn operator for weights modified as follows: let γ_x and γ_y be dual paths in G_1 avoiding edges of \mathcal{C}_0 , with respective homology class $(1, 0)$ and $(0, 1)$, and whose lifts delimit the fundamental domain of G . The weight of an edge crossing γ_x from left to right (resp. from right to left) is multiplied by z (resp. by z^{-1}). The weight of an edge crossing γ_y from left to right (resp. from right to left) is multiplied by w (resp. by w^{-1}).

The polynomial

$$P(z, w) = \det K(z, w)$$

is called the *characteristic polynomial* of the graph G . The *spectral curve* is the locus of the zeros of P in $(\mathbb{C}^*)^2$. The partition function of the dimer model on G_1 in presence of a

magnetic field (B_x, B_y) , given by formula (1.7), is expressed in terms of the characteristic polynomial P :

$$Z(G_1) = \frac{1}{2}(-P(e^{B_x}, e^{B_y}) + P(-e^{B_x}, e^{B_y}) + P(e^{B_x}, -e^{B_y}) + P(-e^{B_x}, -e^{B_y})) \quad (2.2)$$

The *Newton polygon* $N(P)$ of the polynomial P is the convex hull in \mathbb{R}^2 of the set of integer exponents of monomials in P

$$N(P) = \text{Conv} \left\{ (j, k) \in \mathbb{Z}^2 \mid z^j w^k \text{ is a monomial in } P(z, w) \right\}.$$

The interest of the Newton polygon in the dimer context is given by the following proposition:

Proposition 2.1 ([34]). *$N(P)$ is the set of all possible slopes for an EGM on dimer configurations of G .*

A choice of another reference configuration \mathcal{C}_0 will lead to another characteristic polynomial, differing from P just by a multiplicative term of the form $z^k w^l$, whose Newton polygon is obtained from $N(P)$ by a translation. The spectral curve is invariant by this modification.

The *amœba* $A(P)$ of the polynomial P is the image of the curve $P(z, w) = 0$ by the application

$$\begin{aligned} \text{Log} : (\mathbb{C}^*)^2 &\rightarrow \mathbb{R}^2 \\ (z, w) &\mapsto (\log |z|, \log |w|). \end{aligned}$$

A related object is the *Ronkin function* $F(x, y)$ of the polynomial P , defined by the following integral

$$F(x, y) = \iint_{\substack{|z|=e^x \\ |w|=e^y}} \log P(z, w) \frac{dz}{2i\pi z} \frac{dw}{2i\pi w} \quad (2.3)$$

These objects coming from algebraic geometry have a direct probabilistic interpretation, as we will see in the following sections. It is important to note that the integral in (2.3) is singular if and only if $(x, y) \in A(P)$. The Ronkin function is linear over each component of the amœba's complement, and strictly convex over the interior of the amœba [40].

The locus of the zeros of P define an algebraic curve in \mathbb{C}^2 of a very special kind. More precisely, it is a *Harnack curve*. The consequences of this algebraic fact will be explained in section 2.4.

2.3 Changing the magnetic field and computing...

Theorem 2.1 states that the set of EGMs for a given periodic energy function \mathcal{E} on the \mathbb{Z}^2 -periodic graph G is a two-parameter family. To obtain one of these measures, instead

of taking limits of the conditioned measures $\mu_n(s, t)$, one can fix a value (B_x, B_y) for the magnetic field, and take the limit of the Boltzmann measures on $\mathcal{M}(G_n)$ for the *magnetically modified weights*: let $\tilde{\gamma}_x^n$ be a lift of $n \cdot \gamma_x$ to G_n and $\tilde{\gamma}_y^n$ a lift of $n \cdot \gamma_y$. Multiply the weight of an edge of G_n crossing $\tilde{\gamma}_x^n$ (resp. of $\tilde{\gamma}_y^n$) to by $e^{\pm n B_x}$ (resp. by $e^{\pm n B_y}$) according to its orientation.

Let $K_{n,B}$ be a Kasteleyn operator on G_n for these weights.

2.3.1 ... the partition function

The partition function of the dimer model on G_n for these weights can be computed from formula (1.7).

$$Z(G_n, B) = \frac{1}{2} \left(-\det K_{n,B}^{(00)} + \det K_{n,B}^{(01)} + \det K_{n,B}^{(10)} + \det K_{n,B}^{(11)} \right) \quad (2.4)$$

where $K_{n,B}^{(\theta\tau)}$ are the four modifications of $K_{n,B}$ where the entries of $K_{n,B}$ corresponding to edges crossing $\tilde{\gamma}_x^n$ (resp. $\tilde{\gamma}_y^n$) are multiplied by $(-1)^\theta$ (resp. by $(-1)^\tau$). Using the action of $(\mathbb{Z}/n\mathbb{Z})^2$ by translation, the operators $K_{n,B}^{(\theta\tau)}$ can be diagonalized by blocks by discrete Fourier transform: the diagonal blocks are of the form $K(\zeta, \xi)$ where ζ and ξ are n th roots of $(-1)^\tau e^{n B_x}$ and $(-1)^\theta e^{n B_y}$ respectively. The different determinants can be computed in terms of P :

$$\det K_{n,B}^{\theta\tau} = \prod_{\substack{\zeta^n = (-1)^\tau e^{n B_x} \\ \xi^n = (-1)^\theta e^{n B_y}}} P(\zeta, \xi). \quad (2.5)$$

The normalized logarithm of such a determinant is thus a Riemann sum on the torus

$$\frac{1}{n^2} \log \det K_{n,B}^{\theta\tau} = \frac{1}{n^2} \sum_{\substack{\zeta^n = (-1)^\tau e^{n B_x} \\ \xi^n = (-1)^\theta e^{n B_y}}} \log P(\zeta, \xi) \quad (2.6)$$

approximating the integral

$$F(B_x, B_y) = \iint_{\substack{|z|=e^{B_x} \\ |w|=e^{B_y}}} \log P(z, w) \frac{dz}{2i\pi z} \frac{dw}{2i\pi w}. \quad (2.7)$$

In fact, one can show that the asymptotics of the four terms in (2.4) are the same, and by a standard subadditivity argument [8] that

$$\lim_{n \rightarrow \infty} \frac{1}{n^2} \log Z(G_n, B) = F(B_x, B_y). \quad (2.8)$$

Thus, the Ronkin function gives the free energy of the model for the measure $\mu(B_x, B_y)$. On the other hand, from formula (1.9) and the definition of the free energy, we have

$$F(B_x, B_y) = \max_{s,t} (-\sigma(s, t) + s B_x + t B_y) \quad (2.9)$$

since the slope of the limit measure $\mu(B_x, B_y)$ minimizes the surface tension corresponding to the magnetically modified weights. In other words, the Ronkin function is the Legendre transform of the surface tension σ . Since the surface tension is strictly convex, the Legendre transform is involutive, and σ is the Legendre transform of the Ronkin function F .

The gradient of F maps \mathbb{R}^2 to the Newton polygon $N(P)$. the facets of F correspond to the cusps of σ . The slopes of the facets of F are integer points of $N(P)$ [40].

2.3.2 ... the local statistics

One may also want to compute the local statistics for the measure $\mu(B_x, B_y)$. What is the probability that k given edges $\mathbf{e}_1 = (\mathbf{w}, \mathbf{b}_1), \dots, \mathbf{e}_k = (\mathbf{w}_k, \mathbf{b}_k)$ appear in the random dimer configuration ? For the finite graph G_n , the answer is given by formula (1.8).

$$\begin{aligned} \mu_n(B_x, B_y)[\mathbf{e}_1, \dots, \mathbf{e}_k] &= \left(\prod_{l=1}^k \mathbf{K}_{\mathbf{w}_l \mathbf{b}_l} \right) \times \frac{1}{2} \left(-\frac{Z_{n,B}^{(00)}}{Z_{n,B}} \det(\mathbf{K}_{n,B}^{(00)})_{\mathbf{b}_i, \mathbf{w}_j}^{-1} + \right. \\ &\quad \left. \frac{Z_{n,B}^{(10)}}{Z_{n,B}} \det(\mathbf{K}_{n,B}^{(10)})_{\mathbf{b}_i, \mathbf{w}_j}^{-1} + \frac{Z_{n,B}^{(01)}}{Z_{n,B}} \det(\mathbf{K}_{n,B}^{(01)})_{\mathbf{b}_i, \mathbf{w}_j}^{-1} + \frac{Z_{n,B}^{(11)}}{Z_{n,B}} \det(\mathbf{K}_{n,B}^{(11)})_{\mathbf{b}_i, \mathbf{w}_j}^{-1} \right) \end{aligned} \quad (2.10)$$

where $Z_{n,B}^{(\theta\tau)} = \det \mathbf{K}^{(\theta\tau)}$ and $Z_{n,B} = \frac{1}{2}(-Z_{n,B}^{(00)} + Z_{n,B}^{(00)} + Z_{n,B}^{(01)} + Z_{n,B}^{(10)} + Z_{n,B}^{(11)})$ and the indices i and j in the determinants range from 1 to k .

The inverses of the operators $\mathbf{K}_{n,B}^{(\theta\tau)}$ can be also explicitly computed by discrete Fourier transform. Their entries are Riemann sums. Let \mathbf{w} and \mathbf{b} be respectively a white and a black vertex in G_1 . Denote by $\mathbf{w}_{x,y}$ the lift of \mathbf{w} in the fundamental domain (x, y) of G_n , and $\mathbf{b}_{x',y'}$ the lift of \mathbf{b} in fundamental domain (x', y') . The entry of $\mathbf{K}_{n,B}^{(\theta\tau)}$ between $\mathbf{b}_{x',y'}$ and $\mathbf{w}_{x,y}$ is

$$\begin{aligned} (\mathbf{K}_{n,B}^{(\theta\tau)})_{\mathbf{b}_{x',y'}, \mathbf{w}_{x,y}}^{-1} &= \frac{1}{n^2} \sum_{\substack{\zeta^n = (-1)^\tau e^{nB_x} \\ \xi^n = (-1)^\theta e^{nB_y}}} (K(\zeta, \xi)^{-1})_{\mathbf{b}, \mathbf{w}} \zeta^{-(y'-y)} \xi^{x'-x} \\ &= \frac{1}{n^2} \sum_{\substack{\zeta^n = (-1)^\tau e^{nB_x} \\ \xi^n = (-1)^\theta e^{nB_y}}} \frac{Q_{\mathbf{b}\mathbf{w}}(\zeta, \xi)}{P(\zeta, \xi)} \zeta^{-(y'-y)} \xi^{x'-x} \end{aligned} \quad (2.11)$$

where $Q_{\mathbf{b}, \mathbf{w}}(z, w)$ is the cofactor of the matrix $K(z, w)$ obtained after removing the line corresponding to white vertex \mathbf{w} and the column corresponding to black vertex \mathbf{b} . When n goes to $+\infty$, the entries $(\mathbf{K}_{n,B}^{(\theta\tau)})_{\mathbf{b}_{x',y'}, \mathbf{w}_{x,y}}^{-1}$ converge to the integrals

$$\mathbf{K}_B^{-1}(\mathbf{b}_{x',y'}, \mathbf{w}_{x,y}) = \int_{\substack{|z|=e^{B_x} \\ |w|=e^{B_y}}} \frac{z^{-(y'-y)} w^{x'-x} Q_{\mathbf{b}\mathbf{w}}(z, w)}{P(z, w)} \frac{dz}{2i\pi z} \frac{dw}{2i\pi w} \quad (2.12)$$

The operator K_B^{-1} is the inverse of the operator K over the space $\ell_B^2(G)$, the completion of the space of functions with finite support for the scalar product

$$\langle f, g \rangle_B = \sum_{x,y} (e^{-xB_y + yB_x})^2 \sum_{\substack{v \in \text{fund.} \\ \text{domain}}} \overline{f(v_{xy})} g(v_{xy}) \quad (2.13)$$

and the probability converges to

$$\mu_{(B_x, B_y)}[\mathbf{e}_1, \dots, \mathbf{e}_k] = \left(\prod_{l=1}^k K_{\mathbf{w}_l \mathbf{b}_l} \right) \det(K_B^{-1}(\mathbf{b}_i, \mathbf{w}_j)) \quad (2.14)$$

A natural topology on the set $\mathcal{M}(G)$ of dimer configurations of G is the product topology, for which two dimer configurations are close if they coincide on a large ball around the origin. For this topology, $\mathcal{M}(G)$ is compact and the convergence of finite dimensional distributions is equivalent to the weak convergence of probability measures $\mu_n(B_x, B_y)$ to $\mu_{(B_x, B_y)}$.

The way we chose to compute the correlations in presence of a magnetic field leads to a nice interpretation of the magnetic field, as the size of the torus over which we integrate to get the expression of the free energy and of the operator K^{-1} giving the correlations. However, the drawback of this procedure is that the entries of the operator K_B^{-1} are unbounded for a non-zero magnetic field.

Another way to get local statistics for the measure $\mu_{(B_x, B_y)}$ is to take limits of Boltzmann measures on G_n for weights in the same equivalence class, but for another gauge. The magnetically modified weights are defined as follows: we multiply the original weights of an edge crossing any lift of γ_x (resp. γ_y) to G_n by $e^{\pm B_x}$ (resp. by $e^{\pm B_y}$) according to its orientation. We get then the following expression for the (new) inverse Kasteleyn operator K_B^{-1}

$$K_B^{-1}(\mathbf{b}_{xy}, \mathbf{w}) = \int_{\mathbb{T}^2} \frac{z^{-y} w^x Q_{\mathbf{b}\mathbf{w}}(e^{B_x} z, e^{B_y} w)}{P(e^{B_x} z, e^{B_y} w)} \frac{dz}{2i\pi z} \frac{dw}{2i\pi w} \quad (2.15)$$

where \mathbb{T}^2 is the unit torus. This expression for the entries of K_B^{-1} differs from (2.12) by a factor $e^{yB_x - xB_y}$. However, the special expression of this factor implies that formula (2.14) used to compute local statistics are unchanged, thanks to their determinantal form. The entries of this new operator are bounded for any value of the magnetic field. The price to pay to use this expression is that we have to modify the Kasteleyn operator itself: in presence of a magnetic field, every edge crossing a lift of the horizontal cycle γ_x (resp. the vertical cycle γ_y) has its weight multiplied by $e^{\pm B_x}$ (resp. by $e^{\pm B_y}$), leading to a new Kasteleyn operator K_B . Following [34], we will in fact adopt this second point of view and use (2.15) to compute K_B^{-1} .

2.4 Harnack curves and consequences of maximality

As we said briefly in section 2.2, the curves arising as spectral curves of bipartite dimer models are algebraic real curves of a special kind. They are called *Harnack curves* or *maximal curves*. While all complex curves of a given degree have the same topology, the number and the position of ovals of real curves can be different. Harnack curves are the curves with the largest number of ovals in the “best possible” position. A precise topological definition can be found in [40]. Recently, Mikhalkin and Rullgård gave alternative characterizations of Harnack curves

Theorem 2.2 ([41]). *Let P a polynomial with real coefficients whose Newton polygon $N(P)$ has positive area. Then the three following assertions are equivalent*

- i) The real curve $\{P(z, w) = 0\}$ is a Harnack curve.*
- ii) The mapping from the complex curve $\{P(z, w) = 0\}$ to its amœba is at most¹ 2-to-1.*
- iii) $\text{Area } A(P) = \pi^2 \text{Area } N(P)$*

The right hand side of *iii)* is in fact an upper bound for the area of the amœba of a curve with a given Newton polygon [47]. Harnack curves have thus the property that the area of their amœba is maximal among those of the curves with the same Newton polygon. This explains why Harnack curves are also called maximal curves. Several proofs of maximality of spectral curves of bipartite planar dimer models were given [32, 34, 36].

The 2-to-1 property implies that, generically, the polynomial P has 2 or 0 roots on the torus $\{|z| = e^{B_x}, |w| = e^{B_y}\}$ depending on whether (B_x, B_y) lies in the amœba or in its complement. The number of roots of P on this torus has an influence on the asymptotics of K_B^{-1} , that has an impact on the decay of correlations between dimers.

One distinguishes three phases, depending on the behavior of the correlations at long range:

- in the *gaseous phase*, the correlations decay exponentially fast,
- in the *liquid phase*, the correlations decay as a power law,
- in the *solid phase*, there exist edges arbitrary far from each other such that the correlation between them is 1.

The relation between the magnetic field and the phase of the corresponding measure $\mu_{(B_x, B_y)}$ has been investigated in [34] and is summarized in the theorem:

Theorem 2.3 ([34]). *The measure $\mu_{(B_x, B_y)}$ is gaseous, liquid or solid respectively when (B_x, B_y) is in the closure of a bounded complementary component of $A(P)$, in the interior of $A(P)$, or in the closure of an unbounded complementary component of $A(P)$.*

¹This mapping is 2-to-1 over the interior of the amœba except at the real nodes of the curve.

The components of the boundary of the amoeba are the curves separating the different phases of the dimer model. They form the *phase diagram* of the model.

Another consequence of the 2-to-1 property is that to any lattice point of the Newton polygon corresponds either a bounded component of the amoeba complement or an isolated real node of the spectral curve. In particular, the number of gaseous phases of a dimer model equals the genus of the spectral curve [34]. For a generic choice of weights, the dimer model has a gaseous phase for every lattice point in the interior of the Newton polygon $N(P)$ and a frozen phase for every lattice point on the boundary of $N(P)$. When the curve has the maximal possible number of real nodes, the amoeba has no holes. The spectral curve has genus 0 and therefore corresponds to an isoradial dimer model [30, 32, 10], that have particular properties of locality.

The next three sections describe more in details the quantitative behaviour of the different phases. We will use short notations for magnetically altered quantities

$$P^B(z, w) = P(e^{B_x} z, e^{B_y} w), \quad K^B(z, w) = K(e^{B_x} z, e^{B_y} w), \quad Q^B(z, w) = Q(e^{B_x}, e^{B_y} z).$$

As introduced before, K_B and K_B^{-1} will stand for the Kasteleyn operator and its inverse in presence of the magnetic field $B = (B_x, B_y)$.

2.5 The gaseous phase

When (B_x, B_y) belongs to a bounded complementary component of the amoeba, the polynomial $P^B(z, w) = P(e^{B_x} z, e^{B_y} w)$ has no root on the unit torus. For any choice of black and white vertices \mathbf{b} and \mathbf{w} , the rational fraction

$$\frac{Q_{\mathbf{bw}}^B(z, w)}{P^B(z, w)} \tag{2.16}$$

is analytic over the unit torus. Therefore, the coefficients $K_B^{-1}(\mathbf{b}_x, \mathbf{w})$ decay exponentially when $|\mathbf{x}| \rightarrow \infty$. As a consequence, the height variance $\text{Var}(h(\mathbf{f}_1) - h(\mathbf{f}_2))$ stays bounded independently from the distance between \mathbf{f}_1 and \mathbf{f}_2 .

2.6 The liquid phase

We suppose in this section that (B_x, B_y) is in the interior of the amoeba. When (B_x, B_y) is a generic point in the interior of the amoeba, the polynomial $P^B(z, w)$ has two roots on the unit torus. We describe some features of liquid measures assuming that (B_x, B_y) is such a generic point. Similar statements can be given when (B_x, B_y) is a real node.

2.6.1 Map from G^* to \mathbb{R}^2

When given a liquid measure on dimer configurations of G , there is a natural application Ψ from the dual graph G^* to \mathbb{R}^2 , described by the following lemma. This application seems to give the good geometry to study liquid dimer models. In particular, when dimer weights are *critical*, Ψ coincides with the *isoradial embedding* of G^* [30].

Lemma 2.1. *Let (z_0, w_0) be a root of the characteristic polynomial on the unit torus. The 1-form*

$$\mathbf{e} = (\mathbf{w}, \mathbf{b}) \mapsto iK_{\mathbf{w}\mathbf{b}}^B(z_0, w_0)Q_{\mathbf{b}\mathbf{w}}^B(z_0, w_0) \quad (2.17)$$

is a divergence-free flow. Its dual is therefore the gradient of a mapping from G^ to $\mathbb{R}^2 \simeq \mathbb{C}$.*

This mapping Ψ is Λ -periodic, where Λ is the two-dimensional lattice generated by $\hat{x} = iz_0\partial_1 P(z_0, w_0)$ and $\hat{y} = iw_0\partial_2 P(z_0, w_0)$.

Proof:

The divergence of the 1-form $\omega : \mathbf{e} \mapsto iK_{\mathbf{w}\mathbf{b}}^B(z_0, w_0)Q_{\mathbf{b}\mathbf{w}}^B(z_0, w_0)$ at some black vertex \mathbf{b} is given by

$$\begin{aligned} (\operatorname{div}\omega)(\mathbf{b}) &= \sum_{\mathbf{w}' \sim \mathbf{b}} iK_{\mathbf{w}'\mathbf{b}}^B(z_0, w_0)Q_{\mathbf{b}\mathbf{w}'}^B(z_0, w_0) \\ &= i(Q^B(z_0, w_0) \cdot K^B(z_0, w_0))_{\mathbf{b}, \mathbf{b}} = iP^B(z_0, w_0) = 0 \end{aligned}$$

Similarly, one can check that the divergence of this flow is 0 at every white vertex \mathbf{w} . Thus, since G is planar, there exists an application $\Psi : G^* \rightarrow \mathbb{C}$ such that $\omega = d\Psi$.

The fact that Ψ is periodic is a consequence of the fact that G and the Kasteleyn operator are both periodic. There exist two complex numbers \hat{x} and \hat{y} such that for every $v \in G^*$ and every $(x, y) \in \mathbb{Z}^2$, the difference between the image of $v_{x,y}$ the translated of v by (x, y) and that of v itself is given by

$$\Psi(v_{x,y}) - \Psi(v) = x\hat{x} + y\hat{y}. \quad (2.18)$$

Define α and β to be the partial derivatives of P^B at the root (z_0, w_0) with respect to the first and the second variable respectively

$$\alpha = \partial_1 P^B(z_0, w_0), \quad \beta = \partial_2 P^B(z_0, w_0). \quad (2.19)$$

Let us prove now that the numbers \hat{x} and \hat{y} are given by $iz_0\alpha$ and $iw_0\beta$ respectively. Let $\tilde{\gamma}_x$ and $\tilde{\gamma}_y$ be respectively the lift of γ_x and γ_y starting at the same face of G . The complex number \hat{x} equals the sum of the complex numbers $\pm\omega(\mathbf{e})$ over all edges \mathbf{e} crossing $\tilde{\gamma}_x$ (see figure 2.1). These are exactly the edges of G_1 whose weights have been multiplied by

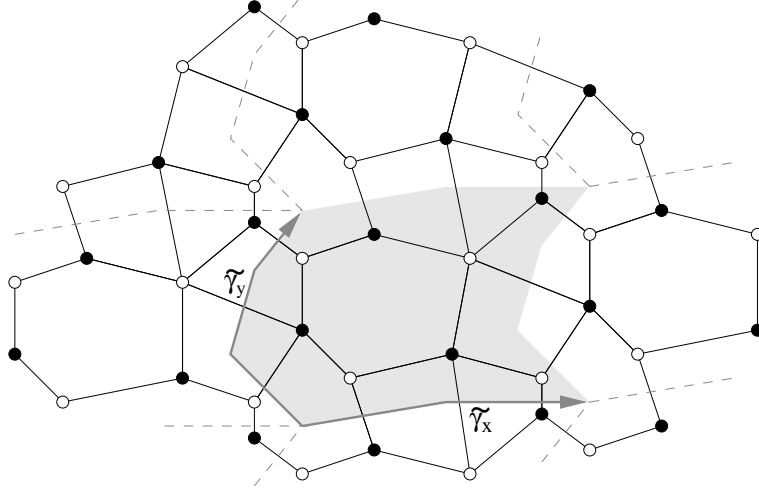


Figure 2.1: A piece of a planar bipartite periodic graph. The shaded zone represents its fundamental domain, delimited by the two paths γ_x and γ_y .

$z^{\pm 1}$ in the magnetically altered Kasteleyn operator $K^B(z, w)$, and the sign of the power of z is the same as that in front of $\omega(\mathbf{e})$. Noticing that

$$z \frac{\partial}{\partial z} z^m = m z^m = \begin{cases} z & \text{if } m = 1 \\ -z^{-1} & \text{if } m = -1 \\ 0 & \text{if } m = 0 \end{cases} \quad (2.20)$$

we can write

$$\begin{aligned} \hat{x} &= \sum_{\mathbf{w}, \mathbf{b} \in G_1} i(z_0 \partial_1 K_{\mathbf{w}\mathbf{b}}^B(z_0, w_0)) Q_{\mathbf{b}\mathbf{w}}^B(z_0, w_0) \\ &= iz_0 \operatorname{tr} (\partial_1 K^B(z_0, w_0) \cdot Q_{\mathbf{b}\mathbf{w}}^B(z_0, w_0)). \end{aligned}$$

On the other hand, recall that the characteristic polynomial $P^B(z, w)$ is the determinant of $K^B(z, w)$. Therefore if the black and white vertices of G_1 are labeled from 1 to n , then

$$iz_0 \alpha = iz_0 \partial_1 P(z_0, w_0) = iz_0 \sum_{j=1}^n \det(K_{\mathbf{b}_1}^B(z_0, w_0), \dots, \partial_1 K_{\mathbf{b}_j}^B(z_0, w_0), \dots, K_{\mathbf{b}_n}^B(z_0, w_0)) \quad (2.21)$$

where $K_{\mathbf{b}_j}^B(z, w)$ is the j th column of the matrix $K^B(z, w)$. Expanding each determinant with respect to the column containing derivatives, we get

$$\begin{aligned} iz_0 \alpha &= iz_0 \sum_{j=1}^n \sum_{k=1}^n \partial_1 K_{\mathbf{w}_k \mathbf{b}_j}^B(z_0, w_0) \times \\ &\quad \operatorname{Cof}_{\mathbf{w}_k \mathbf{b}_j} (K_{\mathbf{b}_1}^B(z_0, w_0), \dots, \partial_1 K_{\mathbf{b}_j}^B(z_0, w_0), \dots, K_{\mathbf{b}_n}^B(z_0, w_0)) \quad (2.22) \end{aligned}$$

Since the cofactor $\text{Cof}_{\mathbf{w}_k \mathbf{b}_j}(K_{\mathbf{b}_1}^B, \dots, \partial_1 K_{\mathbf{b}_j}(z_0, w_0), \dots, K_{\mathbf{b}_n}^B(z_0, w_0))$ does not depend on the j th column, we can replace it by $K_{\mathbf{b}_j}^B(z_0, w_0)$. This cofactor by definition is $Q_{\mathbf{b}_j \mathbf{w}_k}^B(z_0, w_0)$. Thus,

$$iz_0 \alpha = iz_0 \sum_{j=1}^n \sum_{k=1}^n \partial_1 K_{\mathbf{w}_k \mathbf{b}_j}^B(z_0, w_0) Q_{\mathbf{b}_j \mathbf{w}_k}^B(z_0, w_0) \quad (2.23)$$

$$= iz_0 \text{tr}(\partial_1 K^B(z_0, w_0) \cdot Q^B(z_0, w_0)) = \hat{x}. \quad (2.24)$$

The same argument applied to $\tilde{\gamma}_y$ gives the formula

$$iw_0 \beta = \hat{y}. \quad (2.25)$$

□

In what follows, to construct the application from G^* to \mathbb{R}^2 , we will choose between the root (z_0, w_0) on the unit torus for which the frame (\hat{x}, \hat{y}) is direct. This is equivalent to requiring that

$$\text{Im} \left(\frac{w_0 \beta}{z_0 \alpha} \right) > 0 \quad (2.26)$$

2.6.2 Asymptotics of $K_B^{-1}(\mathbf{b}, \mathbf{w})$

The coefficients of K_B^{-1} decays linearly. More precisely, if \mathbf{b} and \mathbf{w} are in the same fundamental domain, and $\mathbf{b}_{x,y}$ is a translate of \mathbf{b} by (x, y) , then we have the following asymptotics for $K_B^{-1}(\mathbf{b}_{x,y}, \mathbf{w})$:

Lemma 2.2. *Let (z_0, w_0) the root of P^B on the unit torus satisfying (2.26). Then the asymptotic expression for the coefficients of K^{-1} are given by*

$$K_B^{-1}(\mathbf{b}_{x,y}, \mathbf{w}) = -\text{Re} \left(\frac{z_0^{-y} w_0^x Q_{\mathbf{b}, \mathbf{w}}^B(z_0, w_0)}{\pi(x\hat{x} + y\hat{y})} \right) + O \left(\frac{1}{|x|^2 + |y|^2} \right) \quad (2.27)$$

The proof of this lemma is given in [34].

Note that the geometry of the map from G^* to \mathbb{R}^2 appears in this analytical result. The denominator up to a factor π is the vector separating the image of the fundamental domains of $\mathbf{b}_{x,y}$ and \mathbf{w} under this mapping. Moreover, if \mathbf{b} and \mathbf{w} are the ends of an edge \mathbf{e} then (2.27) can be rewritten as

$$K_B(\mathbf{w}, \mathbf{b}) K_B^{-1}(\mathbf{b}_{x,y}, \mathbf{w}) = \text{Re} \left(\frac{z_0^{-y} w_0^x i \mathbf{e}^*}{\pi(x\hat{x} + y\hat{y})} \right) + O \left(\frac{1}{|x|^2 + |y|^2} \right) \quad (2.28)$$

In particular, this lemma implies that the correlations between two distant dimers \mathbf{e}_1 and \mathbf{e}_2 decays as $\text{dist}(\mathbf{e}_1, \mathbf{e}_2)^{-2}$. As a consequence, the variance of the difference of height between two faces grows like the logarithm of the distance between the images of the two faces by Ψ .

2.7 The solid phase

Let ω_0 be a periodic white-to-black unit flow. Since a probability measure μ on dimer configurations of G gives also rise to a periodic white-to-black unit flow ω_μ , by the formula

$$\omega_\mu(\mathbf{e}) = \mathbb{P}_\mu[\mathbf{e}], \quad (2.29)$$

the difference $\omega_\mu - \omega_0$ is a divergence-free flow and the corresponding flux is the average height function h .

For \mathbf{f}_1 and \mathbf{f}_2 two adjacent faces of G and $\vec{\mathbf{e}}$ the (oriented) edge having face \mathbf{f}_1 on its left and \mathbf{f}_2 on its right, define $d(\mathbf{f}_1, \mathbf{f}_2)$ to be the maximal possible amount of flow $\omega_\mu - \omega_0$ through the edge $\vec{\mathbf{e}}$. Thus quantity is called the *capacity* of the edge $\vec{\mathbf{e}}$.

For two any faces \mathbf{f} and \mathbf{f}' , define $D(\mathbf{f}, \mathbf{f}')$ as

$$D(\mathbf{f}, \mathbf{f}') = \min_\gamma \sum_{j=1}^n d(\mathbf{f}_{\gamma(j)}, \mathbf{f}_{\gamma(j+1)}) \quad (2.30)$$

where the minimum is taken over all dual paths $\gamma = (\mathbf{f}_{\gamma(1)}, \mathbf{f}_{\gamma(2)}, \dots, \mathbf{f}_{\gamma(n)})$ from $\mathbf{f} = \mathbf{f}_{\gamma(1)}$ to $\mathbf{f}' = \mathbf{f}_{\gamma(n)}$.

The *max flow-min cut theorem* states that the quantity $D(\mathbf{f}, \mathbf{f}')$ is equal to the maximum flux through any dual path from \mathbf{f} to \mathbf{f}' . This theorem can be stated as follows:

Theorem 2.4 (max flow-min cut). *For any dimer configuration \mathcal{C} , the difference of height between faces \mathbf{f} and \mathbf{f}' satisfies*

$$h(\mathbf{f}') - h(\mathbf{f}) \leq D(\mathbf{f}, \mathbf{f}') \quad (2.31)$$

If there exist no dimer configuration with slope (s, t) , then there exists a face \mathbf{f} and a translated of it $\mathbf{f}_{x,y}$ such that

$$D(\mathbf{f}, \mathbf{f}_{x,y}) < sx + ty \quad (2.32)$$

In this case, there exists a dual path $\gamma = (\mathbf{f}_1, \dots, \mathbf{f}_k)$ between $\mathbf{f} = \mathbf{f}_1$ and $\mathbf{f}_{x',y'} = \mathbf{f}_k$ a translated of \mathbf{f} (maybe different from $\mathbf{f}_{x,y}$) using at most once each type of face, such that

$$D_\gamma(\mathbf{f}, \mathbf{f}_{x',y'}) = \sum_{j=1}^{k-1} d(\mathbf{f}_j, \mathbf{f}_{j+1}) < sx' + ty' \quad (2.33)$$

There is a finite number of such paths, and each paths of this type gives a constraint on the slope of a height function. In particular, the Newton polygon representing the set of all possible slopes is the convex set defined by the intersection of the half-planes

$$\{(s, t) \mid D_\gamma(\mathbf{f}, \mathbf{f}_{x',y'}) \geq sx' + ty'\} \quad (2.34)$$

when γ runs through the set of such paths. The case of equality in the inequality corresponding to a path γ means that the flux through this dual path is maximal: the amount of flow ω_μ through an edge crossing γ is either 0 or 1. In other words, the state of the edges crossing γ is completely deterministic. The path γ is called a *frozen path*. One can always manage to deform slightly γ so that any edge crossing γ appears with probability zero in the random configuration.

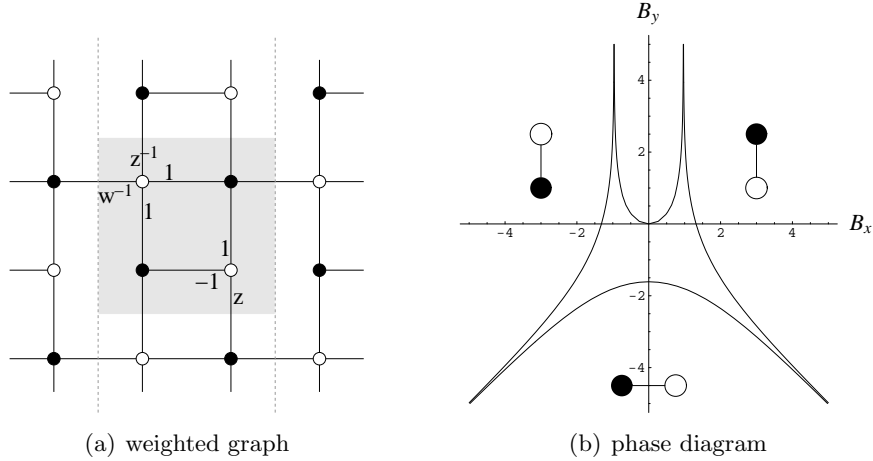


Figure 2.2: The graph and the phase diagram of a dimer model comporting a non-frozen solid phase. The multipliers used to compute the Fourier transform of K are indicated on the graph. On the phase diagram are drawn the type of edges appearing with probability 1 in each frozen solid phase. The fourth solid phase is not completely frozen. The frozen paths corresponding to this phase are represented by dotted lines.

Every weighted bipartite graph is equivalent² to a honeycomb graph with a $n \times n$ fundamental domain. Generically, all the weights are non zero, and the Newton polygon is an isocetes right triangle. It has $3n$ lattice points on the boundary, each corresponding to a solid phase of the model. These different solid phases are easily described. For example, the vertical side of the Newton polygon corresponds to n frozen paths in the \hat{x} -direction. The strips between two neighbouring frozen paths admit only two dimers configurations (see fig.) with generically different energy, given by a succession of edges in one of the two directions allowed. The choice between the two directions depends on the magnetic field. The transition from a solid phase to another happens when the magnetic field makes one of these strips switch from one direction to another.

A typical tiling with a height lying on this side of the Newton polygon will be a succession of rows of edges of the same type separated by frozen paths. Two solid phases will differ from each other by the direction each rows has.

In this generic situation the solid phases are really frozen: every edge appears in the random dimer configuration with probability 1 or 0.

²The equivalence relation for dimer graphs means that one can pass from one graph to another by a succession of elementary moves that preserves dimer properties. See [52]

This is however not always the case, as shows the following example. Let us consider the dimer model presented on figure 2.2.

This model presents 4 solid phases, 3 of them being completely frozen. The fourth one is of a different kind: between two neighbouring vertical frozen paths, the strips admit an infinity of dimer configurations corresponding to tilings of infinite strips of width 2 by 2×1 dominos. Dimer configurations in different strips are independent.

2.8 The dimer on the honeycomb lattice

In this section we discuss the different aspects introduced in this chapter on a particular graph: the honeycomb lattice H . The dual graph of H is the triangular lattice, and a dimer configuration can be seen by duality as a rule to glue the triangular faces of H^* by pairs, leading to a tiling of the plane by rhombi.

Every edge of the lattice is assigned a weight equal to 1. A system of coordinates (x, y) is chosen to label fundamental domains of the graph consisting of a white and a black vertex.

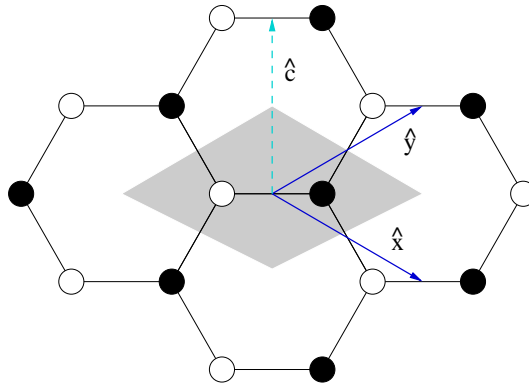


Figure 2.3: A piece of the honeycomb lattice. The shaded area represents the fundamental domain of this lattice. The unit vectors \hat{x} and \hat{y} drawn with solid lines define the system of coordinates (x, y) we use to label vertices. Another system of coordinates (c, y) is used, using vector \hat{c} in dotted lines.

The characteristic polynomial for this model is $P(z, w) = 1 + z + \frac{1}{w}$. For a given choice of magnetic field (B_x, B_y) , the inverse Kasteleyn operator is given by the formula

$$\mathbb{K}_B^{-1}(\mathbf{b}_{x,y}, \mathbf{w}) = \iint_{\mathbb{T}^2} \frac{z^{-y} w^x}{1 + e^{B_x} z + e^{-B_y} \frac{1}{w}} \frac{dz}{2i\pi z} \frac{dw}{2i\pi w}. \quad (2.35)$$

If the three inequalities

$$e^{B_x} + e^{-B_y} > 1, \quad 1 + e^{B_x} > e^{-B_y}, \quad 1 + e^{-B_y} > e^{B_x}, \quad (2.36)$$

are fulfilled, the polynomial $P^B(z, w) = P(e^{B_x z}, e^{B_y w})$ has two zeros on the unit torus \mathbb{T}^2 and the corresponding Gibbs measure is liquid. If one of these inequalities is not satisfied, the Gibbs measure is frozen: with probability 1, we will see only one type of edge. All the Gibbs measures have the *conditional uniform property*: the probability measure induced by conditioning on an annular region on the tilings inside this region is the uniform probability measure.

Imposing a magnetic field in this case is in fact equivalent to assigning different weights to edges according to their orientation, as in figure 2.4.

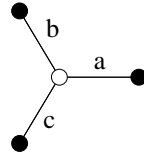


Figure 2.4: The weights assigned to edges of the honeycomb lattice, according to their orientation.

These weights a, b and c are related to the magnetic field by

$$B_x = \log\left(\frac{c}{a}\right) \quad B_y = -\log\left(\frac{b}{a}\right) \quad (2.37)$$

This is the point of view we adopt in this section.

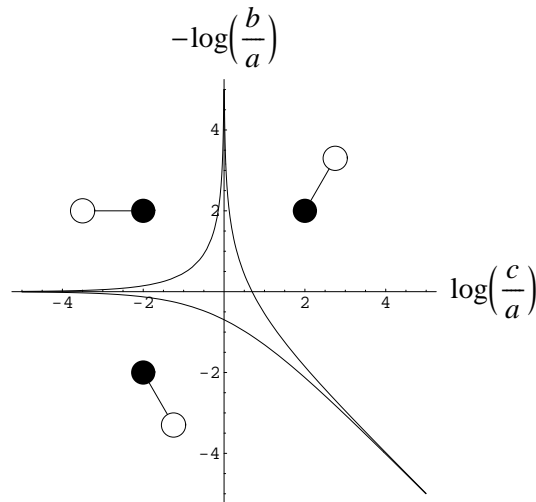


Figure 2.5: The amœba of the dimer model on the honeycomb lattice. The connected complement of the complementary represent the solid phases of the model. The type of edge appearing with probability 1 in each of these phases are represented.

The spectral curve of this dimer model is a Harnack curve of genus zero, whose amoeba is represented on figure 2.5. The dimer model has only two phases, instead of three: there is no gaseous phase. It belongs thus to the class of the *isoradial dimer model* with *critical weights* introduced in [30] by Kenyon: there is an embedding of H^* in the plane such that every face is inscribable in a circle of radius 1, and the length of any dual edge is proportional to the weight of the corresponding primal edge³. The faces of H^* are triangles with side length proportional to a , b and c .

A dimer configuration on H can be interpreted as a surface in \mathbb{R}^3 through the height function: the corresponding tiling is the projection of a landscape of unit cubes in the plane perpendicular to $(1, 1, 1)$ direction, and the height function is the coordinate in the direction $(1, 1, 1)$.

It is sometimes more convenient to use another system of coordinates to label vertices of H . We decide to use (\mathbf{c}, y) where $\mathbf{c} = x + y$ labels the columns of hexagons of H . The inverse Kasteleyn operator in these new coordinates is given by

$$\mathbb{K}^{-1}(\mathbf{b}_y^{\mathbf{c}}, \mathbf{w}) = \int_{\mathbb{T}^2} \frac{u^{-y} w^{\mathbf{c}}}{a + \frac{1}{w}(b + cu)} \frac{du}{2i\pi u} \frac{dw}{2i\pi w}.$$

In the special case when $\mathbf{c} = 0$, this integral can be completely computed by the method of residues. If $y \neq 0$, $\mathbb{K}^{-1}(\mathbf{b}_y^{(0)}, \mathbf{w})$ equals

$$\mathbb{K}^{-1}(\mathbf{b}_y^{(0)}, \mathbf{w}) = \frac{\sin(\theta_0 y)}{\pi a y}.$$

where $\theta_0 = \text{Arccos}\left(\frac{a^2 - b^2 - c^2}{2bc}\right)$. The inverse Kasteleyn operator, restricted to a column is a *discrete sine kernel*. In the continuous framework, the sine kernel describes the statistics of eigenvalues in the bulk the spectrum of large random Hermitian matrices. Several between random tilings and discrete sine process have been presented in [21]

In chapters 4 and 5, we will see that in some particular limit cases, the distributions of dimers in a column converge to that of the eigenvalues of large Hermitian random matrices. In chapter 4, we discuss the case when θ_0 converges to π . The case when θ_0 goes to 0 is developed in chapter 5 and generalized in chapter 6.

Before that, we introduce in the next chapter some definitions and basic facts about *determinant random fields*, giving the necessary framework to describe the two examples of such random processes discussed here, namely the dimer model on a bipartite planar graph, and the statistics of the eigenvalues of large Hermitian random matrices.

³The usual embedding of the triangular lattice H^* with equilateral triangles is a case of isoradial embedding, corresponding to equal weights $a = b = c$.

3 Determinant random point fields

In the random dimer model on a bipartite planar graph, the probabilistic quantities of interest, like the correlations between edges, are given by determinants. It is an example of a *determinant random point field*.

In this chapter, we present some background on the theory of *determinant random point fields*. Here are collected definitions and basic properties about these objects that will be necessary in the sequel. These facts as well as an exposition of some recent results can be found in [56].

3.1 Definitions

Let E be a separable Hausdorff space, called the *one-particle space* and Ω be a space of countable configurations of particles in E . In our examples, E will be a product $\prod_{j=1}^m E_j$, with $E_j = \mathbb{R}$ or \mathbb{Z} , or the set of edges of an infinite biperiodic graph G .

To a Borel set B of E and to a configuration $\omega \in \Omega$ is associated an integer $N_B(\omega)$ representing the number of particles in B . We assume that each configuration $\omega = (x_i)_{i \in \mathbb{Z}}$ of X is locally finite, *i.e.* that $N_K(\omega)$ in any compact set $K \subset E$ is finite.

We refer to a set of the form

$$C_B^n = \{\omega \in \Omega \mid N_B(\omega) = n\}$$

as a cylinder set. The σ -algebra \mathcal{F} of measurable subset of Ω is the σ -algebra generated by the cylinder sets.

Definition 3.1. A *random point field* is a triplet $(\Omega, \mathcal{F}, \mathbb{P})$ where \mathbb{P} is a probability measure on (X, Ω) .

Such a probability measure can be constructed, at least in the cases we will consider, by Kolmogorov extension theorem [37]. Suppose we are able to construct a joint distribution of non-negative integer-valued random variables N_B for a sufficiently large class \mathcal{R} of sets B^1 such that the following finite-additivity condition holds: if B_1, \dots, B_m are disjoint sets of the class \mathcal{R} and $B = \bigcup_{j=1}^m B_j$, then

$$N_B = \sum_{j=1}^m N_{B_j} \quad \text{almost surely.} \quad (3.1)$$

¹When $E = \mathbb{R}^d$ for instance, it is sufficient to consider the class \mathcal{R} of all finite unions of open, closed or semi-closed rectangles with rational integers.

The joint distribution of random variables $N_B, B \in \mathcal{R}$ determines uniquely a probability distribution on (Ω, \mathcal{F}) .

We now define the correlation functions.

Definition 3.2. Locally integrable function $\rho_n : E^n \rightarrow \mathbb{R}^+$ is called the n -point correlation function of the random point field $(\Omega, \mathcal{F}, \mathbb{P})$ if for any disjoint bounded Borel subset B_1, \dots, B_k of E and any integers n_1, \dots, n_k , the following holds

$$\mathbb{E} \left[\prod_{j=1}^k \frac{N_{B_j}!}{(N_{B_j} - n_j)!} \right] = \int_{B_1^{n_1} \times \dots \times B_k^{n_k}} \rho_n(x_1, \dots, x_n) dx_1 \cdots dx_n \quad (3.2)$$

where $n = \sum_{j=1}^k n_j$ and \mathbb{E} is the mathematical expectation with respect to \mathbb{P} .

The probabilistic interpretation of ρ_n is the following: for $j \in \{1, \dots, k\}$, if $[x_j, x_j + dx_j]$ is an infinitesimally small box around x_j of volume dx_j , the probability to find a particle in each box is

$$\rho_n(x_1, \dots, x_n) dx_1 \cdots dx_n \quad (3.3)$$

One can construct from these correlation functions a generating function for the joint distribution of $(N_{B_1}, \dots, N_{B_k})$. If

$$n = (n_1, \dots, n_k), \quad z = (z_1, \dots, z_k), \quad B = (B_1, \dots, B_k),$$

it will be convenient to use following multi-index notations

$$n! = \prod_{j=1}^k n_j!, \quad |n| = \sum_{j=1}^k n_j, \quad B^n = B_1^{n_1} \times \dots \times B_k^{n_k}, \quad z^n = z_1^{n_1} \cdots z_k^{n_k}.$$

The generating function $Q_B(z)$ is given by the formula

$$\begin{aligned} Q_B(z) &= \mathbb{E} \left[\prod_{j=1}^k (1 - z_j)^{N_{B_j}} \right] = \sum_{n \in \mathbb{N}^k} \frac{(-z)^n}{n!} \mathbb{E} \left[\prod_{j=1}^k \frac{N_{B_j}!}{(N_{B_j} - n_j)!} \right] \\ &= \sum_{n \in \mathbb{N}^k} \frac{(-z)^n}{n!} \int_{B^n} \rho_n(x_1, \dots, x_n) dx_1 \cdots dx_n \end{aligned}$$

The probability to find exactly n_j particles in B_j for every j is obtained from $Q_B(z)$ by differentiation

$$\mathbb{P} [\forall j \in \{1, \dots, k\} N_{B_j} = n_j] = \frac{(-1)^{|n|}}{n!} \frac{\partial^n}{\partial z^n} Q_B(z) \Big|_{z=(1, \dots, 1)} \quad (3.4)$$

3. Determinant random point fields

where $\frac{\partial^n}{\partial z^n}$ stands for the differential operator $\frac{\partial^{n_1}}{\partial z_1} \cdots \frac{\partial^{n_k}}{\partial z_k}$. In particular, the probability of having no particle in a Borel set B is given by the alternating series

$$\mathbb{P} [N_B = 0] = \sum_{n=0}^{\infty} \frac{(-1)^n}{n!} \int \cdots \int_{B^n} \rho_n(x_1, \dots, x_n) dx_1 \cdots dx_n. \quad (3.5)$$

We now introduce the notion of determinantal random point field, which will be useful in the next chapters:

Definition 3.3. A random point field in E is called *determinantal* or *fermionic* if its n -point correlation functions are given by

$$\rho_n(x_1, \dots, x_n) = \det_{1 \leq i, j \leq n} [J(x_i, x_j)] \quad (3.6)$$

where $J(x, y)$ is the integral kernel of a non-negative locally trace class operator on $L^2(E)$, also denoted by J .

For a determinantal random point field $(\Omega, \mathcal{F}, \mathbb{P})$, the generating function of the distribution of the number of particles N_B in a bounded Borel set B equals the *Fredholm determinant*² of $\text{Id} - zJ_B$, with $J_B : f \mapsto \int_B J(\cdot, y)f(y)dy$, whose expression is

$$Q_B(z) = \text{Det}(\text{Id} - zJ_B) = \sum_{n=0}^{+\infty} \frac{(-z)^n}{n!} \int \cdots \int_{B^n} \det[J(x_i, x_j)] dx_1 \cdots dx_n. \quad (3.7)$$

Similar formulæ exist for the generating function of the joint distribution of the numbers of particles N_{B_1}, \dots, N_{B_k} in disjoint bounded Borel:

$$\begin{aligned} Q_B(z) &= \text{Det}(\text{Id} - \sum_{j=1}^k z_j \cdot J_{B_j}) \\ &= \sum_{n \in \mathbb{N}^k} \frac{(-z)^n}{n!} \int \cdots \int_{B_1^{n_1} \times \cdots \times B_k^{n_k}} \det[J(x_i, x_j)] dx_1 \cdots dx_n \end{aligned} \quad (3.8)$$

If the kernel $J(x, y)$ is bounded, say by M , then the series $Q_B(z_1, \dots, z_n)$ is an entire function of $z \in \mathbb{C}^k$. Indeed, Hadamard's inequality states that the determinant of a matrix is bounded by the product of the ℓ^2 -norms of its columns:

²Fredholm determinants are used to solve integral equation of the form

$$\varphi(x) - \lambda \int J(x, y)\varphi(y)dy = f(x).$$

The coefficient

$$\frac{1}{n!} \int \cdots \int_{B^n} \det[J(x_i, x_j)] dx_1 \cdots dx_n$$

is in fact the trace of the operator J_B acting on functions on the n -th exterior power of E . This formula is thus a generalization of the usual formula $\det(\text{Id} - A)$ for matrices.

Lemma 3.1. *Hadamard's inequality*

$$\forall A \in \mathcal{M}_n(\mathbb{R}), \quad |\det(A)| \leq \prod_{j=1}^n \left(\sum_{i=1}^n A_{ij}^2 \right)^{1/2} \quad (3.9)$$

Consequently, the n th term in the series (3.8) is bounded in absolute value by

$$\begin{aligned} \left| \frac{(-z)^n}{n!} \int_{B^n} \det[J(x_i, x_j)] d^n x \right| &\leq \frac{|z|^n}{n!} \int_{B^n} [J(x_i, x_j)] d^n x \\ &\leq \frac{|z|^n}{n!} \int_{B^n} (|n|M^2)^{|n|/2} d^2 x \leq \left(\prod_{j=1}^k \frac{(M|B_j||z_j|)^{n_j}}{n_j!} \right) |n|^{|n|/2}. \end{aligned}$$

The series $Q_B(z_1, \dots, z_n)$ converges normally on every compact set of \mathbb{C}^k and is thus an entire function of z . In particular, the joint distribution of N_{B_1}, \dots, N_{B_k} is completely determined by the correlation functions.

The generating functions $Q_B(z)$ can be useful to prove weak convergence of random point fields. Indeed, the space \mathcal{N}_E of all locally-finite, integer-valued measures on E is usually endowed with the topology defined by the usual notion of convergence for measures: a sequence (μ_n) converges to μ if for all functions f with compact support in E ,

$$\lim_{n \rightarrow +\infty} \int f d\mu_n = \int f d\mu. \quad (3.10)$$

With this topology on \mathcal{N}_E , weak convergence of random point fields, or equivalently, of probability measures on \mathcal{N}_E , is equivalent to the convergence of finite dimensional distributions [9].

Let (μ_n) be a sequence of determinantal random point fields with kernel $J^{(n)}$. Suppose we can prove that for every finite collection of Borel sets $B = (B_1, \dots, B_k)$, the series

$$Q_B^{(n)}(z) = \text{Det} \left(\text{Id} - \sum_{j=1}^k z_j \cdot J_{B_j}^{(n)} \right) \quad (3.11)$$

converges to a Fredholm determinant

$$\text{Det} \left(\text{Id} - \sum_{j=1}^k z_j \cdot J_{B_j}^{(\infty)} \right), \quad (3.12)$$

and that this series has a positive radius of convergence around $z = (1, \dots, 1)$. Then by a standard argument [4], the joint distribution of $(N_{B_1}, \dots, N_{B_k})$ converges, and thus the determinantal random field μ_n converges to a random point field μ with a kernel $J^{(\infty)}$.

3.2 Examples of determinantal random point fields

3.2.1 Eigenvalues of Random matrices

The archetypical example in random matrix theory is the so-called *Gaussian Unitary Ensemble*. See for example [16] for a review. Gaussian ensembles belong both to the family of invariant ensembles – for which the probability measure is invariant under the action of some continuous symmetry group – and to the family of ensembles with independent identically distributed entries.

Let \mathcal{H}_N be the set of Hermitian matrices of size N . A matrix $H \in \mathcal{H}_N$ has N^2 real degrees of freedom: one can choose arbitrarily the N real entries on the diagonal, and the real and imaginary part of the $\frac{N(N-1)}{2}$ complex entries above the diagonal. \mathcal{H}_N can be identified with \mathbb{R}^{N^2} , and we define a probability measure ν_N on \mathcal{H}_N by giving the expression of its density with respect to the Lebesgue measure on \mathbb{R}^{N^2} , denoted by dH . If f is a measurable function on \mathcal{H}_N , its expectation with respect to this probability measure is

$$\mathbb{E}_{\nu_N} [f(H)] = \frac{1}{Z_N} \int_{\mathcal{H}_N} f(H) e^{-\frac{1}{2N} \text{tr}(H^2)} dH \quad (3.13)$$

where Z_N is a renormalization factor to ensure we deal with a probability measure. The denomination of Gaussian Unitary ensemble is justified by the fact that $\frac{1}{2N} \text{tr}(H^2)$ is a positive definite quadratic form invariant under the transformation $H \rightarrow U^{-1} H U$, where U is a unitary matrix, implying that the probability measure ν_N is a Gaussian measure preserved by the action of $U(N)$. With respect to μ_N , the different degrees of freedom (h_{ii} , $\text{Re}(h_{ij})$ and $\text{Im}(h_{ij})$ for $j > i$) are independent random variables with Gaussian distribution.

The $U(N)$ invariance can be used to “integrate out” the dependence on the eigenvectors of the random matrix H_N , and to get a probability measure μ_N on eigenvalues $\lambda = (\lambda_1, \dots, \lambda_N)$

$$\mathbb{E}_{\mu_N} [g(\lambda)] = \frac{1}{Z'_N} \int_{\mathbb{R}^N} g(\lambda) \prod_{i < j} (\lambda_j - \lambda_i)^2 e^{-\frac{1}{2N} (\lambda_1^2 + \dots + \lambda_N^2)} d^N \lambda \quad (3.14)$$

Rewriting the square of the Vandermonde of λ as an exponential

$$\prod_{i < j} (\lambda_j - \lambda_i)^2 = e^{\sum_{i \neq j} \log |\lambda_i - \lambda_j|}$$

one can give a new interpretation of μ_N as a Boltzmann measure of a system with N particles with mass $\frac{1}{N}$, repelling each other by Coulomb interaction.

The statistics of the eigenvalues of the random matrix H can be studied, making use of the method of orthogonal polynomials, involving in this case Plancherel-Rotach asymptotics of Hermite polynomials.

The empirical measure

$$M_N = \frac{1}{N} \sum_{j=1}^N \delta_{\lambda_j} \quad (3.15)$$

converges weakly when N goes to $+\infty$ to a probability measure with support $[-2, 2]$ whose density d_∞ with respect to Lebesgue's measure is

$$d_\infty(x) = \frac{1}{2\pi} \sqrt{4 - x^2} \mathbb{1}_{[-2, 2]}(x). \quad (3.16)$$

This is the *Wigner semicircle law*. This tells us that roughly, the spacing between two neighbouring eigenvalues in the bulk is of order $\frac{1}{N}$. If we rescale properly the eigenvalues λ around $x_0 \in (-2, 2)$ by posing

$$\xi = \pi N d_\infty(x_0)(\lambda - x_0), \quad (3.17)$$

then letting N going to infinity, we get the convergence of the distribution of the random points ξ to a determinantal random point field whose correlation functions are

$$\rho_k(\xi_1, \dots, \xi_k) = \det \left[\frac{\sin(\xi_i - \xi_j)}{\pi(\xi_i - \xi_j)} \right]. \quad (3.18)$$

The kernel $\frac{\sin(x-y)}{\pi(x-y)}$ is called the *sine kernel*.

At the edge of the spectrum, the density goes to zero. The typical distant between two successive eigenvalues is of order $N^{-1/3}$ and the scaling needs to be modified. At the edge of the spectrum, the distribution of the rescaled eigenvalues

$$\zeta = N^{2/3}(\lambda - 2), \quad (3.19)$$

converges when N goes to infinity to a determinantal random point field with the *Airy kernel*

$$A(x, y) = \frac{\text{Ai}(x)\text{Ai}'(y) - \text{Ai}(y)\text{Ai}'(x)}{x - y} \quad (3.20)$$

where the $\text{Ai}(x)$ is the Airy function

$$\text{Ai}(x) = \frac{1}{\pi} \int_{-\infty}^{+\infty} e^{ixt + i\frac{t^3}{3}} dt. \quad (3.21)$$

The GUE ensemble furnishes two examples of determinantal random point fields with hermitian kernels. If an evolution of the system in time is wanted, one can replace the Gaussian random variables by Gaussian stochastic processes, like Brownian motion or Ornstein-Uhlenbeck processes. The eigenvalues depend now on time, modelling the motion of charged particles, not allowed to cross each other. Determinantal expressions for probabilities involving non intersecting paths is a well known phenomenon in probability theory [23] as well as in combinatorics [17].

In a suitable scaling limit, the distribution of the time-dependent eigenvalues converge to a generalization of the determinantal random point fields described above, with the so-called *extended sine kernel* and *extended Airy kernel*. Note that these kernel are not hermitian any more. The distribution in time of the first eigenvalue of the random matrix, referred to as the *Airy process*, introduced in [50], appears as the scaling limit of random growth system, crystal melting or also in random tilings of the so-called *Aztec diamond* [22]. The extended sine kernel will be discussed more in details in the following chapter.

3.2.2 Dimer models

The dimer model is another example of determinantal random point field. Let G be a \mathbb{Z}^2 -periodic, with positive weights on edges, and K the associated Kasteleyn operator. If μ is a probability measure on dimers configuration of G as described in the previous chapter: μ is a Boltzmann measure if G is finite, and a Gibbs measure if G is \mathbb{Z}^2 -periodic.

The one-particle space is the set of edges of E , endowed with the discrete topology

The correlation functions are given by determinants. In this discrete setting, the expression of the n -point correlation function ρ_n evaluated at edges $\mathbf{e}_1 = (\mathbf{w}_n, \mathbf{b}_n), \dots, \mathbf{e}_n = (\mathbf{w}_1, \mathbf{b}_1)$ is

$$\rho_n(\mathbf{e}_1, \dots, \mathbf{e}_n) = \mathbb{P}_\mu[\mathbf{e}_1, \dots, \mathbf{e}_n \in \mathcal{C}] = \left(\prod_{k=1}^n K(\mathbf{w}_k, \mathbf{b}_k) \right) \det_{1 \leq i, j \leq n} [K^{-1}(\mathbf{b}_j, \mathbf{w}_i)] \quad (3.22)$$

$$= \det_{1 \leq i, j \leq n} [J(\mathbf{e}_j, \mathbf{e}_i)] \quad (3.23)$$

where $J(\mathbf{e}_j, \mathbf{e}_i) = K(\mathbf{w}_j, \mathbf{b}_j)K^{-1}(\mathbf{b}_j, \mathbf{w}_i)$.

If an explicit embedding of the graph G in the plane is used, the dimer model can be interpreted as a determinant random point field on the plane. Suppose that the fundamental domain of G contains n edges, whose translates define n classes of edges. A dimer of a configuration is identified with the image under the embedding of its white end, labelled with the class of edges it belongs to. The probability distribution of the position of the labelled points is a (multitype) determinantal random field. The kernel of this random field is singular, since the particles are forced to sit on a set of Lebesgue measure 0 (the image of the white vertices).

We would like to indicate that the dimer model is not the only model from statistical physics whose correlations have a determinantal form. We cite the example of the random uniform spanning tree model [5]. A spanning tree of a graph G is a connex subgraph without cycles covering all the vertices of G . For a finite graph, the number of spanning trees equals the determinant of the discrete Laplacian of the graph. The probability that k edges appear in a uniform spanning tree is the determinant of a matrix whose entries are *transfert impedances*, which are combinations of Green functions. Temperley [59] discovered a bijection between the uniform spanning tree model on (a piece of) \mathbb{Z}^2 and

the random tilings with dominos. This correspondence has been widely extended to other graphs [35, 36].

4 Lozenge tilings and the Dyson model

A dimer configuration on the honeycomb lattice H is, by duality, in correspondence with a tiling of the plane with three different types of rhombi, which can be viewed as a three-dimensional landscape made of cubes piled up.

This three-dimensional interpretation of dimer configurations on subgraphs of H has been used for example to modelize a melting crystal corner [7, 44]. A dimer configuration of H with asymptotic constraints on the slope of the height function, as the one represented on figure 4.1 can be viewed as the corner of an infinitely large crystal from which some atoms (small cubes) escaped.

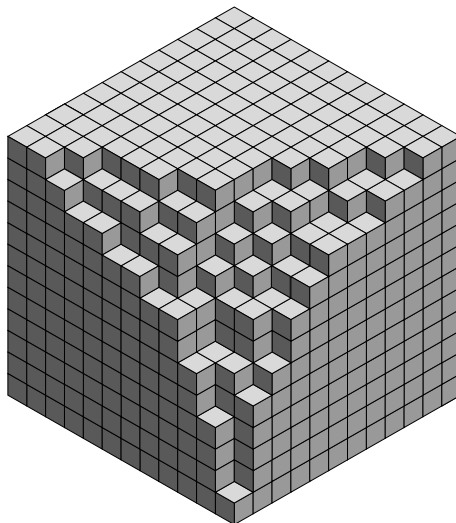


Figure 4.1: A melting crystal corner.

This crystal corner can be described by the family of paths formed by rhombi with a vertical side, separating zones tiled with horizontal rhombi. Using the techniques of [44], Ferrari and Spohn [13] studied the fluctuations of the first ledge, separating the frozen region and the tempered one. The fluctuations of this first ledge are related in the scaling limit (when the size of the atoms goes to zero) to the *Airy process*, which describes the fluctuation of the upper path in a family of N Ornstein-Uhlenbeck processes conditioned not to intersect, also known as the *Dyson model*, in the limit when N goes to $+\infty$.

In the limit of an infinity large crystal corner, the local statistics are given by the Gibbs measure with a slope equal to that of the asymptotic height function [31]. We consider the Gibbs measure corresponding to the local statistics in the neighbourhood of this first ledge. In the random configuration, edges of type b and c form a infinite family of non-intersecting paths. In this chapter, we study the scaling limit of this family of paths and prove that their distribution in the limit coincide with the so-called *sine process* describing the bulk of the Dyson model in the stationary regime.

4.1 Non colliding random paths

A dimer configuration of the honeycomb lattice is in correspondance by duality with a tiling of the plane with rhombi of three different types. The type of a rhombi refers to the orientation – and therefore to the weight a , b or c – of the corresponding edge.

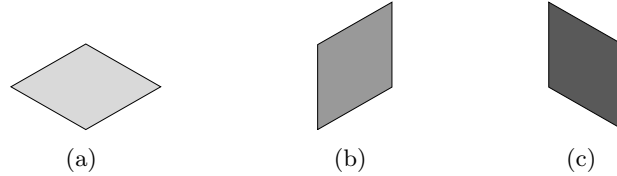


Figure 4.2: The different types of rhombi in a tiling corresponding to a dimer configuration on the honeycomb lattice.

In such a tiling, rhombi of type b and c form infinite paths from left to right that cannot cross each other. This collection of paths characterizes completely the whole tiling. In this chapter, we are interested in the limiting distribution of these paths when the probabilities of apparition of b - and c -rhombi are equal to each other and tend to zero. This is achieved for example by taking $b = c = 1$ and letting a go to 2 from below. Recall that if a is greater than 2, then the system is frozen, and with probability 1, we will see only a -rhombi. To label vertices of the graph, we use the system of coordinates (c, y) described in section 2.8.

Let $\varepsilon > 0$ be small. The inverse Kasteleyn operator K_ε^{-1} for the weights $a = 2 \cos(\frac{\varepsilon}{2})$, $b = c = 1$ between \mathbf{w} and black vertex $\mathbf{b}_y^{(c)}$

$$\begin{aligned} K_\varepsilon^{-1}(\mathbf{b}_y^{(c)}, \mathbf{w}) &= \iint_{\mathbb{T}^2} \frac{z^{-y} w^x}{a + b/w + cz} \frac{dz}{2i\pi z} \frac{dw}{2i\pi w} = \iint_{\mathbb{T}^2} \frac{(zw)^{-y} w^{x+y}}{a + \frac{1}{w}(1 + zw)} \frac{dz}{2i\pi z} \frac{dw}{2i\pi w} \\ &= \int_{-\pi}^{\pi} \int_{S^1} \frac{e^{-iy\theta} w^c}{a + \frac{1}{w}(1 + e^{i\theta})} \frac{dw}{2i\pi w} \frac{d\theta}{2\pi} \\ &= \int_{-\pi}^{\pi} e^{i\theta(-y+c/2)} \left(\int_{S^1} \frac{u^c}{2 \cos(\varepsilon/2)u + 2 \cos(\theta/2)} \frac{du}{2i\pi} \right) \frac{d\theta}{2\pi} \end{aligned}$$

The pole at $u = -\frac{\cos(\theta/2)}{\cos(\varepsilon/2)}$ is outside of the unit disk if and only if $2 \cos(\theta/2) > a$, *i.e.* if and only if $\theta \in (-\varepsilon, \varepsilon)$. The integral over u in the definition of K_ε^{-1} can be computed using residues, and we get the following expressions for the entries of that operator

$$K_\varepsilon^{-1}(\mathbf{b}_y^c, \mathbf{w}) = \begin{cases} \frac{(-1)^{c+1}}{2 \cos(\varepsilon/2)} \int_{[-\varepsilon, \varepsilon]} \left(\frac{\cos(\theta/2)}{\cos(\varepsilon/2)} \right)^c e^{i\theta(-y+c/2)} \frac{d\theta}{2\pi} & \text{if } c < 0 \\ \frac{(-1)^c}{2 \cos(\varepsilon/2)} \int_{[-\pi, \pi] \setminus [-\varepsilon, \varepsilon]} \left(\frac{\cos(\theta/2)}{\cos(\varepsilon/2)} \right)^c e^{i\theta(-y+c/2)} \frac{d\theta}{2\pi} & \text{if } c \geq 0 \end{cases} \quad (4.1)$$

Since a is close to 2, one sees in a typical configuration large zones tiled by rombi of type a , separated by paths made of tiles of type b and c , the distance between paths being larger and larger as a gets closer to 2.

As the paths become more and more distant, they should behave like simple random walks since they do not feel the presence of other paths. Indeed, if we condition on having a path passing through a given point, one can compute the law of the n first steps of the path from this point. The probability that a path of rhombi passes through vertices labelled by $(0, y_0), \dots, (n, y_n)$, given that the horizontal edge $(\mathbf{w}_0^{c_0}, \mathbf{b}_0^{c_0})$ is not covered by a dimer, is given by the following expression

$$\mathbb{P} \left[\begin{array}{c} \text{Diagram of a path of rhombi starting at } (c_0, y_0) \\ \text{Diagram of a rhombus with a dimer crossing it at } (c_0, y_0) \end{array} \right] = \frac{1}{1 - aK_\varepsilon^{-1}(\mathbf{b}_0, \mathbf{w}_0)} \det \begin{bmatrix} K_\varepsilon^{-1}(\mathbf{b}_0, \mathbf{w}_1) & \cdots & K_\varepsilon^{-1}(\mathbf{b}_{n-1}, \mathbf{w}_1) \\ \vdots & \ddots & \vdots \\ K_\varepsilon^{-1}(\mathbf{b}_0, \mathbf{w}_n) & \cdots & K_\varepsilon^{-1}(\mathbf{b}_{n-1}, \mathbf{w}_n) \end{bmatrix} \quad (4.2)$$

where \mathbf{b}_j and \mathbf{w}_j are shortcuts for $\mathbf{b}_j^{c_j}$ and $\mathbf{w}_j^{c_j}$.

Since $K^{-1}(\mathbf{b}_j, \mathbf{w}_j) = \frac{1}{2} + o(1)$, and $K^{-1}(\mathbf{b}_j, \mathbf{w}_i) = \frac{\varepsilon}{2} + O(\varepsilon)$ if $j < i$, the determinant in (4.2) equals up to terms of smaller order

$$\det \begin{bmatrix} 0 & \frac{1}{2} & \star & \cdots & \star \\ 0 & 0 & \frac{1}{2} & \ddots & \vdots \\ \vdots & & \ddots & \ddots & \star \\ 0 & & & 0 & \frac{1}{2} \\ \frac{\varepsilon}{2} & 0 & \cdots & \cdots & 0 \end{bmatrix} = \frac{\varepsilon}{2^n} \quad (4.3)$$

and hence, the probability (4.2) equals

$$\frac{1}{\varepsilon + o(\varepsilon)} \left(\frac{\varepsilon}{2^n} + o(\varepsilon) \right) = \frac{1}{2^n} + o(1) \quad (4.4)$$

When ε goes to zero, this conditional probability converges to the corresponding probability for a simple random walk. In the limit we are left with an infinite collection of

random paths that individually behave like a random walk, but that are conditioned not to intersect with each other. This looks like a discretized version of the so-called *Dyson model*, modeling the diffusion of particles conditioned not to collide, when the number of particles goes to infinity.

4.2 The Dyson model and the sine process

The *Dyson model* [12] is a random process on Hermitian $n \times n$ matrices H , where the independent coefficients of each matrix H independently undergo diffusion. More precisely, they execute independently Brownian motion subject to a harmonic restoring force. When $n = 1$, this is the so-called *Ornstein-Uhlenbeck* process. Dyson observed that the equilibrium measure is the *Gaussian Unitary Ensemble* (GUE) measure of random matrix theory. In a Dyson process, one is generally interested in the distribution of the eigenvalues of the matrix, seen as curves parameterized by time. Given $\tau_1 < \dots < \tau_k$ and a sequence of subsets $(I_j)_{j=1}^k$ of \mathbb{R} , the distribution of the number of curves crossing subset I_k at time τ_k for every k can be expressed in terms of determinants of the *extended Hermite kernel*, a space-time extension of the Hermite kernel appearing in the GUE. In particular, the probability that all the curves avoid all the subsets is given by the *Fredholm determinant* of this kernel.

If we scale the Dyson process in the bulk when n goes to infinity, we get the *sine process* associated with the *extended sine kernel* given by

$$S(t - t', y' - y) = \begin{cases} \int_0^1 e^{-(t'-t)\phi^2/2} \cos(\phi(y' - y)) \frac{d\phi}{\pi} & \text{if } t' \leq t \\ - \int_1^{+\infty} e^{-(t'-t)\phi^2/2} \cos(\phi(y' - y)) \frac{d\phi}{\pi} & \text{if } t' > t \end{cases} \quad (4.5)$$

When $t = t'$, this reduces to the usual *sine kernel* $\frac{\sin(y' - y)}{\pi(y' - y)}$.

The sine process describes an infinite system of particles repulsing each other by Coulomb force, and which is homogeneous both in space and time. Such a system has been studied by [12, 58, 26]

The probability that the number $N_{I_j}(\tau_j)$ of curves crossing I_j equals n_j at time τ_j is given by the following expression

$$\begin{aligned} & \mathbb{P} [\forall j \in \{1, \dots, k\} N_{I_j}(\tau_j) = n_j] \\ &= \sum_{p \in \mathbb{N}^k} \frac{(-1)^{|p|}}{p! n!} \int \dots \int_{(\tau_1, I_1)^{n_1} \times \dots \times (\tau_k, I_k)^{n_k}} \det_{|n+p|}(S(\xi_i - \xi_j)) d^{n+p} \xi \end{aligned} \quad (4.6)$$

where ξ_i stands for the variables (τ, y) ranging over the i th factor of the cartesian product $(\tau_1, I_1)^{n_1} \times \dots \times (\tau_k, I_k)^{n_k}$. In this expression, we used multi-index notations:

$$n! = \prod_{j=1}^k n_j!, \quad |n| = \sum_{j=1}^k n_j.$$

4.3 Convergence to the sine process

For a fixed ε , we represent our paths of rhombi by continuous functions as follows. We first embed the honeycomb lattice H in the plane such that every white vertex with coordinates (\mathbf{c}, y) is mapped to the point $(\frac{\varepsilon^2}{8}\mathbf{c}, \frac{\varepsilon}{2}(2y - \mathbf{c}))$. This diffusive scaling seems natural since the paths of rhombi behave like random walks at small scales.

A path of rhombi is then encoded by the piecewise linear path joining all the white vertices covered by this path. We get a bi-infinite family of paths $(X_n^\varepsilon(t))_{n \in \mathbb{Z}}$, indexed by time $t \in \mathbb{R}$. By convention, the path corresponding to the index 0 is the one passing the closest to $y = 0$ at time 0.

Such a family of paths is in bijection with a random tiling with rhombi. The Gibbs measure on tilings (or equivalently on dimer configurations of H) can therefore be viewed as a probability measure on $\mathcal{C}(\mathbb{R}^\infty)$, the set of continuous functions on \mathbb{R} with values in $\mathbb{R}^\infty = \{\bar{x} = (x_j)_{j \in \mathbb{Z}} \mid \forall j \in \mathbb{Z} \ x_j \in \mathbb{R}\}$. The space \mathbb{R}^∞ is a complete separable metric space with the metric

$$\text{dist}(\bar{x}, \bar{y}) = \sum_{k=-\infty}^{+\infty} \frac{1}{2^{|k|}} \frac{|x_k - y_k|}{1 + |x_k - y_k|}$$

The topology induced by this distance is the topology of coordinatewise convergence, and the sets

$$B_{k,\varepsilon}(\bar{x}) = \{\bar{y} \mid \forall j \in \{-k, \dots, k\} \ |y_j - x_j| < \varepsilon\}$$

form a basis for this topology.

The aim of this section is to prove the following theorem

Theorem 4.1. *The probability measures (\mathbb{P}_ε) , as measures on bi-infinite families of continuous paths on \mathbb{R} , converge weakly in $\mathcal{C}(\mathbb{R}^\infty)$ to the sine process.*

The proof of the convergence of the ensemble of paths to the sine model is based on precise asymptotics of the inverse Kasteleyn operator when ε goes to zero, that are proven in lemma 4.1. These asymptotics allow us to prove the finite dimensional distributions of \mathbb{P}_ε to those for the sine process in proposition 4.1. Then we prove that (\mathbb{P}_ε) is tight in proposition 4.2. A key point of the proof of this proposition is a simple comparison between probability for paths of rhombi and for simple random walks given by lemma 4.2.

Since the proofs of proposition 4.1 and 4.2 are rather long and technical, they are exposed separately in section 4.4 and 4.5 respectively.

Let us begin with the asymptotics of the kernel in the scaling regime described above, when ε goes to zero.

Lemma 4.1. *For every $\varepsilon > 0$, let $(\mathbf{c}_\varepsilon, y_\varepsilon) \in \mathbb{Z}^2$ such that*

$$\lim_{\varepsilon \rightarrow 0} \frac{1}{8} \varepsilon^2 \mathbf{c}_\varepsilon = T \in \mathbb{R}, \quad \lim_{\varepsilon \rightarrow 0} \frac{1}{2} \varepsilon (2y_\varepsilon - \mathbf{c}_\varepsilon) = Y \in \mathbb{R}. \quad (4.7)$$

- If $T \neq 0$, then

$$\lim_{\varepsilon \rightarrow 0} \frac{(-1)^{\mathbf{c}_\varepsilon+1}}{\varepsilon} a \mathbf{K}_\varepsilon^{-1}(\mathbf{c}_\varepsilon, y_\varepsilon) = e^T S(T, Y). \quad (4.8)$$

- If $\mathbf{c}_\varepsilon = 0$ and $y_\varepsilon \neq 0$ for ε small enough,

$$\lim_{\varepsilon \rightarrow 0} \frac{-a}{\varepsilon} \mathbf{K}_\varepsilon^{-1}(0, y_\varepsilon) = \frac{\sin(Y)}{\pi Y} = e^0 S(0, Y). \quad (4.9)$$

- If $\mathbf{c}_\varepsilon = 0$ and $y_\varepsilon = 0$ for ε small enough,

$$\lim_{\varepsilon \rightarrow 0} \frac{1 - a \mathbf{K}_\varepsilon^{-1}(0, 0)}{\varepsilon} = \frac{1}{\pi} = e^0 S(0, 0). \quad (4.10)$$

Moreover, the quantities $\frac{a \mathbf{K}_\varepsilon^{-1}(\mathbf{c}_\varepsilon, y_\varepsilon)}{\varepsilon}$ (or $\frac{1 - a \mathbf{K}_\varepsilon^{-1}(0, 0)}{\varepsilon}$ if $(\mathbf{c}_\varepsilon, y_\varepsilon) = (0, 0)$) are uniformly bounded in ε .

This lemma shows that the discrete kernel for the dimer model on the honeycomb lattice converges, up to a factor e^T and except for the third case, to the extended sine kernel.

Proof:

Suppose first that $T < 0$. In this case, for ε small enough, $\mathbf{c}_\varepsilon < 0$ and

$$\begin{aligned} \mathbf{K}_\varepsilon^{-1}(\mathbf{c}_\varepsilon, y_\varepsilon) &= \frac{(-1)^{\mathbf{c}_\varepsilon+1}}{a} \int_{-\varepsilon}^{\varepsilon} \left(\frac{2 \cos(\theta/2)}{a} \right)^{\mathbf{c}_\varepsilon} e^{i(-y_\varepsilon + \mathbf{c}_\varepsilon/2)\theta} \frac{d\theta}{2\pi} \\ &= \frac{(-1)^{\mathbf{c}_\varepsilon+1}}{a} \int_{-\varepsilon}^{\varepsilon} \left(\frac{\cos(\theta/2)}{\cos(\varepsilon/2)} \right)^{\frac{8T}{\varepsilon^2}(1+o(1))} e^{-i\theta \frac{Y}{\varepsilon}(1+o(1))} \frac{d\theta}{2\pi} \\ &= \frac{\varepsilon (-1)^{\mathbf{c}_\varepsilon+1}}{a} \int_{-1}^1 \left(\frac{\cos(\frac{\varepsilon\phi}{2})}{\cos(\frac{\varepsilon}{2})} \right)^{\frac{8T}{\varepsilon^2}(1+o(1))} e^{-iY\phi(1+o(1))} \frac{d\phi}{\pi} \\ &= \frac{\varepsilon (-1)^{\mathbf{c}_\varepsilon+1}}{a} \int_{-1}^1 \left(1 - \frac{\varepsilon^2(\phi^2 - 1)}{8} + o(\varepsilon^2) \right)^{\frac{8T}{\varepsilon^2}(1+o(1))} e^{-iY\phi+o(1)} \frac{d\phi}{2\pi} \end{aligned}$$

When ε goes to zero, the integrand converges to $e^T e^{-\phi^2 T} e^{-iY\phi}$. A simple application of Lebesgue dominated convergence theorem shows then that

$$\begin{aligned} \lim_{\varepsilon \rightarrow 0} \frac{(-1)^{\mathbf{c}_\varepsilon+1}}{\varepsilon} a \mathbf{K}_\varepsilon^{-1}(\mathbf{c}_\varepsilon, y_\varepsilon) &= e^T \int_{-1}^1 e^{-\phi^2 T} e^{-iY\phi} \frac{d\phi}{2\pi} \\ &= e^T \int_0^1 e^{-\phi^2 T} \cos(Y\phi) \frac{d\phi}{\pi} = S(T, Y). \quad (4.11) \end{aligned}$$

When $T > 0$, $\mathbf{c}_\varepsilon > 0$ for ε small enough, we have

$$\mathbf{K}_\varepsilon^{-1}(\mathbf{c}_\varepsilon, y_\varepsilon) = \frac{(-1)^{\mathbf{c}_\varepsilon}}{a} \int_{[-\pi, \pi] \setminus [-\varepsilon, \varepsilon]} \left(\frac{2 \cos(\theta/2)}{a} \right)^{\mathbf{c}_\varepsilon} e^{i(-y_\varepsilon + \mathbf{c}_\varepsilon/2)\theta} \frac{d\theta}{2\pi} \quad (4.12)$$

$$= \frac{(-1)^{\mathbf{c}_\varepsilon}}{a} \int_\varepsilon^\pi \left(\frac{2 \cos(\theta/2)}{a} \right)^{\mathbf{c}_\varepsilon} \cos((-y + \mathbf{c}/2)\theta) \frac{d\theta}{\pi}. \quad (4.13)$$

$$(4.14)$$

If we change the variable in the integral, defining $\phi = \varepsilon\theta$, we get

$$\begin{aligned} \mathbf{K}_\varepsilon^{-1}(\mathbf{c}_\varepsilon, y_\varepsilon) &= \frac{\varepsilon(-1)^{\mathbf{c}}}{a} \int_1^{\pi/\varepsilon} \left(\frac{\cos(\frac{\varepsilon\phi}{2})}{\cos(\frac{\varepsilon}{2})} \right)^{\frac{8T}{\varepsilon^2}(1+o(1))} \cos(Y\phi + o(1)) \frac{d\phi}{\pi} \\ &= \frac{\varepsilon(-1)^{\mathbf{c}}}{a} \int_1^A \left(\frac{\cos(\frac{\varepsilon\phi}{2})}{\cos(\frac{\varepsilon}{2})} \right)^{\frac{8T}{\varepsilon^2}(1+o(1))} \cos(Y\phi + o(1)) \frac{d\phi}{\pi} \\ &\quad + \frac{\varepsilon(-1)^{\mathbf{c}}}{a} \int_A^{\pi/\varepsilon} \left(\frac{\cos(\frac{\varepsilon\phi}{2})}{\cos(\frac{\varepsilon}{2})} \right)^{\frac{8T}{\varepsilon^2}(1+o(1))} \cos(Y\phi + o(1)) \frac{d\phi}{\pi} \end{aligned}$$

for a given large number A . The second integral can be bounded by

$$\left| \frac{\varepsilon(-1)^{\mathbf{c}}}{a} \int_A^{\pi/\varepsilon} \left(\frac{\cos(\frac{\varepsilon\phi}{2})}{\cos(\frac{\varepsilon}{2})} \right)^{\frac{8T}{\varepsilon^2}(1+o(1))} \cos(Y\phi + o(1)) \frac{d\phi}{\pi} \right| \leq C e^{-T(A-1)+o(1)} \quad (4.15)$$

uniformly in ε for ε small enough. A domination argument shows that the first integral converges to

$$e^T \int_1^A e^{-\phi^2 T} \cos(Y\phi) \frac{d\phi}{\pi} \quad (4.16)$$

As a consequence, letting A go to ∞ , we get

$$\lim_{\varepsilon \rightarrow 0} \frac{(-1)^{\mathbf{c}}}{\varepsilon} a \mathbf{K}_\varepsilon^{-1}(y, \mathbf{c}) = e^T \int_1^{+\infty} e^{-\phi^2 T} \cos(Y\phi) \frac{d\phi}{\pi}. \quad (4.17)$$

When $\mathbf{c}_\varepsilon = 0$, $\mathbf{K}_\varepsilon^{-1}(\mathbf{c}_\varepsilon, y_\varepsilon)$ given by

$$\mathbf{K}_\varepsilon^{-1}(0, y_\varepsilon) = \frac{1}{a} \int_\varepsilon^\pi \cos(y_\varepsilon \theta) \frac{d\theta}{\pi}. \quad (4.18)$$

If $y_\varepsilon \neq 0$, then

$$\frac{(-1)a}{\varepsilon} \mathbf{K}_\varepsilon^{-1}(0, y_\varepsilon) = -\frac{a \sin(\pi y_\varepsilon) - \sin(y_\varepsilon \varepsilon)}{\varepsilon a \pi} = \frac{\sin(Y)}{\pi Y} + o(1). \quad (4.19)$$

However, if $y_\varepsilon = 0$ for ε small enough, $K_\varepsilon^{-1}(0, 0) = \frac{\pi - \varepsilon}{a\pi}$ and thus

$$\lim_{\varepsilon \rightarrow 0} \frac{1 - aK_\varepsilon^{-1}(0, 0)}{\varepsilon} = \frac{1}{\pi}. \quad (4.20)$$

The uniform bounds are obtained directly from the expression of K_ε^{-1} given by (4.1). When $T < 0$,

$$\left| \frac{a}{\varepsilon} K_\varepsilon^{-1}(\mathbf{c}_\varepsilon, y_\varepsilon) \right| = \left| \frac{1}{\varepsilon} \int_{-\varepsilon}^{\varepsilon} \left(\frac{2 \cos(\theta/2)}{a} \right)^c e^{i\theta(-y+\mathbf{c}/2)} \frac{d\theta}{2\pi} \right| \leq \frac{1}{\pi} \left(1 - \left(\frac{\varepsilon}{2} \right)^2 \right)^{-c_\varepsilon/2} \leq C. \quad (4.21)$$

When $T > 0$,

$$\begin{aligned} \left| \frac{a}{\varepsilon} K_\varepsilon^{-1}(\mathbf{c}_\varepsilon, y_\varepsilon) \right| &= \left| \frac{1}{\varepsilon} \int_{[-\pi, \pi] \setminus [-\varepsilon, \varepsilon]} \left(\frac{2 \cos(\theta/2)}{a} \right)^c e^{i\theta(-y+\mathbf{c}/2)} \frac{d\theta}{2\pi} \right| \\ &\leq \frac{1}{\pi} \left(1 - \left(\frac{\varepsilon}{2} \right)^2 \right)^{-c_\varepsilon/2} \int_1^{\frac{\pi}{\varepsilon}} e^{-\frac{\varepsilon^2 c_\varepsilon}{8} t^2} dt \leq C. \end{aligned} \quad (4.22)$$

When $c_\varepsilon = 0$, the bound is obtained by a direct evaluation of (4.1). \square

As in the case of the sine process, for given times τ_1, \dots, τ_k and unions of intervals I_1, \dots, I_k , we can compute for every ε the probability that for every j , the number $N_{I_j}^\varepsilon(\tau_j)$ of paths in I_j at time τ_j equals n_j . The following proposition states that these probabilities converges to the corresponding probabilities for the sine process.

Proposition 4.1. *The finite dimensional distributions of X^ε converge to that of the extended sine process.*

For all $\tau_1, \dots, \tau_m \in \mathbb{R}$, and $I_1, \dots, I_m \subset \mathbb{R}$ finite unions of intervals,

$$\lim_{\varepsilon \rightarrow 0} \mathbb{P}_\varepsilon [N_{I_1}^\varepsilon(\tau_1) = n_1, \dots, N_{I_k}^\varepsilon(\tau_k) = n_k] = \mathbb{P} [N_{I_1}(t_1) = n_1, \dots, N_{I_k}(t_k) = n_k] \quad (4.23)$$

We prove also tightness of the family of probability measures (\mathbb{P}_ε) in $\mathcal{C}(\mathbb{R}^\infty)$. Since \mathbb{R}^∞ is a nice complete separable metric space, tightness is characterized by the following two properties [3] we have to check:

Proposition 4.2.

i) *The sequence of distributions of $(X^\varepsilon(0))$ is tight: for each $\eta > 0$, there exists a sequence of closed intervals $([-a_k, a_k])_{k \in \mathbb{Z}}$ such that*

$$\forall \varepsilon, \quad \mathbb{P}_\varepsilon [\exists k \in \mathbb{Z}, X_k(0) \notin [-a_k, a_k]] < \eta \quad (4.24)$$

ii) *For each $L > 0$, for each positive δ and η , there exists an $\alpha \in (0, L)$ such that*

$$\forall \varepsilon, \quad \mathbb{P}_\varepsilon \left[\sup_{\substack{-L/2 < s, t < L/2 \\ |s-t| < \alpha}} \text{dist}((X(s), X(t)) > \delta \right] < \eta \quad (4.25)$$

Tightness and convergence of finite dimensional distributions of the family (\mathbb{P}_ε) imply the weak convergence of this family to a probability measure on $\mathcal{C}(\mathbb{R}^\infty)$ whose finite distributions coincide with that of the sine process. The family of discrete random paths therefore converges weakly to the family of random continuous paths described by the sine process.

4.4 Proof of proposition 4.1

This section is devoted to the proof of the convergence of finite dimensional distributions of the family (\mathbb{P}_ε) . It makes use of standard objects in the theory of random point fields, described in the previous chapter.

We denote by τ^ε the quantity $\lfloor \frac{\tau}{8\varepsilon^2} \rfloor$ and $(I)_\tau^\varepsilon$ the set of integers $\{y \in \mathbb{Z} \mid \varepsilon(y - \frac{1}{2}\tau^\varepsilon) \in I\}$. The set of white vertices with coordinates $(\mathbf{c}, y) \in \{\tau^\varepsilon\} \times (I)_\tau^\varepsilon$ are the white vertices the closest to $\{\tau\} \times I$.

The function Q^ε of the variable $z = (z_1, \dots, z_k) \in \mathbb{C}^k$ defined by

$$Q^\varepsilon(z) = \mathbb{E}_\varepsilon \left[\prod_{j=1}^k (1 - z_j)^{N_{I_j}(\tau_j^\varepsilon)} \right] = \sum_{n \in \mathbb{N}^k} \mathbb{E}_\varepsilon \left[\prod_{j=1}^k \frac{N_{I_j}^\varepsilon!}{(N_{I_j}^\varepsilon - n_j)!} \right] \frac{(-z)^n}{n!} \quad (4.26)$$

where $z^n = \prod_{j=1}^k z_j^{n_j}$, is a generating function for the probabilities we are interested in. Indeed, an inclusion-exclusion argument shows that

$$\mathbb{P}_\varepsilon [N_{I_1}^\varepsilon(t_1) = n_1, \dots, N_{I_k}^\varepsilon(t_k) = n_k] = \sum_{p \in \mathbb{N}^k} \frac{(-1)^p}{n! p!} \mathbb{E}_\varepsilon \left[\prod_{j=1}^k \frac{N_{I_j}^\varepsilon!}{(N_{I_j}^\varepsilon - (n_j + p_j))!} \right] \quad (4.27)$$

$$= \frac{(-1)^n}{n!} \frac{\partial^n}{\partial z^n} Q^\varepsilon(z) \Big|_{z=(1, \dots, 1)}. \quad (4.28)$$

We will show that Q^ε converges to the corresponding generating function for the sine process. For this, we first compute the quantities $\mathbb{E}_\varepsilon \left[\prod_{j=1}^k \frac{N_{I_j}^\varepsilon!}{(N_{I_j}^\varepsilon - n_j)!} \right]$ and their limit when ε goes to 0. Up to smaller terms, these quantities are given by the sum over all distinct n_j -tuples of white vertices in $\{\tau_j^\varepsilon\} \times (I_j)_{\tau_j}^\varepsilon$ for $j \in \{1, \dots, k\}$ of the probability that these white vertices are covered by a path of rhombi, or equivalently, that the horizontal edges with weight a incident with these vertices are not present in the random dimer configuration. We have

$$\mathbb{E}_\varepsilon \left[\prod_{j=1}^k \frac{N_{I_j}^\varepsilon!}{(N_{I_j}^\varepsilon - n_j)!} \right] = \sum_{\substack{j=1, \dots, k \\ y_{(j,1)}, \dots, y_{(j,n_j)} \in (I_j)_{\tau_j}^\varepsilon \\ \text{distinct}}} \mathbb{P}_\varepsilon \left[\mathbf{a}_{\tau_1^\varepsilon, y_{(1,1)}}, \dots, \mathbf{a}_{\tau_1^\varepsilon, y_{(1,n_1)}}, \dots, \mathbf{a}_{\tau_k^\varepsilon, y_{(k,n_k)}} \notin \mathcal{C} \right] \quad (4.29)$$

where $\mathbf{a}_{\mathfrak{c},y}$ is the horizontal edge with weight a incident with the white vertex with coordinates (\mathfrak{c}, y) .

Using the multilinearity of the determinant, one can write each of these probabilities

$$\mathbb{P}_\varepsilon \left[\mathbf{a}_{\tau_1^\varepsilon, y(1,1)}, \dots, \mathbf{a}_{\tau_1^\varepsilon, y(1, n_1)}, \dots, \mathbf{a}_{\tau_k^\varepsilon, y(k, n_k)} \notin \mathcal{C} \right] \quad (4.30)$$

as a determinant by formula (1.6)

$$\det(\delta_{i,j} - aK_\varepsilon^{-1}(\tau_{\langle i \rangle}^\varepsilon - \tau_{\langle j \rangle}^\varepsilon, y_i - y_j)) = \det_{|n|} \begin{bmatrix} 1 - aK_\varepsilon^{-1}(\tau_1^\varepsilon - \tau_1^\varepsilon, y(1,1) - y(1,1)) & \cdots & -aK_\varepsilon^{-1}(\tau_k^\varepsilon - \tau_1^\varepsilon, y(k, n_k) - y(1,1)) \\ \vdots & & \vdots \\ \vdots & \ddots & \vdots \\ \vdots & & \vdots \\ -aK_\varepsilon^{-1}(\tau_1^\varepsilon - \tau_k^\varepsilon, y(1, n_1) - y(k, n_k)) & \cdots & 1 - aK_\varepsilon^{-1}(\tau_k^\varepsilon - \tau_k^\varepsilon, y(k, n_k) - y(k, n_k)) \end{bmatrix} \quad (4.31)$$

where i and j belong to the following list of indices

$$((1, 1), \dots, (1, n_1), \dots, (k, 1), \dots, (k, n_k)) \quad (4.32)$$

and the angular brackets of a couple $\langle (i, j) \rangle$ represent its first factor i .

The determinant is unchanged if we multiply each column i by $e^{-\tau_{\langle i \rangle}^\varepsilon}(-1)^{\tau_{\langle i \rangle}^\varepsilon}$ and each line by $e^{\tau_{\langle j \rangle}^\varepsilon}(-1)^{-\tau_{\langle j \rangle}^\varepsilon}$. It follows from lemma 4.1 that this determinant is asymptotic to

$$\varepsilon^{|n|} \det(S(\tau_{\langle i \rangle}^\varepsilon - \tau_{\langle j \rangle}^\varepsilon), Y_i^\varepsilon - Y_j^\varepsilon) \quad (4.33)$$

where $Y_j^\varepsilon = \varepsilon(y_j - \tau_{\langle j \rangle}^\varepsilon) \in I_j$. The sum (4.29) becomes a Riemann sum converging as ε goes to zero to the following integral

$$\int \cdots \int_{(\tau_1, I_1)^{n_1} \times \cdots \times (\tau_k, I_k)^{n_k}} \det(S(\xi_i - \xi_j)) d^n \xi. \quad (4.34)$$

Therefore, the coefficients of $Q^\varepsilon(z)$ converge to those of $Q(z)$, the generating function for the sine process. By lemma 4.1, the entries of the matrix in (4.31) are uniformly bounded, say by M . By applying Hadamard's lemma, we bound the sum (4.29) by

$$\left| \mathbb{E}_\varepsilon \left[\prod_{j=1}^k \frac{N_{I_j}^\varepsilon!}{(N_{I_j}^\varepsilon - n_j)!} \right] \right| \leq \left(\prod_{j=1}^k |I_j|^{n_j} \right) (|n|M^2)^{|n|/2} \quad (4.35)$$

uniformly in ε . Thus, by Lebesgue's dominated convergence theorem, all the derivatives of the series $Q^\varepsilon(z)$ converge uniformly on compact sets of \mathbb{C}^k to the corresponding derivatives of the generating function $Q(z)$ for the sine process. In particular,

$$\lim_{\varepsilon \rightarrow 0} \mathbb{P}_\varepsilon [N_{I_1}^\varepsilon(t_1) = n_1, \dots, N_{I_k}^\varepsilon(t_k) = n_k] = \mathbb{P} [N_{I_1}(t_1) = n_1, \dots, N_{I_k}(t_k) = n_k].$$

4.5 Proof of proposition 4.2

This section is devoted to the proof of the tightness of the family of probability measures $(\mathbb{P}_\varepsilon)_{\varepsilon>0}$.

First, we check the the first point $i)$ of proposition 4.2. Let $\eta > 0$. We look for a sequence of segments such that

$$\forall \varepsilon, \quad \mathbb{P}_\varepsilon [\exists k \in \mathbb{Z}, X_k(0) \notin [-a_k, a_k]] < \eta$$

is satisfied. If we take a sequence verifying that

$$\forall k \in \mathbb{N} \quad a_k = a_{-k} \quad \text{and} \quad a_{k+1} > a_k \tag{4.36}$$

then the condition (4.24) is equivalent to

$$\forall \varepsilon > 0 \quad \mathbb{P}_\varepsilon [\exists k \in \mathbb{N}, N_{a_k} < 2k + 1] < \eta \tag{4.37}$$

where $N_{a_k} = N_{[-a_k, a_k]}(0)$ is the number of paths crossing the interval $[-a_k, a_k]$ at time 0. We will use Chebyshev inequality to get a bound on the probability (4.37). For this, we need first to estimate and bound the average and the variance of the random variable $N_L = N_{[-L, L]}^\varepsilon(0)$ for any $L > 0$.

The average of N_L under \mathbb{P}_ε is given by

$$\mathbb{E}_\varepsilon [N_L] = \sum_{y \in [-\frac{L}{\varepsilon}, \frac{L}{\varepsilon}] \cap \mathbb{Z}} \mathbb{P}_\varepsilon [\exists \text{ a path crossing at } (0, \varepsilon y)] \tag{4.38}$$

$$= \sum_{y \in [-\frac{L}{\varepsilon}, \frac{L}{\varepsilon}] \cap \mathbb{Z}} (1 - \mathbb{P}_\varepsilon [\mathbf{a}_y \in \mathcal{C}]) \tag{4.39}$$

$$= \left(2 \left\lfloor \frac{L}{\varepsilon} \right\rfloor + 1 \right) \frac{\varepsilon}{\pi} = \frac{2L}{\pi} (1 + o(1)) \tag{4.40}$$

Moreover, the variance of N_L is given by

$$\text{Var}_\varepsilon(N_L) = \mathbb{E}_\varepsilon [N_L^2] - \mathbb{E}_\varepsilon [N_L]^2 \tag{4.41}$$

$$= \mathbb{E}_\varepsilon [N_L(N_L - 1)] - \mathbb{E}_\varepsilon [N_L]^2 + \mathbb{E}_\varepsilon [N_L] < \mathbb{E}_\varepsilon [N_L] \tag{4.42}$$

Indeed, $\mathbb{E}_\varepsilon [N_L(N_L - 1)] - \mathbb{E}_\varepsilon [N_L]^2$, given by the following expression

$$\sum_{\substack{y, y' \in [-\frac{L}{\varepsilon}, \frac{L}{\varepsilon}] \cap \mathbb{Z} \\ y \neq y'}} \mathbb{P}_\varepsilon [\mathbf{a}_y, \mathbf{a}_{y'} \notin \mathcal{C}] - \left(\sum_{y \in [-\frac{L}{\varepsilon}, \frac{L}{\varepsilon}] \cap \mathbb{Z}} \mathbb{P}_\varepsilon [\mathbf{a}_y \notin \mathcal{C}] \right)^2 = \quad (4.43)$$

$$= \sum_{\substack{y, y' \in [-\frac{L}{\varepsilon}, \frac{L}{\varepsilon}] \cap \mathbb{Z} \\ y \neq y'}} \det \begin{bmatrix} 1 - a\mathbf{K}_\varepsilon^{-1}(0, 0) & -a\mathbf{K}_\varepsilon^{-1}(0, y - y') \\ -a\mathbf{K}_\varepsilon^{-1}(0, y' - y) & 1 - a\mathbf{K}_\varepsilon^{-1}(0, 0) \end{bmatrix} - \left(\sum_{y \in [-\frac{L}{\varepsilon}, \frac{L}{\varepsilon}] \cap \mathbb{Z}} 1 - a\mathbf{K}_\varepsilon^{-1}(0, 0) \right)^2 \quad (4.44)$$

$$= - \sum_{\substack{y, y' \in [-\frac{L}{\varepsilon}, \frac{L}{\varepsilon}] \cap \mathbb{Z} \\ y \neq y'}} a^2 \mathbf{K}^{-1}(0, y - y')^2 - (1 - a\mathbf{K}_\varepsilon^{-1}(0, 0))^2 (2 \lfloor \frac{L}{\varepsilon} \rfloor + 1) < 0 \quad (4.45)$$

is a sum of negative terms. By Chebyshev inequality, we get

$$\mathbb{P}_\varepsilon \left[N_L < \frac{L}{\pi} \right] \leq \mathbb{P}_\varepsilon \left[|N_L - \mathbb{E}_\varepsilon [N_L]| < \frac{L}{\pi} \right] \leq \frac{\text{Var}_\varepsilon(N_L)}{(L/\pi)^2} \leq \frac{2\pi}{L} + o(1) \quad (4.46)$$

Thus, for $\eta \leq \frac{\pi^2}{6}$, taking $a_k = \frac{\pi^3(k+1)^2}{3\eta}$, we finally get that

$$\mathbb{P}_\varepsilon [\exists k \in \mathbb{N}, N_{a_k} < k] \leq \sum_{k=0}^{+\infty} \mathbb{P}_\varepsilon [N_{a_k} < k] \quad (4.47)$$

$$\leq \sum_{k=0}^{+\infty} \mathbb{P}_\varepsilon \left[N_{a_k} < \frac{\pi^2(k+1)^2}{6\eta} \right] \quad (4.48)$$

$$\leq \sum_{k=0}^{+\infty} \frac{6\eta}{\pi^2(k+1)^2} = \eta \quad (4.49)$$

Therefore, the family of distributions of $(X(0))$ under \mathbb{P}_ε is tight.

The proof of point *ii*) goes as follows. First, as the topology on \mathbb{R}^∞ is that of coordinatewise convergence, the condition (4.25) is equivalent to

$$\forall L > 0, \forall \eta > 0, \forall k \in \mathbb{N}, \exists \alpha \in (0, L),$$

$$\forall \varepsilon > 0, \forall j \in \{-k, \dots, k\} \quad \mathbb{P}_\varepsilon \left[\sup_{\substack{s, t \in (-\frac{L}{2}, \frac{L}{2}) \\ |s-t| < \alpha}} |X_j(s) - X_j(t)| > \delta \right] < \eta \quad (4.50)$$

It is therefore sufficient to check this condition for each path separately. It is well-known that this property is true for simple random walks: for any $\delta > 0$, there exists an $\alpha > 0$ such that the number of properly rescaled walks (Y^ε) with $N = \lfloor L/\varepsilon \rfloor$ steps such that

$$\sup_{\substack{s, t \in (-\frac{L}{2}, \frac{L}{2}) \\ |s-t| < \alpha}} |Y(s) - Y(t)| > \delta \quad (4.51)$$

is less than $\eta 2^N$ uniformly in ε . Therefore, by the following, rather technical lemma 4.2, since the probability of a sequence of steps of X_j is bounded by a constant times the same probability for a simple random walk, we get by decomposing the event realisation by realisation of the path X_j from 0 to L ,

$$\mathbb{P}_\varepsilon \left[\sup_{\substack{s,t \in (-\frac{L}{2}, \frac{L}{2}) \\ |s-t| < \alpha}} |X_j(s) - X_j(t)| > \delta \right] < \text{Cst} \cdot \eta \quad (4.52)$$

where the constant Cst depends only in L .

Lemma 4.2. *Let $L > 0$. There exists a $c_L > 0$ such that for every ε small enough and every $(\omega_n)_{0 \leq n \leq \lfloor L/\varepsilon \rfloor}$ sequence of upward and downward steps, the probability that the first $\lfloor L/\varepsilon \rfloor$ steps of a path of rhombi X_j^ε , conditioned on its starting position (x_0, y_0) , is bounded by*

$$\mathbb{P}_\varepsilon \left[\text{first } \left\lfloor \frac{L}{\varepsilon} \right\rfloor \text{ steps of } X_j^\varepsilon \text{ coincide with } (\omega_n) \middle| X_j^\varepsilon \text{ starts at } (x_0, y_0) \right] \leq \frac{c_L}{2^{\lfloor L/\varepsilon \rfloor}} \quad (4.53)$$

Proof:

Define

$$g(\mathbf{c}, y) = \frac{1}{2} \int_{-\varepsilon}^{\varepsilon} (\cos \frac{\theta}{2})^{\mathbf{c}} e^{i\theta(-y+\mathbf{c}/2)} \frac{d\theta}{2\pi}. \quad (4.54)$$

Since

$$\int_{-\pi}^{\pi} (2 \cos(\theta/2))^{\mathbf{c}} e^{i\theta(-y+\mathbf{c}/2)} \frac{d\theta}{2\pi} = \sum_{k=0}^{\mathbf{c}} \binom{\mathbf{c}}{k} \int_{-\pi}^{\pi} e^{i\frac{\theta}{2}(2k-\mathbf{c})} e^{i\frac{\theta}{2}(-2y+\mathbf{c})} \frac{d\theta}{2\pi} = \binom{\mathbf{c}}{y}, \quad (4.55)$$

$\mathbf{K}^{-1}(\mathbf{c}, y)$ can be rewritten as

$$\mathbf{K}_\varepsilon^{-1}(\mathbf{c}, y) = \begin{cases} \left(-\frac{2}{a}\right)^{\mathbf{c}+1} g(\mathbf{c}, y) & \text{if } \mathbf{c} < 0, \\ \left(-\frac{2}{a}\right)^{\mathbf{c}+1} \left(g(\mathbf{c}, y) - \frac{1}{2^{\mathbf{c}+1}} \binom{\mathbf{c}}{y} \right) & \text{if } \mathbf{c} \geq 0 \end{cases} \quad (4.56)$$

Let $N = \lfloor \frac{L}{\varepsilon} \rfloor$. Suppose that the sequence (ω_n) corresponds to a path covering the vertices

$$\mathbf{b}_0 = \mathbf{b}_{y_0}^{(0)}, \mathbf{w}_1 = \mathbf{w}_{y_1}^{(1)}, \mathbf{b}_1 = \mathbf{b}_{y_1}^{(1)}, \dots, \mathbf{b}_{N-1} = \mathbf{b}_{y_{N-1}}^{(N-1)}, \mathbf{w}_N = \mathbf{w}_{y_N}^{(N)} \quad (4.57)$$

with $y_{i+1} - y_i = \frac{1+\omega_i}{2}$.

The probability that a path goes through these vertices is given by

$$\begin{aligned} \mathbb{P}_\varepsilon [\exists \text{ path through } \mathbf{b}_0, \mathbf{w}_1, \dots, \mathbf{b}_{N-1}, \mathbf{w}_N] &= \det(\mathbf{K}_\varepsilon^{-1}(\mathbf{b}_{j-1}, \mathbf{w}_i)) \\ &= \det(\mathbf{K}_\varepsilon^{-1}((j-1) - i, y_{j-1} - y_i)) \end{aligned} \quad (4.58)$$

where the indices i and j refer to white and black vertices respectively and range from 1 to N . Multiplying simultaneously each row of the matrix (4.58) i by $(-a)^{-i}$ and each line j by $(-a)^j$ does not affect the determinant. This manipulation cancels the coefficients $(\frac{-1}{a})^{(j-1)-i+1}$ in the expression of $\mathbf{K}^{-1}(\mathbf{b}_{j-1}, \mathbf{w}_i)$, leading to a simpler expression for the determinant (4.58)

$$\begin{aligned} & \mathbb{P}_\varepsilon[\exists \text{ path through } \mathbf{b}_0, \mathbf{w}_1, \dots, \mathbf{b}_{N-1}, \mathbf{w}_N] \\ &= \det \left[g((j-1) - i, y_{j-1} - y_i) - \frac{\delta_{j>i}}{2^{j-i}} \binom{j-1-i}{y_{j-1} - y_i} \right] \end{aligned} \quad (4.59)$$

where $\delta_{j>i} = 1$ is $j > i$ and 0 otherwise. The matrix, the determinant of which we want to compute, is the sum of a matrix with entries $g(\mathbf{c}, y) = O(\varepsilon)$, and a strictly upper triangular matrix.

We have now to find an upper bound for the value of this determinant to get the estimate stated in the lemma. We will use the Hadamard inequality, but a direct application of it would give too approximative a bound. We will have to make some more manipulations on the rows and columns of this matrix.

First, note that for every $\mathbf{c} \in \{-N, \dots, N\}$, and $y' = y$ or $y + 1$,

$$g(\mathbf{c} + 1, y') - g(\mathbf{c}, y) = \frac{1}{2} \int_{-\varepsilon}^{\varepsilon} (\cos \frac{\theta}{2})^{\mathbf{c}} e^{i\frac{\theta}{2}(-2y+\mathbf{c})} (e^{\pm i\frac{\theta}{2}} \cos \frac{\theta}{2} - 1) \frac{d\theta}{2\pi} = O(\varepsilon^3) \quad (4.60)$$

uniformly in \mathbf{c} . Therefore, replacing for $j \in \{2, \dots, N\}$, column C_j by $C_j - C_{j-1}$, we get on the diagonal and under it entries that are $O(\varepsilon^3)$ (except in the first column). It is important to observe that after these operations, the module of the entries (i, j) strictly above the diagonal does not increase, at least at the leading order in ε , and are bounded from above by a constant times $(j - i)^{-1/2}$, since

$$\left| \frac{1}{2^{\mathbf{c}+1}} \binom{\mathbf{c}}{y} - \frac{1}{2^{\mathbf{c}}} \binom{\mathbf{c}-1}{y'} \right| \leq \frac{1}{2^{\mathbf{c}+1}} \binom{\mathbf{c}}{y} \leq \frac{1}{2^{\mathbf{c}+1}} \binom{\mathbf{c}}{\lfloor \mathbf{c}/2 \rfloor} \leq \frac{1}{\sqrt{2\pi\mathbf{c}}}. \quad (4.61)$$

Now, we use the second column to put 0 instead of the first entries of columns $C_j, j > 2$ by making the substitution $C_j \leftarrow C_j + \alpha_{j,2} C_2$ for a suitable value of $\alpha_{j,2}$ in the determinant. From the bound on coefficients, we see that $|\alpha_{j,2}| = O((j-2)^{-1/2})$ and that therefore, the module of the entries of column $C_j, j \leq 3$ does not increase more than by

$$O((j-2)^{-1/2}\varepsilon^3) = o(1). \quad (4.62)$$

We then continue this procedure, and for $3 \leq k \leq N-1$, we use column C_k to eliminate the entries of the $k-1$ th row on columns $C_j, j > k$.

After this succession of operations, the entries (i, j) of the matrix with $j > i + 1$ are 0. The module of the other entries of column $C_j, j \leq 2$ increased at most by

$$O\left(\frac{\varepsilon^3}{\sqrt{j-2}}\right) + O\left(\frac{\varepsilon^3}{\sqrt{j-3}}\right) + \dots + O\left(\frac{\varepsilon^3}{\sqrt{j-(j-1)}}\right) = O(\varepsilon^3 \sqrt{j}) \quad (4.63)$$

The probability we are interested is given by the determinant

$$\det \begin{bmatrix} O(\varepsilon) & \frac{1}{2} + O(\sqrt{2}\varepsilon^3) & 0 & \cdots & 0 \\ O(\varepsilon) & O(\sqrt{2}\varepsilon^3) & \frac{1}{2} + O(\sqrt{3}\varepsilon^3) & & \vdots \\ \vdots & & & \ddots & 0 \\ \vdots & \vdots & \ddots & & \frac{1}{2} + O(\sqrt{N}\varepsilon^3) \\ O(\varepsilon) & O(\sqrt{2}\varepsilon^3) & \cdots & & O(\sqrt{N}\varepsilon^3) \end{bmatrix}. \quad (4.64)$$

Hadamard inequality states that a determinant is bounded by the product of the ℓ^2 -norm of its rows. In this particular case, it gives

$$\begin{aligned} \mathbb{P}_\varepsilon [\exists \text{ path through } \mathbf{b}_0, \mathbf{w}_1, \dots, \mathbf{b}_{N-1}, \mathbf{w}_N] \\ \leq \prod_{j=1}^{N-1} \left(O(\varepsilon)^2 + \sum_{k=2}^j O(\sqrt{k}\varepsilon^3)^2 + \left(\frac{1}{2} + O(\sqrt{j+1}\varepsilon^3) \right)^2 \right)^{\frac{1}{2}} \\ \times \left(O(\varepsilon)^2 + \sum_{k=1}^N O(\sqrt{k}\varepsilon^3)^2 \right)^{\frac{1}{2}} \end{aligned} \quad (4.65)$$

From the fact that we have for $j \in \{1, \dots, N-1\}$

$$\left(O(\varepsilon)^2 + \sum_{k=2}^j O(\sqrt{k}\varepsilon^3)^2 + \left(\frac{1}{2} + O(\sqrt{j+1}\varepsilon^3) \right)^2 \right)^{\frac{1}{2}} = \frac{1}{2} + O(\varepsilon)^2 \quad (4.66)$$

and

$$\left(O(\varepsilon)^2 + \sum_{k=1}^N O(\sqrt{k}\varepsilon^3)^2 \right)^{\frac{1}{2}} = O(\varepsilon), \quad (4.67)$$

it follows that finally

$$\mathbb{P}_\varepsilon [\exists \text{ path through } \mathbf{b}_0, \mathbf{w}_1, \dots, \mathbf{b}_{N-1}, \mathbf{w}_N] \leq \left(\frac{1}{2} + O(\varepsilon^2) \right)^{N-1} \times O(\varepsilon) = O\left(\frac{\varepsilon}{2^N}\right). \quad (4.68)$$

Since the probability that there is a path of rhombi starting from \mathbf{b}_0 is of order ε , we obtain the wanted bound for the conditionnal probability

$$\mathbb{P}_\varepsilon \left[\text{first } \lfloor \frac{L}{\varepsilon} \rfloor \text{ steps of } X_j^\varepsilon \text{ coincide with } (\omega_n) \mid X_j^\varepsilon \text{ starts at } (x_0, y_0) \right] \leq \frac{c_L}{2^N}. \quad (4.69)$$

for some constant c_L depending on L . \square

5 The bead model

In this chapter, we construct Gibbs measures on configurations of points on $\mathbb{Z} \times \mathbb{R}$ respecting a simple geometric condition. These probability measures are ergodic under the action of $\mathbb{Z} \times \mathbb{R}$ by translation, and it turns out that the distribution of points on each factor \mathbb{R} is described by the determinant random field with the sine kernel, also known as the *sine random point field*.

The construction provided of these measures is based on approximation by dimer models on the honeycomb lattice.

5.1 Presentation of the bead model

We consider the collection of configurations of beads strung on an infinite collection of parallel threads lying on the plane. A bead configuration on these threads gives a configuration of points on $\mathbb{Z} \times \mathbb{R}$. We impose the following constraints on the configurations:

- The configuration must be locally finite : the number of beads in each finite interval of a thread must be finite.
- Between two consecutive beads on a thread, there must be exactly one bead on each neighboring thread.

Let Ω be the set of bead configurations satisfying these two conditions.

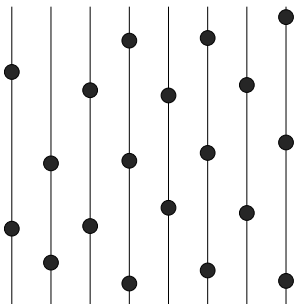


Figure 5.1: A bead configuration.

If there were only a finite number of threads of finite length, and a fixed number of beads on each thread, then the set Ω would be a bounded convex set of \mathbb{R}^N , where N is the total number of beads. Therefore the normalized Lebesgue measure on Ω would give a uniform probability measure.

The aim of this chapter is to construct probability measures for our infinite system Ω that are uniform in a certain sense. More precisely, we look for probability measures that satisfy the two following properties:

- they are ergodic under the action of $\mathbb{Z} \times \mathbb{R}$ by translation
- conditioned in an annular region, they induce the uniform measure on allowed configurations inside this region.

Such a probability measure is called an *ergodic Gibbs measure*. When endowed with an ergodic measure, the set Ω is called a *bead model*.

We now define the σ -algebra of events for our probability measures. To each bounded Borel set B of $\mathbb{Z} \times \mathbb{R}$ and to each bead configuration $\omega \in \Omega$ is associated an integer $X_B(\omega)$. Let \mathcal{F} be the smallest σ -algebra such that all the maps $X_B : \Omega \rightarrow \mathbb{N}$ are measurable. \mathcal{F} is generated by the elementary events

$$\{\omega \in \Omega \mid X_B(\omega) = n\}.$$

If \mathbb{P} is a Gibbs measure on (Ω, \mathcal{F}) , it defines through the application $X : B \mapsto X_B$ a random process with value in the set of boundedly finite, integer-valued measures, *i.e.* in other words, a *random point field*.

We will see that the Gibbs measures we construct on (Ω, \mathcal{F}) define a particular type of random point fields on $\mathbb{Z} \times \mathbb{R}$, named determinant random point fields, for which correlations functions are given by determinants of a kernel J .

We prove the following theorem

Theorem 5.1. *For a fixed average density of beads, there exists a 1-parameter family of ergodic Gibbs measures (\mathbb{P}_γ) on (Ω, \mathcal{F}) . When endowed with one of these measures, (Ω, \mathcal{F}) is a determinantal random point field on $\mathbb{Z} \times \mathbb{R}$ whose marginal on each thread is the sine random point field.*

The sine random point field process is a determinantal random point field on \mathbb{R} whose kernel is the *sine kernel*

$$S(x, y) = \frac{\sin(x - y)}{\pi(x - y)}$$

and describes the statistics of eigenvalues in the bulk of the spectrum of large hermitian random matrices. The parameter is chosen to be the average distance between a bead and its right neighbour just below it and describes the amplitude of a magnetic field that tends to push the beads in some directions.

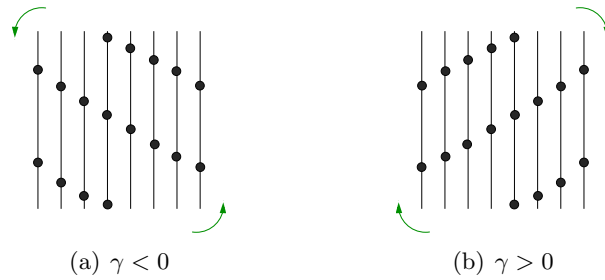


Figure 5.2: Two typical bead configurations for different values of γ . The parameter γ is negative in panel (a), and positive in panel (b).

A way to construct these Gibbs measures is first to consider a discretized version of the bead model. The set of possible configurations $\Omega_{\mathfrak{t}} \subset \Omega$, is constituted by the configurations for which the beads are located at sites of a lattice with mesh \mathfrak{t} . We show that in this discrete setting, there exist probability measures supported by $\Omega_{\mathfrak{t}}$, for which the distribution of the beads is a determinantal random point field, by exhibiting a bijection between the discretized bead model and the dimer model on the honeycomb lattice – or equivalently random tilings of the plane by rhombi. The measures on random tilings have the Gibbs property. Then we prove that the sequence of discrete determinantal processes indexed by \mathfrak{t} converges to a determinantal random point field on $\mathbb{Z} \times \mathbb{R}$ when \mathfrak{t} goes to zero.

5.2 Discrete bead model and dimers

We assume for the moment that the threads are not continuous lines, but one-dimensional lattice with mesh size \mathfrak{t} . The possible positions of the beads are labelled by coordinates

$$(\mathfrak{c}, \mathfrak{t}y) \in \mathbb{Z} \times \mathfrak{t}\mathbb{Z}, \quad (5.1)$$

\mathfrak{c} representing the thread on which the bead lies, and y being the coordinate running along the thread.

There is a correspondence between discrete bead configurations and dimer configurations on the honeycomb lattice H : there is a bead at $(\mathfrak{c}, \mathfrak{t}y)$ if the horizontal edge incident with the white vertex (\mathfrak{c}, y) is in the dimer configuration. A way to see geometrically this correspondence is the following: fix an isoradial embedding of the honeycomb lattice such that the middle of horizontal edges coincide with the possible bead positions. A bead configuration is obtained by putting a bead at a site each time there is an horizontal dimer at this position. Reciprocally, from a bead configuration one can reconstruct a dimer configuration by placing horizontal dimers on edges crossing an occupied site, and completing the configuration. This is always possible, because of the intertwining of bead positions. Moreover, the completion is unique once there is at least one bead on each wire.

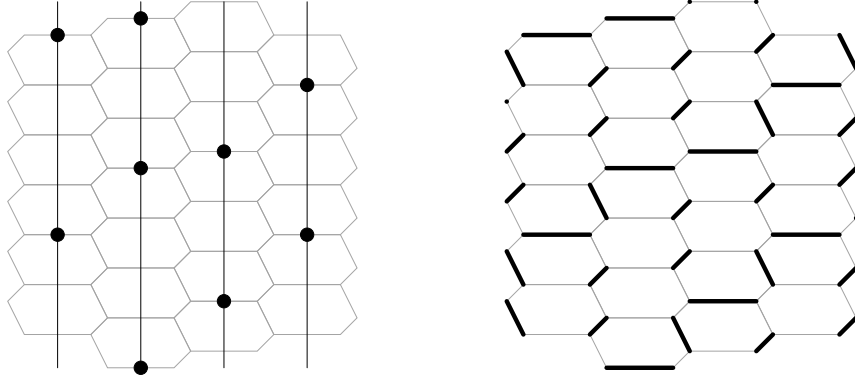


Figure 5.3: A piece of discrete bead configuration and the corresponding piece of dimer configuration on H .

Isoradial embeddings of H are parameterized, up to a global scaling factor, by two quantities $a/b, c/b$ fixing the ratios between the length of dual edges of each type. We take $a = \mathfrak{t}, b = 1, c = e^{\gamma\mathfrak{t}}$.

The parameter $\gamma \in (-1, 1)$ parameterizes the family of isoradial embeddings compatible with the geometric constraints discussed above.

For a fixed \mathfrak{t} , each value of γ corresponds to a liquid Gibbs probability measure on dimer configurations, that can be transported to bead configurations. The local statistics of the beads coincide with that of horizontal dimers. The probability measure on bead configurations benefits from the conditional uniform property of the dimer Gibbs measure.

This procedure defines for a given \mathfrak{t} a family parameterized by γ of probability measures on discrete bead configurations that have the conditioned uniform property. The correlations between beads are given by determinants: the probability of having a bead at the sites $(\mathbf{c}_1, \mathfrak{t}y_1), \dots, (\mathbf{c}_k, \mathfrak{t}y_k)$ in the random bead configuration ω is

$$\mathbb{P}_{\mathfrak{t}, \gamma} [(\mathbf{c}_1, \mathfrak{t}y_1), \dots, (\mathbf{c}_k, \mathfrak{t}y_k) \in \omega] = t^k \det_{1 \leq i, j \leq k} \mathbf{K}_{\mathfrak{t}, \gamma}^{-1}(\mathbf{b}_{y_i}^{\mathbf{c}_i}, \mathbf{w}_{y_j}^{\mathbf{c}_j}) \quad (5.2)$$

where $\mathbf{K}_{\mathfrak{t}, \gamma}^{-1}$ is defined by

$$\mathbf{K}_{\mathfrak{t}, \gamma}^{-1}(\mathbf{b}_y^{(\mathbf{c})}, \mathbf{w}) = \iint_{\mathbb{T}^2} \frac{u^{-y} w^{\mathbf{c}}}{\mathfrak{t} + \frac{1}{w}(1 + ue^{\gamma\mathfrak{t}})} \frac{du}{2i\pi u} \frac{dw}{2i\pi w} \quad (5.3)$$

We will determine the asymptotics of this kernel for a fixed γ and a small t , and then prove the convergence of the corresponding determinantal process when t goes to zero.

5.3 Explicit expression of the Gibbs measures

Before proving theorem 5.1, it is necessary to investigate the behavior of the kernel defining the discrete bead model. In other words, one has to compute the asymptotics of $K_{\gamma,t}^{-1}(\mathbf{b}_y^{\mathbf{c}}, \mathbf{w})$ when t becomes small and y large. Such asymptotics are given by the following lemma.

Lemma 5.1. *In the vertical scaling limit*

$$t \rightarrow 0, \quad ty \rightarrow \xi \quad (5.4)$$

the coefficients $(-1)^y K_{\gamma,t}^{-1}(\mathbf{b}_y^{\mathbf{c}}, \mathbf{w})$ converge to

$$J_{\gamma}(\mathbf{c}, \xi) = \begin{cases} \frac{1}{2\pi} \int_{[-\sqrt{1-\gamma^2}, \sqrt{1-\gamma^2}]} e^{-i\xi\phi} (\gamma + i\phi)^{\mathbf{c}} d\phi & \text{if } \mathbf{c} \geq 0, \\ \frac{-1}{2\pi} \int_{\mathbb{R} \setminus [-\sqrt{1-\gamma^2}, \sqrt{1-\gamma^2}]} e^{-i\xi\phi} (\gamma + i\phi)^{\mathbf{c}} d\phi & \text{if } \mathbf{c} < 0. \end{cases} \quad (5.5)$$

In particular, when $\mathbf{c} = 0$,

$$J_{\gamma}(0, \xi) = \int_{[-\sqrt{1-\gamma^2}, \sqrt{1-\gamma^2}]} e^{i\xi\phi} d\phi = \frac{\sin(\sqrt{1-\gamma^2}\xi)}{\pi\xi} \quad (5.6)$$

Proof:

As we said before, the entries of the inverse Kasteleyn operator are given by

$$K^{-1}(\mathbf{b}_y^{\mathbf{c}}, \mathbf{w}) = \iint_{\mathbb{T}^2} \frac{z^{-y} w^x}{a + b/w + cz} \frac{dz}{2i\pi z} \frac{dw}{2i\pi w} = \iint_{\mathbb{T}^2} \frac{u^{-y} w^{\mathbf{c}}}{t + \frac{1}{w} (1 + ue^{\gamma t})} \frac{du}{2i\pi u} \frac{dw}{2i\pi w}$$

To evaluate this integral, we first perform the integration over w by the method of residues. If $\mathbf{c} \geq 0$, the rational fraction

$$f_u(w) = \frac{w^{\mathbf{c}}}{tw + u(1 + ue^{\gamma t})}$$

has one pole at $w = w_0(u) = -\frac{1+ue^{\gamma t}}{t}$.

By Cauchy's theorem, the integral

$$\frac{1}{2i\pi} \int_{\mathbb{S}^1} f_u(w) dw$$

is zero unless the pole $w_0(u)$ is in the unit disc, *i.e.*

$$\operatorname{Re}(u) < -\frac{1 + e^{2\gamma t} - t^2}{2e^{\gamma t}} = -1 + (1 - \gamma^2)t^2 + O(t^3) \quad (5.7)$$

Define $\theta_0 = \text{Arccos}\left(\frac{1+e^{2\gamma\mathfrak{t}}-t^2}{2e^{\gamma\mathfrak{t}}}\right) = \mathfrak{t}\sqrt{1-\gamma^2} + O(\mathfrak{t}^2)$. The constraint (5.7) on the pole to be inside the unit disk can be rewritten as

$$\arg(u) \in (\pi - \theta_0, \pi + \theta_0)$$

Posing $u = -e^{i\theta} = -e^{i\mathfrak{t}\phi}$ in the integral, we get

$$\mathbf{K}^{-1}(\mathbf{b}_y^{(\mathfrak{c})}, \mathbf{w}) = \int_{\text{Re}(u) < -\frac{1+e^{2\gamma\mathfrak{t}}-t^2}{2e^{\gamma\mathfrak{t}}}} u^{-y} \left(-\frac{1+ue^{\gamma\mathfrak{t}}}{t}\right)^{\mathfrak{c}} \frac{du}{2\pi\mathfrak{t}iu} \quad (5.8)$$

$$= (-1)^y \int_{-\theta_0}^{\theta_0} e^{-iy\theta} \left(\frac{e^{\gamma\mathfrak{t}}e^{i\theta} - 1}{\mathfrak{t}}\right)^{\mathfrak{c}} \frac{d\theta}{2\pi\mathfrak{t}} \quad (5.9)$$

$$= \frac{(-1)^y}{2\pi} \int_{-\theta_0/\mathfrak{t}}^{\theta_0/\mathfrak{t}} e^{-i\mathfrak{t}y\phi} \left(\frac{e^{\mathfrak{t}(\gamma+i\phi)} - 1}{\mathfrak{t}}\right)^{\mathfrak{c}} d\phi \quad (5.10)$$

In the vertical scaling limit $\mathfrak{t} \rightarrow 0, \mathfrak{t}y \rightarrow \xi$, we have

$$\lim_{\mathfrak{t}} \frac{\theta_0}{\mathfrak{t}} = \sqrt{1-\gamma^2}, \quad \lim e^{-i\mathfrak{t}y\phi} = e^{-i\xi\phi}, \quad \lim \frac{e^{\mathfrak{t}(\gamma+i\phi)} - 1}{\mathfrak{t}} = \gamma + i\phi.$$

Thus, the integral above, multiplied by $(-1)^y$, converges to

$$\lim(-1)^y \mathbf{K}^{-1}(\mathbf{b}_y^{(\mathfrak{c})}, \mathbf{w}) = \frac{1}{2\pi} \int_{[-\sqrt{1-\gamma^2}, \sqrt{1-\gamma^2}]} e^{-i\xi\phi} (\gamma + i\phi)^{\mathfrak{c}} d\phi.$$

When $\mathfrak{c} < 0$, $f_u(w)$ has two poles: there is a pole at $w = 0$ in addition to that located at $w = w_0(u) = -\frac{1+u^{-1}e^{\gamma\mathfrak{t}}}{\mathfrak{t}}$. Since $wf_u(w)$ goes to zero when u goes to infinity, the sum of the residues is zero. Therefore the integral of $f_u(w)$ on the unit circle is not zero only if $w_0(u)$ is outside of the unit disc. It equals in that case the opposite of the residue at $w_0(u)$. Again with the change of variable $u = -e^{i\theta} = -e^{i\mathfrak{t}\phi}$, we have

$$\mathbf{K}^{-1}(\mathbf{b}_y^{(\mathfrak{c})}, \mathbf{w}) = - \int_{\text{Re}(w) > -\frac{1+e^{2\gamma\mathfrak{t}}-t^2}{2e^{\gamma\mathfrak{t}}}} u^{-y} \left(-\frac{1+ue^{\gamma\mathfrak{t}}}{\mathfrak{t}}\right)^{\mathfrak{c}} \frac{du}{2\pi\mathfrak{t}iu} \quad (5.11)$$

$$= (-1)^{y+1} \left(\int_{-\pi}^{-\theta_0} + \int_{\theta_0}^{\pi} \right) e^{-iy\theta} \left(\frac{e^{\gamma\mathfrak{t}}e^{i\theta} - 1}{\mathfrak{t}}\right)^{\mathfrak{c}} \frac{d\theta}{2\pi\mathfrak{t}} \quad (5.12)$$

$$= (-1)^{y+1} \left(\int_{-\pi/\mathfrak{t}}^{-\theta_0/\mathfrak{t}} + \int_{\theta_0/\mathfrak{t}}^{\pi/\mathfrak{t}} \right) e^{-i\mathfrak{t}y\phi} \left(\frac{e^{\gamma\mathfrak{t}}e^{i\mathfrak{t}\phi} - 1}{\mathfrak{t}}\right)^{\mathfrak{c}} \frac{d\phi}{2\pi} \quad (5.13)$$

Thus in the scaling limit, by Lebesgue dominated convergence theorem,

$$\lim(-1)^y \mathbf{K}^{-1}(\mathbf{b}_y^{(\mathfrak{c})}, \mathbf{w}) = \frac{-1}{2\pi} \int_{\mathbb{R} \setminus [-\sqrt{1-\gamma^2}, \sqrt{1-\gamma^2}]} e^{-i\xi\phi} (\gamma + i\phi)^{\mathfrak{c}} d\phi$$

what terminates the proof of the lemma. \square

From the exact expressions (5.10) and (5.13) of $K^{-1}(\mathbf{b}_y^{(\mathfrak{c})}, \mathbf{w})$, one can easily check that the entries are uniformly bounded in y and \mathfrak{t} for a given value of \mathfrak{c} , leading to the following lemma:

Lemma 5.2. $\forall \mathfrak{c} \in \mathbb{Z} \quad \exists M_{\mathfrak{c}} > 0 \quad \forall t < t_0 \quad \forall y \in \mathbb{R} \quad \left| K^{-1}(\mathbf{b}_y^{(\mathfrak{c})}, \mathbf{w}) \right| \leq M_{\mathfrak{c}}$

These two lemmas will now be used to prove theorem 5.1, stating that this family converges weakly to the determinantal random point field on $\mathbb{Z} \times \mathbb{R}$ with kernel J_{γ} .

Theorem 5.2. *For each value of $\gamma \in (-1, 1)$, the discrete bead model converges weakly when t goes to 0 to a determinantal random point field on $\mathbb{Z} \times \mathbb{R}$, the marginal of which on each factor \mathbb{R} is the sine random field of the eigenvalues of large random Hermitian matrices. The kernel J_{γ} of this limiting determinant random point field is given by*

$$J_{\gamma}(\mathfrak{c}, \xi) = \begin{cases} \int_{[-\sqrt{1-\gamma^2}, \sqrt{1-\gamma^2}]} e^{-i\xi\phi} (\gamma + i\phi) \frac{\mathfrak{c} d\phi}{2\pi} & \text{if } x \geq 0 \\ - \int_{\mathbb{R} \setminus [-\sqrt{1-\gamma^2}, \sqrt{1-\gamma^2}]} e^{-i\xi\phi} (\gamma + i\phi) \frac{\mathfrak{c} d\phi}{2\pi} & \text{if } x < 0. \end{cases} \quad (5.14)$$

Proof:

Since tightness is automatic for random point fields [9], it is sufficient to prove the convergence of finite dimensional distributions in order to prove the weak convergence of the family of random point fields $(\Omega, \mathcal{F}, \mathbb{P}_{\gamma, \mathfrak{t}})$.

Let I_1, \dots, I_k be segments on wire $\mathfrak{c}_1, \dots, \mathfrak{c}_k$ respectively. It will be convenient to use multi-index notations

$$n! = \prod_{j=1}^k n_j!, \quad |n| = \sum_{j=1}^k n_j, \quad I^n = I_1^{n_1} \times \dots \times I_k^{n_k}, \quad z^n = z_1^{n_1} \dots z_k^{n_k}$$

We will prove the convergence of the moment generating function $G_{\gamma, \mathfrak{t}}^{(I)}(z_1, \dots, z_k)$ of the joint law of $(X_{I_1}, \dots, X_{I_k})$

$$G_{\gamma, \mathfrak{t}}^{(I)}(z) = \mathbb{E}_{\gamma, \mathfrak{t}} \left[\prod_{j=1}^k (1 - z_j)^{X_{I_j}} \right] = \sum_{n \in \mathbb{N}^k} \mathbb{E}_{\gamma, \mathfrak{t}} \left[\prod_{j=1}^k \frac{(X_{I_j})!}{(X_{I_j} - n_j)!} \right] \frac{(-z)^n}{n!}. \quad (5.15)$$

The factorial moments

$$A_{\gamma, \mathfrak{t}}^{(I)}(n_1, \dots, n_k) = \mathbb{E}_{\gamma, \mathfrak{t}} \left[\prod_{i=1}^k \frac{X_{I_i}!}{(X_{I_i} - n_i)!} \right] \quad (5.16)$$

are quite easy to compute. They are given by the formula:

$$A_{\gamma, \mathbf{t}}^{(I)}(n_1, \dots, n_k) = \sum_{\substack{y_1^1 \dots y_{n_1}^1 \in I_1 / \mathbf{t} \\ y_1^k \dots y_{n_k}^k \in I_k / \mathbf{t}}} \mathbb{P}_{\gamma, \mathbf{t}} \left[\text{there are beads at } (\mathbf{c}_1, \mathbf{t}y_1^1), \dots, (\mathbf{c}_k, \mathbf{t}y_{n_k}^k) \right] \quad (5.17)$$

where the sum is performed over all the distinct n_j tuples of I_j , $j = 1, \dots, k$. By equation (5.2), this can be rewritten in terms of determinants of matrices with blocks of size n_1, \dots, n_k

$$A_{\gamma, \mathbf{t}}^{(I)}(n) = \sum_{\substack{y_1^1 \dots y_{n_1}^1 \in I_1 / \mathbf{t} \\ y_1^k \dots y_{n_k}^k \in I_k / \mathbf{t}}} \mathbf{t}^{|n|} \det \left[\begin{array}{c|c|c} \mathbf{K}_{\gamma, \mathbf{t}}^{-1}(\mathbf{b}_{y_{i_1}^1}, \mathbf{w}_{y_{j_1}^1}) & \cdots & \mathbf{K}_{\gamma, \mathbf{t}}^{-1}(\mathbf{b}_{y_{i_1}^1}, \mathbf{w}_{y_{j_1}^1}) \\ \vdots & \ddots & \vdots \\ \mathbf{K}_{\gamma, \mathbf{t}}^{-1}(\mathbf{b}_{y_{i_1}^k}, \mathbf{w}_{y_{j_k}^k}) & \cdots & \mathbf{K}_{\gamma, \mathbf{t}}^{-1}(\mathbf{b}_{y_{i_1}^k}, \mathbf{w}_{y_{j_k}^k}) \end{array} \right]_{\substack{1 \leq i_1, j_1 \leq n_1 \\ 1 \leq i_k, j_k \leq n_k}} \quad (5.18)$$

which converges when \mathbf{t} goes to zero to

$$A_{\gamma}^{(I)}(n) = \int_{I^n} \det \left[\begin{array}{c|c|c} J_{\gamma}(\mathbf{c}_1 - \mathbf{c}_1, \xi_{i_1}^{(1)} - \xi_{j_1}^{(1)}) & \cdots & J_{\gamma}(\mathbf{c}_1 - \mathbf{c}_k, \xi_{i_1}^{(1)} - \xi_{j_k}^{(k)}) \\ \vdots & \ddots & \vdots \\ J_{\gamma}(\mathbf{c}_k - \mathbf{c}_1, \xi_{i_k}^{(k)} - \xi_{j_1}^{(1)}) & \cdots & J_{\gamma}(\mathbf{c}_k - \mathbf{c}_k, \xi_{i_k}^{(k)} - \xi_{j_k}^{(k)}) \end{array} \right] d^n \xi \quad (5.19)$$

where the integration variable $\xi = (\xi_1^{(1)}, \dots, \xi_{n_1}^{(1)}, \dots, \xi_{n_k}^{(k)})$. Since the coefficients of $\mathbf{K}_{\gamma, \mathbf{t}}^{-1}$ are bounded uniformly in \mathbf{t} and y , say by M , then using Hadamard inequality, we get a uniform bound on the coefficients $A_{\gamma, \mathbf{t}}^{(I)}(n_1, \dots, n_k)$

$$|A_{\gamma, \mathbf{t}}^{(I)}(n)| \leq \prod_{j=1}^k |I_j|^{n_j} (\sqrt{|n|} M)^{|n|} \quad (5.20)$$

Therefore, by an argument of dominated convergence, the entire series $Q_{\gamma, \mathbf{t}}^{(I)}(z)$, $z \in \mathbb{C}^k$ converges uniformly on compact sets towards

$$Q_{\gamma}^{(I)}(z) = \sum_{n \in \mathbb{N}^k} A_{\gamma}^{(I)}(n) \frac{(-z)^n}{n!} \quad (5.21)$$

which is the moment generating function for the limit distribution of $(X_{I_1}, \dots, X_{I_k})$. The probability of having for all $j \in \{1, \dots, k\}$ exactly n_j beads in I_j is given by the following formula

$$\mathbb{P}_{\gamma} [X_{I_1} = n_1, \dots, X_{I_k} = n_k] = \frac{(-1)^{|n|}}{n!} \frac{\partial^n}{\partial z^n} Q_{\gamma}^{(I)}(z) \Big|_{z=(1, \dots, 1)}. \quad (5.22)$$

In particular, the probability of having no bead in a Borel set B is given by the Fredholm determinant

$$\mathbb{P}_{\gamma} [X_B = 0] = \text{Det}(\text{Id} - \chi_B \mathbf{K}_{\gamma}^{-1} \chi_B) = Q_{\gamma}^B(1) = \sum_{n=0}^{\infty} \frac{(-1)^n}{n!} \int_{B^n} \det[\mathbf{K}_{\gamma}^{-1}(\xi_i - \xi_j)] d^n \xi \quad (5.23)$$

The restriction of the process to one line is a determinantal random point field on \mathbb{R} with kernel

$$J_\gamma(0, \xi - \xi') = \frac{\sin(\sqrt{1 - \gamma^2}(\xi - \xi'))}{\pi(\xi - \xi')}. \quad (5.24)$$

It is thus, up to a scaling factor, the sine random point field. \square

5.4 Comments and possible developments

5.4.1 The bead model as an asymmetric exclusion process

A bead configuration can be interpreted as the history of a collection of particles located on a one dimensional lattice \mathbb{Z} and jumping from left to right. Time is continuous and is flowing vertically along the threads, and there is a lattice site between two successive threads. Joining every bead to the bead just above it on the neighbouring right thread, one gets an infinite collection of monotonous paths representing the trajectories of the particles: a bead on a thread corresponds to a jump of a particle from the site at the left of the thread to the site on its right. Because of the geometric constraint on beads, these paths cannot touch each other. Consequently, the particles are submitted to an exclusion rule: a particle cannot jump to a site if this one is already occupied by another particle.

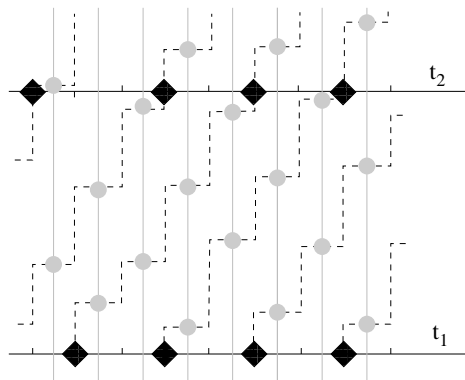


Figure 5.4: The trajectories corresponding to the bead configuration of figure 5.1 and positions of particles (black squares) at different times t_1 and t_2 .

The Gibbs measures \mathbb{P}_γ on bead configurations, viewed as families of monotonous paths constructed as above, are probability measures on all possible evolutions of particles. The Gibbs property and ergodicity imply that the marginal of these measures for a fixed time (*i.e.* along an horizontal line) give stationary measures for some Markovian dynamics.

The discrete bead model gives a discrete version of this particle system: in this picture a particle is represented by a c -rhombus, and a hole by a b -rhombus. Under \mathbb{P}_γ , the average particle density ρ is equal to the limit of the probability of a c -rhombus, and therefore related to γ by the following expression

$$\rho = \lim_{\mathfrak{t} \rightarrow 0} \mathbb{P}_{\mathfrak{t}, \gamma} \left[\begin{array}{c} \blacktriangleleft \\ \blacktriangleright \end{array} \right] = 1 - \frac{\arccos \gamma}{\pi} \quad (5.25)$$

so that the density is an increasing function of γ .

ASEP¹ is also an example of particle systems with the same constraint of exclusion. Its evolution is Markovian, and the transition rates from an allowed configuration to another is constant. The translation invariant stationary measures for this model are Bernoulli probability measure, whose parameter is the density.

If the particles are not located on the vertices of the finite lattice \mathbb{Z} but on a finite annulus $\mathbb{Z}/N\mathbb{Z}$, then the number of particles is a conserved quantity. For a fixed number of particles, the stationary measure is uniform for ASEP. This is not the case for the bead model with a finite number of beads² the probability of a configuration of particles depends not only on the number of particles, but also on their positions.

The properties of the particle system coming from the bead model differ from that of ASEP. It would be interesting to study more in details these properties using the dimer microscopic structure, and to compare them with that of ASEP, that are also related to random matrix theory [49].

5.4.2 The bead model and spanning trees

In [59], Temperley gives a bijection between dimer model on \mathbb{Z}^2 and the uniform spanning tree model on \mathbb{Z}^2 . This correspondance has been considerably extended [35, 36]: for any bipartite planar graph G with weighted edges, there exist a T-graph G^T and a weight-preserving bijection between spanning trees of a G^T and the (marked) dimer configurations of G . A piece of the T-graph corresponding to the dimer model on the honeycomb lattice with weights $a = \mathfrak{t} = 0.1, b = 1, c = 1$, shown on figure 5.5, looks like fish scales. When \mathfrak{t} goes to zero, the envelopes of these fish scales approach a collection of superimposed cycloids. Using Wilson's algorithm [63], one can sample a spanning tree on that T-graph, and thus a bead configuration using loop-erased random walks. It would be interesting to understand more in details how a random walk can sample a sine random field.

¹ASEP: Asymmetric Simple Exclusion Process.

²A bead model for a finite number of threads can be constructed following the same procedure as in the beginning of this chapter. We impose the number of threads N to be even to ensure that the geometric constraint on beads makes sense. We get leading to a 1-parameter family of determinantal random fields, whose kernel is obtained by replacing the integral in (5.5) by a discrete sum.

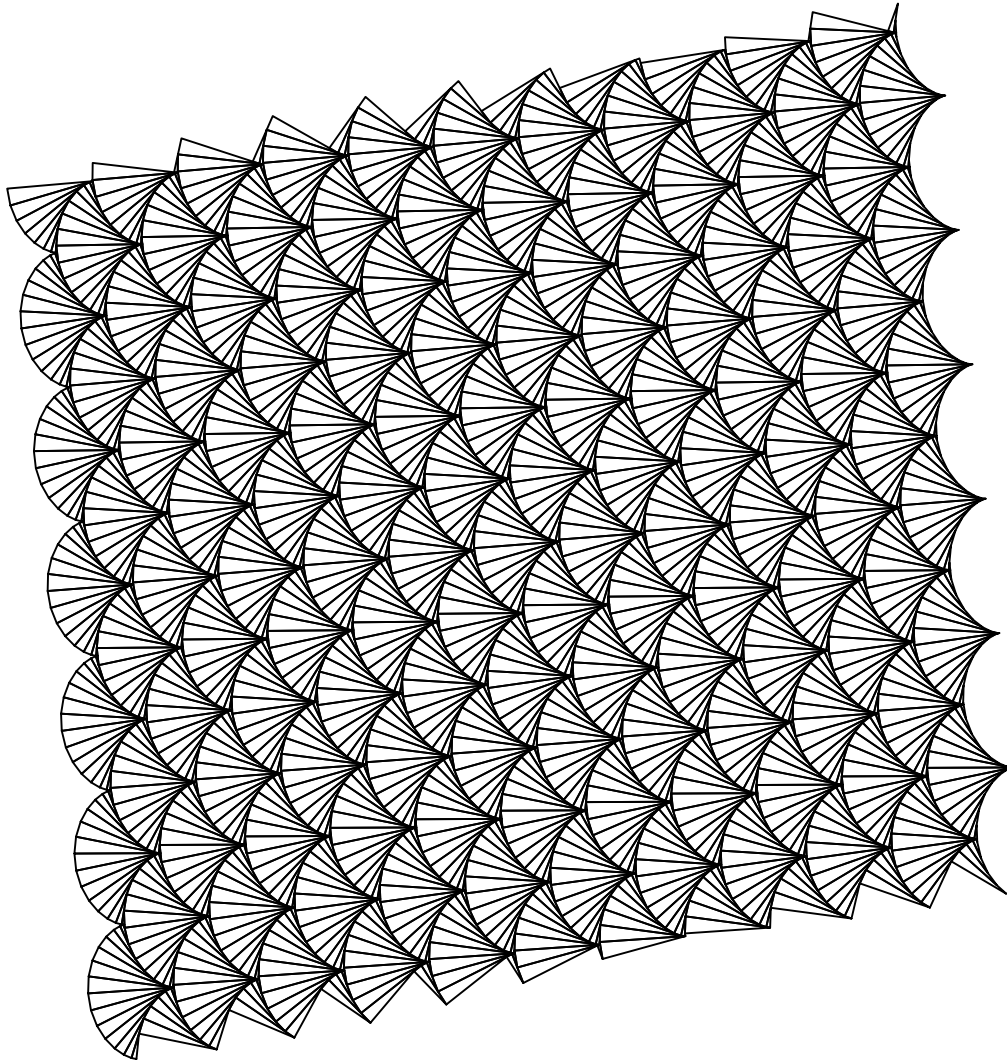


Figure 5.5: A piece of the graph on which the spanning tree model is in bijection with the dimer model on the honeycomb lattice with weights $a = \tau = 0.2, b = 1, c = 1$. The faces of this graph are triangles similar to the isosceles triangle with side lengths a, b and c .

6 The bead model – Generalization

Although the bead model was presented in the last section as the limit of the dimer model on the honeycomb lattice, it turns out to be much more general. Indeed, we will see in this chapter that the bead model appears as the limit of any dimer model on a planar \mathbb{Z}^2 -periodic bipartite graph.

Let G be a planar \mathbb{Z}^2 -periodic graph, and K the Kasteleyn operator corresponding to some periodic weight function on the edges of G . There is a two-parameter family of Gibbs measures on dimer configurations of G for these weights, parameterized by two order parameters (B_x, B_y) . The characteristic polynomial $P(z, w)$ is the determinant of the Fourier transform of the periodic operator K , and the phase diagram describing the behaviour of the measures in function of B_x and B_y is given by the *amoeba* of the *spectral curve* $P(z, w) = 0$, *i.e.* the image of $P(z, w) = 0$ by the mapping

$$\begin{aligned} \text{Log} : (\mathbb{C}^*)^2 &\rightarrow \mathbb{R}^2 \\ (z, w) &\mapsto (\log |z|, \log |w|). \end{aligned}$$

The structure of this amoeba is related to the geometry of $N(P)$, the Newton polygon of P , which is the convex hull of the exponents of monomials of P , representing all the possible slopes of a Gibbs measure.

Before explaining how to find the bead model in this setting, we need some more information about the local geometry of the amoeba, in particular about its unbounded outgrowths of the amoeba, the *tentacles*.

6.1 Tentacles of the amoeba

Consider a particular side of the Newton polygon $N(P)$. Changing the basis of the \mathbb{Z}^2 lattice acting on G by translation induces a linear transformation¹ of $N(P)$. After possibly such an operation, we can assume that this side is horizontal, and that the polygon lies above it. Recall that the Newton polygon represent the possible slopes for a Gibbs measure on the dimer model on G . When the slope of a Gibbs measure is a lattice point of the boundary of $N(P)$, the system is a solid phase.

We want to investigate the geometry of the phase diagram for values of the magnetic field inducing measures with slope close to the particular side of $N(P)$ we chose. In particular,

¹A change of basis of \mathbb{Z}^2 is encoded by an element M of $\text{SL}_2(\mathbb{Z})$. The linear transformation acting on $N(P)$ is $(M^{-1})^T$.

we seek for the shape of the curve in the neighborhood of the frontier between the liquid phase and the different solid phases, corresponding to the points of the particular side of the polygon.

To get a measure with a slope close to that side of $N(P)$, we apply to the system a magnetic field oriented essentially downward $(B_x, B_y) = (c, -R)$. To remain close to the notations used in the previous chapter, we introduce the small parameter $\mathfrak{t} = e^{-R}$.

When \mathfrak{t} is small, the leading terms in the characteristic polynomial $P(e^c z, \mathfrak{t}w)$ are those with the smallest power in w , say δ_0 .

$$P(e^c z, \mathfrak{t}w) = (\mathfrak{t}w)^{\delta_0} \left(\sum_{\gamma} a_{\gamma\delta_0} (e^c z)^{\gamma} + O(\mathfrak{t}) \right) \quad (6.1)$$

By a suitable choice of the origin of the Newton polygon, one can assume that $\delta_0 = 0$ and that all the roots of $P_0(X) = \sum_{\gamma} a_{\gamma 0} X^{\gamma}$ are positive.

If e^c is not a root of $P_0(X) = \sum_{\gamma} a_{\gamma 0} X^{\gamma}$, then for \mathfrak{t} small enough, $P(e^c z, e^{-R}w)$ has no roots on the unit torus. In this case, the magnetic field $(B_x, B_y) = (c, -R)$ belongs to a unbounded component of the amoeba. The corresponding measure $\mu(B_x, B_y)$ is frozen. On the contrary, if e^c is a root of this polynomial, then for every R large enough, the polynomial has two complex conjugated roots on the unit torus: we are in the liquid phase. The amoeba defining the liquid phase has therefore *tentacles* going to infinity with asymptotes the straight lines $x = c$. For generic weights, the asymptotes are all distinct, and there is one asymptote for each segment between to lattice points on the side of $N(P)$. Moreover, one can give an asymptotic expansion for the equation of the boundary of the amoeba: since the boundary of the amoeba is the image of the real locus of the curve, it is given by the equation

$$P(e^{B_x}, \pm e^{B_y}) = 0 \quad (6.2)$$

In the neighborhood of $(B_x, B_y) = (c, -\infty)$, B_x admits an asymptotic expansion in $\mathfrak{t} = e^{-B_y}$: $B_x = c + c_1 \mathfrak{t} + O(\mathfrak{t}^2)$. Since $P(e^c, 0) = 0$, we have

$$P(e^{B_x}, \pm e^{B_y}) = P(e^{c+c_1\mathfrak{t}+O(\mathfrak{t}^2)}, \pm \mathfrak{t}) = (c_1 e^c \partial_1 P(e^c, 0) \pm \partial_2 P(e^c, 0)) \mathfrak{t} + O(\mathfrak{t}^2) \quad (6.3)$$

Therefore the coefficient c_1 in the expansion is defined by

$$c_1 = \pm \frac{\partial_2 P(e^c, 0)}{e^c \partial_1 P(e^c, 0)} \quad (6.4)$$

and the two curves $B_x = c \pm e^{-c} \frac{\partial_2 P(e^c, 0)}{\partial_1 P(e^c, 0)} e^{B_y}$ define asymptotic branches of the boundary of the amoeba in the neighborhood of $(c, -\infty)$. Define β as

$$\beta = -e^{-c} \frac{\partial_2 P(e^c, 0)}{\partial_1 P(e^c, 0)} \quad (6.5)$$

For any $\gamma \in (-1, 1)$, the curve

$$B_x = c + \gamma \beta e^{B_y} \quad (6.6)$$

lies inside the amoeba for B_y negative enough.

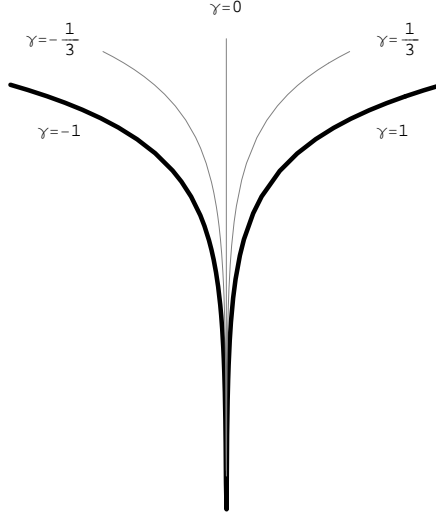


Figure 6.1: A tentacle (in thick lines) and curves described above, for different values of γ .

6.2 Deep inside a tentacle

6.2.1 Analytic results about the roots of P

Let us fix c to be equal to the logarithm of one of the roots of P_0 . For a fixed z , the polynomial $P(e^{c+\gamma\beta\mathfrak{t}}z, W)$ has d roots $W_0(z), \dots, W_{d-1}(z)$. Since e^c is a root of P_0 , one of these $W_j(z)$, say it is W_0 , equals 0 when $z = 1$. If all the roots of P_0 are distinct, $W_0(z)$ is the only zero having this property. The 2-to-1 property shows that $W_0(z)$ does not equal zero for $z \neq 1$

Therefore, by compactness of \mathbb{S}^1 there exists an $\epsilon > 0$ such that

$$\forall j \in \{1, \dots, d-1\}, \quad \forall z \in \mathbb{S}^1 \quad |W_j(z)| \geq \epsilon \quad (6.7)$$

Continuity of the roots with respect to the coefficients and symmetry by complex conjugation imply that there exists $\theta(\mathfrak{t}) = \theta_0\mathfrak{t} + O(\mathfrak{t}^2)$, with $\theta_0 > 0$ such that

$$|W_0(z)| \leq \mathfrak{t} \Leftrightarrow z \in [e^{-i\theta(\mathfrak{t})}, e^{i\theta(\mathfrak{t})}] \quad (6.8)$$

In fact, an expansion of P similar to (6.3) shows that when $\arg(z) = O(\mathfrak{t})$

$$W_0(z) = \gamma\mathfrak{t} + \frac{i \arg(z)}{\beta} + O(\mathfrak{t}^2), \quad (6.9)$$

and therefore, $\theta(\mathfrak{t}) = \mathfrak{t}\beta\sqrt{1-\gamma^2} + O(\mathfrak{t}^2)$.

6.2.2 Asymptotics of the inverse Kasteleyn operator for beads

Recall that the Newton polygon $N(P)$ is an intersection of half-planes, where all the inequalities (2.34) are satisfied by the average slope of the Gibbs measure. The side of the Newton polygon we are looking at is a segment of one of the straight lines delimiting one of these half-planes. When the average slope of the Gibbs measure lies on this line, there exists two translates of a face between which the difference of height equals the capacity of a dual path Γ joining them. All the translated of this path form a collection of infinite parallel paths perpendicular to the side of $N(P)$, that are *frozen* when the slope of the Gibbs measure lies on that boundary of $N(P)$: with probability 1, no dimer will cross these *frozen paths*. These possibly frozen paths will be the threads of our bead model. When the slope is not exactly on that boundary of $N(P)$, some dimers may cross these paths. We will see that these *defects* will play the role of beads strung along these threads.

Let $\mathbf{e} = (\mathbf{w}, \mathbf{b})$ be an edge of G crossing one of these threads. When the slope of the Gibbs measure is on the side of the Newton polygon, this edge appears in the random dimer configuration with probability 0. In particular, there is no dimer configuration on the torus G_1 corresponding to a lattice point of the side of $N(P)$ containing this edge. As the cofactor $Q_{\mathbf{e}}(z, w) = Q_{\mathbf{bw}}(z, w)$ is up to a sign the determinant of the Kasteleyn operator on $G_1 \setminus \{\mathbf{w}, \mathbf{b}\}$, it contains only monomials of degree at least 1 in w .

We determine now the asymptotic expression for the coupling function $K_{\gamma, \mathbf{t}}^{-1}(\mathbf{b}_x, \mathbf{w})$ corresponding to our magnetic field $(B_x, B_y) = (c + \beta\gamma\mathbf{t}, \log \mathbf{t})$, between \mathbf{w} and the black end \mathbf{b}_x of a translate \mathbf{e}_x of \mathbf{e} by $x = (x, y) \in \mathbb{Z}^2$

$$K_{\gamma, \mathbf{t}}^{-1}(\mathbf{b}_x, \mathbf{w}) = \iint \frac{z^{-y} w^x Q_{\mathbf{e}}(e^{c+\beta\gamma\mathbf{t}} z, \mathbf{t}w)}{P(e^{c+\beta\gamma\mathbf{t}} z, \mathbf{t}w)} \frac{dz}{2i\pi z} \frac{dw}{2i\pi w}. \quad (6.10)$$

Proposition 6.1. *Denote by $J_\gamma(x, \xi)$ the kernel of the bead model.*

$$J_\gamma(x, \xi) = \begin{cases} \int_{[-\sqrt{1-\gamma^2}, \sqrt{1-\gamma^2}]} e^{-i\xi\phi} (\gamma + i\phi)^x \frac{d\phi}{2\pi} & \text{if } x \geq 0 \\ - \int_{\mathbb{R} \setminus [-\sqrt{1-\gamma^2}, \sqrt{1-\gamma^2}]} e^{-i\xi\phi} (\gamma + i\phi)^x \frac{d\phi}{2\pi} & \text{if } x < 0 \end{cases} \quad (6.11)$$

In the scaling limit

$$\mathbf{t} \rightarrow 0, \quad , \quad \mathbf{t}\beta y \rightarrow \xi, \quad (6.12)$$

the coefficients $K_{\gamma, \mathbf{t}}^{-1}(\mathbf{b}_x, \mathbf{w})$ have the following asymptotics

$$K_{\gamma, \mathbf{t}}^{-1}(\mathbf{b}_x, \mathbf{w}) \sim \mathbf{t}\rho_{\mathbf{e}} J_\alpha(x, \xi) \quad (6.13)$$

The quantity $\rho_{\mathbf{e}}$ is given by

$$\rho_{\mathbf{e}} = \frac{e^c \beta \partial_1 Q_{\mathbf{e}}(e^c, 0) + \partial_2 Q_{\mathbf{e}}(e^c, 0)}{\partial_2 P(e^c, 0)}. \quad (6.14)$$

Once multiplied by $K_{\mathbf{e}}$, it represents the proportion of this type of edges among the defects along a thread.

Proof:

We denote by $f(z, w)$ the rational fraction inside the integral (6.10)

$$f(z, w) = \frac{z^{-y-1}w^{x-1}Q_{\mathbf{e}}(e^{c+\beta\gamma\mathbf{t}}z, \mathbf{t}w)}{P(e^{c+\beta\gamma\mathbf{t}}z, \mathbf{t}w)}. \quad (6.15)$$

The integral defining $K_{\gamma, \mathbf{t}}^{-1}$ is evaluated by performing first the integral over w . Suppose first that $x \geq 0$. There is no singularity at $w = 0$, since $\deg_w Q \geq 1$. The only pole in the unit disc is $W_0(z)/\mathbf{t}$ when $z \in [e^{-i\theta(\mathbf{t})}, e^{i\theta(\mathbf{t})}] = I_{\mathbf{t}}$. In this case,

$$\begin{aligned} K_{\gamma, \mathbf{t}}^{-1}(\mathbf{b}_x, \mathbf{w}) &= \int_{I_{\mathbf{t}}} \frac{u^{-y}(W_0(z)/\mathbf{t})^{x-1}Q_{\mathbf{e}}(e^{c+\beta\gamma\mathbf{t}}z, W_0(z))}{\partial_2 P(z, W_0(z))\mathbf{t}} \frac{dz}{2i\pi z} \\ &= \int_{-\sqrt{1-\gamma^2}+O(\mathbf{t})}^{\sqrt{1-\gamma^2}+O(\mathbf{t})} \frac{e^{-i\beta\mathbf{t}y\phi}(\gamma + i\phi + O(\mathbf{t}))^{x-1}Q_{\mathbf{e}}(e^{c+\mathbf{t}\beta\gamma+i\mathbf{t}\beta\phi}, (\gamma + i\phi)\mathbf{t} + O(\mathbf{t}^2))}{\partial_2 P(e^{c+\mathbf{t}\beta\gamma+i\mathbf{t}\beta\phi}, (\gamma + i\phi)\mathbf{t} + O(\mathbf{t}^2))} \frac{\beta d\phi}{2\pi} \end{aligned}$$

For a small \mathbf{t} and a fixed ϕ , we have

$$Q_{\mathbf{e}}(e^{c+\mathbf{t}\beta\gamma+i\mathbf{t}\beta\phi}, (\gamma + i\phi)\mathbf{t} + O(\mathbf{t}^2)) = \mathbf{t}(\gamma + i\phi)(\beta e^c \partial_1 Q_{\mathbf{e}} + \partial_2 Q_{\mathbf{e}}) + O(\mathbf{t}^2), \quad (6.16)$$

$$\partial_2 P(e^{c+\mathbf{t}\beta\gamma+i\mathbf{t}\beta\phi}, (\gamma + i\phi)\mathbf{t} + O(\mathbf{t}^2)) = \partial_2 P + O(\mathbf{t}). \quad (6.17)$$

where the derivatives of polynomials P and $Q_{\mathbf{e}}$ are evaluated at $(e^c, 0)$. Therefore,

$$K_{\gamma, \mathbf{t}}^{-1}(\mathbf{b}_x, \mathbf{w}) = \frac{\mathbf{t}\beta(e^c \partial_1 Q_{\mathbf{e}} + \partial_2 Q_{\mathbf{e}})}{\partial_2 P} \left(\int_{[-\sqrt{1-\gamma^2}, \sqrt{1-\gamma^2}]} e^{-i\xi\phi}(\gamma + i\phi)^x \frac{d\phi}{2\pi} + O(\mathbf{t}) \right)$$

When $x < 0$, the rational fraction in the integral has a multiple pole at $w = 0$ which is hard to evaluate directly. However the rational fraction is a $o(\frac{1}{w})$ when $|w| \rightarrow \infty$, and hence the sum of all residues in the plane is 0.

Let us bound the residues at the simple roots of P : $W_1(z), \dots, W_{d-1}(z)$. We know already from (6.7) that there exists ϵ such that for every $j \in \{1, \dots, d-1\}$, $|W_j(z)| \geq \epsilon$ for every $z \in \mathbb{S}^1$. By the same argument of compactness, there exists a constant $M > 0$ such that for \mathbf{t} small enough,

$$\forall j \in \{1, \dots, d-1\} \quad \forall z \in \mathbb{S}^1$$

$$|\partial_2 P(e^{c+\beta\gamma\mathbf{t}}z, W_j(z))| \geq \frac{1}{M} \quad \text{and} \quad \left| \frac{Q_{\mathbf{e}}(e^{c+\beta\gamma\mathbf{t}}z, W_j(z))}{W_j(z)} \right| \leq M \quad (6.18)$$

and therefore,

$$\left| \frac{(W_j(z)/\mathbf{t})^x Q_{\mathbf{e}}(e^{c+\beta\gamma\mathbf{t}}z, W_j(z))}{W_j(z) \partial_2 P(e^{c+\beta\gamma\mathbf{t}}z, W_j(z))} \right| \leq (\epsilon/\mathbf{t})^x M^2 = O(\mathbf{t}^{-x}) \quad (6.19)$$

Thus the contribution of these residues is negligible as soon as $x \leq -2$. In that case, we have:

$$\begin{aligned} \mathsf{K}_{\gamma, \mathfrak{t}}^{-1}(\mathbf{b}_x, \mathbf{w}) &= \int_{\mathbb{S}^1} \operatorname{Res}_{w=0} f(z, w) \frac{dz}{2i\pi} + \int_{I_{\mathfrak{t}}} \operatorname{Res}_{w=W_0(z)/\mathfrak{t}} f(z, w) \frac{dz}{2i\pi} \\ &= - \sum_{j=1}^{d-1} \int_{\mathbb{S}^1} \operatorname{Res}_{w=W_j(z)/\mathfrak{t}} f(z, w) \frac{dz}{2i\pi} - \int_{\mathbb{S}^1 \setminus I_{\mathfrak{t}}} \operatorname{Res}_{w=W_0(z)/\mathfrak{t}} f(z, w) \frac{dz}{2i\pi} \end{aligned} \quad (6.20)$$

Using the estimates (6.16) and (6.17), we find that

$$\begin{aligned} \int_{\mathbb{S}^1 \setminus I_{\mathfrak{t}}} \operatorname{Res}_{w=W_0(z)/\mathfrak{t}} f(z, w) \frac{dz}{2i\pi} &= \int_{\mathbb{S}^1 \setminus I_{\mathfrak{t}}} \frac{z^{-y} \left(\frac{W_0(z)}{\mathfrak{t}}\right)^{x-1} Q_{\mathbf{e}}(e^{c+\gamma\beta\mathfrak{t}}z, W_0(z))}{\mathfrak{t}\partial_2 P(e^{c+\gamma\beta\mathfrak{t}}z, W_0(z))} \frac{dz}{2i\pi z} \\ &= \int_{\left[-\frac{\pi}{|\beta|}, -\sqrt{1-\gamma^2}+o(1)\right] \cup \left[\sqrt{1-\gamma^2}+o(1), \frac{\pi}{|\beta|}\right]} \frac{e^{-iy\beta\mathfrak{t}\phi} (\gamma + i\phi + O(\mathfrak{t}))^{x-1} Q_{\mathbf{e}}(e^{c+\mathfrak{t}\beta\gamma+it\beta\phi}, W_0(e^{it\beta\phi}))}{\mathfrak{t}\partial_2 P(e^{c+\mathfrak{t}\beta\gamma+it\beta\phi}, W_0(e^{it\beta\phi}))} \frac{\mathfrak{t}\beta d\phi}{2\pi}. \end{aligned} \quad (6.21)$$

By Lebesgue's dominated convergence theorem, the integral in the scaling limit

$$\mathfrak{t} \rightarrow 0, \quad \mathfrak{t}\beta y \rightarrow \xi$$

is asymptotic to the following expression

$$\frac{\mathfrak{t}\beta(e^c\beta\partial_1 Q_{\mathbf{e}} + \partial_2 Q_{\mathbf{e}})}{\partial_2 P} \int_{\mathbb{R} \setminus [-\sqrt{1-\gamma^2}, \sqrt{1-\gamma^2}]} e^{-i\phi\xi} (\gamma + i\phi)^x \frac{d\phi}{2\pi} \quad (6.22)$$

and thus,

$$\mathsf{K}_{\gamma, \mathfrak{t}}^{-1}(\mathbf{b}_x, \mathbf{w}) = \frac{\mathfrak{t}\beta(e^c\beta\partial_1 Q_{\mathbf{e}} + \partial_2 Q_{\mathbf{e}})}{\partial_2 P} \left(- \int_{\mathbb{R} \setminus [-\sqrt{1-\gamma^2}, \sqrt{1-\gamma^2}]} e^{-i\phi\xi} (\gamma + i\phi)^x \frac{d\phi}{2\pi} + o(1) \right). \quad (6.23)$$

When $x = -1$, the residues at the poles $W_1(z), \dots, W_{d-1}(z)$ are not negligible any more. However, in this case, the pole at $w = 0$ is simple. A direct evaluation of the integral shows:

$$\begin{aligned} \mathsf{K}_{\gamma, \mathfrak{t}}^{-1}(\mathbf{b}_x, \mathbf{w}) &= \int_{\mathbb{S}^1} \operatorname{Res}_{w=0} f(z, w) \frac{dz}{2i\pi} + \int_{I_{\mathfrak{t}}} \operatorname{Res}_{w=W_0(z)/\mathfrak{t}} f(z, w) \frac{dz}{2i\pi} \\ &= \int_{\mathbb{S}^1} \frac{z^{-y} \mathfrak{t} \partial_2 Q_{\mathbf{e}}(e^{c+\beta\gamma\mathfrak{t}}z, 0)}{P(e^{c+\beta\gamma\mathfrak{t}}z, 0)} \frac{dz}{2i\pi z} + \int_{I_{\mathfrak{t}}} \frac{z^{-y} \left(\frac{W_0(z)}{\mathfrak{t}}\right)^{-2} Q_{\mathbf{e}}(e^{c+\beta\gamma\mathfrak{t}}z, W_0(z))}{\mathfrak{t}\partial_2 P(e^{c+\beta\gamma\mathfrak{t}}z, W_0(z))} \frac{dz}{2i\pi z} \end{aligned} \quad (6.24)$$

Posing $z = e^{i\beta\mathfrak{t}\phi}$, one has

$$\begin{aligned} \mathsf{K}_{\gamma, \mathfrak{t}}^{-1}(\mathbf{b}_x, \mathbf{w}) &= \mathfrak{t}^2 \beta \int_{-\frac{\pi}{|\beta|\mathfrak{t}}}^{\frac{\pi}{|\beta|\mathfrak{t}}} \frac{e^{-i\beta\varphi\mathfrak{t}y} \partial_2 Q_{\mathbf{e}}(e^{c+\beta\gamma\mathfrak{t}+i\beta\phi\mathfrak{t}}, 0)}{P(e^{c+\beta\gamma\mathfrak{t}+i\beta\phi\mathfrak{t}}, 0)} \frac{d\phi}{2\pi} \\ &\quad + \mathfrak{t}^2 \beta \int_{-\sqrt{1-\gamma^2}+o(1)}^{\sqrt{1-\gamma^2}+o(1)} \frac{e^{-i\beta\varphi\mathfrak{t}y} Q_{\mathbf{e}}(e^{c+\beta\gamma\mathfrak{t}+i\beta\phi\mathfrak{t}}, 0)}{W_0(e^{i\beta\phi\mathfrak{t}})^2 \partial_2 P(e^{c+\beta\gamma\mathfrak{t}+i\beta\phi\mathfrak{t}}, 0)} \frac{d\phi}{2\pi} \end{aligned} \quad (6.25)$$

Using the following estimates from Taylor's formula

$$\begin{aligned} \partial_2 Q(e^{c+\beta\gamma\mathfrak{t}+i\beta\phi\mathfrak{t}}, 0) &= \frac{Q_{\mathbf{e}}(e^{c+\beta\gamma\mathfrak{t}+i\beta\phi\mathfrak{t}}, W_0(z)) - Q_{\mathbf{e}}(e^{c+\beta\gamma\mathfrak{t}+i\beta\phi\mathfrak{t}}, 0)}{W_0(z)} + O(\mathfrak{t}) \\ &= \beta e^c \partial_1 Q_{\mathbf{e}} + \partial_2 Q_{\mathbf{e}} + O(\mathfrak{t}) \end{aligned} \quad (6.26)$$

$$\begin{aligned} P(e^{c+\beta\gamma\mathfrak{t}+i\beta\phi\mathfrak{t}}, 0) &= P(e^{c+\beta\gamma\mathfrak{t}+i\beta\phi\mathfrak{t}}, W_0(z)) - W_0(z) \partial_2 P(e^{c+\beta\gamma\mathfrak{t}+i\beta\phi\mathfrak{t}}, W_0(z)) + O(\mathfrak{t}^2) \\ &= -(\gamma + i\phi)\mathfrak{t} \partial_2 P + O(\mathfrak{t}^2) \end{aligned} \quad (6.27)$$

together with (6.16) and (6.17), and applying Lebesgue dominated convergence theorem after an integration by parts, one can prove that in the scaling limit, the coefficient of the inverse Kasteleyn operator $\mathbf{K}_{\gamma, \mathfrak{t}}^{-1}(\mathbf{b}_x, \mathbf{w})$ is asymptotic to

$$-\mathfrak{t} \beta \frac{e^c \beta \partial_1 Q + \partial_2 Q}{\partial_2 P} \int_{\mathbb{R} \setminus [-\sqrt{1-\gamma^2}, \sqrt{1-\gamma^2}]} e^{-i\phi\xi} (\gamma + i\phi)^{-1} \frac{d\phi}{2\pi}$$

□

Remark. The ratio $(e^c \beta \partial_1 Q_{\mathbf{e}} + \partial_2 Q_{\mathbf{e}}) / \partial_2 P$ controls the density of the limiting bead model. If plugging $\phi = \sqrt{1-\gamma^2}$ into (6.16) and (6.17), one can see that it is up, to terms of higher order in \mathfrak{t} , equal to

$$\frac{i Q_{\mathbf{e}}(e^{c+\beta\gamma\mathfrak{t}} z_0, \mathfrak{t} w_0)}{i \partial_2 P(e^{c+\beta\gamma\mathfrak{t}} z_0, \mathfrak{t} w_0) \mathfrak{t} w_0} \quad (6.28)$$

where (z_0, w_0) are zeros of the characteristic polynomial $P(e^{c+\beta\gamma\mathfrak{t}} \cdot, \mathfrak{t} \cdot)$ on the unit torus. When multiplied by $\mathbf{K}_{\mathbf{e}}$, the numerator is the length of the dual edge \mathbf{e}^* in the natural application from the dual graph G^* to \mathbb{R}^2 described in section 2.6 while the denominator is that of the vertical side of the fundamental domain.

Proposition 6.1 shows that the kernel giving the correlations has the same form as the original bead model. However, in order to recover the bead model, one can not just look at one type of edges on threads but at all of them.

Since the frozen paths have been chosen to cross no dimer when the slope is on the side of the particular Newton polygon we are looking at, they are bordered by white vertices on their left, and black vertices on their right. For a reason of parity between white and black vertices, there is no dimer configuration of the graph G_1 deprived of the projection of these two vertices having a height change² on the side of $N(P)$. Therefore the arguments of the proof of proposition 6.1 can be applied to obtain similar asymptotics as those given in that proposition for the coefficients of $\mathbf{K}_{\gamma, \mathfrak{t}}^{-1}$ between these vertices.

²The term *height change* here is an abuse of notations, since the difference between the reference unit flow and the one corresponding to any dimer configuration of G_1 deprived of the two vertices has a non-zero divergence. What we mean here by this expression is in fact the powers in z and w in the weight of the configuration computed using the magnetically altered Kasteleyn operator $K(z, w)$ divided by that of the reference dimer configuration.

Proposition 6.2. *Let $\mathbf{b}_{x,y}$ and \mathbf{w} be respectively a black and a white vertex each bordering one of these paths, and in fundamental domains separated by a lattice translation (x, y) . In the scaling limit*

$$\mathfrak{t} \rightarrow 0, \quad \mathfrak{t}\beta y \rightarrow \xi, \quad (6.29)$$

the coefficient $K_{\gamma, \mathfrak{t}}^{-1}(\mathbf{b}_{x,y}, \mathbf{w})$ has the following asymptotics

$$K_{\gamma, \mathfrak{t}}^{-1}(\mathbf{b}_{x,y}, \mathbf{w}) \sim \mathfrak{t} \rho_{\mathbf{b}\mathbf{w}} J_\gamma(x, \xi), \quad (6.30)$$

where

$$\rho_{\mathbf{b}\mathbf{w}} = \frac{e^c \beta \partial_1 Q_{\mathbf{b}\mathbf{w}}(e^c, 0) + \partial_2 Q_{\mathbf{b}\mathbf{w}}(e^c, 0)}{\partial_2 P(e^c, 0)}. \quad (6.31)$$

These coefficients $\rho_{\mathbf{b}\mathbf{w}}$ are in fact the product of two terms, one depending only on \mathbf{b} and the other on \mathbf{w} . This property is stated in the following lemma

Lemma 6.1. *The rank of the matrix $e^c \beta \partial_1 Q(e^c, 0) + \partial_2 Q(e^c, 0)$, restricted to projections of vertices bordering a thread, is equal to 1. In particular, for any \mathbf{b} and any \mathbf{w} bordering a thread, there exist $U_{\mathbf{b}}$ and $V_{\mathbf{w}}$ such that*

$$\rho_{\mathbf{b}\mathbf{w}} = U_{\mathbf{b}} V_{\mathbf{w}}. \quad (6.32)$$

Proof:

The matrix $e^c \beta \partial_1 Q(e^c, 0) + \partial_2 Q(e^c, 0)$ is the limit when \mathfrak{t} goes to zero of

$$\frac{1}{\mathfrak{t} w_0} Q(e^{c+\beta\gamma\mathfrak{t}} z_0, \mathfrak{t} w_0) \quad (6.33)$$

where (z_0, w_0) are zeros on the unit torus of $P(e^{c+\beta\gamma\mathfrak{t}} z, \mathfrak{t} w)$. These zeros depend on \mathfrak{t} and γ and their first term in their expansion in \mathfrak{t} is obtained by plugging $\phi = \pm\sqrt{1-\gamma^2}$ into equations (6.16) and (6.17):

$$z_0 = 1 + O(\mathfrak{t}), \quad w_0 = \gamma \pm i\sqrt{1-\gamma^2} + O(\mathfrak{t}). \quad (6.34)$$

Since $(e^{c+\beta\gamma\mathfrak{t}} z_0, \mathfrak{t} w_0)$ is not real, it is a simple zero of $P = \det K$. Q is the comatrix of K , its rank is 1 at a simple zero of P . Therefore, as the limit of sequence of rank 1 matrices, the matrix $e^c \beta \partial_1 Q(e^c, 0) + \partial_2 Q(e^c, 0)$ has a rank at most 1. As there is at most a non-zero entry in this matrix, the rank is equal to 1.

The coefficient $\rho_{\mathbf{b}\mathbf{w}}$ is a multiple the entry (\mathbf{b}, \mathbf{w}) of this matrix. Its decomposition into a product comes from the representation of a rank-1 matrix as a tensor product of a vector and a linear form. \square

6.3 Convergence to the bead model

We already said that the threads of our bead model would be the infinite collection of vertical paths, translated one from another, that are frozen, *i.e.* they do not cross any dimer when the slope of the measure lies on the boundary of the Newton polygon. The beads are represented by the dimers crossing these paths when the magnetic field lies in one of the vertical tentacles of the amoeba.

Like in chapter 5, as the magnetic field goes deeper into the tentacle of the amoeba, the picture of the graph in the plane is rescaled in such a way that although the probability of seeing a dimer crossing these “almost-frozen” paths goes to zero, the average number of such edges by centimeter of thread stays almost constant. The scaling limit we perform is

$$\mathfrak{t} \rightarrow 0, \quad \mathfrak{t}\beta y \rightarrow \xi \in \mathbb{R}. \quad (6.35)$$

To find the limiting distribution of this beads, we first evaluate the quantities

$$\mathbb{E} \left[\frac{X_{I_1}!}{(X_{I_1} - n_1)!} \cdots \frac{X_{I_k}!}{(X_{I_k} - n_k)!} \right] \quad (6.36)$$

where X_{I_j} is the number of dimers crossing the (rescaled) thread interval. We look in details at the case $k = 1$ when only one thread interval is at stake. The other cases are similar. For a given n , and a fixed value of γ and of the scaling parameter \mathfrak{t} , we have

$$\mathbb{E}_{\gamma, \mathfrak{t}} \left[\frac{X_I!}{(X_I - n)!} \right] = \sum_{\substack{\mathbf{e}_1, \dots, \mathbf{e}_n \in I \\ \text{distinct}}} \mathbb{P}_{\gamma, \mathfrak{t}} [\mathbf{e}_1, \dots, \mathbf{e}_n \in \mathcal{C}] \quad (6.37)$$

where the sum is over all possible n -tuples of edges crossing the thread interval I . The edges crossing I are labelled by their type (*i.e.* their projection on $G_1 = G/\mathbb{Z}^2$) and the coordinates of the fundamental domain they belong to. The edge \mathbf{e}_x^j represents the edge of type j in the fundamental domain with coordinates $x = (x, y)$. The type label j ranges from 1 to d . Since the probability of having two such edges in the same fundamental domain is negligible, we can rewrite this sum of probabilities, as a sum over the fundamental domains and the types of edges crossing the thread interval.

$$\mathbb{E}_{\gamma, \mathfrak{t}} \left[\frac{X_I!}{(X_I - n)!} \right] = \sum_{\substack{x_1, \dots, x_n \in I \\ \text{distinct}}} \sum_{j_1, \dots, j_n=1}^n \mathbb{P}_{\gamma, \mathfrak{t}} [\mathbf{e}_{x_1}^{j_1}, \dots, \mathbf{e}_{x_n}^{j_n} \in \mathcal{C}] + O(\mathfrak{t}) \quad (6.38)$$

The different probabilities $\mathbb{P}_{\gamma, \mathfrak{t}} [\mathbf{e}_{x_1}^{j_1}, \dots, \mathbf{e}_{x_n}^{j_n} \in \mathcal{C}]$ are given by the determinant of a $n \times n$ matrix that is equal to

$$\mathfrak{t}^n \left(\prod_{l=1}^n \mathbf{K}_{j_l} \right) \times \det_{1 \leq k, l \leq n} [\rho_{j_k j_l} J_\gamma(x_k - x_l, \mathfrak{t}\beta(y_k - y_l))] + O(\mathfrak{t}^{n+1}) \quad (6.39)$$

Since ρ_{jk} is the product of two terms $U_j V_k$, by carrying out of the determinant by n -linearity these coefficients, equation (6.39) becomes

$$\begin{aligned} \mathfrak{t}^n \left(\prod_{l=1}^n \mathsf{K}_{j_l} \right) &\times \det_{1 \leq k, l \leq n} [U_{j_k} V_{j_l} J_\gamma(x_k - x_l, \mathfrak{t}\beta(y_k - y_l))] + O(\mathfrak{t}^{n+1}) \\ &\mathfrak{t}^n \left(\prod_{l=1}^n \mathsf{K}_{j_l} U_{j_l} V_{j_l} \right) \times \det_{1 \leq k, l \leq n} [J_\gamma(x_k - x_l, \mathfrak{t}\beta(y_k - y_l))] + O(\mathfrak{t}^{n+1}) \\ &\mathfrak{t}^n \left(\prod_{l=1}^n \mathsf{K}_{j_l} \rho_{j_l} \right) \times \det_{1 \leq k, l \leq n} [J_\gamma(x_k - x_l, \mathfrak{t}\beta(y_k - y_l))] + O(\mathfrak{t}^{n+1}) \end{aligned} \quad (6.40)$$

Summing now over the different types of edges, one gets

$$\begin{aligned} \sum_{j_1, \dots, j_n=1}^d \mathbb{P}_{\gamma, \mathfrak{t}} [\mathbf{e}_{x_1}^{j_1}, \dots, \mathbf{e}_{x_n}^{j_n} \in \mathcal{C}] &= \\ \mathfrak{t}^n \left(\sum_{j=1}^d \mathsf{K}_{j_l} \rho_{j_l} \right)^n &\det_{1 \leq k, l \leq n} [J_\gamma(x_k - x_l, \mathfrak{t}\beta(y_k - y_l))] + O(\mathfrak{t}^{n+1}) \end{aligned} \quad (6.41)$$

$\mathsf{K}_j \rho_j$ is the proportion of edges of type j along the thread. These coefficients sum up to 1, and we have finally that expression (6.38) is a Riemann sum of

$$\int \cdots \int_{I^n} \det_{1 \leq k, l \leq n} [J_\gamma(x_k - x_l, \xi_k - \xi_l)] d^n \xi \quad (6.42)$$

and the same argument of domination as in the proof of theorem 5.2 implies that the distribution of X_I converges to the distribution of beads in the interval I in the bead model of parameter γ . The generalization to any finite dimensional distribution is notationally cumbersome, but straightforward. These considerations give thus the proof of the following theorem

Theorem 6.1. *Let $\gamma \in (-1, 1)$. In the scaling limit $\mathfrak{t} \rightarrow 0$, $\mathfrak{t}\beta y \rightarrow \xi$, the point process describing the position of rare edges on the threads, identified with the almost frozen paths converges to the bead model of index γ , i.e. the determinantal point process on $\mathbb{Z} \times \mathbb{R}$ with kernel J_γ .*

Recall that γ describes the different possible ways to go deep into a tentacle. This theorem states that the bead model, with its 1-parameter family of Gibbs measures, is the universal limiting behaviour of any dimer model on a bipartite periodic planar graph when the order parameters (B_x, B_y) go to infinity in staying in the liquid phase.

6.4 Interaction between bead models

It often happens that a side of the Newton polygon is not the result of a unique frozen path, but that different paths give the same constraint on the slope (2.34). In that case,

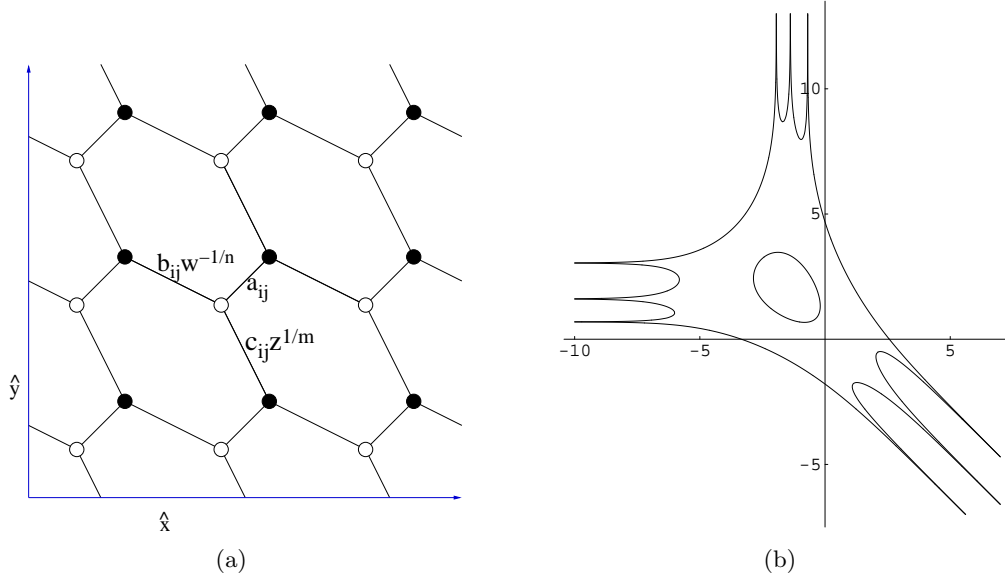
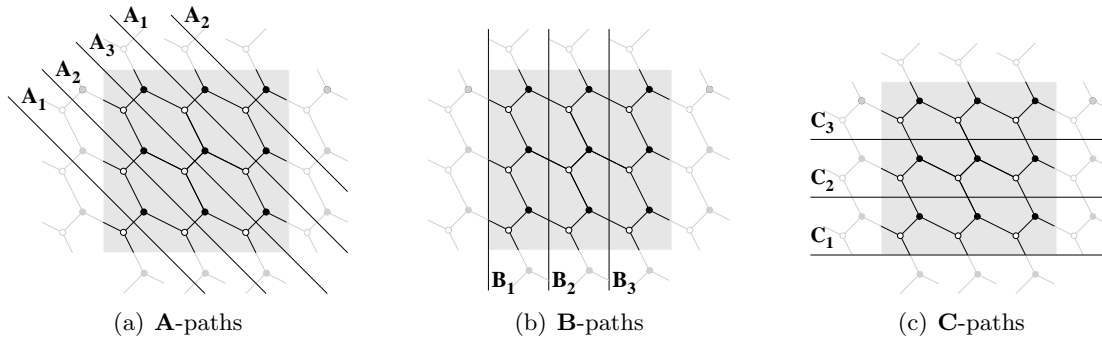


Figure 6.2: (a) A 3×3 fundamental domain of the honeycomb lattice. Weights of edges around white vertex \mathbf{w}_{ij} are a_{ij} , b_{ij} and c_{ij} . The Fourier multipliers have been distributed over the edges by gauge transformation. (b) The amoeba for generic weights on the graph represented on the left panel. This amoeba presents a gaseous phase, and three tentacles in three directions, each corresponding to a collection of frozen paths drawn on figure 6.3.

we do not have just one family of frozen paths, but several parallel families of thread, carrying all in the scaling limit a bead model. In this section, we describe the interaction between these different bead models in the case of the generic case of the honeycomb lattice H with a $n \times m$ fundamental domain.

The fundamental domain of this periodic planar graph is represented on figure 6.2. The vertices of the quotient H_1 by the action of \mathbb{Z}^2 by translation are labelled by two integers, i and j ranging respectively from 1 to n , and from 1 to m . The weights of the edges around the white vertex labelled by (i, j) are denoted by a_{ij} , b_{ij} and c_{ij} . By an appropriate gauge transformation, one can spread the factors z and w in the magnetically altered Kasteleyn matrix $K(z, w)$ so that the coefficients of this operator be a_{ij} , $b_{ij}w^{-1/n}$ and $c_{ij}z^{1/m}$. The reference dimer configuration we will use is the configuration containing a -edges.

One distinguishes three special classes of dual cycles in G_1 , say **A**, **B** and **C** that cross only edges of a given type (repectively a , b and c). The lifts of these classes to H are represented on figure 6.3. The **B** class is constituted by n vertical straight paths with homology class $(0, 1)$, whereas the **C** class contains the m horizontal straight paths with homology class $(1, 0)$. The **A** class contains $d = \gcd(n, m)$ paths with homology $(\frac{m}{d}, \frac{n}{d})$. The three classes of cycles lift to H , forming three classes of parallel families of straight lines.

Figure 6.3: the three classes of possible frozen paths: **A**, **B** and **C**.

The Newton polygon of the weighted dimer graph G is a right triangle. Each side of the triangle corresponds to Gibbs measures for which all the paths of one of the three classes are frozen. The horizontal side contains $n + 1$ lattice points. The amoeba of the associated spectral curve exhibits n vertical tentacles separating $n + 1$ unbounded complementary components – solid phases in the phase diagram – each corresponding to a lattice point of the horizontal side.

As explained in chapter 2, the frozen configurations are obtained as follows: when the Gibbs measure's slope lies, say, on the horizontal side of the Newton polygon, there is almost surely no edge crossing the **B** class of paths. These paths delimit thin strips where one sees either an infinite succession of a -edges or an infinite collection of c -edges. On G_1 and in presence of a magnetic field (B_x, B_y) , the associated patterns have weights $\prod_{i=1}^m a_{ij}$ and $e^{B_x} \prod_{i=1}^m c_{ij}$. The patterns with the highest weight correspond to the type of columns appearing in the configuration with probability 1. When the horizontal component of the magnetic field is very negative, the weight of the ' a ' patterns are greater than the ' c ' ones, but as B_x increases, the weight of the second pattern becomes more important, and at some point, it becomes bigger than the first one. In the graph G the a -edges that were filling the space between the two **B** paths switch to c -edges. Generically the values of B_x corresponding to such a switch are all different. They correspond to the abscissæ of the vertical tentacles of the amoeba.

In a fixed window and when B_y is very large, one sees columns of edges of the same type (a , or c) with a probability close to 1. When the magnetic field lies in a tentacle of the phase diagram, the system hesitates between two states for a given type of columns. With a probability p bounded away from 0 and 1, the column is filled with a -edges, and with probability $1 - p$, it is filled with c -edges. If one rescales vertically the graph in the same time as B_y goes to $+\infty$, then one will be able to see the transition between these two possibilities: between the two types of fillings, a b -edge is inserted. The edge creates a defect in the neighbouring column that is supposed to be frozen. This discussion is quantified in the following proposition:

Proposition 6.3. *If*

$$B_x < \sum_{i=1}^m \log \frac{a_{ij_0}}{c_{ij_0}}, \quad (6.43)$$

then with probability going to 1 when B_y goes to infinity, the columns of type j_0 will be filled with a -edges.

If the inequality is strict in the other direction, then they will be filled with c -edges with probability going to 1 when B_y goes to infinity.

Proof:

When the vertical component of the magnetic field is very negative, the main contribution to the characteristic polynomial is given by the configurations on G_1 that contain no b -edges. One can choose to fill each strip of G_1 between two consecutive frozen cycles either by a -edges or by c -edges. Choosing a filling with c edges induces a height change of m in the vertical direction. Therefore

$$P^B(z, w) = \prod_{j=1}^n \left(\prod_{i=1}^m a_{ij} - (-1)^m e^{B_x} z \prod_{i=1}^m c_{ij} \right) + O(t) \quad (6.44)$$

where $t = e^{B_y}$ is small.

Let \mathbf{b} and \mathbf{w} two vertices in the same strip j_0 in G_1 . Denote by \mathbf{b}_y and \mathbf{w}_0 lifts of \mathbf{b} and \mathbf{w} in the same column of G , separated by y fundamental domains. The entry of the inverse Kasteleyn operator between these two vertices is easily evaluated: recall that $Q_{\mathbf{bw}}$ is the characteristic polynomial of the graph G where all the translated of \mathbf{b} and \mathbf{w} have been removed. Repeating the argument given above, we find the main contribution to it,

$$Q_{\mathbf{bw}}^B = M_{\mathbf{bw}} z^\delta \prod_{\substack{j=1 \\ j \neq j_0}}^n \left(\prod_{i=1}^m a_{ij} - (-1)^m e^{B_x} z \prod_{i=1}^m c_{ij} \right) + O(t) \quad (6.45)$$

where $M_{\mathbf{bw}} z^\delta$ is the weight of the dimer configuration of the strip j_0 of G_1 deprived of \mathbf{b} and \mathbf{w} . The coefficient of the inverse Kasteleyn operator corresponding to these two vertices whose fundamental domains are separated by the lattice vector (x, y) is given by

$$\mathbb{K}_B^{-1}(\mathbf{b}_y, \mathbf{w}_0) = \iint_{\mathbb{T}^2} \frac{z^{-y} w^0 Q_{\mathbf{bw}}^B(z, w)}{P^B(z, w)} \frac{dz}{2i\pi z} \frac{dw}{2i\pi w} \quad (6.46)$$

$$= \iint_{\mathbb{T}^2} \frac{z^{-y+\delta} M_{\mathbf{bw}}}{\left(\prod_{i=1}^m a_{ij_0} - (-1)^m e^{B_x} z \prod_{i=1}^m c_{ij_0} \right)} \frac{dz}{2i\pi z} \frac{dw}{2i\pi w} + O(t) \quad (6.47)$$

$$= \int_{\mathbb{S}^1} \frac{z^{-y+\delta} M_{\mathbf{bw}}}{\left(\prod_{i=1}^m a_{ij_0} - (-1)^m e^{B_x} z \prod_{i=1}^m c_{ij_0} \right)} \frac{dz}{2i\pi z} + O(t) \quad (6.48)$$

Suppose that $B_x < \sum_{i=1}^m \log \frac{a_{ij_0}}{c_{ij_0}}$, the other case is similar. In that case, the pole located at

$$z = (-1)^m \frac{\prod_{i=1}^m a_{ij_0}}{e^{B_x} \prod_{i=1}^m c_{ij_0}} \quad (6.49)$$

is outside of the unit disk. If $y - \delta < 0$, then there is no pole at all in the unit disk, and therefore the integral over z is zero. However, if $y - \delta \geq 0$, then the integral equals the opposite of the residue at z_0 , and

$$\mathbf{K}_B^{-1}(\mathbf{b}_y, \mathbf{w}_0) = \frac{M_{\mathbf{b}\mathbf{w}}}{(-1)^m e^{B_x} \prod_{i=1}^m c_{ij_0}} \left(\frac{\prod_{i=1}^m a_{ij_0}}{(-1)^m e^{B_x} \prod_{i=1}^m c_{ij_0}} \right)^{-y-1} + O(\mathfrak{t}) \quad (6.50)$$

When \mathbf{b}_y and \mathbf{w}_0 are the ends of an edge with weight $a_{i_0 j_0}$, $M_{\mathbf{b}\mathbf{w}} = \prod_{i \neq i_0} a_{ij_0}$ and y and δ equal 0. It follows that

$$\mathbf{K}_B^{-1}(\mathbf{b}_y, \mathbf{w}_0) = \frac{M_{\mathbf{b}\mathbf{w}}}{\prod_{i=1}^m a_{ij_0}} + O(\mathfrak{t}) = \frac{1}{a_{i_0 j_0}} + O(\mathfrak{t}) \quad (6.51)$$

Thus, the probability of this a -edge, given by $a_{i_0 j_0} \mathbf{K}_B^{-1}(\mathbf{b}_y, \mathbf{w}_0)$ goes to 1 when \mathfrak{t} goes to zero.

On the other hand, in the case when \mathbf{b} and \mathbf{w} are the ends of a ' c '-type edge, then either $y = -1$ or $\delta = 1$. In both cases, $\mathbf{K}_B^{-1}(\mathbf{b}_y, \mathbf{w}_0)$ is $O(\mathfrak{t})$. Thus the probability of this edge goes to zero when \mathfrak{t} goes to zero. Such an edge is called *non typical*. \square

A sequence of non-typical edges in a frozen column is initiated by the presence of a bead (a ' b '-edge) crossing a neighbouring wire. The analysis we made of the inverse Kasteleyn operator allows us to determine the distribution of the sequence of non typical edges in a frozen column.

Proposition 6.4. *The length of a succession of non typical edges in a frozen column has a geometric distribution. The parameter of the geometric distribution has an explicit expression in terms of lengths of dual edges.*

Proof:

We suppose that in the frozen column j_0 , we only see a -edges with probability close to 1. The following inequality

$$B_x < \sum_{i=1}^m \log \frac{a_{ij_0}}{c_{ij_0}} \quad (6.52)$$

is satisfied. Since we work only in one column, we will drop the index j_0 for the sake of simplicity. Given that the edge $\mathbf{e} = (\mathbf{w}, \mathbf{b})$ with weight b_{i_0} is present in the dimer configuration, we compute the probability of seeing N successive c -edges after this bead. Denote by $\mathbf{e}_1^c = (\mathbf{w}_1, \mathbf{b}_1), \dots, \mathbf{e}_N^c = (\mathbf{w}_N, \mathbf{b}_N)$ the N c -edges. The weights of the edges around vertex \mathbf{w}_i are $a_{[i]}, b_{[i]}, c_{[i]}$, where $[i] = (i_0 + i \bmod m) + 1$. The conditional probability we want to compute is give by the following formula

$$\mathbb{P} \left[\mathbf{e} \in \mathcal{C} \text{ and } \forall i = 1, \dots, N \mathbf{e}_i^c \in \mathcal{C} \mid \mathbf{e} \in \mathcal{C} \right] = \frac{\mathbb{P} [\mathbf{e} \in \mathcal{C} \text{ and } \forall i = 1, \dots, N \mathbf{e}_i^c \in \mathcal{C}]}{\mathbb{P} [\mathbf{e} \in \mathcal{C}]} = \left(\prod_{i=1}^N c_{[i]} \right) \frac{\det A_{N+1}}{\mathbb{K}^{-1}(\mathbf{b}, \mathbf{w})} \quad (6.53)$$

where A_{N+1} is the following square matrix whose entries are inverse Kasteleyn operator coefficients:

$$A = \left[\begin{array}{c|ccc} \mathbb{K}^{-1}(\mathbf{b}, \mathbf{w}) & \cdots & \mathbb{K}^{-1}(\mathbf{b}_j, \mathbf{w}) & \cdots \\ \vdots & \ddots & \vdots & \\ \mathbb{K}^{-1}(\mathbf{b}, \mathbf{w}_i) & & \mathbb{K}^{-1}(\mathbf{b}_j, \mathbf{w}_i) & \\ \vdots & & \vdots & \ddots \end{array} \right] \quad (6.54)$$

Since \mathbf{w} and the white vertices \mathbf{w}_i stand on different sides of a frozen path, the associated coefficients $\mathbb{K}^{-1}(\mathbf{b}, \mathbf{w}_i)$ are $O(\mathfrak{t})$. More precisely, from (6.30), one has

$$\mathbb{K}^{-1}(\mathbf{b}, \mathbf{w}_i) = \mathfrak{t} \rho_{\mathbf{b}\mathbf{w}_i} + O(\mathfrak{t}^2). \quad (6.55)$$

Besides, if $i \leq j$, the power of z in the numerator of (6.46) is positive, and it follows from computations made above that $\mathbb{K}^{-1}(\mathbf{b}_j, \mathbf{w}_i)$ is also $O(\mathfrak{t})$.

For $i \in \{1, \dots, N\}$ and with the convention that $\mathbf{w}_0 = \mathbf{w}$, \mathbf{w}_{i-1} and \mathbf{b}_i are the ends of an a -edge with weight $a_{[i-1]}$. Therefore, the same computations as above show that $\mathbb{K}^{-1}(\mathbf{b}_i, \mathbf{w}_{i-1}) = \frac{1}{a_{[i-1]}}$. As a consequence, the asymptotic expansion of the determinant of A_{N+1} is given by the product of these elements just above the diagonal times the last element of the first column.

$$\det A_{N+1} = \mathfrak{t} \rho_{\mathbf{b}\mathbf{w}_N} \prod_{i=1}^N \frac{1}{a_{[i-1]}} + O(\mathfrak{t}^2) \quad (6.56)$$

As the probability of the bead is $b_{i_0} \rho_{\mathbf{b}\mathbf{w}} \mathfrak{t} + O(\mathfrak{t}^2)$, the conditional probability we want is given by

$$\mathbb{P} [N \text{ successive } c\text{-edges} \mid \text{bead}] = \frac{\rho_{\mathbf{b}\mathbf{w}}}{\rho_{\mathbf{b}\mathbf{w}_N}} \prod_{i=1}^N \frac{c_{[i]}}{a_{[i-1]}} + O(\mathfrak{t}) \quad (6.57)$$

Using proposition 6.1, one can rewrite $\rho_{\mathbf{b}\mathbf{w}_N} / \rho_{\mathbf{b}\mathbf{w}}$ as the following telescopic product

$$\frac{\rho_{\mathbf{b}\mathbf{w}_N}}{\rho_{\mathbf{b}\mathbf{w}}} = \frac{U_{\mathbf{b}} V_{\mathbf{w}_N}}{U_{\mathbf{b}} V_{\mathbf{w}}} = \prod_{i=1}^N \frac{U_{\mathbf{b}_i} V_{\mathbf{w}_i}}{U_{\mathbf{b}_i} V_{\mathbf{w}_{i-1}}}. \quad (6.58)$$

Plugging this into (6.57), one gets

$$\mathbb{P} [N \text{ successive } c\text{-edges} \mid \text{bead}] = \prod_{i=1}^N \frac{c_{[i]} U_{\mathbf{b}_i} V_{\mathbf{w}_i}}{a_{[i-1]} U_{\mathbf{b}_i} V_{\mathbf{w}_{i-1}}} + O(\mathfrak{t}) = \prod_{i=1}^N \frac{\ell(c_{[i]})}{\ell(a_{[i-1]})} + O(\mathfrak{t}) \quad (6.59)$$

where $\ell(a_{[i-1]})$ and $\ell(c_{[i]})$ are respectively the length of the dual edges with weight $a_{[i-1]}$ and $c_{[i]}$ given by the mapping described in lemma 2.1. In particular, in the limit $\tau \rightarrow 0$, the probability that the length L of this succession of non typical edges exceeds p fundamental domains equals

$$\mathbb{P}[L \geq p] = \left(\prod_{i=1}^m \frac{\ell(c_i)}{\ell(a_i)} \right)^p. \quad (6.60)$$

Thus, in the limit, L has a geometric distribution. \square

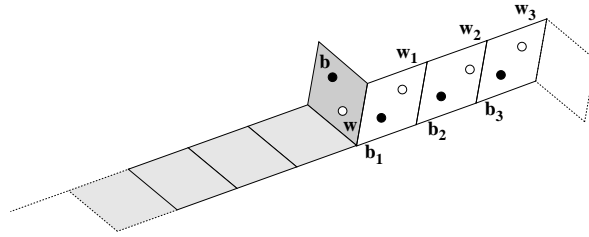


Figure 6.4: Illustration of proposition 6.4. Here is represented a frozen column of (horizontal) a -rhombi, perturbed by the presence of a defect (the b -rhombus corresponding to the edge (\mathbf{w}, \mathbf{b})), followed by a finite sequence of c -rhombi.

A corollary of the above computations of the lengths of the non typical sequences of edges in frozen columns is the following:

Corollary. *The limiting bead models on the different families of threads \mathbf{B}_j are perfectly correlated: the distance between beads on each side of a frozen column converges in probability to zero.*

Proof:

If one proceeds as in lemma 4.2, then one can easily see that, for every τ , the probability that a sequence of non typical edges in a frozen column exceeds, say, $\frac{1}{\sqrt{\tau}}$ is of order $q^{1/\sqrt{\tau}}$, and thus decays very fast when τ goes to zero. Thus, in the vertically rescaled graph, the distance between two beads at the extremity of a sequence of non typical edges is close to 1. In the scaling limit, the distance between these beads converges in probability to 0. \square

As a consequence, the picture of a typical dimer configuration for a Gibbs measure corresponding to a point in a tentacle of the phase diagram looks like the figure 6.5.

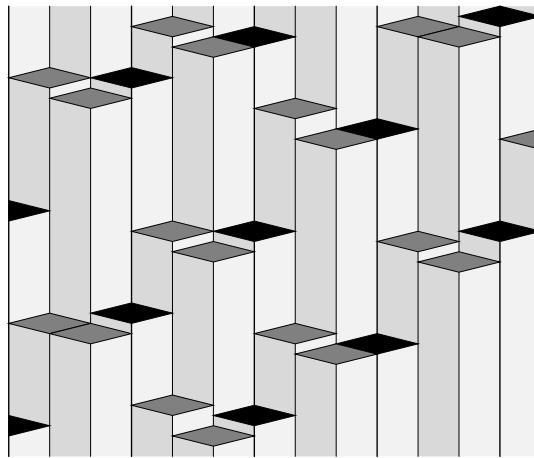


Figure 6.5: A typical tiling for a Gibbs measure corresponding to a point in a tentacle. The black beads mark the transition between the two dominant type of edges. Next to them, bead also appear on the other threads to compensate the defect created in frozen columns.

7 Pattern densities in fluid dimer models

7.1 Introduction

The aim of statistical mechanics is to describe systems made of a large number of simple components. The notion of Gibbs measure for the dimer model on an infinite graph gives a mathematical description of such an infinite system, at a microscopic scale: these probability measures describe the local statistics of the system, when the boundary of the system is sent to infinity.

If one wants to capture long range properties of the system, one has to adopt a macroscopic point of view, where the size of the simple components goes to zero, whereas the number of components goes to infinity, the global size of the system being fixed. This double limit procedure is referred to as scaling limit. Several quantities of interest can be studied from this point of view. Two examples of such observables are the height function, and the pattern densities.

This chapter is devoted to the proof of the convergence of pattern density fields in the scaling limit, in both liquid and gaseous phases of the dimer model on a bipartite \mathbb{Z}^2 -periodic graph, to a continuous random object, which can be described as the sum of a derivative of the Gaussian Free Field in the plane and an independent white noise.

7.1.1 Scaling limits of pattern densities

A dimer configuration on a bipartite planar graph can be interpreted through the height function as a discrete surface. From this point of view, scaling limits of dimer models on planar bipartite graphs have already been the object of several studies. A law of large number has been established [8, 33] showing that this discrete surface approaches a *limit shape* when the mesh size goes to zero. The fluctuations of the height function around the limit shape have also been studied in the case of a graph embedded in a bounded region, as well as in the case of an *isoradial* infinite graph with critical weights [10]. The continuous limiting object for these fluctuations is the *Gaussian Free Field* [54, 18].

In this chapter, we are interested in the scaling limit of dimer models on \mathbb{Z}^2 -periodic planar graphs but from a different standpoint. Instead of looking at the height function, we consider other observables, called *pattern density fields*.

Let G be a \mathbb{Z}^2 -periodic planar bipartite graph. A *geometric realization* of G is an application from G to \mathbb{R}^2 preserving the \mathbb{Z}^2 -periodicity of G : vertices of G are mapped to points of \mathbb{R}^2 , edges to segments, and \mathbb{Z}^2 acts on the image of G by translation.

Let Ψ a geometric realization of G such that the quotient of \mathbb{R}^2 by the action of \mathbb{Z}^2 has area 1. For each scaling factor $\varepsilon > 0$, we define the scaled geometric realization $\Psi^\varepsilon = \varepsilon\Psi$ and $G^\varepsilon = \Psi^\varepsilon(G)$ the image of G by the application Ψ^ε .

A *pattern* \mathcal{P} is a finite set of edges $\{\mathbf{e}_1, \dots, \mathbf{e}_k\}$, together with a marked vertex. The position of the pattern in G^ε is given by the coordinates of the image by Ψ^ε of this marked vertex. The probability of seeing such a pattern in a random dimer configuration is given by a determinant involving the Kasteleyn operator and its inverse: if \mathbf{e}_j goes from white vertex \mathbf{w}_j to black vertex \mathbf{b}_j , then

$$\mathbb{P}[\mathcal{P}] = \left(\prod_{j=1}^k \mathbf{K}(\mathbf{w}_j, \mathbf{b}_j) \right) \det_{1 \leq i, j \leq k} [\mathbf{K}^{-1}(\mathbf{b}_i, \mathbf{w}_j)]$$

In order to get some information about spatial distribution of patterns, and the way they interact with each other, we define for every pattern \mathcal{P} a family of (discrete) random fields $N_{\mathcal{P}}^\varepsilon$, called *pattern density fields*. For a given ε , $N_{\mathcal{P}}^\varepsilon$ is a random distribution, associating to every domain D the number of copies of \mathcal{P} seen in D in a random dimer configuration of G^ε . More precisely, if u^ε is the image of the marked vertex related to \mathcal{P} the action of $N_{\mathcal{P}}^\varepsilon$ on a smooth test function φ is given by

$$N_{\mathcal{P}}^\varepsilon(\varphi) = \sum_{\mathbf{x} \in \mathbb{Z}^2} \varphi(u_{\mathbf{x}}^\varepsilon) \mathbb{1}_{\mathcal{P}_{\mathbf{x}}} = \sum_{\mathbf{x} \in \mathbb{Z}^2} \varphi(u_{\mathbf{x}}^\varepsilon) \mathcal{P}_{\mathbf{x}}$$

where $\mathcal{P}_{\mathbf{x}}$ and $u_{\mathbf{x}}^\varepsilon$ are the translated by \mathbf{x} of \mathcal{P} an u^ε . For the sake of simplicity, $\mathcal{P}_{\mathbf{x}}$ will also represent the indicator function $\mathbb{1}_{\mathcal{P}_{\mathbf{x}}}$ of the pattern $\mathcal{P}_{\mathbf{x}}$, equal to 1 or 0 whether $\mathcal{P}_{\mathbf{x}}$ is in the random dimer configuration \mathcal{C} or not.

$\varepsilon^2 \mathbb{E} [N_{\mathcal{P}}^\varepsilon(\varphi)]$ is a Riemann sum of $\mathbb{P}[\mathcal{P}]\varphi$, and thus converges to $\mathbb{P}[\mathcal{P}] \int \varphi(u) |du|$ when ε goes to 0.

The aim of the following chapters is to prove the convergence of the fluctuations of this field around its mean value

$$\tilde{N}_{\mathcal{P}}^\varepsilon = \varepsilon (N_{\mathcal{P}}^\varepsilon - \mathbb{E} [N_{\mathcal{P}}^\varepsilon]) \tag{7.1}$$

towards a continuous Gaussian field. Such central limit theorems exist for a broad class of determinantal random fields [57] but only for Hermitian kernels, contrary to the cases presented here.

Before stating the main results, we recall some basics facts about the fluid phases of the dimer model and about Gaussian fields.

7.1.2 The fluid phases of the dimer model

We recall here some basic facts about liquid and gaseous phases of the dimer model on a planar bipartite periodic graph G , presented in details in chapter 2. The phase diagram of the dimer model is given by the amoeba of the spectral curve $P(z, w) = 0$, where the

characteristic polynomial P is the determinant of the Fourier transform of the Kasteleyn operator on G .

Liquid phase of dimer models

The liquid phase corresponds to the interior of the amoeba. In this phase, the characteristic polynomial $P(z, w)$ has two conjugate zeros (maybe merged) on the unit torus \mathbb{T}^2 . Generically, these two zeros are distinct. Let (z_0, w_0) be the zero satisfying $\text{Im}\left(\frac{\beta w_0}{\alpha z_0}\right) \geq 0$. P has the following expansion near (z_0, w_0)

$$P(z, w) = \alpha(z - z_0) + \beta(w - w_0) + o(\|(z, w) - (z_0, w_0)\|). \quad (7.2)$$

Recall from section 2.6.1 that generically, when the two zeros on the torus are distinct, there is a natural geometric realisation of G^* , with a fundamental domain spanned by vectors proportional to $\hat{x} = i\alpha z_0$ and $\hat{y} = i\beta w_0$, from which a geometric realisation of G can be deduced. The asymptotics of the inverse Kasteleyn operator are given in lemma 2.2. In particular, if \mathbf{b} and \mathbf{w} are adjacent,

$$\begin{aligned} \mathbf{K}(\mathbf{w}, \mathbf{b}) \mathbf{K}^{-1}(\mathbf{b}_{x,y}, \mathbf{w}) &= -\text{Re} \left(\frac{z_0^{-y} w_0^x \mathbf{K}(\mathbf{w}, \mathbf{b}) Q_{\mathbf{bw}}(z_0, w_0)}{\pi(x\hat{x} + y\hat{y})} \right) + O \left(\frac{1}{|x|^2 + |y|^2} \right) \\ &= \varepsilon \text{Re} \left(\frac{z_0^{-y} w_0^x i \mathbf{e}^*}{\pi u_{x,y}^\varepsilon} \right) + O \left(\frac{\varepsilon^2}{u_{x,y}^\varepsilon{}^2} \right), \end{aligned} \quad (7.3)$$

where $u_{x,y}^\varepsilon = \Psi^\varepsilon(\mathbf{b}_{x,y}) - \Psi^\varepsilon(\mathbf{w})$ and \mathbf{e}^* is the complex number representing the dual of $\mathbf{e} = (\mathbf{w}, \mathbf{b})$ in Ψ . The correlations between edges decay polynomially with the distance.

Gaseous phase

This phase corresponds to bounded components of the complementary of the amoeba. The characteristic polynomial P has no zero on the unit torus. If \mathbf{b} and \mathbf{w} are a black and a white vertex of G , the fraction $Q_{\mathbf{bw}}/P$ is analytic on the unit torus and its Fourier coefficients $\mathbf{K}^{-1}(\mathbf{b}_x, \mathbf{w})$ decay exponentially with x . Hence the correlations also decay exponentially.

7.1.3 Gaussian Fields

These definitions are borrowed from [20].

Definition 7.1 (Random field). A *random distribution* or *random field* F is a continuous linear functional on the set $\mathcal{C}_c^\infty(\mathbb{R}^2)$ of smooth functions on \mathbb{R}^2 with compact support. F associates to every test function $\varphi \in \mathcal{C}_c^\infty(\mathbb{R}^2)$ a random variable $F(\varphi)$. The continuity here means that if the sequence (φ_k) converges to φ in $\mathcal{C}_c^\infty(\mathbb{R}^2)$, then $F(\varphi_k)$ converges to $F(\varphi)$ in distribution.

$\tilde{N}_{\mathcal{P}}^\varepsilon$ is an example of random field. A particular class of random fields is given by the Gaussian fields:

Definition 7.2 (Gaussian field). A *Gaussian random field* F is a random field such that for $\varphi \in \mathcal{C}_c^\infty(\mathbb{R}^2)$, $F(\varphi)$ is a Gaussian random variable.

A Gaussian field is somehow a infinite dimensional generalization of the notion of Gaussian vector. As in the classical situation with a Gaussian vector, all the moments can be expressed in terms of the second moment, by Wick's formula:

Theorem 7.1 (Wick's formula). *Let W be a Gaussian field. All the moments of W are determined by the covariance: Let $\varphi_1, \dots, \varphi_n$ be smooth test functions. Then*

$$\mathbb{E} [W(\varphi_1) \cdots W(\varphi_n)] = \begin{cases} 0 & \text{if } n \text{ is odd} \\ \sum_{\tau \text{ pairing}} \prod_{k=1}^{n/2} \mathbb{E} [W(\varphi_{i_k}) W(\varphi_{j_k})] & \text{if } n \text{ is even} \end{cases} \quad (7.4)$$

In particular, if all the test functions are taken to be equal and $\mathbb{E} [W(\varphi)^2] = \sigma^2$, then we recover the usual formula for the moments of a Gaussian random variable:

$$\mathbb{E} [W(\varphi)^n] = \begin{cases} 0 & \text{if } n \text{ is odd} \\ (n-1)!! \sigma^n & \text{if } n \text{ is even} \end{cases} \quad (7.5)$$

where $(n-1)!! = (n-1) \cdots 3 \cdot 1$ is the number of pairings of n elements.

7.1.4 Statement of the result and structure of the proof

We prove the following Central Limit Theorem when the measure on dimer configurations is fluid (i.e liquid or gaseous).

Theorem 7.2. *Consider the dimer model on a planar bipartite \mathbb{Z}^2 -periodic graph G with a generic liquid or gaseous Gibbs measure μ . Let \mathcal{P} be a pattern of G and $\tilde{N}_{\mathcal{P}}^\varepsilon$ be the random field of density fluctuations of pattern \mathcal{P} . Then when ε goes to 0, $\tilde{N}_{\mathcal{P}}^\varepsilon$ converges weakly in distribution to a Gaussian random field $\mathcal{N}_{\mathcal{P}}$.*

- *If the measure is liquid, then $\mathcal{N}_{\mathcal{P}}$ is a linear combination of a directional derivative of the masslessfree field and an independent white noise and its covariance structure has the form*

$$\mathbb{E} [\mathcal{N}_{\mathcal{P}}(\varphi_1) \mathcal{N}_{\mathcal{P}}(\varphi_2)] = \alpha \iint_{\mathbb{R}^2 \times \mathbb{R}^2} \partial \varphi_1(u) \partial \varphi_2(v) G(u, v) du dv + \beta \int_{\mathbb{R}^2} \varphi_1(u) \varphi_2(u) du \quad (7.6)$$

where $G(u, v) = -\frac{1}{2\pi} \log |u - v|$ is the Green function on the plane.

- If μ is gaseous, then $\tilde{N}_{\mathcal{P}}^\varepsilon$ is a white noise and

$$\mathbb{E} [\mathcal{N}_{\mathcal{P}}(\varphi_1)\mathcal{N}_{\mathcal{P}}(\varphi_2)] = \beta \int_{\mathbb{R}^2} \varphi_1(u)\varphi_2(u)du \quad (7.7)$$

In other terms, for any choice of $\varphi_1, \dots, \varphi_n \in \mathcal{C}_c^\infty(\mathbb{R}^2)$, the distribution of the random vector $(\tilde{N}_{\mathbf{e}}^\varepsilon\varphi_1, \dots, \tilde{N}_{\mathbf{e}}^\varepsilon\varphi_n)$ converges to that of the Gaussian vector $(\mathcal{N}_{\mathbf{e}}\varphi_1, \dots, \mathcal{N}_{\mathbf{e}}\varphi_n)$ whose covariance structure is mentioned in the theorem. As the distribution of a Gaussian vector is characterized by its moments, it is sufficient to prove the convergence of the moments of $(\tilde{N}_{\mathbf{e}}^\varepsilon\varphi_1, \dots, \tilde{N}_{\mathbf{e}}^\varepsilon\varphi_n)$ to those of $(\mathcal{N}_{\mathbf{e}}\varphi_1, \dots, \mathcal{N}_{\mathbf{e}}\varphi_n)$, given by Wick's formula (7.4).

The proof goes in two steps: first we prove the convergence of the second moment of the fluctuation field $\tilde{N}_{\mathcal{P}}^\varepsilon$ to the covariance of $\mathcal{N}_{\mathcal{P}}$, and then we prove that Wick's formula is satisfied asymptotically.

As the arguments are different for a liquid and a gaseous measure, the proof of theorem 7.2 is decomposed into three cases. In section 7.2, we give the proof for a pattern made of a single edge in the generic liquid case and discuss briefly what happens in the non generic case. In section 7.3, the proof is extended to any admissible pattern (*i.e.* a pattern appearing with positive probability) in the generic liquid case. The case of a gaseous measure is discussed in section 7.4.

7.1.5 Density fields and partition function

In this paragraph, the calculations are purely formal and try to give some heuristics on the information one can get from these pattern density fields.

Consider a dimer model for which we assign to a configuration \mathcal{C} the weight $w(\mathcal{C})$. Let Z_0 be the partition function of this model

$$Z_0 = \sum_{\mathcal{C}} w(\mathcal{C}) \quad (7.8)$$

We now perturb the partition function by modifying locally the configuration weights. Let φ be a smooth test function. Fix a pattern \mathcal{P} and a $\varepsilon > 0$. We multiply every weight $w(\mathcal{C})$ by a factor $e^{t\varepsilon\varphi(u_x^\varepsilon)}$ whenever there is a copy of a given pattern \mathcal{P} located at \mathbf{x} . Up to a multiplicative constant $\exp(t\varepsilon\mathbb{P}[\mathcal{P}]\sum_{\mathbf{x}}\varphi(u_x^\varepsilon))$, the new partition function for the model with these new weights is

$$Z_t = \sum_{\mathcal{C}} w(\mathcal{C})e^{t\varepsilon\sum_{\mathbf{x}}\varphi(u_x^\varepsilon)(\mathbb{1}_{\mathcal{P}_{\mathbf{x}}} - \mathbb{P}[\mathcal{P}])} = \sum_{\mathcal{C}} w(\mathcal{C})e^{t\tilde{N}_{\mathcal{P}}^\varepsilon(\varphi)}$$

This can be generalized to a perturbation involving several patterns. Formally, the successive derivatives of Z_t/Z_0 at $t = 0$ are the moments of the random variable $\tilde{N}_{\mathcal{P}}^\varepsilon(\varphi)$ with respect to the unperturbed probability measure.

$$\left. \frac{d^k}{dt^k} \frac{Z_t}{Z_0} \right|_{t=0} = \mathbb{E}_0 \left[(\tilde{N}_{\mathcal{P}}^\varepsilon \varphi)^k \right]$$

Thus, an information on the moments of $\tilde{N}_{\mathfrak{p}}^\varepsilon$ gives an infinitesimal information on the perturbed partition function that could be hopefully integrated to construct probability measures corresponding to the modified weights.

7.2 The liquid case: edge densities

This section is devoted to the proof of one particular case of theorem 7.2. We suppose that the probability measure on dimer configurations of G is liquid, and consider the fluctuations of the density random field $\tilde{N}_{\mathbf{e}}^\varepsilon$ for a pattern consisting in a single edge $\mathbf{e} = (\mathbf{w}, \mathbf{b})$. The precise statement we prove in this section is the following:

Theorem 7.3. *The random field $\tilde{N}_{\mathbf{e}}^\varepsilon$ converges weakly in distribution, as ε goes to 0, to a Gaussian random field $\mathcal{N}_{\mathbf{e}}$ with covariance*

$$\mathbb{E} [\mathcal{N}_{\mathbf{e}}(\varphi_1)\mathcal{N}_{\mathbf{e}}(\varphi_2)] = \frac{1}{\pi} \iint \partial_{\mathbf{e}^*} \varphi_1(u) G(u, v) \partial_{\mathbf{e}^*} \varphi_2(v) dudv + A \int \varphi_1(u)\varphi_2(u)du \quad (7.9)$$

for a certain $A \geq 0$.

As we discussed in the previous section, we first prove the convergence of the second moment, and then that of higher moments. In this section, as we will be interested in copies of an edge $\mathbf{e} = (\mathbf{w}, \mathbf{b})$, the only vertices we will deal with are most of the time translates of \mathbf{w} and \mathbf{b} . To simplify notations, we will write $K^{-1}(\mathbf{z} - \mathbf{z}')$ instead of $K^{-1}(\mathbf{b}_{\mathbf{z}}, \mathbf{w}_{\mathbf{z}'})$ and $K_{\mathbf{e}}$ will stand for $K(\mathbf{w}, \mathbf{b})$.

7.2.1 Convergence of the second moment

The second moment $(\varphi_1, \varphi_2) \mapsto \mathbb{E} [\tilde{N}_{\mathbf{e}}^\varepsilon(\varphi_1)\tilde{N}_{\mathbf{e}}^\varepsilon(\varphi_2)]$ of $\tilde{N}_{\mathbf{e}}^\varepsilon$ is a continuous bilinear positive form on $\mathcal{C}_c^\infty(\mathbb{R}^2)$. In this section, we prove that this bilinear form converges to a non degenerate bilinear form, that will define the covariance structure for the limit Gaussian field $\mathcal{N}_{\mathbf{e}}$.

Proposition 7.1. *There exists a non-negative constant A such that*

$$\begin{aligned} \forall \varphi_1, \varphi_2 \in \mathcal{C}_c^\infty(\mathbb{R}^2) \\ \lim_{\varepsilon \rightarrow 0} \mathbb{E} [\tilde{N}_{\mathbf{e}}^\varepsilon(\varphi_1)\tilde{N}_{\mathbf{e}}^\varepsilon(\varphi_2)] = \frac{1}{\pi} \iint_{\mathbb{R}^2 \times \mathbb{R}^2} \partial_{\mathbf{e}^*} \varphi_1(u_1) G(u_1, u_2) \partial_{\mathbf{e}^*} \varphi_2(u_2) |du_1| |du_2| \\ + A \int_{\mathbb{R}^2} \varphi_1(u)\varphi_2(u) |du| \quad (7.10) \end{aligned}$$

where $G(u, v) = -\frac{1}{2\pi} \log |u - v|$ is the Green function on the plane.

The right hand side can be physically interpreted as the energy of interaction between two electric dipoles with moment density $\varphi_1 \mathbf{e}^*$ and $\varphi_2 \mathbf{e}^*$, plus a term of interaction at very short range.

Proof:

Using the invariance by translation of the Kasteleyn operator and hence of the correlations, we rewrite the second moment as a convolution of two distributions applied to a test function.

$$\mathbb{E} \left[\tilde{N}_{\mathbf{e}}^\varepsilon(\varphi_1) \tilde{N}_{\mathbf{e}}^\varepsilon(\varphi_2) \right] = \varepsilon^2 \sum_{\mathbf{x}, \mathbf{x}' \in \mathbb{Z}^2} \varphi_1(u_{\mathbf{x}}) \varphi_2(u_{\mathbf{x}'}) \mathbb{E} [(\mathbf{e}_{\mathbf{x}} - \bar{\mathbf{e}})(\mathbf{e}_{\mathbf{x}'} - \bar{\mathbf{e}})] \quad (7.11)$$

$$= \varepsilon^2 \sum_{\mathbf{x}, \mathbf{x}' \in \mathbb{Z}^2} \varphi_1(u_{\mathbf{x}}) \varphi_2(u_{\mathbf{x}'}) \mathbb{E} [(\mathbf{e} - \bar{\mathbf{e}})(\mathbf{e}_{\mathbf{x}-\mathbf{x}'} - \bar{\mathbf{e}})] \quad (7.12)$$

$$= \langle \varphi_1^\varepsilon * F^\varepsilon, \varphi_2 \rangle \quad (7.13)$$

where $\bar{\mathbf{e}} = \mathbb{P}[\mathbf{e}]$ and the two distributions φ_1^ε and F^ε are defined by

$$\varphi_1^\varepsilon = \varepsilon^2 \sum_{xy} \varphi_1(u_{\mathbf{x}}) \delta_{u_{\mathbf{x}}} \quad F^\varepsilon = \sum_{\mathbf{x}} \mathbb{E} [(\mathbf{e} - \bar{\mathbf{e}})(\mathbf{e}_{\mathbf{x}} - \bar{\mathbf{e}})] \delta_{u_{\mathbf{x}}}.$$

The distribution φ_1^ε converges weakly to φ_1 when ε goes to zero. We will now prove the convergence of F^ε to some distribution F , what will ensure that $\varphi_1^\varepsilon * F^\varepsilon$ converges weakly to $\varphi_1 * F$, since the support of φ_1^ε is contained in the fixed compact $\text{supp}(\varphi_1)$, and hence, that $\langle \varphi_1^\varepsilon * F^\varepsilon, \varphi_2 \rangle$ converges.

Let ψ be a smooth test function with compact support. Let us prove the convergence of

$$\langle F^\varepsilon, \psi \rangle = \sum_{\mathbf{x}} \mathbb{E} [(\mathbf{e} - \bar{\mathbf{e}})(\mathbf{e}_{\mathbf{x}} - \bar{\mathbf{e}})] \psi(u_{\mathbf{x}}^\varepsilon) = \sum_{\mathbf{x}} \text{Cov}(\mathbf{e}, \mathbf{e}_{\mathbf{x}}) \psi(u_{\mathbf{x}}^\varepsilon). \quad (7.14)$$

At first sight, $\langle F^\varepsilon, \psi \rangle$ looks like a Riemann sum of a particular function. The problem is that due to the asymptotics of K^{-1} , the function would behave as $1/u^2$, which is not integrable in the vicinity of 0. Therefore, we decompose the sum on \mathbf{x} in the definition of F^ε depending on whether the norm of \mathbf{x} is larger than $M = \lfloor 1/\varepsilon \rfloor$ or not, that is if $u_{\mathbf{x}}^\varepsilon$ is in $\mathcal{B} = \{-i(\alpha z_0 s - \beta z_0 t) ; (s, t) \in [-1, 1]^2\}$.

$$\begin{aligned} \langle F^\varepsilon, \psi \rangle &= \sum_{|\mathbf{x}| > M} \psi(u_{\mathbf{x}}^\varepsilon) \text{Cov}(\mathbf{e}, \mathbf{e}_{\mathbf{x}}) + \sum_{|\mathbf{x}| \leq M} \psi(u_{\mathbf{x}}^\varepsilon) \text{Cov}(\mathbf{e}, \mathbf{e}_{\mathbf{x}}) \\ &= \sum_{|\mathbf{x}| > M} \psi(u_{\mathbf{x}}^\varepsilon) \text{Cov}(\mathbf{e}, \mathbf{e}_{\mathbf{x}}) + \sum_{|\mathbf{x}| \leq M} (\psi(u_{\mathbf{x}}^\varepsilon) - \psi(0)) \text{Cov}(\mathbf{e}, \mathbf{e}_{\mathbf{x}}) + \psi(0) \sum_{|\mathbf{x}| \leq M} \text{Cov}(\mathbf{e}, \mathbf{e}_{\mathbf{x}}) \end{aligned} \quad (7.15)$$

The fact we subtracted and added $\psi(0)$ in the second sum removed the non integrable singularity at 0. The following two lemmas state the convergence of the three sums.

Lemma 7.1.

$$\lim_{\varepsilon \rightarrow 0} \sum_{|x| > [1/\varepsilon]} \psi(u_x^\varepsilon) \text{Cov}(\mathbf{e}, \mathbf{e}_x) = \frac{1}{2\pi^2} \int_{\mathbb{R}^2 \setminus \mathcal{B}} \psi(z) \text{Re} \left(\frac{\mathbf{e}^*}{u} \right)^2 |du| \quad (7.16)$$

$$\lim_{\varepsilon \rightarrow 0} \sum_{|x| \leq [1/\varepsilon]} (\psi(u_x^\varepsilon) - \psi(0)) \text{Cov}(\mathbf{e}, \mathbf{e}_x) = \frac{1}{2\pi^2} \int_{\mathcal{B}} (\psi(z) - \psi(0)) \text{Re} \left(\frac{\mathbf{e}^*}{u} \right)^2 |du| \quad (7.17)$$

Moreover the sum of the two previous limit can be rewritten as

$$\frac{1}{\pi} \int_{\mathbb{R}^2} \partial_{\mathbf{e}^*} \psi(u) \partial_{\mathbf{e}^*} G(u, 0) |du| + A_1 \psi(0).$$

for some constant A_1 .

Proof:

If $x \neq (0, 0)$, the covariance between edges $\mathbf{e} = \mathbf{e}_{(0,0)}$ and \mathbf{e}_x is given by

$$\begin{aligned} \text{Cov}(\mathbf{e}, \mathbf{e}_x) &= \mathbb{P}[\mathbf{e} \text{ and } \mathbf{e}_x] - \mathbb{P}[\mathbf{e}]^2 = \mathbf{K}_e^2 \det \begin{bmatrix} \mathbf{K}^{-1}(0) & \mathbf{K}^{-1}(x) \\ \mathbf{K}^{-1}(-x) & \mathbf{K}^{-1}(0) \end{bmatrix} - (\mathbf{K}_e \mathbf{K}^{-1}(0))^2 \\ &= -\mathbf{K}_e^2 \mathbf{K}^{-1}(x) \mathbf{K}^{-1}(-x) \end{aligned}$$

Using asymptotics of \mathbf{K}^{-1} for large x , we get the following asymptotic expression for the covariance between two distinct edges

$$\begin{aligned} \text{Cov}(\mathbf{e}, \mathbf{e}_x) &= -\frac{\varepsilon^2}{\pi^2} \text{Re} \left(\frac{z_0^{-y} w_0^x i \mathbf{e}^*}{u_x^\varepsilon} \right) \text{Re} \left(\frac{z_0^y w_0^{-x} i \mathbf{e}^*}{-u_x^\varepsilon} \right) + O \left(\frac{\varepsilon}{u_x^\varepsilon} \right)^3 \\ &= -\frac{\varepsilon^2}{2\pi^2} \text{Re} \left(\frac{\mathbf{e}^*}{u_x^\varepsilon} \right)^2 + \frac{\varepsilon^2}{2\pi^2} \text{Re}(z_0^{2y} w_0^{-2x}) \left| \frac{\mathbf{e}^*}{u_x^\varepsilon} \right|^2 + O \left(\frac{\varepsilon}{u_x^\varepsilon} \right)^3 \end{aligned}$$

Since the second term is oscillating, it will not contribute to the limit. The sum in the LHS of (7.16), modulo the oscillating terms, can be interpreted as the integral of a piecewise constant function approximating

$$-\frac{1}{2\pi^2} \psi(u) \text{Re} \left(\frac{\mathbf{e}^{*2}}{u^2} \right) \mathbb{1}_{\mathbb{R}^2 \setminus \mathcal{B}}(u)$$

As the approximating functions are bounded uniformly in ε by an integrable function, and converge almost everywhere, then by Lebesgue theorem, the first sum converges to

$$-\int_{\mathbb{R}^2 \setminus \mathcal{B}} \frac{1}{2\pi^2} \text{Re} \left(\frac{\mathbf{e}^{*2}}{u^2} \right) \psi(z) |du| \quad (7.18)$$

In the same way, the sum in the LHS of (7.17) is the integral of a piecewise constant function approximating

$$-\frac{1}{2\pi^2}(\psi(u) - \psi(0))\operatorname{Re}\left(\frac{\mathbf{e}^{*2}}{u^2}\right)\mathbb{1}_{\mathcal{B}}(u)$$

and for the same reasons, it converges to

$$-\int_{\mathcal{B}}\frac{1}{2\pi^2}\operatorname{Re}\left(\frac{\mathbf{e}^{*2}}{u^2}\right)(\psi(z) - \psi(0))|du| \quad (7.19)$$

We rewrite the sum of the limit using Green's formula inside and outside of \mathcal{B} , noticing that $\frac{1}{2\pi}\operatorname{Re}\left(\frac{\mathbf{e}^*}{u}\right)^2$ is the second derivative of the Green function $G(\cdot, 0)$ along the vector \mathbf{e}^* .

$$\begin{aligned} \int_{\mathbb{R}^2 \setminus \mathcal{B}} \frac{1}{\pi} \partial_{\mathbf{e}^*}^2 G(u, 0) \psi(z) |du| = \\ \frac{1}{\pi} \oint_{\partial \mathcal{B}} \psi(u) \partial_{\mathbf{e}^*} G(u, 0) \langle \vec{n}_{in}, \mathbf{e}^* \rangle d\sigma - \frac{1}{\pi} \int_{\mathbb{R}^2 \setminus \mathcal{B}} \partial_{\mathbf{e}^*} \psi(u) \partial_{\mathbf{e}^*} G(u, 0) |du| \end{aligned} \quad (7.20)$$

$$\begin{aligned} \int_{\mathcal{B}} \frac{1}{\pi} \partial_{\mathbf{e}^*}^2 G(u, 0) (\psi(u) - \psi(0)) |du| = \\ \frac{1}{\pi} \oint_{\partial \mathcal{B}} (\psi(u) - \psi(0)) \partial_{\mathbf{e}^*} G(u, 0) \langle \vec{n}_{out}, \mathbf{e}^* \rangle d\sigma - \frac{1}{\pi} \int_{\mathcal{B}} \partial_{\mathbf{e}^*} \psi(u) \partial_{\mathbf{e}^*} G(u, 0) |du| \end{aligned} \quad (7.21)$$

where \vec{n}_{in} and \vec{n}_{out} are the unit normal vector fields on $\partial \mathcal{B}$ pointing respectively inwards and outwards. The two integrals on \mathcal{B} and $\mathbb{R}^2 \setminus \mathcal{B}$ combine to give an integral over \mathbb{R}^2 . The two integrals on $\partial \mathcal{B}$ cancel out partially. It remains only

$$-\psi(0) \oint_{\partial \mathcal{B}} \partial_{\mathbf{e}^*} G(u, 0) \langle \vec{n}_{ext}, \mathbf{e}^* \rangle d\sigma = A_1 \psi(0)$$

This establishes the convergence of the two first sums, which completes the proof of the lemma. \square

We now prove the convergence of the third sum.

Lemma 7.2. $\sum_{|x| \leq M} \operatorname{Cov}(\mathbf{e}, \mathbf{e}_x)$ converges when M goes to infinity to a limit A_2 .

Proof:

The sum of the covariances is given in terms of \mathbf{K} and \mathbf{K}^{-1} by

$$\begin{aligned} \sum_{|x| \leq M} \operatorname{Cov}(\mathbf{e}, \mathbf{e}_x) &= \mathbb{P}[\mathbf{e}](1 - \mathbb{P}[\mathbf{e}]) + \sum_{0 < |x| \leq M} \operatorname{Cov}(\mathbf{e}, \mathbf{e}_x) \\ &= \mathbf{K}_e \mathbf{K}^{-1}(0) - \mathbf{K}_e^2 \sum_{|x| \leq M} \mathbf{K}^{-1}(x) \mathbf{K}^{-1}(-x) \end{aligned} \quad (7.22)$$

$K^{-1}(\mathfrak{x})$ is by definition the \mathfrak{x} th Fourier coefficient of the function $f = Q/P$ defined on the unit torus \mathbb{T}^2 . As P has simple zeros, f is in $L^1(\mathbb{T}^2)$. The convolution

$$(f * f)(z, w) = \iint_{\mathbb{T}^2} f(u, v) f(zu, wv) \frac{du}{2i\pi u} \frac{dv}{2i\pi v} \quad (7.23)$$

is also in $L^1(\mathbb{T}^2)$ and its \mathfrak{x} th Fourier coefficient is exactly $K^{-1}(\mathfrak{x})K^{-1}(-\mathfrak{x})$. Establishing the convergence of the sum is now a problem of pointwise convergence of a Fourier series. If f was continuous at $(z, w) = (1, 1)$, then the Fourier series would have converged to $f(1, 1)$. The problem is that the function $f(u, v)f(\bar{u}, \bar{v})$ is not integrable and thus, the function $f * f$ is not defined when z and w are both equal to 1. However, $f * f$ is smooth in a punctured neighborhood of $(1, 1)$, has directional limits when (z, w) converges to $(1, 1)$, varying continuously with the direction. We can then prove an analogue in two dimensions of Dini's theorem¹ for $f * f$. If $t = \arg(w)/\arg(z)$ and $\ell(t)$ the limit of $f * f$ when (z, w) goes to $(1, 1)$ with t fixed, then

$$\lim_{M \rightarrow +\infty} \sum_{|\mathfrak{x}| \leq M} K^{-1}(\mathfrak{x})K^{-1}(-\mathfrak{x}) = \frac{1}{\pi^2} \int_{-\infty}^{+\infty} \ell(t) \log \left| \frac{1+t}{1-t} \right| \frac{dt}{t} \quad (7.26)$$

And thus $\sum_{|\mathfrak{x}| \leq M} \text{Cov}(\mathbf{e} - \bar{\mathbf{e}})(\mathbf{e}_{\mathfrak{x}} - \bar{\mathbf{e}})$ converges to a limit that we denote by A_2 . \square

We now come back to the proof of the convergence of the distribution F^ε . The three sums in 7.15 defining $\langle F^\varepsilon, \psi \rangle$ converge and the sum of the limits is

$$\langle F, \psi \rangle = \frac{1}{\pi} \int_{\mathbb{R}^2} \partial_{\mathbf{e}^*} \psi(u) \partial_{\mathbf{e}^*} G(u, 0) |du| + A\psi(0) \quad (7.27)$$

where $A = A_1 + A_2$. Thus, when ε goes to 0, F^ε converges to a distribution F defined by the formula above, and hence $\varphi_1^\varepsilon * F^\varepsilon$ to $\varphi_1 * F$. Denoting by $\partial^{(u)}$ and $\partial^{(v)}$ respectively the operator of partial differentiation with respect to the variable u and v , and noticing that, since $G(u, v) = G(u - v)$, we have

$$\partial^{(u)} G(u, v) = -\partial^{(v)} G(u, v),$$

¹This theorem states that if a function f is piecewise continuous on \mathbb{S}^1 , the partial Fourier series

$$S_n(f)(z) = \sum_{k=-n}^n z^{-k} \int_{\mathbb{S}^1} f(w) w^k \frac{dw}{2i\pi w} \quad (7.24)$$

converges pointwise and

$$\lim_{n \rightarrow +\infty} S_n(f)(e^{i\theta_0}) = \frac{1}{2} \left(\lim_{\theta \rightarrow \theta_0^-} f(e^{i\theta}) + \lim_{\theta \rightarrow \theta_0^+} f(e^{i\theta}) \right). \quad (7.25)$$

we get the following expression for the limit covariance structure

$$\lim_{\varepsilon \rightarrow 0} \mathbb{E} \left[(\tilde{N}_{\mathbf{e}}^\varepsilon \varphi_1)(\tilde{N}_{\mathbf{e}}^\varepsilon \varphi_2) \right] = \langle \varphi_1 * F, \varphi_2 \rangle \quad (7.28)$$

$$= \frac{1}{\pi} \iint_{\mathbb{R}^2 \times \mathbb{R}^2} \partial_{\mathbf{e}^*} \varphi_1(u) \partial_{\mathbf{e}^*}^{(u)} G(u, v) \varphi_2(v) |du| |dv| + A \int_{\mathbb{R}^2} \varphi_1(u) \varphi_2(u) |du| \quad (7.29)$$

$$= -\frac{1}{\pi} \iint_{\mathbb{R}^2 \times \mathbb{R}^2} \partial_{\mathbf{e}^*} \varphi_1(u) \partial_{\mathbf{e}^*}^{(v)} G(u, v) \varphi_2(v) |du| |dv| + A \int_{\mathbb{R}^2} \varphi_1(u) \varphi_2(u) |du| \quad (7.30)$$

$$= \frac{1}{\pi} \iint_{\mathbb{R}^2 \times \mathbb{R}^2} \partial_{\mathbf{e}^*} \varphi_1(u) G(u, v) \partial_{\mathbf{e}^*} \varphi_2(v) |du| |dv| + A \int_{\mathbb{R}^2} \varphi_1(u) \varphi_2(u) |du| \quad (7.31)$$

Thus the covariance of $\tilde{N}_{\mathbf{e}}^\varepsilon$ converges to the expression given in proposition 7.1. \square

7.2.2 Convergence of higher moments

In this section, we prove the convergence of the moments of order ≥ 3 of $\tilde{N}_{\mathbf{e}}^\varepsilon$ to those of $\mathcal{N}_{\mathbf{e}}$.

Proposition 7.2. *For every $n \geq 3$, The n th moment of $\tilde{N}_{\mathbf{e}}^\varepsilon$ converges to that of $\mathcal{N}_{\mathbf{e}}$ when ε goes to zero. In other words, for every $\varphi_1, \dots, \varphi_n \in \mathcal{C}_c^\infty(\mathbb{R}^2)$,*

$$\lim_{\varepsilon \rightarrow 0} \mathbb{E} \left[\tilde{N}_{\mathbf{e}}^\varepsilon \varphi_1 \cdots \tilde{N}_{\mathbf{e}}^\varepsilon \varphi_n \right] = \mathbb{E} [\mathcal{N}_{\mathbf{e}} \varphi_1 \cdots \mathcal{N}_{\mathbf{e}} \varphi_n]$$

Since $\mathcal{N}_{\mathbf{e}}$ is Gaussian, it is sufficient to show that in the limit, the moments of $\tilde{N}_{\mathbf{e}}^\varepsilon$ satisfy Wick's formula. Moreover, as $(\varphi_1, \dots, \varphi_n) \mapsto \mathbb{E} \left[\tilde{N}_{\mathbf{e}}^\varepsilon \varphi_1 \cdots \tilde{N}_{\mathbf{e}}^\varepsilon \varphi_n \right]$ is a symmetric n -linear form, we just have to prove proposition 7.2 when all the φ_i are equal to some test function ψ , the general case being obtained by polarization. The previous proposition reduces then to showing that

Proposition 7.3.

$$\lim_{\varepsilon \rightarrow 0} \mathbb{E} \left[(\tilde{N}_{\mathbf{e}}^\varepsilon \psi)^n \right] = \mathbb{E} [(\mathcal{N}_{\mathbf{e}} \psi)^n] = \begin{cases} 0 & \text{if } n \text{ is odd} \\ (n-1)!! \mathbb{E} [(\mathcal{N}_{\mathbf{e}} \psi)^2]^{n/2} & \text{if } n \text{ is even} \end{cases}$$

In this section, we are thus interested in the limit of

$$\mathbb{E} \left[(\tilde{N}_{\mathbf{e}}^\varepsilon \psi)^n \right] = \varepsilon^n \sum_{\mathbf{x}_1, \dots, \mathbf{x}_n} \psi(u_{\mathbf{x}_1}^\varepsilon) \cdots \psi(u_{\mathbf{x}_n}^\varepsilon) \mathbb{E} [(\mathbf{e}_{\mathbf{x}_1} - \bar{\mathbf{e}}) \cdots (\mathbf{e}_{\mathbf{x}_n} - \bar{\mathbf{e}})] \quad (7.32)$$

A first step in the proof is to study the convergence of a related quantity $\Xi_n^\varepsilon(\psi)$, defined by a sum of the same general term as for $\mathbb{E} \left[(\tilde{N}_{\mathbf{e}}^\varepsilon \psi)^n \right]$, but with a set of indices restricted to distinct points:

$$\Xi_n^\varepsilon(\psi) = \varepsilon^n \sum_{\substack{\mathbf{x}_1, \dots, \mathbf{x}_n \\ \text{distinct}}} \psi(u_{\mathbf{x}_1}^\varepsilon) \cdots \psi(u_{\mathbf{x}_n}^\varepsilon) \mathbb{E} [(\mathbf{e}_{\mathbf{x}_1} - \bar{\mathbf{e}}) \cdots (\mathbf{e}_{\mathbf{x}_n} - \bar{\mathbf{e}})]. \quad (7.33)$$

Convergence of $\Xi_n^\varepsilon(\psi)$

To prove the convergence of $\Xi_n^\varepsilon(\psi)$, we have to understand the asymptotic behavior of the correlation between distinct edges, when they are far from each other. A simple expression is given by Kenyon in [28] to compute this correlation using a unique determinant.

Lemma 7.3 ([28]). *Let $\mathbf{e}_1 = (\mathbf{w}_1, \mathbf{b}_1), \dots, \mathbf{e}_n = (\mathbf{w}_n, \mathbf{b}_n)$ be distinct edges. Their correlation is given by*

$$\mathbb{E}[(\mathbf{e}_1 - \bar{\mathbf{e}}_1) \cdots (\mathbf{e}_n - \bar{\mathbf{e}}_n)] = \left(\prod_{j=1}^n \mathbf{K}(\mathbf{w}_j, \mathbf{b}_j) \right) \det_{1 \leq i, j \leq n} \begin{bmatrix} 0 & & \mathbf{K}^{-1}(\mathbf{b}_i, \mathbf{w}_j) \\ & \ddots & \\ \mathbf{K}^{-1}(\mathbf{b}_j, \mathbf{w}_i) & & 0 \end{bmatrix}$$

Proof:

This lemma is proven by induction, using the fact that

$$\det \begin{bmatrix} a_{11} & a_{12} & \cdots & a_{1n} \\ a_{21} & a_{22} & \cdots & a_{2n} \\ \vdots & \vdots & & \vdots \\ a_{n1} & a_{n2} & \cdots & a_{nn} \end{bmatrix} = \det \begin{bmatrix} a_{11} & 0 & \cdots & 0 \\ 0 & a_{22} & \cdots & a_{2n} \\ \vdots & \vdots & & \vdots \\ 0 & a_{n2} & \cdots & a_{nn} \end{bmatrix} + \det \begin{bmatrix} 0 & a_{12} & \cdots & a_{1n} \\ a_{21} & a_{22} & \cdots & a_{2n} \\ \vdots & \vdots & & \vdots \\ a_{n1} & a_{n2} & \cdots & a_{nn} \end{bmatrix}$$

□

This formula allows us to give an explicit expression for $\Xi_n^\varepsilon(\psi)$ in terms of the operators \mathbf{K} and \mathbf{K}^{-1} . Since the matrix in lemma 7.3 has zeros on the diagonal, only permutations with no fixed point will contribute to the determinant expressed as a sum over the symmetric group. Let $\tilde{\mathfrak{S}}_n$ be the set of such permutations. Every permutation $\sigma \in \tilde{\mathfrak{S}}_n$ is decomposed as a product of disjoint cycles $\gamma_1 \cdots \gamma_p$. The supports of these cycles form a partition $(\Gamma_l)_{l=1}^p$ of $\{1, \dots, n\}$, whose parts Γ_l have cardinal at least 2. The terms coming from permutations leading to the same partition are put together and we get

$$\begin{aligned} \varepsilon^n \sum_{\substack{\mathbf{x}_1 \cdots \mathbf{x}_n \\ \text{distinct}}} \mathbb{E} \left[\prod_{j=1}^n \psi(u_{\mathbf{x}_j}^\varepsilon) (\mathbf{e}_{\mathbf{x}_j} - \bar{\mathbf{e}}) \right] &= \varepsilon^n \mathbf{K}_e^n \sum_{\substack{\mathbf{x}_1 \cdots \mathbf{x}_n \\ \text{distinct}}} \sum_{\sigma \in \tilde{\mathfrak{S}}_n} \text{sgn}(\sigma) \prod_{j=1}^n \psi(u_{\mathbf{x}_j}^\varepsilon) \mathbf{K}^{-1}(\mathbf{x}_{\sigma(j)} - \mathbf{x}_j) \\ &= \sum_{\{\Gamma\}_{l=1}^p} \prod_{l=1}^p \sum_{\substack{\gamma \text{ cycle} \\ \text{supp}(\gamma) = \Gamma_l}} \left(\text{sgn}(\gamma) \varepsilon^{|\gamma|} \sum_{\substack{\mathbf{x}_{j_1}, \dots, \mathbf{x}_{j_{|\gamma|}} \\ \text{distinct}}} \prod_{k=1}^{|\gamma|} \psi(u_{\mathbf{x}_{j_k}}^\varepsilon) \mathbf{K}_e \mathbf{K}^{-1}(\mathbf{x}_{\gamma(j_k)} - \mathbf{x}_{j_k}) + o(1) \right) \end{aligned} \quad (7.34)$$

The error term $o(1)$ comes from the fact that in the second line, we allow two \mathbf{x}_j whose indices are in different components of (Γ) to be equal.

We now examine the convergence of a term in brackets, associated to a cycle γ

$$\operatorname{sgn}(\gamma)(\varepsilon \mathbf{K}_e)^{|\gamma|} \sum_{\substack{\mathbf{x}_{j_1}, \dots, \mathbf{x}_{j_{|\gamma|}} \\ \text{distinct}}} \prod_{k=1}^{|\gamma|} \psi(u_{\mathbf{x}_{j_k}}^\varepsilon) \mathbf{K}^{-1}(\mathbf{x}_{\gamma(j_k)} - \mathbf{x}_{j_k})$$

According to subsection 7.2.1, we know that when γ is a transposition the corresponding term converges. When the length of γ is at least 3, we have the following lemma.

Lemma 7.4. *For any cycle γ of length $m \geq 3$, and any $\psi \in \mathcal{C}_c^\infty(\mathbb{R}^2)$, we have*

$$\begin{aligned} \lim_{\varepsilon \rightarrow 0} \varepsilon^m \sum_{\substack{\mathbf{x}_1, \dots, \mathbf{x}_m \\ \text{distinct}}} \prod_{k=1}^m \psi(u_{\mathbf{x}_k}^\varepsilon) \mathbf{K}_e \mathbf{K}^{-1}(\mathbf{x}_{\gamma(k)} - \mathbf{x}_k) = \\ \frac{1}{2^{m-1} \pi^m} \int_{(\mathbb{R}^2)^m} \operatorname{Re} \left(\frac{(i\mathbf{e}^*)^m \psi(u_1) \cdots \psi(u_m)}{(u_{\gamma(1)} - u_1) \cdots (u_{\gamma(m)} - u_m)} \right) |du_1| \cdots |du_m| \end{aligned} \quad (7.35)$$

Proof:

From the behavior of \mathbf{K}^{-1} at long range, we get an asymptotic expression for the product

$$\begin{aligned} \prod_{j=1}^m \mathbf{K}_e \mathbf{K}^{-1}(\mathbf{x}_{\gamma(j)} - \mathbf{x}_j) &= \prod_{j=1}^m \operatorname{Re} \left(\frac{\varepsilon z_0^{-(y_{\gamma(j)} - y_j)} w_0^{+(x_{\gamma(j)} - x_j)} i\mathbf{e}^*}{\pi(u_{\mathbf{x}_{\gamma(j)}} - u_{\mathbf{x}_j}^\varepsilon)} \right) + \text{small terms} \\ &= \frac{\varepsilon^m}{2^{m-1} \pi^m} \operatorname{Re} \left(\frac{(i\mathbf{e}^*)^m}{(u_{\mathbf{x}_{\gamma(1)}}^\varepsilon - u_{\mathbf{x}_1}^\varepsilon) \cdots (u_{\mathbf{x}_{\gamma(m)}}^\varepsilon - u_{\mathbf{x}_m}^\varepsilon)} \right) + \text{oscillating terms} \end{aligned} \quad (7.36)$$

The oscillating part of this asymptotic expansion once summed on $\mathbf{x}_1, \dots, \mathbf{x}_m$ will not contribute to the limit. The sum of the leading term multiplied by $\varepsilon^m \psi(u_{\mathbf{x}_1}^\varepsilon) \cdots \psi(u_{\mathbf{x}_m}^\varepsilon)$ can be interpreted as the integral of a piecewise constant function, converging almost surely to

$$\frac{1}{2^{m-1} \pi^m} \psi(u_1) \cdots \psi(u_m) \operatorname{Re} \left(\prod_{j=1}^m \frac{i\mathbf{e}^*}{u_{\gamma(j)} - u_j} \right) \quad (7.38)$$

As all the functions are dominated by a constant times the integrable function

$$\frac{|\psi(u_1) \cdots \psi(u_m)|}{|(u_{\gamma(1)} - u_1) \cdots (u_{\gamma(m)} - u_m)|},$$

the convergence follows from Lebesgue theorem. \square

Once proven the convergence of all these terms, we can combine their limit to get the limit of $\Xi_n^\varepsilon(\psi)$. When summing over all cycles with a given support $\Gamma = \{j_1, \dots, j_m\}$ of cardinality $m \geq 3$, we get the following limit :

$$\begin{aligned} \lim_{\varepsilon \rightarrow 0} \sum_{\substack{\gamma \text{ cycle} \\ \text{supp}(\gamma) = \Gamma}} \left(\varepsilon^m \sum_{\substack{x_{j_1}, \dots, x_{j_m} \\ \text{distinct}}} \prod_{k=1}^m \psi(u_{x_{j_k}}^\varepsilon) \mathbf{K}_e \mathbf{K}^{-1}(x_{\gamma(j_k)} - x_{j_k}) + o(1) \right) \\ = \frac{1}{2^{m-1} \pi^m} \int_{(\mathbb{R}^2)^m} \prod_{j \in \Gamma} \psi(u_j) \text{Re} \left(\sum_{\substack{\gamma \text{ cycle} \\ \text{supp} \gamma = \Gamma}} \prod_{j \in \Gamma} \frac{1}{u_{\gamma(j)} - u_j} \right) |du_1| \cdots |du_m| \end{aligned}$$

which equals zero according to the following lemma :

Lemma 7.5. *Let $m \geq 3$, and u_1, \dots, u_m be distinct complex numbers. Then*

$$\sum_{\substack{\gamma \in \mathfrak{S}_m \\ m\text{-cycles}}} \prod_{i=1}^m \frac{1}{u_{\gamma(i)} - u_i} = 0 \quad (7.39)$$

Proof:

Denote by f the function of u_1, \dots, u_m defined by the left hand side of (7.39). When m is odd, the result is obvious, since γ and γ^{-1} give opposite contributions. For a general m , since m -cycles form a conjugation class in the group of permutations \mathfrak{S}_m , the function f is a rational fraction invariant under permutation of the variables u_1, \dots, u_m . The denominator of this fraction is the Vandermonde $V = \prod_{i < j} (u_i - u_j)$, and the numerator is of lower degree than V . Since V is antisymmetric under permutation, the denominator has to be as well. But the only antisymmetric polynomial of lower degree than V is 0. \square

In the limit of equation (7.34) will contribute only partitions whose all components have cardinality 2. If n is odd, $\{1, \dots, n\}$ cannot be partitionned into parts of two elements, and the limit $\Xi_n(\psi)$ of $\Xi_n^\varepsilon(\psi)$ is zero. When n is even, there are $(n-1)!!$ such partitions, corresponding each to a pairing. The limit $\Xi_n(\psi)$ of $\Xi_n^\varepsilon(\psi)$ is then

$$\begin{aligned} \Xi_n(\psi) &= \sum_{\substack{\text{pairings} \\ \{i_1, j_1\}, \dots, \{i_{n/2}, j_{n/2}\}}} \prod_{k=1}^{n/2} \left(\lim_{\varepsilon \rightarrow 0} \varepsilon^2 \sum_{x_{i_k} \neq x_{j_k}} \psi(u_{x_{i_k}}^\varepsilon) \psi(u_{x_{j_k}}^\varepsilon) \text{Cov}(\mathbf{e}_{x_{i_k}}, \mathbf{e}_{x_{j_k}}) \right) \\ &= (n-1)!! (\Xi_2(\psi))^{n/2} \end{aligned}$$

For the moment, we discussed the limit of a restricted sum on distinct edges, which is not exactly the expression for the n th moment. We will now deal with the case when edges can coincide.

Proof of proposition 7.3

In the expression of the n th moment

$$\varepsilon^n \sum_{\mathfrak{x}_1, \dots, \mathfrak{x}_n} \psi(u_1^\varepsilon) \cdots \psi(u_n^\varepsilon) \mathbb{E} [(\mathbf{e}_{\mathfrak{x}_1} - \bar{\mathbf{e}}) \cdots (\mathbf{e}_{\mathfrak{x}_n} - \bar{\mathbf{e}})]$$

the correlations are not given by lemma 7.3 as soon as at least two edges coincide. To understand the behavior of this expression, we must be able to express in terms of \mathbf{K} and \mathbf{K}^{-1} correlations of the form

$$\mathbb{E} [(\mathbf{e}_{\mathfrak{x}_1} - \bar{\mathbf{e}})^{k_1} \cdots (\mathbf{e}_{\mathfrak{x}_p} - \bar{\mathbf{e}})^{k_p}] \quad (7.40)$$

when $\mathbf{e}_1, \dots, \mathbf{e}_p$ are distinct. Using the fact that the indicator function of an edge \mathbf{e} satisfies $\mathbf{e}^j = \mathbf{e}$ for $j \geq 1$, Newton formula yields

$$(\mathbf{e} - \bar{\mathbf{e}})^k = \sum_{j=0}^k \binom{k}{j} \mathbf{e}^j (-\bar{\mathbf{e}})^{k-j} = \mathbf{e} \sum_{j=1}^k \binom{k}{j} (-\bar{\mathbf{e}})^{k-j} + (-\bar{\mathbf{e}})^k = \alpha_k^{\mathbf{e}} (\mathbf{e} - \bar{\mathbf{e}}) + \beta_k^{\mathbf{e}}$$

where $\alpha_k^{\mathbf{e}}$ and $\beta_k^{\mathbf{e}}$ are deterministic, depending only on $\bar{\mathbf{e}}$ and k . In the case we consider, all the edges have the same probability, and we will simply denote these coefficients by α_k and β_k . Note the particular values of α_k and β_k that will be useful later

$$\alpha_1 = 1 \quad \beta_1 = 0 \quad \beta_2 = \bar{\mathbf{e}}(1 - \bar{\mathbf{e}})$$

Therefore correlation 7.40 can be rewritten as

$$\mathbb{E} [(\mathbf{e}_{\mathfrak{x}_1} - \bar{\mathbf{e}})^{k_1} \cdots (\mathbf{e}_{\mathfrak{x}_p} - \bar{\mathbf{e}})^{k_p}] = \mathbb{E} [(\alpha_{k_1} (\mathbf{e}_1 - \bar{\mathbf{e}}) + \beta_{k_1}) \cdots (\alpha_{k_p} (\mathbf{e}_p - \bar{\mathbf{e}}) + \beta_{k_p})] \quad (7.41)$$

$$= \sum_{J \subset \{1, \dots, p\}} \tilde{\alpha}_J \tilde{\beta}_J \mathbb{E} \left[\prod_{j \in J} (\mathbf{e}_j - \bar{\mathbf{e}}) \right] \quad (7.42)$$

where $\tilde{\alpha}_J = \prod_{j \in J} \alpha_{k_j}$ and $\tilde{\beta}_J = \prod_{j \notin J} \beta_{k_j}$.

In equation (7.32), $\mathbb{E} [(\tilde{N}_{\mathbf{e}}^\varepsilon \psi)^n]$ is expressed as a sum over all edges. We want now to rewrite this sum as a sum over distinct edges, using partitions of $\{1, \dots, n\}$. Such a partition $\{\Gamma_l\}_{l=1}^p$ is associated naturally to every n -tuple of lattice points $(\mathfrak{x}_1, \dots, \mathfrak{x}_n)$: each component Γ_l of this partition is an equivalence class for the relation

$$i \sim j \Leftrightarrow \mathfrak{x}_i = \mathfrak{x}_j.$$

Denoting by n_l the cardinal of Γ_l , we rewrite equation (7.32) as

$$\begin{aligned} \mathbb{E} \left[(\tilde{N}_{\mathbf{e}}^\varepsilon \psi)^n \right] &= \varepsilon^n \sum_{\{\Gamma_l\}_{l=1}^p} \sum_{\substack{\mathbf{x}_1, \dots, \mathbf{x}_p \\ \text{distinct}}} \mathbb{E} \left[\prod_{j=1}^p \psi^{n_j}(u_{\mathbf{x}_j}^\varepsilon) (\mathbf{e}_{\mathbf{x}_j} - \bar{\mathbf{e}})^{n_j} \right] \\ &= \varepsilon^n \sum_{\{\Gamma_l\}_{l=1}^p} \sum_{J \subset \{1, \dots, p\}} \tilde{\alpha}_J \tilde{\beta}_J \sum_{\substack{(\mathbf{x}_j)_{j \in J} \\ \text{distinct}}} \mathbb{E} \left[\prod_{j \in J} \psi^{n_j}(u_{\mathbf{x}_j}^\varepsilon) (\mathbf{e}_{\mathbf{x}_j} - \bar{\mathbf{e}}) \right] \sum'_{(\mathbf{x}_l)_{l \notin J}} \prod_{l \notin J} \psi^{n_l}(u_{\mathbf{x}_l}^\varepsilon) \end{aligned} \quad (7.43)$$

where Σ' means the sum over (\mathbf{x}_l) distinct, but also distinct from values of any $\mathbf{x}_j, j \in J$. Denote by q the number of Γ_l reduced to a single element. As $\beta_1 = 0$, $\tilde{\beta}_J$ is zero unless J contains the indices of these Γ_l . Thus, the cardinal of a subset J giving a non-zero contribution must be at least q . For such a J , the last sum over $(\mathbf{x}_l)_{l \notin J}$ in (7.43) is a Riemann sum, and therefore is $O(\varepsilon^{-2(p-|J|)})$.

Furthermore, the sum over $(\mathbf{x}_J)_{j \in J}$ can be expressed by polarization in terms of $\Xi_{|J|}^\varepsilon$, and is therefore a $O(\varepsilon^{-|J|})$. Since $|J| \geq q$ and

$$n = \sum_{l=1}^p n_l \geq q + 2(p - q) = 2p - q,$$

the contribution of J to (7.43) is at most $O(\varepsilon^{n-2p+|J|})$ which will be negligible in the limit except when $|J| = q$ and $n_l = 2$ for all $l \notin J$. For such J and (Γ_l) , we have

$$\tilde{\alpha}_J = 1 \quad \tilde{\beta}_J = (\bar{\mathbf{e}}(1 - \bar{\mathbf{e}}))^{(n-q)/2} \quad (7.44)$$

Thus the only partitions that will contribute to the limit are “partial pairings”, matching by pairs $2m = (n - q)$ elements of $\{1, \dots, n\}$. For a fixed m , there are

$$\binom{n}{2m} (2m - 1)!! = \frac{n!}{2^m m! (n - 2m)!}$$

such partitions, all giving the same contribution. Summing over m we get

$$\mathbb{E} \left[(\tilde{N}_{\mathbf{e}}^\varepsilon \psi)^n \right] = \sum_{m=0}^{\lfloor n/2 \rfloor} \binom{n}{2m} (2m - 1)!! \Xi_{n-2m}^\varepsilon(\psi) \left(\varepsilon^2 \bar{\mathbf{e}}(1 - \bar{\mathbf{e}}) \sum_{\mathbf{x}} \psi^2(u_{\mathbf{x}}^\varepsilon) \right)^m + O(\varepsilon)$$

If n is odd, so is $n - 2m$. In this case, $\lim_{\varepsilon \rightarrow 0} \Xi_{n-2m}^\varepsilon(\psi) = 0$, and therefore

$$\lim_{\varepsilon \rightarrow 0} \mathbb{E} \left[(\tilde{N}_{\mathbf{e}}^\varepsilon \psi)^n \right] = 0 \quad (7.45)$$

If n is even,

$$\lim_{\varepsilon \rightarrow 0} \Xi_{n-2m}^\varepsilon(\psi) = \Xi_{n-2m}(\psi) = (n - 2m - 1)!! \Xi_2(\psi)^{n/2-m} \quad (7.46)$$

$$= \frac{(n - 2m)!}{2^{n/2-m} (n/2 - m)!} \Xi_2(\psi)^{n/2-m}. \quad (7.47)$$

Therefore, the limit of $\mathbb{E} \left[(\tilde{N}_{\mathbf{e}}^\varepsilon \psi)^n \right]$ is given by

$$\begin{aligned} \lim_{\varepsilon \rightarrow 0} \mathbb{E} \left[(\tilde{N}_{\mathbf{e}}^\varepsilon \psi)^n \right] &= \sum_{m=0}^{n/2} \frac{n!}{2^m m! (n-2m)!} \frac{(n-2m)! \Xi_2(\psi)^{n/2-m}}{2^{n/2-m} (n/2-m)!} \left(\bar{\mathbf{e}}(1-\bar{\mathbf{e}}) \int \psi^2(u) |du| \right)^m \\ &= (n-1)!! \sum_{m=0}^{n/2} \binom{n/2}{m} \Xi_2(\psi)^{n/2-m} \left(\bar{\mathbf{e}}(1-\bar{\mathbf{e}}) \int \psi^2(u) |du| \right)^m \\ &= (n-1)!! \left(\Xi_2(\psi) + \bar{\mathbf{e}}(1-\bar{\mathbf{e}}) \int \psi^2(u) |du| \right)^{n/2} \\ &= (n-1)!! \left(\mathbb{E} [\mathcal{N}_{\mathbf{e}}(\psi)^2] \right)^{n/2} \end{aligned}$$

what is exactly what we wanted to prove. This therefore ends the proof of theorem 7.2 for a pattern made of one edge and a generic liquid Gibbs measure.

7.2.3 A word about the non generic case

When the two roots of the characteristic polynomial $P(z, w)$ on the unit torus coincide, the measure is still liquid, and the correlations between edges at distance r still decay like r^{-2} . However, since z_0 and w_0 are real, the leading term is the asymptotics of \mathbf{K}^{-1} is not oscillating anymore, what will induce a resonance phenomenon in the system.

The two first sums in equation (7.15) defining the distribution F^ε appearing in the study of the convergence of the second moment still have a finite limit when ε goes to zero. On the contrary, due to the resonance, the third sum

$$\sum_{|x| \leq \lfloor 1/\varepsilon \rfloor} \text{Cov}(\mathbf{e}, \mathbf{e}_x)$$

in this case diverges. More precisely, this sum is $O(\log(1/\varepsilon))$. Therefore the second moment diverges. However, one can prove that $(\log(1/\varepsilon))^{-1} \tilde{N}_{\mathbf{e}}^\varepsilon$ converges weakly in distribution to a white noise. We will not show it here.

7.3 The liquid case: general pattern densities

This section is devoted to the proof of an analogue of theorem 7.3 for multi-edged patterns. Let $\tilde{N}_{\mathcal{P}}^\varepsilon$ the density fluctuation field of a pattern \mathcal{P} for a generic liquid Gibbs measure.

Theorem 7.4. *When ε goes to zero, $\tilde{N}_{\mathcal{P}}^\varepsilon$ converges weakly in distribution to the Gaussian*

field $\mathcal{N}_{\mathcal{P}}$ whose covariant structure is given by

$$\begin{aligned} \mathbb{E} [\mathcal{N}_{\mathcal{P}}(\varphi_1)\mathcal{N}_{\mathcal{P}}(\varphi_2)] &= \frac{1}{\pi} \iint_{\mathbb{R}^2 \times \mathbb{R}^2} \partial_{\mathcal{P}^*} \varphi_1(u_1) G(u_1, u_2) \partial_{\mathcal{P}^*} \varphi_2(u_2) |du_1| |du_2| \\ &\quad + A \int_{\mathbb{R}^2} \varphi_1(u_1) \varphi_2(u) |du| \end{aligned}$$

where the vector \mathcal{P}^* and the positive constant A depend only on the pattern \mathcal{P} and the Gibbs measure.

The scheme of the proof is very similar to that of theorem 7.3 for edge density fluctuations. The problem is that there is no simple analogue of lemma 7.3 for correlations between non overlapping patterns, that is why the proof needs a little more combinatorial work in this case.

After having introduced the different notations required to deal easily with these patterns, we prove the theorem, following the structure of the proof given in the last chapter, and explaining in details only parts that are specific to patterns formed by more than one edge.

7.3.1 Notations

Let \mathcal{P} be a pattern containing k distinct edges $\mathbf{e}^1 = (\mathbf{w}^1, \mathbf{b}^1), \dots, \mathbf{e}^k = (\mathbf{w}^k, \mathbf{b}^k)$. The probability of such a pattern to appear in a random dimer configuration is

$$\bar{\mathbb{P}}[\mathcal{P}] = \mathbb{K}_{\mathbf{e}^1} \cdots \mathbb{K}_{\mathbf{e}^k} \det \begin{bmatrix} \mathbb{K}^{-1}(\mathbf{b}^1, \mathbf{w}^1) & \cdots & \mathbb{K}^{-1}(\mathbf{b}^1, \mathbf{w}^k) \\ \vdots & \ddots & \vdots \\ \mathbb{K}^{-1}(\mathbf{b}^k, \mathbf{w}^1) & \cdots & \mathbb{K}^{-1}(\mathbf{b}^k, \mathbf{w}^k) \end{bmatrix} \quad (7.48)$$

More generally, the probability to see n non-overlapping copies $\mathcal{P}_1, \dots, \mathcal{P}_n$ of \mathcal{P} obtained respectively by translation of a lattice vector $\mathbf{x}_1, \dots, \mathbf{x}_n$ is given up to a constant by a determinant of matrix $nk \times nk$ defined by blocks

$$\mathbb{P}[\mathcal{P}_1 \cdots \mathcal{P}_n] = (\mathbb{K}_{\mathbf{e}^1} \cdots \mathbb{K}_{\mathbf{e}^k})^n \det \begin{bmatrix} A_{11} & \cdots & A_{1n} \\ \vdots & \ddots & \vdots \\ A_{n1} & \cdots & A_{nn} \end{bmatrix} \quad (7.49)$$

where the entries of the block A_{IJ} are coefficients of \mathbb{K}^{-1} between black vertices of \mathcal{P}_I and white vertices of \mathcal{P}_J

$$A_{IJ} = \begin{bmatrix} \mathbb{K}^{-1}(\mathbf{b}_{\mathbf{x}_I}^1, \mathbf{w}_{\mathbf{x}_J}^1) & \cdots & \mathbb{K}^{-1}(\mathbf{b}_{\mathbf{x}_I}^1, \mathbf{w}_{\mathbf{x}_J}^k) \\ \vdots & \ddots & \vdots \\ \mathbb{K}^{-1}(\mathbf{b}_{\mathbf{x}_I}^k, \mathbf{w}_{\mathbf{x}_J}^1) & \cdots & \mathbb{K}^{-1}(\mathbf{b}_{\mathbf{x}_I}^k, \mathbf{w}_{\mathbf{x}_J}^k) \end{bmatrix} \quad (7.50)$$

When $I = J$ the matrix A_{IJ} does not depend on I . We denote by E this matrix, whose determinant is used to compute $\mathbb{P}[\mathcal{P}]$. Defining B_{IJ} as the product $E^{-1}A_{IJ}$ and B as the whole block matrix (B_{IJ}) , we can rewrite the joint probability of $\mathcal{P}_1, \dots, \mathcal{P}_n$ as

$$\mathbb{P}[\mathcal{P}_1 \cdots \mathcal{P}_n] = (\bar{\mathcal{P}})^n \det \begin{bmatrix} \mathbb{1}_k & B_{1,2} & \cdots & B_{1,n} \\ B_{2,1} & \mathbb{1}_k & & \vdots \\ \vdots & & \ddots & \vdots \\ B_{n,1} & \cdots & B_{n,n-1} & \mathbb{1}_k \end{bmatrix} \quad (7.51)$$

Instead of using a single integer i to denote the line (resp. the column) of an entry in such a matrix defined by blocks, it will be more convenient to use a couple of integers (I, α) , where I is the index of the block line (resp. of the block column) and α is the relative position in the I th block line (resp. block column). The relation between the two sets of indices is simply

$$i = I(k - 1) + \alpha.$$

If the coordinates \mathbf{x}_j are all distinct but some patterns overlap, define $\tilde{\mathcal{P}}_j = \mathcal{P}_j \setminus \bigcup_{i=1}^{j-1} \mathcal{P}_i$ for all $j \in \{1, \dots, n\}$. We have then

$$\mathbb{P}[\mathcal{P}_1 \cdots \mathcal{P}_n] = \mathbb{P}[\tilde{\mathcal{P}}_1 \cdots \tilde{\mathcal{P}}_n]$$

Up to a relabelling of the patterns, we can assume that none of the $\tilde{\mathcal{P}}_j$ is empty. Thus the joint probability of these patterns is also given by the determinant of a matrix defined by blocks of size $|\tilde{\mathcal{P}}_1| + \cdots + |\tilde{\mathcal{P}}_n|$.

7.3.2 Asymptotics of correlations

The following lemma gives asymptotic correlations between distant patterns.

Lemma 7.6. *Let $(\mathbf{x}_j) = \mathbf{x}_1, \dots, \mathbf{x}_n$ be n distinct lattice points. The correlations between the patterns $\mathcal{P}_{\mathbf{x}_1}, \dots, \mathcal{P}_{\mathbf{x}_n}$ can be rewritten as*

$$\mathbb{E}[(\mathcal{P}_{\mathbf{x}_1} - \bar{\mathcal{P}}) \cdots (\mathcal{P}_{\mathbf{x}_n} - \bar{\mathcal{P}})] = \sum_{S \in \hat{\mathfrak{S}}_n} \left(\prod_{\gamma \text{ cycle of } S} H_\gamma((\mathbf{x}_j)) \right) (1 + o(1))$$

where the functions H_γ have the following asymptotic behaviour

$$H_\gamma((\mathbf{x}_j)) = \text{sgn } \gamma \frac{\varepsilon^{|\gamma|}}{2^{|\gamma|-1} \pi^{|\gamma|}} \text{Re} \left(\frac{\text{tr}((E^{-1}Q)^{|\gamma|})}{\prod_{j \in \text{supp } \gamma} u_{\mathbf{x}_{\gamma(j)}}^\varepsilon - u_{\mathbf{x}_j}^\varepsilon} \right) + \begin{matrix} \text{oscillating} \\ \text{terms} \end{matrix}$$

and satisfy

$$|H_\gamma((\mathbf{x}_j))| \leq \varepsilon^{|\gamma|} \frac{C}{\prod_{j \in \text{supp } \gamma} |u_{\gamma(j)} - u_j|}$$

for every u_1, \dots, u_n in a ε -neighborhood of $u_{x_1}^\varepsilon, \dots, u_{x_n}^\varepsilon$. The error term $o(1)$ is uniformly bounded in x_1, \dots, x_n and goes to zero when the distance between the patterns goes to infinity.

Proof:

We first derive the asymptotic expression for the correlations when the patterns are far from each other. When $|x_i - x_j|$ are large enough for every $i \neq j$, the patterns are disjoint and expression (7.51) for correlations can be used. Expanding the products in the expectation, we get

$$\begin{aligned} \mathbb{E} [(\mathcal{P}_{x_1} - \bar{\mathcal{P}}) \cdots (\mathcal{P}_{x_n} - \bar{\mathcal{P}})] &= \sum_{j_1, \dots, j_p} (-\bar{\mathcal{P}})^{n-p} \mathbb{E} [\mathcal{P}_{x_{j_1}} \cdots \mathcal{P}_{x_{j_p}}] \\ &= \mathbb{P} [\mathcal{P}]^n \sum_{C \subset \{1, \dots, n\}} (-1)^{n-|C|} \det \begin{bmatrix} \mathbb{1}_n & \delta_{12} B_{12} & \cdots & \delta_{1n} B_{1n} \\ \delta_{21} B_{21} & \mathbb{1}_n & & \\ \vdots & & \ddots & \\ \delta_{n1} B_{n1} & & & \mathbb{1}_n \end{bmatrix} \end{aligned} \quad (7.52)$$

where the non diagonal bloc (I, J) is either B_{IJ} or 0 depending on whether (I, J) belongs to $C \times C$ or not.

Expressing each determinant as a sum over the symmetric group \mathfrak{S}_{nk} and gathering the terms coming from the same permutation, one can notice that the contributions of permutations fixing a whole block are vanishing, due to the alternating sign in the sum over C . The permutations contributing to the correlations are those whose support intersects each block. Therefore, we have

$$\mathbb{E} [(\mathcal{P}_{x_1} - \bar{\mathcal{P}}) \cdots (\mathcal{P}_{x_n} - \bar{\mathcal{P}})] = \mathbb{P} [\mathcal{P}]^n \sum_{\substack{\sigma \in \mathfrak{S}_{nk} \\ \text{fixing no block}}} \text{sgn}(\sigma) \prod_{I, \alpha} B_{(I, \alpha), \sigma((I, \alpha))}$$

To each such σ can be associated (in a non canonical way) a fixed-point free permutation $S \in \hat{\mathfrak{S}}_n$: as σ does not fix the first block, there exists an index $(1, \alpha_1)$ that is not sent to an index of the first block by σ . Define $S(1)$ as the label of the block to which belongs $\sigma((1, \alpha_1))$. The index $\sigma((1, \alpha_1))$ is not a fixed point either. Thus its image under S belongs to a block labelled by $S^2(1) \neq S(1)$. Define in the same way the iterated images of 1 under S until that $S^k(1) = 1$ for some $k > 1$. If all the blocks have been visited once, then the definition of S is complete and S is a n -cycle. If some block J has not been visited, then, as σ does not fix block J , one can find a non-fixed index (J, α_J) and follow the orbit of this index under σ until the first return to block J to define the orbit of J under S . This construction is reiterated until each block has been visited. It provides a partition of the set of permutations fixing no blocks indexed by elements of $\hat{\mathfrak{S}}_n$. The class of permutations σ leading to a given $S \in \hat{\mathfrak{S}}_n$ is denoted $[S]$.

In each class there are ‘‘special’’ permutations, the support of which intersects each block exactly once. For each class $[S]$, there are k^n such elements, corresponding to the

different possible choices of non fixed points $(1, \alpha_1), \dots, (n, \alpha_n)$. These permutations will give the main contribution, whereas the contributions of the permutations with more than one non fixed point by block will be negligible in the limit, since non diagonal terms are small when the patterns are far from each other. Thus,

$$\mathbb{E} \left[\prod_{j=1}^n (\mathcal{P}_{\mathbb{X}_j} - \bar{\mathcal{P}}) \right] = \mathbb{P} [\mathcal{P}]^n \sum_{S \in \hat{\mathfrak{S}}_n} \sum_{\sigma \in [S]} \text{sgn}(\sigma) \prod_{I, \alpha} B_{(I, \alpha), \sigma((I, \alpha))} \quad (7.53)$$

$$= \mathbb{P} [\mathcal{P}]^n \sum_{S \in \hat{\mathfrak{S}}_n} \sum_{\sigma \in [S]} \text{sgn}(S) \left(\prod_{I=1}^n \sum_{\alpha_I=1}^k (B_{I, S(I)})_{\alpha_I, \alpha_{S(I)}} \right) (1 + o(1)) \quad (7.54)$$

where $o(1)$ corresponds to the contributions of the non “special” permutations. As \mathbb{K}^{-1} is a bounded operator, and goes to zero at infinity, this error term is bounded by a constant uniformly in the positions of the patterns, and goes to zero when the distance between patterns goes to infinity.

The main term in equation (7.54) has an expression in terms of traces of products of block matrices B_{IJ}

$$\prod_{I=1}^n \sum_{\alpha_I=1}^k (B_{I, S(I)})_{\alpha_I, \alpha_{S(I)}} = \prod_{\substack{\gamma=(I_1, \dots, I_p) \\ \text{cycle of } S}} \text{tr} (B_{I_1, I_2} \cdots B_{I_p, I_1}) \quad (7.55)$$

Let us have a look to a particular trace $\text{tr} (B_{I_1, I_2} \cdots B_{I_p, I_1})$. Recall that B_{IJ} is the product of E^{-1} whose entries will be denoted by $e_{\alpha\beta}$ and A_{IJ} whose entries are $\mathbb{K}^{-1}(\mathbf{b}_{\mathbb{X}_I}^\alpha, \mathbf{w}_{\mathbb{X}_J}^\beta)$, the coefficient of \mathbb{K}^{-1} taken between black vertex ‘ α ’ of pattern I and white vertex ‘ β ’ of pattern J , whose asymptotics when patterns are far away from each other are given by lemma 2.2

$$(A_{IJ})_{\alpha\beta} = -\frac{\varepsilon}{\pi} \text{Re} \left(\frac{z_0^{-y_J+y_I} w_0^{+x_J-x_I} Q_{\alpha\beta}(z_0, w_0)}{u_{\mathbb{X}_J}^\varepsilon - u_{\mathbb{X}_I}^\varepsilon} \right) + \text{small terms} \quad (7.56)$$

To simplify notations, we introduce

$$\zeta_{IJ} = \frac{z_0^{-y_J+y_I} w_0^{+x_J-x_I}}{u_{\mathbb{X}_J}^\varepsilon - u_{\mathbb{X}_I}^\varepsilon}. \quad (7.57)$$

The trace $\text{tr} (B_{I_1, I_2} \cdots B_{I_p, I_1})$ can therefore be rewritten as

$$\begin{aligned}
 \operatorname{tr} (B_{I_1, I_2} \cdots B_{I_p, I_1}) &= \sum_{\alpha_1, \dots, \alpha_k} (E^{-1} A_{I_1 I_2})_{\alpha_1 \alpha_2} \cdots (E^{-1} A_{I_p I_1})_{\alpha_p \alpha_1} \\
 &= \sum_{\substack{\alpha_1, \dots, \alpha_k \\ \beta_1, \dots, \beta_k}} \left(\frac{-\varepsilon}{\pi} \right)^p e_{\alpha_1 \beta_1} \cdots e_{\alpha_p \beta_p} \operatorname{Re} (Q_{\beta_1 \alpha_2} \zeta_{I_1 I_2}) \cdots \operatorname{Re} (Q_{\beta_p \alpha_1} \zeta_{I_p I_1}) + \text{small terms}
 \end{aligned}$$

As in the case of edge densities, there will be only two non oscillating terms in the expansion of this product of real parts: those for which the phases contained in the ζ_{IJ} compensate exactly.

$$\operatorname{tr} (B_{I_1, I_2} \cdots B_{I_p, I_1}) = \tag{7.58}$$

$$= \sum_{\substack{\alpha_1, \dots, \alpha_k \\ \beta_1, \dots, \beta_k}} \left(\frac{-\varepsilon}{2\pi} \right)^p \prod_{j=1}^p e_{\alpha_j \beta_j} (Q_{\beta_j \alpha_{j+1}} \zeta_{I_j I_{j+1}} + \overline{Q_{\beta_j \alpha_{j+1}} \zeta_{I_j I_{j+1}}}) + \text{small terms} \tag{7.59}$$

$$= \sum_{\substack{\alpha_1, \dots, \alpha_k \\ \beta_1, \dots, \beta_k}} \frac{(-\varepsilon)^p}{2^p \pi^p} \left(\prod_{j=1}^p e_{\alpha_j \beta_j} Q_{\beta_j \alpha_{j+1}} \zeta_{I_j I_{j+1}} + \prod_{j=1}^p e_{\alpha_j \beta_j} \overline{Q_{\beta_j \alpha_{j+1}} \zeta_{I_j I_{j+1}}} \right) + \text{oscillating terms} \tag{7.60}$$

The product of the $\zeta_{I_k I_{k+1}}$ is equal to

$$\prod_{j=1}^p \zeta_{I_j, I_{j+1}} = \prod_{j=1}^p \frac{1}{u_{I_{j+1}}^\varepsilon - u_{I_j}^\varepsilon} \tag{7.61}$$

and we can rewrite the trace of $B_{I_1, I_2} \cdots B_{I_p, I_1}$ as

$$\operatorname{tr} (B_{I_1, I_2} \cdots B_{I_p, I_1}) = \frac{(-\varepsilon)^p}{2^{p-1} \pi^p} \operatorname{Re} \frac{\operatorname{tr}((E^{-1} Q)^p)}{(u_{I_2}^\varepsilon - u_{I_1}^\varepsilon) \cdots (u_{I_1}^\varepsilon - u_{I_p}^\varepsilon)} + \text{oscillating terms} \tag{7.62}$$

giving the asymptotics for H_γ .

When the patterns are not disjoint anymore, then a similar analysis can be done, in defining new patterns as the connected components of $\mathcal{P}_1 \cup \cdots \cup \mathcal{P}_n$. The bound can be extended to this case. \square

7.3.3 Convergence of the second moment

Proposition 7.4.

$$\begin{aligned} \forall \varphi_1, \varphi_2 \in \mathcal{C}_c^\infty(\mathbb{R}^2) \\ \lim_{\varepsilon \rightarrow 0} \mathbb{E} \left[\tilde{N}_{\mathcal{P}}^\varepsilon(\varphi_1) \tilde{N}_{\mathcal{P}}^\varepsilon(\varphi_2) \right] = \frac{1}{\pi} \iint_{\mathbb{R}^2 \times \mathbb{R}^2} \partial_{\mathcal{P}^*} \varphi_1(u_1) G(u_1, u_2) \partial_{\mathcal{P}^*} \varphi_2(u_2) |du_1| |du_2| \\ + A \int_{\mathbb{R}^2} \varphi_1(u) \varphi_2(u) |du| \end{aligned} \quad (7.63)$$

The proof of the convergence of the second moment goes exactly as that of section 7.2. The second moment of $\tilde{N}_{\mathcal{P}}^\varepsilon$ can be expressed as a convolution of two distributions applied to a test function

$$\mathbb{E} \left[(\tilde{N}_{\mathcal{P}}^\varepsilon \varphi_1)(\tilde{N}_{\mathcal{P}}^\varepsilon \varphi_2) \right] = \langle \varphi^\varepsilon * F^\varepsilon, \varphi_2 \rangle \quad (7.64)$$

with the same definitions as before for φ_1^ε and F^ε .

$$\varphi_1^\varepsilon = \varepsilon^2 \sum_{\mathbf{x}} \varphi_1(u_{\mathbf{x}}^\varepsilon) \delta(\cdot - u_{\mathbf{x}}^\varepsilon) \quad F^\varepsilon = \sum_{\mathbf{x}} \text{Cov}(\mathcal{P}, \mathcal{P}_{\mathbf{x}}) \delta(\cdot - u_{\mathbf{x}}^\varepsilon) \quad (7.65)$$

φ_1^ε converges weakly to φ_1 . The convergence of F^ε to a distribution F is proven in exactly in the same way as in section 7.2. The only difficulty that could appear is the analogue of lemma 7.2 proving the convergence of $\sum_{\mathbf{x}} \text{Cov}(\mathcal{P}, \mathcal{P}_{\mathbf{x}})$. $\text{Cov}(\mathcal{P}, \mathcal{P}_{\mathbf{x}})$ is a linear combination of products of diverse values of \mathbf{K}^{-1} . If we interpret these products as Fourier coefficients of a convolution of functions, then the convergence becomes more obvious: we saw in section 7.2 that the function whose Fourier coefficients are the product of two \mathbf{K}^{-1} is not defined at $(1, 1)$, but has directional limits when (z, w) converges to $(1, 1)$, and the sum of the Fourier coefficient was an average of these directional limits. When more than \mathbf{K}^{-1} are involved, the function is even continuous thanks to the multiple convolutions, and the Fourier series converges at $(z, w) = 1$.

The complex number representing the vector \mathcal{P}^* along which are taken the derivatives is a square root of $\text{tr}(E^{-1}QE^{-1}Q)$.

7.3.4 Convergence of higher moments

Proposition 7.5. *Let $n \geq 3$, and $\varphi_1, \dots, \varphi_n \in \mathcal{C}_c^\infty(\mathbb{R}^2)$.*

$$\lim_{\varepsilon \rightarrow 0} \mathbb{E} \left[\tilde{N}_{\mathcal{P}}^\varepsilon(\varphi_1) \cdots \tilde{N}_{\mathcal{P}}^\varepsilon(\varphi_n) \right] = \begin{cases} 0 & \text{if } n \text{ is odd} \\ \sum_{\text{pairings}} \prod_{l=1}^{n/2} \mathbb{E} [\mathcal{N}_{\mathcal{P}}(\varphi_{i_l}) \mathcal{N}_{\mathcal{P}}(\varphi_{j_l})] & \text{if } n \text{ is even} \end{cases} \quad (7.66)$$

Proof:

As usually, it is sufficient to study the case where all the φ_i are equal to some fixed smooth test function ψ . The n th moment is then given by

$$\mathbb{E} \left[(\tilde{N}_{\bar{\mathcal{P}}}^\varepsilon \psi)^n \right] = \varepsilon^n \sum_{\mathbf{x}_1, \dots, \mathbf{x}_n} \mathbb{E} \left[\prod_{l=1}^n \psi(u_l^\varepsilon) (\mathcal{P}_{\mathbf{x}_l} - \bar{\mathcal{P}}) \right]. \quad (7.67)$$

We know from lemma 7.6 the asymptotics of the general term of the sum

$$\begin{aligned} & \varepsilon^n \mathbb{E} \left[\prod_{l=1}^n \psi(u_l^\varepsilon) (\mathcal{P}_{\mathbf{x}_l} - \bar{\mathcal{P}}) \right] \\ &= \sum_{S \in \tilde{\mathcal{C}}_n} \prod_{\gamma \text{ cycle of } S} \operatorname{sgn} \gamma \frac{2\varepsilon^{2|\gamma|}}{(2\pi)^{|\gamma|}} \operatorname{Re} \left(\operatorname{tr}((E^{-1}Q)^{|\gamma|}) \prod_{l \in \operatorname{supp} \gamma} \frac{\psi(u_l^\varepsilon)}{u_{\mathbf{x}_{\gamma(l)}}^\varepsilon - u_{\mathbf{x}_l}^\varepsilon} \right) \\ & \qquad \qquad \qquad + \text{oscillating terms} + \text{small terms} \\ &= \sum_{(\Gamma_l)_1^p} \prod_{l=1}^p (-2) \left(\frac{-\varepsilon}{2\pi} \right)^{|\Gamma_l|} \operatorname{Re} \left(\operatorname{tr}((E^{-1}Q)^{|\Gamma_l|}) \sum_{\substack{\gamma \text{ cycle} \\ \operatorname{supp} \gamma = \Gamma_l}} \prod_{j \in \Gamma_l} \frac{\psi(u_j^\varepsilon)}{u_{\mathbf{x}_{\gamma(j)}}^\varepsilon - u_{\mathbf{x}_j}^\varepsilon} \right) \\ & \qquad \qquad \qquad + \text{small terms} + \text{oscillating terms} \end{aligned}$$

where the (Γ_l) are partitions of $\{1, \dots, n\}$ whose components have size at least 2. The expression we obtained is very close to that of equation (7.36). From this point, the same arguments as for edges yield the proof of the proposition. \square

7.4 The gaseous case

In a gaseous phase, K^{-1} decays exponentially. There exist two constants C_1 and C_2 such that

$$\forall \mathbf{x} \in \mathbb{Z}^2, \quad |K^{-1}(\mathbf{b}_{\mathbf{x}}, \mathbf{w}_{00})| \leq C_1 \cdot e^{-C_2|\mathbf{x}|}$$

The precise statement of theorem 7.2 in this particular context for a pattern consisting in a single edge \mathbf{e} is the following:

Theorem 7.5. *The random field $\tilde{N}_{\mathbf{e}}^\varepsilon$ converges weakly in distribution to a white noise of amplitude $\sqrt{\frac{\partial^2 F}{\partial^2 \log K_{\mathbf{e}}}}$.*

The proof is exposed in the first two subsections, and the case of a more complex pattern is briefly discussed in subsection 7.4.3

7.4.1 Convergence of the second moment

Proposition 7.6.

$$\forall \varphi_1, \varphi_2 \in \mathcal{C}_c^\infty(\mathbb{R}^2) \quad \lim_{\varepsilon \rightarrow 0} \mathbb{E} \left[\tilde{N}_{\mathbf{e}}^\varepsilon(\varphi_1) \tilde{N}_{\mathbf{e}}^\varepsilon S(\varphi_2) \right] = \frac{\partial^2 F}{\partial \log \mathbf{K}_{\mathbf{e}}^2} \int_{\mathbb{R}^2} \varphi_1(z) \varphi_2(z) |dz|.$$

Proof:

As in section 7.2, the covariance $\mathbb{E} \left[\tilde{N}_{\mathbf{e}}^\varepsilon(\varphi_1) \tilde{N}_{\mathbf{e}}^\varepsilon S(\varphi_2) \right]$ is a convolution of distributions $\varphi_1^\varepsilon * F^\varepsilon$ applied to the test function φ_2 , where

$$\varphi_1^\varepsilon = \varepsilon^2 \sum_{xy} \varphi_1(u_x) \delta(\cdot - u_x^\varepsilon) \quad \text{and} \quad F^\varepsilon = \sum_{\mathbf{x}} \text{Cov}(\mathbf{e}, \mathbf{e}_{\mathbf{x}}) \delta(\cdot - u_{\mathbf{x}}^\varepsilon).$$

φ_1^ε converges weakly to φ_1 . We have now to prove that the distribution F^ε converges toward the distribution $F = \frac{\partial^2 \mathcal{F}}{\partial \log \mathbf{K}_{\mathbf{e}}^2} \delta$. The limit of the second moment will be then

$$\langle \varphi_1 * F, \varphi_2 \rangle = \frac{\partial^2 \mathcal{F}}{\partial \log \mathbf{K}_{\mathbf{e}}^2} \langle \varphi_1 * \delta, \varphi_2 \rangle = \frac{\partial^2 \mathcal{F}}{\partial \log \mathbf{K}_{\mathbf{e}}^2} \int_{\mathbb{R}^2} \varphi_1(u) \varphi_2(u) |du|. \quad (7.68)$$

If $\mathbf{x} \neq (0, 0)$, the covariance between edges \mathbf{e} and $\mathbf{e}_{\mathbf{x}}$ is given by

$$\text{Cov}(\mathbf{e}, \mathbf{e}_{\mathbf{x}}) = \mathbb{E} [(\mathbf{e}_{0,0} - \bar{\mathbf{e}})(\mathbf{e}_{\mathbf{x}} - \bar{\mathbf{e}})] = -\mathbf{K}_{\mathbf{e}}^2 \mathbf{K}^{-1}(\mathbf{x}) \mathbf{K}^{-1}(-\mathbf{x}) \quad (7.69)$$

Let ψ be a smooth test function with compact support, and N a large integer. We decompose the sum over \mathbf{x} in the expression of $\langle F^\varepsilon, \psi \rangle$ depending on whether the norm of \mathbf{x} is larger than N or not.

$$\begin{aligned} \langle F^\varepsilon, \psi \rangle &= \sum_{|\mathbf{x}| > N} \psi(u_{\mathbf{x}}^\varepsilon) \text{Cov}(\mathbf{e}, \mathbf{e}_{\mathbf{x}}) + \sum_{|\mathbf{x}| \leq N} (\psi(u_{\mathbf{x}}^\varepsilon) - \psi(0)) \text{Cov}(\mathbf{e}, \mathbf{e}_{\mathbf{x}}) \\ &\quad + \psi(0) \sum_{|\mathbf{x}| \leq N} \text{Cov}(\mathbf{e}, \mathbf{e}_{\mathbf{x}}) \end{aligned}$$

In the first sum, there are at most $O(\varepsilon^{-2})$ terms since the support of ψ is bounded. As $|\mathbf{x}| > N$, each term in this sum is bounded by some constant times $e^{-2C_2 N}$. Therefore the whole sum is a $O(\varepsilon^{-2} e^{-2C_2 N})$. In the second sum, since $|\mathbf{x}| \leq N$, the distance between

u_x^ε and 0 is less than εN . As ψ is smooth, $(\psi(u_x^\varepsilon) - \psi(0))$ is $O(\varepsilon N)$. The second sum is therefore $O(N^3\varepsilon)$. Choosing for instance N of order $\varepsilon^{-1/4}$, these two sums converge to zero, when ε goes to zero.

The third sum is absolutely convergent, the limit of $\langle F^\varepsilon, \psi \rangle$ is

$$\psi(0) \sum_{x \in \mathbb{Z}^2} \text{Cov}(\mathbf{e}, \mathbf{e}_x).$$

Thus F^ε converges weakly to $\sum_{x \in \mathbb{Z}^2} \text{Cov}(\mathbf{e}, \mathbf{e}_x) \delta$ and the limit of the second moment is proportional to the L^2 scalar product. The coefficient of proportionality

$$\sum_{x \in \mathbb{Z}^2} \text{Cov}(\mathbf{e}, \mathbf{e}_x)$$

can be rewritten in terms of the polynomials $P(z, w)$ and $Q_{\mathbf{e}}(z, w)$.

$$\begin{aligned} \sum_{x \in \mathbb{Z}^2} \text{Cov}(\mathbf{e}, \mathbf{e}_x) &= \mathbb{E}[(\mathbf{e} - \bar{\mathbf{e}})(\mathbf{e} - \bar{\mathbf{e}})] + \sum_{x \neq (0,0)} \mathbb{E}[(\mathbf{e}_{0,0} - \bar{\mathbf{e}})(\mathbf{e}_x - \bar{\mathbf{e}})] \\ &= \mathbb{P}[\mathbf{e}] (1 - \mathbb{P}[\mathbf{e}]) - \mathbb{K}_{\mathbf{e}}^2 \sum_{x \neq (0,0)} \mathbb{K}^{-1}(x) \mathbb{K}^{-1}(-x) \\ &= \mathbb{K}_{\mathbf{e}} \mathbb{K}^{-1}(0) - \mathbb{K}_{\mathbf{e}}^2 \sum_x \mathbb{K}^{-1}(x) \mathbb{K}^{-1}(-x) \\ &= \iint_{\mathbb{T}^2} \frac{\mathbb{K}_{\mathbf{e}} Q_{\mathbf{e}}(z, w)}{P(z, w)} - \frac{\mathbb{K}_{\mathbf{e}}^2 Q_{\mathbf{e}}(z, w)^2}{P(z, w)^2} \frac{dz}{2\pi iz} \frac{dw}{2\pi iw} \\ &= \mathbb{K}_{\mathbf{e}} \frac{\partial}{\partial \mathbb{K}_{\mathbf{e}}} \mathbb{K}_{\mathbf{e}} \frac{\partial}{\partial \mathbb{K}_{\mathbf{e}}} \iint_{\mathbb{T}^2} \log(P(z, w)) \frac{dz}{2\pi iz} \frac{dw}{2\pi iw} \\ &= \frac{\partial^2 \mathcal{F}}{\partial \log \mathbb{K}_{\mathbf{e}}^2} \end{aligned}$$

where \mathcal{F} is the free energy of the system. □

7.4.2 Higher moments

Proposition 7.7. *The Wick formula is verified in the limit.*

$$\lim_{\varepsilon \rightarrow 0} \mathbb{E} \left[(\tilde{N}_{\mathbf{e}}^\varepsilon \psi)^n \right] = \begin{cases} 0 & \text{if } n \text{ is odd,} \\ (n-1)!! \mathbb{E} \left[(\tilde{N}_{\mathbf{e}}^\varepsilon)^2 \right]^{n/2} & \text{if } n \text{ is even.} \end{cases}$$

Proof:

As in the case of a generic liquid measure, the proof begins with the study of the restricted

n th moment $\Xi_n^\varepsilon(\psi)$ defined by equation (7.33). Lemma 7.3 yields the same asymptotic expression as in the generic liquid case (7.34):

$$\Xi_n^\varepsilon(\psi) = \sum_{\{\Gamma\}_{l=1}^p} \prod_{l=1}^p \sum_{\substack{\gamma \text{ cycle} \\ \text{supp}(\gamma)=\Gamma_l}} \left(\text{sgn}(\gamma)(\varepsilon \mathbf{K}_e)^{|\gamma|} \times \sum_{\substack{\mathbf{x}_{j_1}, \dots, \mathbf{x}_{j_{|\gamma|}} \\ \text{distinct}}} \prod_{k=1}^{|\gamma|} \psi(u_{\mathbf{x}_{j_k}}^\varepsilon) \mathbf{K}^{-1}(\mathbf{x}_{\gamma(j_k)} - \mathbf{x}_{j_k}) + o(1) \right) \quad (7.70)$$

The contributions of cycles of length greater than 3 vanish in the limit, thanks to the following lemma:

Lemma 7.7.

$$\forall m \geq 3, \quad \lim_{\varepsilon \rightarrow 0} \varepsilon^m \sum_{\mathbf{x}_1, \dots, \mathbf{x}_m} \prod_{j=1}^m \psi(u_{\mathbf{x}_j}^\varepsilon) \mathbf{K}^{-1}(\mathbf{x}_{j+1} - \mathbf{x}_j) = 0$$

Proof:

Define $\mathbf{x}' = \mathbf{x}_1$ and for $j \geq 2$ $\mathbf{x}'_j = \mathbf{x}_j - \mathbf{x}_{j-1}$. The sum can be rewritten using these new notations and invariance by translation of operator \mathbf{K}^{-1} as

$$\varepsilon^m \sum_{\mathbf{x}'} \psi(u_{\mathbf{x}'}^\varepsilon) \sum_{\mathbf{x}'_2, \dots, \mathbf{x}'_m} \left(\prod_{j=2}^m \psi(u_{\mathbf{x}' + \mathbf{x}'_2 + \dots + \mathbf{x}'_j}^\varepsilon) \mathbf{K}^{-1}(\mathbf{x}'_j) \right) \mathbf{K}^{-1}(-\mathbf{x}' - \mathbf{x}'_2 \cdots - \mathbf{x}'_m)$$

As ψ is a continuous function on a compact set, it is bounded. The sum on \mathbf{x}' has $O(\varepsilon^{-2})$ terms. $\mathbf{K}^{-1}(\mathbf{b}_{-\mathbf{x}' - \mathbf{x}'_2 \cdots - \mathbf{x}'_m}, \mathbf{w})$ is bounded independently from the \mathbf{x}'_j 's. As \mathbf{K}^{-1} decays exponentially, the sum on $\mathbf{x}'_2, \dots, \mathbf{x}'_m$ is bounded. The whole sum is thus a $O(\varepsilon^{m-2})$, which goes to zero when ε goes to zero as soon as $m \geq 3$. \square

Thus $\Xi_n^\varepsilon(\psi)$ converges to $\Xi_n(\psi) = (n-1)!! \Xi_2(\psi)$. The end of the proof deals with collisions between edges, which is identical to what has been done for proposition 7.3, leading to the result. \square

7.4.3 Patterns in gaseous phase

Combining the notations and the techniques introduced in 7.3 to deal with correlations between patterns, and following the steps of the proof of theorem 7.5, one can prove the following

Theorem 7.6. *Let \mathcal{P} be a pattern in a dimer model endowed with a gaseous Gibbs measure. The random field $\tilde{N}_{\mathcal{P}}^{\varepsilon}$ of density fluctuation of pattern \mathcal{P} converges weakly in distribution to a white noise.*

The proof is omitted here.

7.5 Correlations between density fields

In the previous sections, only fluctuations of the density field associated to one fixed pattern was considered. One can ask what happens for correlations between density fields associated to different patterns. To what extent a high density of some pattern in a given region of the plane has an influence on the density of another pattern in another region ?

This question is answered by the following theorem generalizing the results of the previous sections.

Theorem 7.7. *Consider a dimer model with a generic liquid Gibbs measure μ .*

- *Let \mathcal{P}_1 and \mathcal{P}_2 be two patterns. The bilinear form $\mathbb{E} \left[\tilde{N}_{\mathcal{P}_1}^{\varepsilon}(\cdot) \tilde{N}_{\mathcal{P}_2}^{\varepsilon}(\cdot) \right]$ on $\mathcal{C}_c^{\infty}(\mathbb{R}^2)$ converges when ε goes to zero to a bilinear form $\mathbb{E} [\mathcal{N}_{\mathcal{P}_1}(\cdot) \mathcal{N}_{\mathcal{P}_2}(\cdot)]$.*
- *If μ is a generic liquid Gibbs measure, there exists a constant $A_{\mathcal{P}_1 \mathcal{P}_2}$ such that for every test functions φ_1 and φ_2 ,*

$$\begin{aligned} \mathbb{E} [\mathcal{N}_{\mathcal{P}_1}(\varphi_1) \mathcal{N}_{\mathcal{P}_2}(\varphi_2)] &= \frac{1}{\pi} \iint_{\mathbb{R}^2 \times \mathbb{R}^2} \partial_{\mathcal{P}_1^*} \varphi_1(u) G(u, v) \partial_{\mathcal{P}_2^*} \varphi_2(v) |du| |dv| \\ &\quad + A_{\mathcal{P}_1 \mathcal{P}_2} \int_{\mathbb{R}^2} \varphi_1(u) \varphi_2(u) |du| \quad (7.71) \end{aligned}$$

- *If μ is gaseous, there exists a constant $A_{\mathcal{P}_1 \mathcal{P}_2}$ such that for every test functions φ_1 and φ_2 ,*

$$\mathbb{E} [\mathcal{N}_{\mathcal{P}_1}(\varphi_1) \mathcal{N}_{\mathcal{P}_2}(\varphi_2)] = A_{\mathcal{P}_1 \mathcal{P}_2} \int_{\mathbb{R}^2} \varphi_1(u) \varphi_2(u) |du|$$

- *Let $\mathcal{P}_1, \dots, \mathcal{P}_n$ be patterns (not necessarily distinct). When ε goes to zero, the multilinear form $\mathbb{E} \left[\tilde{N}_{\mathcal{P}_1}^{\varepsilon}(\cdot) \cdots \tilde{N}_{\mathcal{P}_n}^{\varepsilon}(\cdot) \right]$ converges. The limit $\mathbb{E} [\mathcal{N}_{\mathcal{P}_1}(\cdot) \cdots \mathcal{N}_{\mathcal{P}_n}(\cdot)]$ is given by Wick formula: for every test functions $\varphi_1, \dots, \varphi_n$,*

$$\mathbb{E} [\mathcal{N}_{\mathcal{P}_1}(\varphi_1) \cdots \mathcal{N}_{\mathcal{P}_n}(\varphi_n)] = \begin{cases} 0 & \text{if } n \text{ is odd} \\ \sum_{\text{pairing } k=1}^{n/2} \prod_{k=1}^{n/2} \mathbb{E} [\mathcal{N}_{\mathcal{P}_{i_k}}(\varphi_{i_k}) \mathcal{N}_{\mathcal{P}_{j_k}}(\varphi_{j_k})] & \text{if } n \text{ is even} \end{cases}$$

Let \mathbf{v} be a vertex of the graph, and denote by $\mathbf{e}_1, \dots, \mathbf{e}_m$ the edges incident with \mathbf{v} . The complex numbers $\mathbf{e}_1^*, \dots, \mathbf{e}_m^*$ sum to zero since they represent the edges of the dual face \mathbf{v}^* . Even more, for every $\varepsilon > 0$, the linear combination $\tilde{N}_{\mathbf{e}_1}^\varepsilon + \dots + \tilde{N}_{\mathbf{e}_m}^\varepsilon$ is identically zero. Indeed, for every $\mathbf{x} \in \mathbb{Z}^2$, there is exactly one edge incident with $\mathbf{v}_\mathbf{x}$ in the random dimer configuration. Therefore the sum of indicator functions $(\mathbf{e}_1)_\mathbf{x} + \dots + (\mathbf{e}_m)_\mathbf{x}$ is always equal to 1. This relation between the random fields $\tilde{N}_{\mathbf{e}_j}^\varepsilon$ at a microscopic level yields relations between the different coefficients $A_{\mathbf{e}_i \mathbf{e}_j}$. Precisely,

$$\sum_{i=1}^m \sum_{j=1}^m A_{\mathbf{e}_i \mathbf{e}_j} = 0 \quad (7.72)$$

7.6 Examples

The theorems in the previous sections state a convergence of density fluctuation in the scaling limit to a linear combination of a derivative of the massless free field and a white noise. However, they do not give an explicit form for the white noise amplitude. In this section we present some cases for which a closed expression for the white noise amplitude can be provided in terms of the weights on edges. The first case is the dimer model on the graph \mathbb{Z}^2 with periodic weights a, b, c, d around white vertices. The second case is the dimer model on the square octagon graph.

7.6.1 Tilings of the plane by dominos

The graph we consider here is the graph \mathbb{Z}^2 with a bipartite coloring of its vertices. Weights are assigned to edges according to their directions: a, b, c, d counterclockwise around white vertices and clockwise around black vertices. If none of the weights is greater than the sum of the others, the corresponding dimer model is critical [30]: the graph can be embedded in the plane such that all the faces of the graph as well as those of the dual graph are inscribed in circles of a given radius. The Gibbs measure with no magnetic field on dimer configurations is liquid. The primal and dual faces are similar to the cyclic quadrilateral with sides a, b, c and d . The area of such a quadrilateral is

$$\text{Area} = \frac{1}{4} \sqrt{(-a + b + c + d)(a - b + c + d)(a + b - c + d)(a + b + c - d)}$$

and the radius R of its circumscribed circle is defined by the relation

$$R^2 = \frac{(ab + cd)(ac + bd)(ad + cb)}{(-a + b + c + d)(a - b + c + d)(a + b - c + d)(a + b + c - d)}.$$

The fact we chose the fundamental domain to have area 1 leads to the following expression for the complex numbers representing the dual edges in the embedding of \mathbb{Z}^2 :

$$a^* = \frac{ia}{\sqrt{2} \text{Area}} \quad b^* = \frac{ib}{w_0 \sqrt{2} \text{Area}} \quad c^* = \frac{-icz_0}{w_0 \sqrt{2} \text{Area}} \quad d^* = \frac{idz_0}{\sqrt{2} \text{Area}}$$

where (z_0, w_0) is the root of the the characteristic polynomial

$$P(z, w) = a + \frac{b}{w} - \frac{cz}{w} + dz$$

on the unit torus, with the additional constraint that $\text{Im}(z_0) > 0$.

The following theorem is a particular case of theorem 7.7.

Theorem 7.8. *Let GFF a Gaussian free field in the plane and W an independent white noise. The vector-valued random field*

$$\tilde{N}^\varepsilon = \begin{pmatrix} \tilde{N}_a^\varepsilon \\ \tilde{N}_b^\varepsilon \\ \tilde{N}_c^\varepsilon \\ \tilde{N}_d^\varepsilon \end{pmatrix}$$

converges weakly in distribution to the vector-valued Gaussian Field

$$\begin{pmatrix} \mathcal{N}_a \\ \mathcal{N}_b \\ \mathcal{N}_c \\ \mathcal{N}_d \end{pmatrix} = \frac{1}{\sqrt{\pi}} \begin{pmatrix} \partial_{a^*} \\ \partial_{b^*} \\ \partial_{c^*} \\ \partial_{d^*} \end{pmatrix} \text{GFF} + \sqrt{\frac{abcd}{8\pi R^2 \text{Area}}} \begin{pmatrix} +1 \\ -1 \\ +1 \\ -1 \end{pmatrix} W$$

where R is the radius of the circumscribed circle of a face, given by

$$R^2 = \frac{(ab + cd)(ac + bd)(ad + cb)}{(-a + b + c + d)(a - b + c + d)(a + b - c + d)(a + b + c - d)}.$$

Proof:

The only point we have to explain is the computation of the white noise amplitude. This coefficient can be identified from the limit of the second moment of \tilde{N}_a^ε . The proof of the convergence of the second moment, as before, goes through the proof of the convergence of the distribution F^ε defined by (7.14). The sum over \mathbf{x} in the definition of F^ε is decomposed into two parts depending on whether $u_{\mathbf{x}}^\varepsilon$ belongs to some neighborhood of 0 or not. In the general case, we considered the neighborhood $\mathcal{B} = \{i(\alpha z_0 s + \beta z_0 t) ; (s, t) \in [-1, 1]^2\}$. However, here we will take an infinite strip

$$\mathcal{S} = \{i(\alpha z_0 s + \beta z_0 t) ; (s, t) \in \mathbb{R} \times [-1, 1]\}.$$

The condition on $\mathbf{x} = (x, y)$ corresponding to $u_{\mathbf{x}}^\varepsilon \in \mathcal{S}$ is $x \in \mathbb{Z}$ and $|y| \leq M$ where $M = \lfloor 1/\varepsilon \rfloor$. We have

$$\langle F^\varepsilon, \psi \rangle = \sum_{\substack{x \in \mathbb{Z} \\ |y| > M}} \psi(u_{\mathbf{x}}^\varepsilon) \text{Cov}(\mathbf{e}, \mathbf{e}_x) + \sum_{\substack{x \in \mathbb{Z} \\ |y| \leq M}} (\psi(u_{\mathbf{x}}^\varepsilon) - \psi(0)) \text{Cov}(\mathbf{e}, \mathbf{e}_x) + \psi(0) \sum_{\substack{x \in \mathbb{Z} \\ |y| \leq M}} \text{Cov}(\mathbf{e}, \mathbf{e}_x).$$

The inverse Kasteleyn operator in this case is given by

$$\mathbf{K}^{-1}(x, y) = \mathbf{K}^{-1}(\mathbf{b}_x, \mathbf{w}_0) = \int_{\mathbb{T}^2} \frac{z^{-y} w^x}{a + b/w - cz/w + dz} \frac{dz}{2i\pi z} \frac{dw}{2i\pi w}.$$

The fact we have an infinite strip allows us to make use of one dimensional Fourier series in the x -direction to compute the third sum. Indeed, $\mathbf{K}^{-1}(x, y)$ is the x th Fourier coefficient of the function $f_y(w)$ defined by

$$f_y(w) = \int \frac{z^{-y}}{a + b/w - cz/w + dz} \frac{dz}{2i\pi z}.$$

Hence, for a fixed y ,

$$\sum_{x \in \mathbb{Z}} \mathbf{K}^{-1}(x, y) \mathbf{K}^{-1}(-x, -y) = \int f_y(w) f_{-y}(w) \frac{dw}{2i\pi w}.$$

For $y \neq 0$, the functions f_y and f_{-y} have disjoint support, therefore the sum above is zero. When $y = 0$, the sum is equal to

$$\sum_{x \in \mathbb{Z}} \mathbf{K}^{-1}(x, 0) \mathbf{K}^{-1}(-x, 0) = \int f_0^2(w) \frac{dw}{2i\pi w} = \int_{\left| \frac{a+bw}{cw-d} \right| > 1} \frac{dw}{2i\pi (a + b/w)^2 w}.$$

The third sum equals

$$\begin{aligned} \psi(0) \sum_{\substack{x \in \mathbb{Z} \\ |y| \leq M}} \text{Cov}(\mathbf{e}_x, \mathbf{e}_x) &= \psi(0) \left(a \mathbf{K}^{-1}(0) - a^2 \sum_{|y| \leq M} \sum_{x \in \mathbb{Z}} \mathbf{K}^{-1}(x, y) \mathbf{K}^{-1}(-x, -y) \right) \\ &= \psi(0) \left(\int_{\left| \frac{a+bw}{cw-d} \right| > 1} \frac{adz}{(a + b/w) 2i\pi w} - \int_{\left| \frac{a+bw}{cw-d} \right| > 1} \frac{a^2 dz}{(a + b/w)^2 2i\pi w} \right) = \psi(0) \frac{-ab \text{Im}(w_0)}{\pi |a + b/w_0|^2}. \end{aligned}$$

The other term coming from the application of Green formula can also be computed and turns out to be equal to

$$-\psi(0) \frac{1}{2\text{Area}} \frac{1}{\pi} \left(\frac{-ab \text{Im}(w_0)}{\left| a + \frac{b}{w_0} \right|} \right)^2.$$

Hence the variance of the white noise appearing in the limit of \tilde{N}_a^ε is given, after some calculations, by

$$\frac{1}{\pi} \frac{-ab \text{Im}(w_0)}{|a + b/w_0|^2} \left(1 + \frac{ab \text{Im}(w_0)}{2\text{Area}} \right) = \frac{abcd}{8\pi R^2 \text{Area}}$$

A similar computation for $\mathbb{E} \left[\tilde{N}_a^\varepsilon(\varphi_1) \tilde{N}_b^\varepsilon(\varphi_2) \right]$ leads to the same expression, with a negative sign. As the expression of the coefficient is invariant under cyclic permutation of

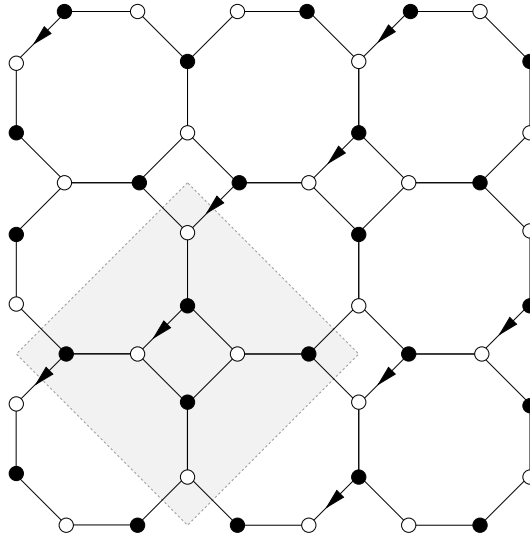


Figure 7.1: A portion of the square-octagon graph. Edges are oriented from white end to black end, except those whose orientation is represented on the figure.

a, b, c, d , the amplitudes for the other pairs are easily deduced. □

When $c = 0$, the dimer model on \mathbb{Z}^2 is equivalent to that on the honeycomb lattice with periodic weights a, b, d . One can notice that in this case, the amplitude of the white noise vanishes. The interaction between dimers on the honeycomb lattice is purely electrostatic. We conjecture that it is true only for that particular model.

7.6.2 Dimer densities on the square-octagon graph

The square-octagon graph is a \mathbb{Z}^2 -periodic graph whose fundamental domain is presented in figure 7.1. It contains four white and four black vertices. When every edge is assigned a weight equal to 1, the characteristic polynomial is given by

$$P(z, w) = \det \begin{bmatrix} 1 & \frac{1}{w} & 0 & -\frac{1}{z} \\ 1 & 1 & 1 & 0 \\ 0 & z & 1 & w \\ -1 & 0 & 1 & 1 \end{bmatrix} = 5 - z - \frac{1}{z} - w - \frac{1}{w}$$

The spectral curve has genus 1 and its amoeba is represented on figure 7.2. When the magnetic field is weak, the dimer model is in a gaseous field. The fluctuations of the density field of an edge can be therefore computed by taking derivatives of the free energy of the system with respect to the weights, as explained in section 7.4.

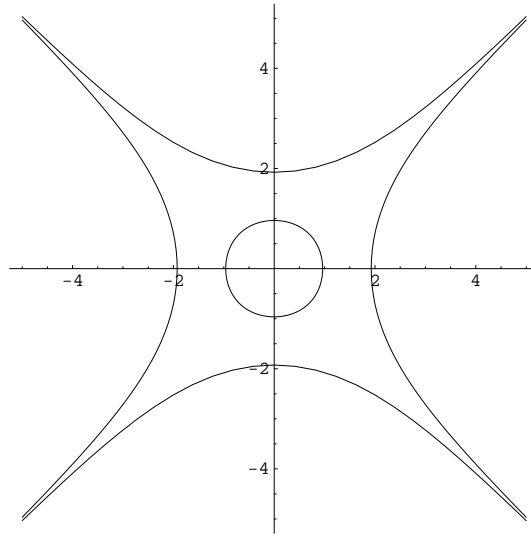


Figure 7.2: The amoeba of the dimer model on the square-octagon graph.

To compute for instance the amplitude of the white noise in the limit density of the edges $(\mathbf{w}_1, \mathbf{b}_1)$, we assign to these edges a weight e^a and to the others a weight equal to 1, and compute the second derivative of the free energy \mathcal{F} associated to this model with respect to a . For these new weights, the spectral curve is now

$$P_a(z, w) = \det \begin{bmatrix} e^a & \frac{1}{w} & 0 & -\frac{1}{z} \\ 1 & 1 & 1 & 0 \\ 0 & z & 1 & w \\ -1 & 0 & 1 & 1 \end{bmatrix} = 4 + e^a - e^a z - \frac{1}{z} - e^a w - \frac{1}{w}.$$

If a is small enough, the dimer model is in a gaseous phase in absence of magnetic field. In every point of this phase, the free energy is constant and given by

$$\begin{aligned} \mathcal{F} &= \iint_{\mathbb{T}^2} \log(P_a(z, w)) \frac{dz}{2i\pi z} \frac{dw}{2i\pi w} \\ &= \log(4 + e^a) + \iint_{[0, 2\pi]^2} \log \left(1 - \frac{1}{4 + e^a} \left(e^{a+i\theta} + e^{-i\theta} + e^{a+i\phi} + e^{-i\phi} \right) \right) \frac{d\theta}{2\pi} \frac{d\phi}{2\pi} \end{aligned}$$

Performing the change of variables $\alpha = \frac{\theta+\phi}{2}$, $\beta = \frac{\theta-\phi}{2}$ and moving the contour of integration over α from $[0, 2\pi]$ to $[-ia/2, -ia/2 + 2\pi]$ using analyticity and periodicity in α , we

finally get an expression of \mathcal{F} in terms of an absolutely convergent series:

$$\mathcal{F}_a = \log(4 + e^a) + \iint_{[0,2\pi]^2} \log \left(1 - \frac{4e^{a/2}}{4 + e^a} \cos(\alpha) \cos(\beta) \right) \frac{d\alpha}{2\pi} \frac{d\beta}{2\pi} \quad (7.73)$$

$$= \log(4 + e^a) - \sum_{k=1}^{\infty} \frac{1}{k} \left(\frac{4e^{a/2}}{4 + e^a} \right)^k \left(\int_0^{2\pi} \cos^k(\alpha) \frac{d\alpha}{2\pi} \right) \left(\int_0^{2\pi} \cos^k(\beta) \frac{d\beta}{2\pi} \right) \quad (7.74)$$

$$= \log(4 + e^a) - \sum_{k=1}^{\infty} \frac{1}{2k} \left(\frac{e^{a/2}}{4 + e^a} \right)^{2k} \left(\frac{(2k)!}{(k!)^2} \right)^2 \quad (7.75)$$

\mathcal{F}_a can be expressed as the value of a certain generalized hypergeometric function. The Taylor expansion up to order 2, involving the elliptic integrals K and E ²

$$\mathcal{F}_a = \mathcal{F} + \left(\frac{1}{2} - \frac{3K\left(\frac{16}{25}\right)}{5\pi} \right) a + \left(\frac{K\left(\frac{16}{25}\right) - E\left(\frac{16}{25}\right)}{2\pi} \right) \frac{a^2}{2} + O(a^3)$$

gives information on the statistics of the copies of edge $(\mathbf{w}_1, \mathbf{b}_1)$. The constant coefficient is the free energy of the initial model, the coefficient of a is the probability of $(\mathbf{w}_1, \mathbf{b}_1)$

$$\mathbb{P}[(\mathbf{w}_1, \mathbf{b}_1)] = \frac{1}{2} - \frac{3K\left(\frac{16}{25}\right)}{5\pi},$$

and the coefficient of $a^2/2$ gives the amplitude of the white noise describing the scaling limit of the fluctuations of the number of edges $(\mathbf{w}_1, \mathbf{b}_1)$

$$\lim_{\varepsilon \rightarrow 0} \mathbb{E} \left[(\tilde{N}_{(\mathbf{w}_1, \mathbf{b}_1)}^\varepsilon \varphi)^2 \right] = \frac{K\left(\frac{16}{25}\right) - E\left(\frac{16}{25}\right)}{2\pi} \int_{\mathbb{R}^2} \varphi(u)^2 du.$$

Similarly, one can compute the probability of seeing an edge of a square, for example $(\mathbf{w}_2, \mathbf{b}_1)$, and the amplitude of the white noise:

$$\mathbb{P}[(\mathbf{w}_2, \mathbf{b}_1)] = \frac{1}{4} + \frac{3K\left(\frac{16}{25}\right)}{10\pi},$$

$$\lim_{\varepsilon \rightarrow 0} \mathbb{E} \left[(\tilde{N}_{(\mathbf{w}_1, \mathbf{b}_1)}^\varepsilon \varphi)^2 \right] = \frac{2K\left(\frac{16}{25}\right)}{5\pi} \int_{\mathbb{R}^2} \varphi(u)^2 du.$$

The fact we see elliptic functions showing up is not very surprising since the spectral curve in this case is a torus.

²We recall that the complete elliptic integral of first and second class are given by

$$K(m) = \int_0^{\frac{\pi}{2}} \frac{d\phi}{\sqrt{1 - m \sin^2(\phi)}} \quad \text{and} \quad E(m) = \int_0^{\frac{\pi}{2}} \sqrt{1 - m \sin^2(\phi)} d\phi. \quad (7.76)$$

8 Curl-free walks and the lamplighter's problem

This work is a preliminary step to solve the following combinatorial problem proposed by Richard Kenyon. On the lattice \mathbb{Z}^2 , what is (asymptotically) the number of closed paths such that the winding number around each face is equal to zero? These special paths are called *curl-free paths* and an example of length 14 is presented on figure 8.1.

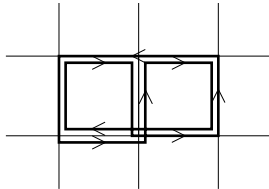


Figure 8.1: An curl-free walk of length 14.

We will solve the following simpler question in the same spirit. Let G be the ladder graph: the vertices of G are indexed by $\mathbb{Z} \times \{0, 1\}$, and there is an edge between $v = (k, z)$ and $v' = (k', z')$ if either $|k - k'| = 1$ and $z = z'$, or $k = k'$ and $z \neq z'$. Edges of the second type are called the *rungs* of the ladder. A piece of the ladder graph is represented on figure 8.2. To simplify, we will use the following notations to label vertices:

$$\bar{k} = (k, 1), \quad \underline{k} = (k, 0).$$

The position of the bar recalls on which side of the ladder the vertex is located.

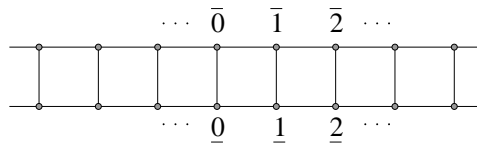


Figure 8.2: A piece of the ladder graph G .

Let \mathcal{P}_n be the set of closed paths on G of length n , starting from $(0, 0)$ and passing an even number of times through every rung of the ladder, and $\mathcal{P} = \bigcup_{n \geq 0} \mathcal{P}_n$. The problem is to determine an asymptotic expression for the cardinal of \mathcal{P}_n .

8.1 The lamplighter's problem

It turns out that this combinatorial problem is equivalent to determining the on-diagonal asymptotics of the heat kernel on the *lamplighter's graph*.

The lamplighter's graph represents an infinite street with an infinite number of lamps labelled by \mathbb{Z} . A vertex of this graph is the collection of the states of all the lamps, in addition to the position of the lamplighter. Two vertices of the graph are linked by an edge if the lamplighter can pass from one state to the other by one of these elementary operations:

- make one step on the left,
- make one step on the right,
- switch the lamp located at his position.

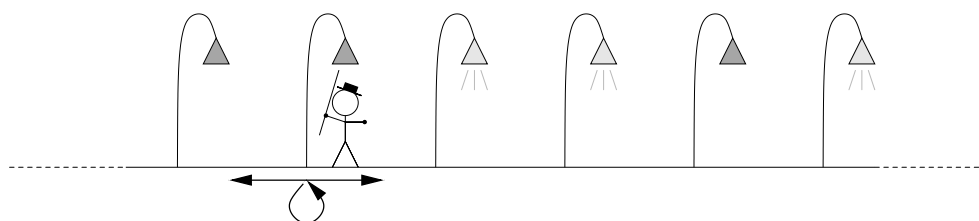


Figure 8.3: The lamplighter switching on and off lamps on a infinite street.

Initially, all the lamps are switched off and the lamplighter stands in front of the lamp labelled by 0. The diagonal entries of the heat kernel represent the probability that the lamplighter will come back to his starting point after a given number of steps, and when he comes back, all the lamp will be switched off.

The correspondence between paths on G and paths on the lamplighter is the following: let γ be a path on G . The projection of γ on the first factor \mathbb{Z} describes the trajectory of the lamplighter, and a crossing of rung k corresponds to a state change of lamp k .

The paths of \mathcal{P} are thus in bijection with loops on the lamplighter's graph, since for the lamplighter to come back to the initial state, he must operate an even number of times all the switches, so that all lamps are switched off when he comes back to 0.

The lamplighter's graph turns out to be the Cayley graph of a group, that can be generated by an automaton [19]. The spectrum of this group is completely known for some random walks [2], and can be used to compute return probabilities. However, we use here an alternative method. See also [53] for another approach.

8.2 Strategy

The method proposed to solve this problem is based on the following combinatorial fact: let M be the adjacency matrix of G . Then $(M^n)_{\underline{0},\underline{0}}$ is exactly the number of loops of length n starting from $\underline{0}$. If we now add weights $\omega(\mathbf{e})$ to the edges \mathbf{e} of the graph, and consider the weighted adjacency matrix M_ω , then $(M_\omega^n)_{\underline{0},\underline{0}}$ is the sum of the weights of these loops of length n , where the weight of a path γ , as usual, is the product of the weights of the edges it contains

$$\omega(\gamma) = \prod_{\mathbf{e} \in \gamma} \omega(\mathbf{e}). \quad (8.1)$$

Let $(\varepsilon_k)_{k \in \mathbb{Z}}$ a sequence of independent identically distributed random variables, such that

$$\mathbb{P}[\varepsilon_k = +1] = \mathbb{P}[\varepsilon_k = -1] = \frac{1}{2}.$$

If we assign weights to the edges of G as follows:

$$\omega(\mathbf{e}) = \begin{cases} 1 & \text{if } \mathbf{e} = (\bar{k}, \overline{k+1}) \text{ or } (\underline{k}, \underline{k+1}) \\ \varepsilon_k & \text{if } \mathbf{e} = (\bar{k}, \underline{k}) \end{cases} \quad (8.2)$$

then the average of $(M_\omega^n)_{\underline{0},\underline{0}}$ is equal to the cardinal of \mathcal{P}_n

$$|\mathcal{P}_n| = \mathbb{E} \left[(M_\omega^n)_{\underline{0},\underline{0}} \right] = \sum_{\substack{\text{length}(\gamma)=n \\ \gamma(0)=\gamma(n)=\underline{0}}} \mathbb{E}[\omega(\gamma)]. \quad (8.3)$$

Indeed, if a path γ crosses a rung, say rung k , an odd number of times, the power of ε_k in $\omega(\gamma)$ is odd, and therefore $\mathbb{E}[\omega(\gamma)] = 0$. On the contrary, if $\gamma \in \mathcal{P}_n$, $\mathbb{E}[\omega(\gamma)] = 1$.

Since a path of length n does not see vertices of G at a distance greater than n of the origin, one can in fact replace the infinite graph G by a smaller one coinciding with G on a large enough neighbourhood of $\underline{0}$. Since G is periodic, it is convenient in order to keep some symmetry to replace G by a quotient of it by a large lattice $G_N = G/N\mathbb{Z}$, for $N > n$. The actual value of N has no importance. One can take for example $N = 2n$.

We will use *bra* and *ket* notations from quantum mechanics to denote functions on vertices and their transpose. For $k \in \mathbb{Z}/N\mathbb{Z}$, $|\bar{k}\rangle$ (resp. $\langle \underline{k}|$) stands for the function equal to 1 on vertex \bar{k} (resp. \underline{k}) and 0 elsewhere.

The graph G_N is invariant under the exchange of the two copies of $\mathbb{Z}/N\mathbb{Z}$. The weighted matrix M_ω

$$M_\omega |\bar{k}\rangle = |\overline{k-1}\rangle + \varepsilon_k |\underline{k}\rangle + |\bar{k}\rangle, \quad M_\omega |\underline{k}\rangle = |\underline{k-1}\rangle + \varepsilon_k |\bar{k}\rangle + |\underline{k}\rangle \quad (8.4)$$

commutes with operator T

$$T|\bar{k}\rangle = |\underline{k}\rangle, \quad T|\underline{k}\rangle = |\bar{k}\rangle. \quad (8.5)$$

The functions $|k^\pm\rangle = \frac{|\bar{k}\rangle \pm |k\rangle}{\sqrt{2}}$ are eigenfunctions of T

$$|k^\pm\rangle = \pm |k^\pm\rangle \quad (8.6)$$

and the matrix of M_ω in the eigenbasis $(|k^+\rangle, |k^-\rangle)$ is block diagonal $\begin{pmatrix} M_\omega^+ & 0 \\ 0 & M_\omega^- \end{pmatrix}$ where

$$M_\omega^\pm = \begin{pmatrix} \pm\varepsilon_0 & 1 & 0 & \cdots & 1 \\ 1 & \pm\varepsilon_1 & 1 & \ddots & \vdots \\ 0 & 1 & \ddots & \ddots & 0 \\ \vdots & \ddots & \ddots & \pm\varepsilon_{N-2} & 1 \\ 1 & \cdots & 0 & 1 & \pm\varepsilon_{N-1} \end{pmatrix} \quad (8.7)$$

It follows then from the iid property of the sequence (ε_k) that

$$\mathbb{E} \left[(M_\omega^n)_{0,0} \right] = \frac{1}{2N} \mathbb{E} [\text{tr}(M_\omega^n)] = \frac{1}{N} \mathbb{E} [\text{tr}(M_\omega^+)] = \frac{1}{N} \sum_{j=1}^N \mathbb{E} [(\lambda_j(\omega))^n] \quad (8.8)$$

where $\lambda_1(\omega) \geq \cdots \geq \lambda_{2N}(\omega)$ are the eigenvalues of M_ω^+ .

The matrix M_ω^+ can be interpreted as the weighted adjacency matrix of the graph represented on figure 8.2.

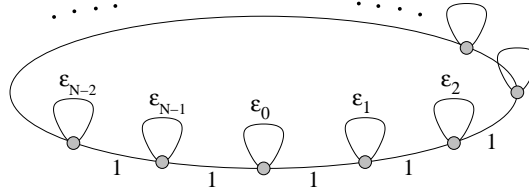


Figure 8.4: The weighted graph represented by M_ω^+

Since the graph G_N is bipartite¹, the walk needs an even number of steps to come back to the origin. Therefore the quantity (8.8) is zero if n is odd. We from now assume that n is even.

When n is large, the main contribution to this sum is given by the edge of the spectrum, λ_1 and λ_N . As G_N is bipartite, we have

$$\lambda_1((\varepsilon_k)) = -\lambda_N((-\varepsilon_k)) \quad (8.9)$$

¹In fact, it is really bipartite only if N is even. We will suppose that it is indeed the case. However, if N is odd, one can still color the vertices such that the bipartite property is verified in a large enough neighbourhood of the origin to contain every n -step walk.

and once again, by the iid property of the sequence (ε_k) , the contribution of these two eigenvalues are equal, and thus

$$|\mathcal{P}_n| \underset{n \rightarrow +\infty}{\sim} \frac{2}{N} \mathbb{E} [\lambda_1(\omega)^n] \quad (8.10)$$

To obtain an asymptotic expression for the cardinal of \mathcal{P}_n , we will give for any realisation of ω an approximation of $\lambda_1(\omega)$ to get an estimate of the main term of (8.8). Then we evaluate the spectral gap in order to control the contribution of the other eigenvalues.

8.3 Approximation of the first eigenvalue

We will work only the block M_ω^+ with a fixed realization of (ε_k) . To simplify notations, we will drop from notations the dependance on ω and superscript $+$.

The diagonal entries of M can be viewed as the period of an infinite succession of $+1$ and -1 . We will see in this section that the greatest eigenvalue is related to the longest sequence of $+1$ in this succession. More precisely, we claim that

Proposition 8.1. *Let ℓ be the longest sequence of $+1$ in $\varepsilon_0, \dots, \varepsilon_{N-1}, \varepsilon_1, \dots$. Then*

$$\lambda_1 = 3e^{-\frac{\pi^2}{3\ell^2} + O\left(\frac{1}{\ell^3}\right)}. \quad (8.11)$$

We prove the proposition in two steps, by first giving a lower bound on λ_1 , and then an upper bound. The error term $O\left(\frac{1}{\ell^3}\right)$ is uniform in ℓ .

8.3.1 Lower bound

The greatest eigenvalue of symmetric matrix M_ω^+ is the maximal value of the associated quadratic form on the unit sphere

$$\lambda_1(\omega) = \sup_{\langle \varphi | \varphi \rangle = 1} \langle \varphi | M | \varphi \rangle. \quad (8.12)$$

To get a lower bound for λ_1 , it is therefore sufficient to evaluate $\langle \varphi | M | \varphi \rangle$ for a suitably chosen function $|\varphi\rangle$.

If $\ell < N$, the restriction of M to the largest interval of $+1$ is equal to $3\text{Id}_\ell + \Delta_\ell$, where Δ_ℓ is the discrete Dirichlet Laplacian on a segment of ℓ points.

Let $|\varphi\rangle$ be the normalized eigenfunction of Δ_ℓ associated to its greatest eigenvalue $2 \cos\left(\frac{\pi}{\ell+1}\right) - 2$. Then

$$\begin{aligned} \lambda_1 &\geq \langle \varphi | M | \varphi \rangle = \langle \varphi | 3\text{Id}_\ell + \Delta_\ell | \varphi \rangle = 1 + 2 \cos\left(\frac{\pi}{\ell+1}\right) \\ &= 3 - \frac{\pi^2}{\ell^2} + \frac{2\pi^2}{\ell^3} + O\left(\frac{1}{\ell^4}\right) = 3e^{-\frac{\pi^2}{3\ell^2} + O\left(\frac{1}{\ell^3}\right)}. \end{aligned} \quad (8.13)$$

8.3.2 Upper bound

A direct rough upper bound for λ_1 is

$$\lambda_1 \leq \sup_i \sum_j |\langle i|M|j\rangle| \leq 3. \quad (8.14)$$

Unfortunately, this is not precise enough to conclude.

Let $|\psi\rangle$ be the eigenfunction of M associated to λ_1 . The upper bound on λ_1 will be given by the greatest eigenvalue μ_1 of a symmetric matrix P such that

$$\lambda_1 = \langle \psi|M|\psi\rangle \leq \langle \psi|P|\psi\rangle \leq \sup_{\langle \varphi|\varphi\rangle=1} \langle \varphi|P|\varphi\rangle = \mu_1 \quad (8.15)$$

To get a first bound on the quadratic form represented by M , one can first replace some $-$ on the diagonal by $+$, without increasing ℓ and so that $-$ come at most by pairs on the diagonal. Then in all pairs of $-$, replace one of them by a $+$. We are left with a matrix \tilde{M} with the same form as M and a ℓ at most increased by 1, whose diagonal consists in a succession of sequences of $+$ separated by one $-$. Let \oplus (resp. \ominus) be the set of indices corresponding to $+$ (resp. $-$) diagonal entries. Let $\overset{\circ}{\oplus} \subset \oplus$ the subset of indices whose neighbours are also in \oplus . We have

$$\langle \psi|\tilde{M}|\psi\rangle = \sum_{j \in \oplus} \psi_j^2 + \sum_{j \in \overset{\circ}{\oplus}} \psi_j(\psi_{j-1} + \psi_{j+1}) + \sum_{j \in \ominus} -\psi_j^2 + 2\psi_j(\psi_{j-1} + \psi_{j+1}). \quad (8.16)$$

Since ψ is the eigenfunction of M associated to λ_1 , we have for $j \in \ominus$ that

$$\lambda_1 \psi_j = \psi_{j-1} - \psi_j + \psi_{j+1} \quad (8.17)$$

and therefore

$$(\lambda_1 + 1)^2 \psi_j^2 = (\psi_{j-1} + \psi_{j+1})^2 \leq 2(\psi_{j-1}^2 + \psi_{j+1}^2) \quad (8.18)$$

from what we get

$$\begin{aligned} -\psi_j^2 + 2\psi_j(\psi_{j-1} + \psi_{j+1}) &= 2\psi_j(\psi_{j-1} - \psi_j + \psi_{j+1}) + \psi_j^2 \\ &= 2\lambda_1 \psi_j^2 + \psi_j^2 \\ &\leq \frac{4\lambda_1}{(\lambda_1 + 1)^2} (\psi_{j-1}^2 + \psi_{j+1}^2) + \psi_j^2 \\ &\leq \frac{4 \times 3}{(2 + 2 \cos(\frac{\pi}{\ell+1}))^2} (\psi_{j-1}^2 + \psi_{j+1}^2) + \psi_j^2 \end{aligned}$$

where in the last line we used the rough upper bound and the lower bound on λ_1 obtained before. Denote by α the coefficient in front of $(\psi_{j-1}^2 + \psi_{j+1}^2)$:

$$\alpha = \frac{4 \times 3}{(2 + 2 \cos(\frac{\pi}{\ell+1}))^2} = \frac{3}{(1 + \cos(\frac{\pi}{\ell+1}))^2} \quad (8.19)$$

This equation in θ can be rewritten as

$$\tan(\tilde{\ell}\theta) = -\frac{(1 - \alpha^2) \sin(\theta)}{(1 + \alpha^2) \cos(\theta) - 2\alpha}. \quad (8.26)$$

This equation has a unique solution in $(0, \frac{\pi}{\tilde{\ell}})$ given by the following expansion

$$\theta = \frac{\pi}{\tilde{\ell}} - \frac{7\pi}{\tilde{\ell}^2} + O\left(\frac{1}{\tilde{\ell}^3}\right). \quad (8.27)$$

The asymptotic expression for μ is thus

$$\mu = 3 - \frac{\pi^2}{\tilde{\ell}^2} + \frac{14\pi^2}{\tilde{\ell}^3} + O\left(\frac{1}{\tilde{\ell}^4}\right) = 3e^{-\frac{\pi^2}{3\tilde{\ell}^2} + O\left(\frac{1}{\tilde{\ell}^3}\right)} \quad (8.28)$$

giving the upper bound we were looking for.

8.4 Main contribution to $|\mathcal{P}_n|$

In order to determine the main term in the asymptotics of $|\mathcal{P}_n|$, one has to first estimate probability that the longest succession of +1 in (ε_k) has size ℓ .

Lemma 8.1.

$$\mathbb{P}[\ell = l_0] = \frac{N}{2^{l_0+2}} \left(1 + O\left(\frac{N}{2^{l_0}}\right)\right) \quad (8.29)$$

Proof:

For $i \in \mathbb{Z}/N\mathbb{Z}$ and $l \in \mathbb{N}$, define $C_i^{(l)}$ to be the following event

$$C_i^{(l)} = \{\text{there is a sequence of } +1 \text{ of length at least } l \text{ starting at position } i\} \quad (8.30)$$

$$= \{\varepsilon_{i-1} = -1 \text{ and } \forall k \in \{i, \dots, i+l-1\}, \varepsilon_k = +1\} \quad (8.31)$$

The probability we want to estimate can be rewritten in terms of these events as

$$\mathbb{P}[\ell = l_0] = \mathbb{P}\left[\bigcup_i C_i^{(l_0)} \setminus \bigcup_i C_i^{(l_0+1)}\right] \quad (8.32)$$

The probability that $C_i^{(l)}$ occurs is $\mathbb{P}[C_i^{(l)}] = 2^{-(l+1)}$ and it is easy to see that

$$\mathbb{P}[C_i^{(l)} \cap C_j^{(l)}] = \begin{cases} \mathbb{P}[C_i^{(l)}] \mathbb{P}[C_j^{(l)}] & \text{if their supports are disjoints,} \\ 0 & \text{if their supports intersect.} \end{cases} \quad (8.33)$$

More generally,

$$\mathbb{P} \left[C_{i_1}^{(l)} \cap \dots \cap C_{i_m}^{(l)} \right] = \begin{cases} \mathbb{P} \left[C_{i_1}^{(l)} \right] \cdots \mathbb{P} \left[C_{i_m}^{(l)} \right] = \frac{1}{2^{m(l+1)}} & \text{if their supports are disjoint,} \\ 0 & \text{otherwise.} \end{cases} \quad (8.34)$$

The number of ways of positioning m sequences of symbols of length $l+1$ so that their support do not intersect on a ring with N sites is equal to $\frac{N}{m} \binom{N-ml-1}{m-1}$. By an inclusion-exclusion argument, the probability that a sequence of $+1$ of length at least l occurs is thus

$$\begin{aligned} \mathbb{P} \left[\bigcup_i C_i^{(l)} \right] &= \sum_i \mathbb{P} \left[C_i^{(l)} \right] + \dots + (-1)^{m+1} \sum_{\substack{i_1, \dots, i_m \\ \text{distinct}}} \mathbb{P} \left[C_{i_1}^{(l)} \cap \dots \cap C_{i_m}^{(l)} \right] \\ &+ \dots + (-1)^{N+1} \mathbb{P} \left[\bigcap_i C_i^{(l)} \right] = \sum_{m=1}^N (-1)^{m+1} \binom{1}{2^{l+1}}^m \frac{N}{m} \binom{N-ml-1}{m-1} \end{aligned} \quad (8.35)$$

This alternate sum is well approximated by its first term, and since $\frac{N}{m} \binom{N-ml-1}{m-1} \leq \frac{N^m}{m!}$, the rest of the sum is bounded by

$$\begin{aligned} \sum_{m=2}^N (-1)^{m+1} \binom{1}{2^{l+1}}^m \frac{N}{m} \binom{N-ml-1}{m-1} &\leq \sum_{m=2}^N \binom{1}{2^{l+1}}^m \frac{N^m}{m!} \\ &\leq e^{\frac{N}{2^{l+1}}} - 1 - \frac{N}{2^{l+1}} = O \left(\left(\frac{N}{2^{l+1}} \right)^2 \right). \end{aligned} \quad (8.36)$$

Consequently, as $\bigcup_i C_i^{(l_0)} \subset \bigcup_i C_i^{(l_0+1)}$, we get finally that

$$\mathbb{P} [\ell = l_0] = \mathbb{P} \left[\bigcup_i C_i^{(l_0)} \right] - \mathbb{P} \left[\bigcup_i C_i^{(l_0+1)} \right] = \frac{N}{2^{l_0+2}} \left(1 + O \left(\frac{N}{2^{l_0}} \right) \right). \quad (8.37)$$

This approximation is valid only for $l \gg \log_2 N$. However, this proof furnishes a uniform upper bound $\mathbb{P} [\ell = l_0] \leq \frac{N}{2^{l_0+1}}$, what will be convenient to control the estimates below. \square

Using proposition 8.1 and lemma 8.1, we can now write the main contribution to $|\mathcal{P}_n|$ as a sum over the length of the longest sequence of $+1$.

$$\begin{aligned} \mathcal{A} &= \frac{2}{N} \mathbb{E} [\lambda_1^n] = \frac{2}{N} \sum_{l=0}^N \mathbb{P} [\ell = l] \lambda_1(l)^n = \frac{2}{N} \sum_{l=0}^N \frac{N}{2^{l+2}} \left(1 + O \left(\frac{N}{2^l} \right) \right) 3^n e^{-\frac{n\pi^2}{3l^2} + O \left(\frac{n}{l^3} \right)} \\ &= 3^n \sum_{l=0}^N \frac{1}{2^{l+1}} e^{-\frac{n\pi^2}{3l^2}} e^{O \left(\frac{N}{2^l} \right) + O \left(\frac{1}{l^3} \right)} = \frac{3^n}{2} \sum_{l=0}^N e^{-f(l)} e^{O \left(\frac{N}{2^l} \right) + O \left(\frac{n}{l^3} \right)} \end{aligned} \quad (8.38)$$

where f is the convex function defined by $f(l) = l \log 2 + \frac{\pi^2 n}{3l^2}$. By Laplace's method, the main contribution to the sum comes from the terms located near the critical point of f , which is

$$l_0 = \sqrt[3]{\frac{2\pi^2}{3 \log 2}} n^{\frac{1}{3}}. \quad (8.39)$$

More precisely, \mathcal{A} is rewritten as

$$\mathcal{A} = \frac{3^n}{2} \sum_{|l-l_0| \leq l_0^{2/3}} e^{-\frac{3}{2} \log 2 l_0 g(l/l_0)} e^{O\left(\frac{N}{2l}\right) + O\left(\frac{n}{l^3}\right)} + \frac{3^n}{2} \sum_{\substack{l=0 \\ |l-l_0| > l_0^{2/3}}}^N e^{-\frac{3}{2} \log 2 l_0 g(l/l_0)} e^{O\left(\frac{N}{2l}\right) + O\left(\frac{n}{l^3}\right)} \quad (8.40)$$

where $g(x) = \frac{2}{3} \left(x + \frac{1}{2x^2}\right)$. In the first sum, l is close to l_0 and one has

$$\begin{aligned} g\left(\frac{l}{l_0}\right) &= g(1) + \frac{1}{2!} \frac{(l-l_0)^2}{l_0^2} g''(1) + O\left(\frac{(l-l_0)^3}{l_0^3} \sup_{|h| \leq l_0^{-\frac{1}{3}}} |g'''(1+h)|\right) \\ &= 1 + \left(\frac{l-l_0}{l_0}\right)^2 + O(n^{-1/3}). \end{aligned} \quad (8.41)$$

In this range of l , the error terms are small, and thus the first sum, interpreted as a Riemann sum with a step $\Delta x = l_0^{-1/2}$, can be compared to a Gaussian integral

$$\begin{aligned} \sum_{|l-l_0| \leq \sqrt{l_0}} e^{-\frac{3}{2} \log 2 l_0 g(l/l_0)} &= \sqrt{l_0} \int_{-\infty}^{+\infty} e^{-\frac{3 \log 2}{2} (l_0 + x^2)} dx (1 + O(\frac{1}{\sqrt{l_0}})) \\ &= \left(\frac{2\pi}{3 \log 2}\right)^{\frac{2}{3}} (\pi n)^{\frac{1}{6}} e^{-\left(\frac{3\pi \log 2}{2}\right)^{\frac{2}{3}} n^{\frac{1}{3}}} (1 + O(n^{-\frac{1}{6}})). \end{aligned} \quad (8.42)$$

The contribution of the other sum is smaller. The fact that g is convex implies that this sum can be bounded by the sum of a geometric series decaying faster than the contribution of the first sum. More precisely,

$$\sum_{\substack{l=0 \\ |l-l_0| > l_0^{2/3}}}^N e^{-\frac{3}{2} \log 2 l_0 g(l/l_0)} e^{O\left(\frac{N}{2l}\right) + O\left(\frac{n}{l^3}\right)} = O\left(e^{-\frac{3}{2} \log 2 l_0}\right) \quad (8.43)$$

what is the order of the error term in (8.42). The error term $O\left(\frac{n}{l^3}\right)$ has to be treated with more care. As this error term is uniform in l , we could have bound from above and from below the function f by functions of the form

$$f_c(l) = l \log 2 + \frac{\pi^2 n}{3l^2} + \frac{cn}{l^3} \quad (8.44)$$

for different values of c . Anyway, the critical point of f_c is still close enough to l_0 not to modify the global asymptotics (exponential decay exponent and polynomial prefactor), except unfortunately the constant in front of (8.42). What we get finally is

Theorem 8.1.

$$|\mathcal{P}_n| \asymp 3^n n^{\frac{1}{6}} e^{-\left(\frac{3\pi \log 2}{2}\right)^{\frac{2}{3}} n^{\frac{1}{3}}} \quad (8.45)$$

where the symbol \asymp means that the ratio between the left hand side and the right hand side is bounded away from 0 and ∞ . To finish the proof, we need to estimate the contribution of the other eigenvalues.

8.5 Spectral gap

With some more work, we prove that the second eigenvalue of M is comparable either to the second eigenvalue of the largest block corresponding to successions of $+1$, either to the first eigenvalue of the second largest block. More precisely,

Lemma 8.2. *If ℓ (resp. ℓ') is the longest (resp. the second longest) succession of $+1$ in the sequence (ε_k) , the second eigenvalue is given by*

$$\lambda_2 \leq \max\left(3e^{-\frac{4\pi^2}{3\ell^2} + O\left(\frac{1}{\ell^3}\right)}, 3e^{-\frac{\pi^2}{3\ell'^2} + O\left(\frac{1}{\ell'^3}\right)}\right) \quad (8.46)$$

We omit the proof of this lemma here.

The contribution of the second eigenvalue is thus given by

$$\begin{aligned} \mathcal{B} &= \frac{1}{N} \sum_{l=0}^N \mathbb{P}[\ell = l] \sum_{l'=0}^l \mathbb{P}[\ell' = l' | \ell] \max\left(3e^{-\frac{4\pi^2}{3l^2} + O\left(\frac{1}{l^3}\right)}, 3e^{-\frac{\pi^2}{3l'^2} + O\left(\frac{1}{l'^3}\right)}\right)^n \\ &= \frac{3^n}{N} \sum_{l=0}^N \mathbb{P}[\ell = l] \sum_{l'=0}^{l/2-1} \mathbb{P}[\ell' = l' | \ell] \left(e^{-\frac{4\pi^2}{3l^2} + O\left(\frac{1}{l^3}\right)}\right)^n \\ &\quad + \frac{3^n}{N} \sum_{l=0}^N \mathbb{P}[\ell = l] \sum_{l'=l/2}^l \mathbb{P}[\ell' = l' | \ell] \left(e^{-\frac{\pi^2}{3l'^2} + O\left(\frac{1}{l'^3}\right)}\right)^n \end{aligned}$$

The first sum can be rewritten, and bounded by

$$\begin{aligned} &\frac{3^n}{N} \sum_{l=0}^N \mathbb{P}[\ell = l] \left(3e^{-\frac{4\pi^2}{3l^2} + O\left(\frac{1}{l^3}\right)}\right)^n \left(\sum_{l'=0}^{l/2-1} \mathbb{P}[\ell' = l' | \ell]\right) \\ &\leq \text{Cst } 3^n \sum_{l=0}^N 2^{-l} e^{-\frac{4n\pi^2}{3l^2} + O\left(\frac{n}{l^3}\right)} = O\left(n^{1/6} 3^n e^{-(3\pi \log 2)^{\frac{2}{3}} n^{\frac{1}{3}}}\right) \quad (8.47) \end{aligned}$$

which is negligible comparing to \mathcal{A} . We invert the order of summation in the second term

$$\begin{aligned} \frac{3^n}{N} \sum_{l=0}^N \mathbb{P}[\ell = l] \sum_{l'=l/2}^l \mathbb{P}[\ell' = l' | \ell] \left(e^{-\frac{\pi^2}{3l'^2} + O\left(\frac{1}{l'^3}\right)} \right)^n \\ = \frac{3^n}{N} \sum_{l'=0}^N \left(e^{-\frac{\pi^2}{3l'^2} + O\left(\frac{1}{l'^3}\right)} \right)^n \left(\sum_{l=l'}^{2l'-1} \mathbb{P}[\ell = l, \ell' = l'] \right) \end{aligned} \quad (8.48)$$

Using the same kind of arguments as in the proof of lemma 8.1, one deduces that the probability that $\ell = l$ and $\ell' = l'$ is bounded by some constant times $\frac{N^2}{2^{l+l'}}$. Therefore, the sum over l is $O\left(\frac{N^2}{2^{2l'}}\right)$, and hence second sum is bounded by

$$\text{Cst } N 3^n \sum_{l'=0}^N \frac{1}{2^{2l'}} \left(e^{-\frac{\pi^2}{3l'^2} + O\left(\frac{1}{l'^3}\right)} \right)^n = O\left(n^{1/6} 3^n e^{-(3\pi \log 2)^{\frac{2}{3}} n^{\frac{1}{3}}} \right) \quad (8.49)$$

which is also negligible.

As the contribution of all the other eigenvalues are dominated by that of λ_2 , one can conclude that the leading term in $|\mathcal{P}_n|$ is really given by \mathcal{A} , and that therefore, theorem 8.1 is proven.

8.6 Generalization

One can extend these results to a little broader context. We suppose that the lamps have not 2 states (*on* or *off*), but p states of different intensity, and that the lamplighter can either increase or decrease the intensity of the lamp (increasing the intensity when the lamp is already in the most intensive state means switching it off).

This can be translated in terms of walks on the graph G . The loops on the lamplighter's graph with p -state lamps are in bijection with closed walks on G passing through every rung an algebraic number of times multiple of p . By algebraic number of times, we mean the number of times from bottom to top, minus the number of times from top to bottom. Let $\mathcal{P}_n(p)$ the set of paths on G of length n having this property.

Our method can be extended to this case: instead of weights ± 1 we assign random, uniformly distributed, complex p th roots of the unity ζ_k to the oriented edge from $|\bar{k}\rangle$ to $|\underline{k}\rangle$, and $\bar{\zeta}_k$ to the backward oriented edge from $|\underline{k}\rangle$ to $|\bar{k}\rangle$ (see figure 8.5).

Let M_ω the random weighted adjacency matrix of G_N for these weights. We claim that the cardinal of $|\mathcal{P}_n(p)|$ is given by

$$|\mathcal{P}_n(p)| = \mathbb{E} [\langle \underline{0} | M_\omega^n | \underline{0} \rangle] = \mathbb{E} \left[\frac{1}{2N} \text{tr}(M_\omega^n) \right] \quad (8.50)$$

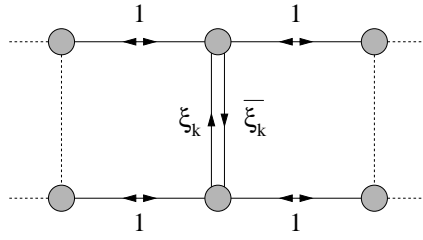


Figure 8.5: weights on edges of G for the problem with lamps with p states.

One can show that for these weights, proposition 8.1 still holds for this weights, and thus $\lambda_1 = 3 \exp\left(-\frac{\pi^2}{3\ell^2}\right)$ where ℓ is the longest succession of identical symbols in the cyclic sequence (ζ_k) . This is done by applying the previous arguments not on M , but on M^2 . As G_N is bipartite, M^2 preserves the subspaces of functions supported on vertices of only one color (white or black). The restriction to M^2 to white vertices can be interpreted as the weighted matrix of the graph represented on figure 8.6. The amplitude of weights of the diagonal edges is maximal when two successive coefficients ξ_k and ξ_{k+1} are equal. The approximation of the first eigenvalue of M^2 (that is the approximation for λ_1^2) is obtained by comparing M^2 with the square of the discrete Laplacian on the longest succession of identic symbols ξ_k , with suitable boundary conditions.

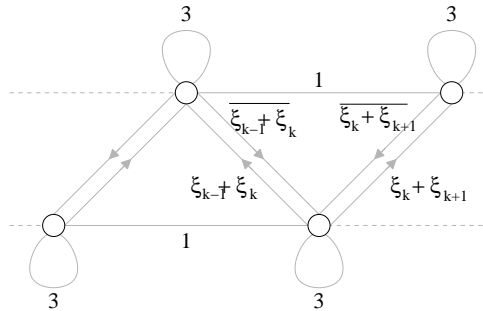


Figure 8.6: The weighted graph described by the *white* block of M^2 , the square of the adjacency matrix of G_N . The module of weights on diagonal edges are maximal when $\xi_k = \xi_{k+1}$.

The probability that the longest succession of identical symbols is l is

$$\frac{N}{(p-1)p^l} \left(1 + O\left(\frac{N}{p^l}\right) \right). \tag{8.51}$$

We apply the same arguments as in the previous sections to compute the asymptotics of $|\mathcal{P}_n(p)|$, and we get finally:

Theorem 8.2.

$$|\mathcal{P}_n(p)| \asymp 3^n n^{\frac{1}{6}} e^{-\left(\frac{3\pi \log p}{2}\right)^{\frac{2}{3}} n^{\frac{1}{3}}} \tag{8.52}$$

These asymptotics have already been obtained by Revelle [53] for the random walk on the lamplighter group in a more precise form, but for other generators.

8.7 Paths counting and random Schrödinger operators

This kind of problem is related to the spectral study of discrete Schrödinger operators with random potential, and more precisely, to a phenomenon called *Lifshitz's tail* describing the behavior of the spectral density at the edge of the spectrum of these operators. The spectral theory of such operators can be found in [48, 6].

Lifshitz gave heuristic arguments to justify that the integrated spectral density \mathcal{N} of a random Schrödinger operator in dimension d near the bottom edge E_0 of the spectrum would have the following behaviour

$$\log \mathcal{N}(E_0 + h) \simeq -\frac{c}{h^{1/(d+1)}}, \quad (8.53)$$

to be compared to the behaviour of another class of random matrices (operators), the GUE ensemble, described by the Wigner semi-circle law (3.16). The same behaviour is expected for every edge of the spectrum.

The proof of this phenomenon has been established rigorously in many examples with different degrees of precision in the asymptotics. The most common type of result is the determination of the *Lifshitz exponent*

$$\lim_{h \rightarrow 0} \frac{\log |\log \mathcal{N}(E_0 + h)|}{\log |h|} = \frac{1}{d+1} \quad (8.54)$$

The operator M_ω^+ on G discussed in the first sections is in fact a discrete Schrödinger operator with a iid random scalar potential

$$M_\omega^+ = \Delta + V_\omega \quad (8.55)$$

The spectrum of this operator is included in $[-3, 3]$, and the quantities counting the paths we are interested are the large moments of the spectral measure:

$$|\mathcal{P}_n| = \mathbb{E} \left[\int \lambda^n d\mathcal{N}(\lambda) \right] \quad (8.56)$$

Precise asymptotics for the Lifshitz's tail and Laplace's method would lead to an approximation of $|\mathcal{P}_n|$ for large n .

The method proposed to solve the initial question raised by Richard Kenyon about the number of *curl-free walks* on \mathbb{Z}^2 of a given length is analogous to that used in the previous sections: assign to each edge \mathbf{e} a weight $\zeta_{\mathbf{e}}$ for one direction and $\bar{\zeta}_{\mathbf{e}}$ for the other direction, where $(\zeta_{\mathbf{e}})$ is a sequence of independent random variables uniformly

distributed on $U(1)$. The weighted adjacency operator for these weights is a discrete Schrödinger operator with random magnetic field in 2 dimensions

$$(M f)(v) = \sum_{w \sim v} \zeta_{(v,w)} f(w). \quad (8.57)$$

the phase of ζ playing the role of magnetic potential. The cardinal of the set \mathcal{Q}_n of curl-free paths of length n is

$$|\mathcal{Q}_n| = \mathbb{E} \left[\int \lambda^n d\mathcal{N}(\lambda) \right]. \quad (8.58)$$

The techniques we used in the 1-dimensional case seems quite difficult to apply to this situation. However, there exist already some results for the Lifshitz's tail of this operator [43] stating that the Lifshitz exponent is given by the formula predicted by Lifshitz

$$\lim_{h \rightarrow 0} \frac{\log |\mathcal{N}(4-h)|}{\log |h|} = \frac{1}{3}, \quad (8.59)$$

implying that

$$\log \left| \log \frac{|\mathcal{Q}_n|}{4^n} \right| = \frac{1}{4} \quad (8.60)$$

i.e. that roughly, Q_n must be of order $4^n e^{-cn^{1/4}}$ up to polynomial prefactors. More precise statements on the behaviour of the spectrum of such operators would lead to full asymptotics for $|\mathcal{Q}_n|$.

Bibliography

- [1] J. BAIK, T. KRIECHERBAUER, K. D. T.-R. MCLAUGHLIN, AND P. D. MILLER, *Uniform asymptotics for polynomials orthogonal with respect to a general class of discrete weights and universality results for associated ensembles: announcement of results*, Int. Math. Res. Not., (2003), pp. 821–858, arXiv:math.CA/0212149.
- [2] L. BARTHOLDI AND W. WOESS, *Spectral computations on lamplighter groups and Diestel-Leader graphs*, J. Fourier Anal. Appl., 11 (2005), pp. 175–202, arXiv:math.GR/0405182.
- [3] P. BILLINGSLEY, *Convergence of probability measures*, John Wiley & Sons Inc., New York, 1968.
- [4] ———, *Probability and measure*, John Wiley & Sons, New York-Chichester-Brisbane, 1979. Wiley Series in Probability and Mathematical Statistics.
- [5] R. BURTON AND R. PEMANTLE, *Local characteristics, entropy and limit theorems for spanning trees and domino tilings via transfer-impedances*, Ann. Probab., 21 (1993), pp. 1329–1371, arXiv:math.PR/0404048.
- [6] R. CARMONA AND J. LACROIX, *Spectral theory of random Schrödinger operators*, Probability and its Applications, Birkhäuser Boston Inc., Boston, MA, 1990.
- [7] R. CERF AND R. KENYON, *The low-temperature expansion of the Wulff crystal in the 3D Ising model*, Comm. Math. Phys., 222 (2001), pp. 147–179.
- [8] H. COHN, R. KENYON, AND J. PROPP, *A variational principle for domino tilings*, J. Amer. Math. Soc., 14 (2001), pp. 297–346 (electronic), arXiv:math.CO/0008220.
- [9] D. J. DALEY AND D. VERE-JONES, *An introduction to the theory of point processes*, Springer Series in Statistics, Springer-Verlag, New York, 1988.
- [10] B. DE TILIÈRE, *Dimères sur les graphes isoradiaux & modèles d’interfaces aléatoires en dimension 2+2*, PhD thesis, Université Paris XI, 2004.
- [11] N. P. DOLBILIN, Y. M. ZINOV’EV, A. S. MISHCHENKO, M. A. SHTAN’KO, AND M. I. SHTOGRIN, *Homological properties of two-dimensional coverings of lattices on surfaces*, Funktsional. Anal. i Prilozhen., 30 (1996), pp. 19–33, 95.
- [12] F. J. DYSON, *A Brownian-motion model for the eigenvalues of a random matrix*, J. Mathematical Phys., 3 (1962), pp. 1191–1198.

-
- [13] P. L. FERRARI AND H. SPOHN, *Step fluctuations for a faceted crystal*, J. Statist. Phys., 113 (2003), pp. 1–46, arXiv:cond-mat/0212456.
- [14] M. E. FISHER, *On the dimer solution of planar Ising models*, J. Math. Phys., 7 (1966), pp. 1776–1781.
- [15] R. H. FOWLER AND G. S. RUSHBROOKE, *Statistical theory of perfect solutions*, Trans. Faraday Soc., 33 (1937), pp. 1272–1294.
- [16] Y. V. FYODOROV, *Introduction to the Random Matrix Theory: Gaussian Unitary Ensemble and Beyond*, (2004), arXiv:math-ph/0412017.
- [17] I. GESSEL AND G. VIENNOT, *Binomial determinants, paths, and hook length formulae*, Adv. in Math., 58 (1985), pp. 300–321.
- [18] J. GLIMM AND A. JAFFE, *Quantum physics*, Springer-Verlag, New York, 1981. A functional integral point of view.
- [19] R. I. GRIGORCHUK AND A. ŽUK, *The lamplighter group as a group generated by a 2-state automaton, and its spectrum*, Geom. Dedicata, 87 (2001), pp. 209–244.
- [20] I. M. GUELFAND AND N. Y. VILENKIN, *Les distributions. Tome 4: Applications de l'analyse harmonique*, Traduit du russe par G. Rideau. Collection Universitaire de Mathématiques, No. 23, Dunod, Paris, 1967.
- [21] K. JOHANSSON, *Non-intersecting paths, random tilings and random matrices*, Probab. Theory Related Fields, 123 (2002), pp. 225–280, arXiv:math.PR/0011250.
- [22] ———, *The arctic circle boundary and the Airy process*, Ann. Probab., 33 (2005), pp. 1–30, arXiv:math.PR/0306216.
- [23] S. KARLIN AND J. MCGREGOR, *Coincidence probabilities*, Pacific J. Math., 9 (1959), pp. 1141–1164.
- [24] P. W. KASTELEYN, *Dimer statistics and phase transitions*, J. Mathematical Phys., 4 (1963), pp. 287–293.
- [25] ———, *Graph theory and crystal physics*, in Graph Theory and Theoretical Physics, Academic Press, London, 1967, pp. 43–110.
- [26] M. KATORI, T. NAGAO, AND H. TANEMURA, *Infinite systems of non-colliding Brownian particles*, in Stochastic analysis on large scale interacting systems, vol. 39 of Adv. Stud. Pure Math., Math. Soc. Japan, Tokyo, 2004, pp. 283–306, arXiv:math.PR/0301143.
- [27] R. KENYON, *Local statistics of lattice dimers*, Ann. Inst. H. Poincaré Probab. Statist., 33 (1997), pp. 591–618, arXiv:math.CO/0105054.

- [28] ———, *Conformal invariance of domino tiling*, Ann. Probab., 28 (2000), pp. 759–795, arXiv:math-ph/9910002.
- [29] ———, *Dominos and the Gaussian free field*, Ann. Probab., 29 (2001), pp. 1128–1137, arXiv:math-ph/0002027.
- [30] ———, *The Laplacian and Dirac operators on critical planar graphs*, Invent. Math., 150 (2002), pp. 409–439, arXiv:math-ph/0202018.
- [31] ———, *Height fluctuations in the honeycomb dimer model*, (2003), arXiv:math-ph/0405052.
- [32] R. KENYON AND A. OKOUNKOV, *Planar dimers and Harnack curves*, (2003), arXiv:math-ph/0311005.
- [33] ———, *Limit shapes and the complex Burgers equation*, (2005), arXiv:math-ph/0507007.
- [34] R. KENYON, A. OKOUNKOV, AND S. SHEFFIELD, *Dimers and amoebae*, (2003), arXiv:math-ph/0311005.
- [35] R. KENYON, J. PROPP, AND D. WILSON, *Trees and matchings*, Electron. J. Combin., 7 (2000), pp. Research Paper 25, 34 pp. (electronic), arXiv:math.CO/9903025.
- [36] R. KENYON AND S. SHEFFIELD, *Dimers, tilings and trees*, J. Combin. Theory Ser. B, 92 (2004), pp. 295–317, arXiv:math.CO/0310195.
- [37] A. N. KOLMOGOROV, *Osnovnye ponyatiya teorii veroyatnostei*, Izdat. “Nauka”, Moscow, second ed., 1974. Probability Theory and Mathematical Statistics Series, Vol. 16.
- [38] M. MATTERA, *Annihilating random walks and perfect matchings of planar graphs*, in Discrete random walks (Paris, 2003), Discrete Math. Theor. Comput. Sci. Proc., AC, Assoc. Discrete Math. Theor. Comput. Sci., Nancy, 2003, pp. 173–180 (electronic).
- [39] B. MCCOY AND F. WU, *The two-dimensional Ising model*, Harvard Univ. Press, 1973.
- [40] G. MIKHALKIN, *Amoebas of algebraic varieties and tropical geometry*, in Different faces of geometry, Int. Math. Ser. (N. Y.), Kluwer/Plenum, New York, 2004, pp. 257–300, arXiv:math.AG/0403015.
- [41] G. MIKHALKIN AND H. RULLGÅRD, *Amoebas of maximal area*, Internat. Math. Res. Notices, (2001), pp. 441–451, arXiv:math.CV/0010087.
- [42] T. NAGAO AND P. J. FORRESTER, *Multilevel dynamical correlation functions for Dyson’s Brownian motion model of random matrices*, Physics Letters A, 247 (1998), pp. 42–46.

-
- [43] S. NAKAMURA, *Lifshitz tail for Schrödinger operator with random magnetic field*, Comm. Math. Phys., 214 (2000), pp. 565–572.
- [44] A. OKOUNKOV AND N. RESHETIKHIN, *Correlation function of Schur process with application to local geometry of a random 3-dimensional Young diagram*, J. Amer. Math. Soc., 16 (2003), pp. 581–603 (electronic), arXiv:math.CO/0107056.
- [45] A. OKOUNKOV, N. RESHETIKHIN, AND C. VAFA, *Quantum Calabi-Yau and classical crystals*, (2003), arXiv:hep-th/0309208.
- [46] H. OSADA, *Dirichlet form approach to infinite-dimensional Wiener processes with singular interactions*, Comm. Math. Phys., 176 (1996), pp. 117–131.
- [47] M. PASSARE AND H. RULLGÅRD, *Amoebas, Monge-Ampère measures, and triangulations of the Newton polytope*, Duke Math. J., 121 (2004), pp. 481–507.
- [48] L. PASTUR AND A. FIGOTIN, *Spectra of random and almost-periodic operators*, vol. 297 of Grundlehren der Mathematischen Wissenschaften [Fundamental Principles of Mathematical Sciences], Springer-Verlag, Berlin, 1992.
- [49] M. PRÄHOFER AND H. SPOHN, *Current fluctuations for the totally asymmetric simple exclusion process*, in In and out of equilibrium (Mambucaba, 2000), vol. 51 of Progr. Probab., Birkhäuser Boston, Boston, MA, 2002, pp. 185–204, arXiv:cond-mat/0101200.
- [50] ———, *Scale invariance of the PNG droplet and the Airy process*, J. Statist. Phys., 108 (2002), pp. 1071–1106, arXiv:math.PR/0105240. Dedicated to David Ruelle and Yasha Sinai on the occasion of their 65th birthdays.
- [51] J. PROPP, *Lattice structure of orientations of graphs*, (2002), arXiv:CO/0209005.
- [52] ———, *Generalized domino-shuffling*, Theoret. Comput. Sci., 303 (2003), pp. 267–301. Tilings of the plane.
- [53] D. REVELLE, *Heat kernel asymptotics on the lamplighter group*, Electron. Comm. Probab., 8 (2003), pp. 142–154 (electronic).
- [54] S. SHEFFIELD, *Gaussian Free Field for mathematicians*, (2003), arXiv:math.PR/0312099.
- [55] ———, *Random Surfaces: Large Deviations Principles and Gradient Gibbs Measure Classifications*, PhD thesis, Stanford University, 2004, arXiv: math.PR/0304049.
- [56] A. SOSHNIKOV, *Determinantal random point fields*, Uspekhi Mat. Nauk, 55 (2000), pp. 107–160, arXiv:math.PR/0002099.
- [57] A. SOSHNIKOV, *Gaussian limit for determinantal random point fields*, Ann. Probab., 30 (2002), pp. 171–187, arXiv:math.PR/0006037.

- [58] H. SPOHN, *Interacting Brownian particles: a study of Dyson's model*, in Hydrodynamic behavior and interacting particle systems (Minneapolis, Minn., 1986), vol. 9 of IMA Vol. Math. Appl., Springer, New York, 1987, pp. 151–179.
- [59] H. N. V. TEMPERLEY, *Enumeration of graphs on a large periodic lattice*, in Combinatorics (Proc. British Combinatorial Conf., Univ. Coll. Wales, Aberystwyth, 1973), Cambridge Univ. Press, London, 1974, pp. 155–159. London Math. Soc. Lecture Note Ser., No. 13.
- [60] H. N. V. TEMPERLEY AND M. E. FISHER, *Dimer problem in statistical mechanics—an exact result*, Philos. Mag. (8), 6 (1961), pp. 1061–1063.
- [61] G. TESLER, *Matchings in graphs on non-orientable surfaces*, J. Combin. Theory Ser. B, 78 (2000), pp. 198–231.
- [62] W. P. THURSTON, *Conway's tiling groups*, Amer. Math. Monthly, 97 (1990), pp. 757–773.
- [63] D. B. WILSON, *Generating random spanning trees more quickly than the cover time*, in Proceedings of the Twenty-eighth Annual ACM Symposium on the Theory of Computing (Philadelphia, PA, 1996), New York, 1996, ACM, pp. 296–303.